Geothermics and hydrogeology of the southern part of the Kenya Rift Valley with emphasis on the Magadi–Nakuru Area

Research Report SD/89/1

Hydrogeology Series

British Geological Survey

BGS Research Report SD/89/1

Geothermics and hydrogeology of the southern part of the Kenya Rift Valley with emphasis on the Magadi–Nakuru area

RESEARCH REPORT SD/89/1

Geothermics and hydrogeology of the southern part of the Kenya Rift Valley with emphasis on the Magadi–Nakuru area

D J Allen, W G Darling and W G Burgess

BRITISH GEOLOGICAL SURVEY

RESEARCH REPORT SD/89/1

Hydrogeology Series

Geothermics and hydrogeology of the southern part of the Kenya Rift Valley with emphasis on the Magadi–Nakuru area

D J Allen, W G Darling and W G Burgess

This report was prepared for the Overseas Development Administration

Cover illustration

Project staff examining hot springs at Lake Bogoria

Authors

BGS Keyworth

D J Allen
W G Darling
W G Burgess

Geographical index

Kenya

Subject index

Geothermal exploration, hydrogeology

Bibliographic reference

Allen, D J, Darling, W G, and Burgess, W G. 1989. Geothermics and hydrogeology of the southern part of the Kenya Rift Valley with emphasis on the Magadi–Nakuru area. *British Geological Survey Research Report* SD/89/1.

ISBN 0 85272 175 7

Keyworth, Nottingham British Geological Survey 1989

BRITISH GEOLOGICAL SURVEY

The full range of Survey publications is available through the Sales Desks at Keyworth and Murchison House, Edinburgh. Selected items can be bought at the BGS London Information Office, and orders are accepted here for all publications. The adjacent Geological Museum bookshop stocks the more popular books for sale over the counter. Most BGS books and reports are listed in HMSO's Sectional List 45, and can be bought from HMSO and through HMSO agents and retailers. Maps are listed in the BGS Map Catalogue and the Ordnance Survey's Trade Catalogue, and can be bought from Ordnance Survey agents as well as from BGS.

The British Geological Survey carries out the geological survey of Great Britain and Northern Ireland (the latter as an agency service for the government of Northern Ireland), and of the surrounding continental shelf, as well as its basic research projects. It also undertakes programmes of British technical aid in geology in developing countries as arranged by the Overseas Development Administration.

The British Geological Survey is a component body of the Natural Environment Research Council.

Keyworth, Nottingham NG12 5GG

☎ Plumtree (060 77) 6111 Telex 378173 BGSKEY G
Fax ☎ 060 77–6602

Murchison House, West Mains Road, Edinburgh EH9 3LA

☎ 031–667 1000 Telex 727343 SEISED G
Fax ☎ 031–668 2683

London Information Office at the Geological Museum, Exhibition Road, South Kensington, London SW7 2DE

☎ 01–589 4090 Fax ☎ 01–584 8270
☎ 01–938 9056/57

19 Grange Terrace, Edinburgh EH9 2LF

☎ 031–667 1000 Telex 727343 SEISED G

St Just, 30 Pennsylvania Road, Exeter EX4 6BX

☎ Exeter (0392) 78312

Bryn Eithyn Hall, Llanfarian, Aberystwyth, Dyfed SY23 4BY

☎ Aberystwyth (0970) 611038 Fax ☎ 0970–624822

Windsor Court, Windsor Terrace, Newcastle upon Tyne NE2 4HB

☎ 091–281 7088 Fax ☎ 091–281 9016

Geological Survey of Northern Ireland, 20 College Gardens, Belfast BT9 6BS

☎ Belfast (0232) 666595

Maclean Building, Crowmarsh Gifford, Wallingford, Oxfordshire OX10 8BB

☎ Wallingford (0491) 38800 Telex 849365 HYDROL G
Fax ☎ 0491–32256

Parent Body

Natural Environment Research Council

Polaris House, North Star Avenue, Swindon, Wiltshire SN2 1EU

☎ Swindon (0793) 411500 Telex 444293 ENVRE G
Fax ☎ 0793–411501

FOREWORD

This report summarizes the findings of the hydrogeological component of the British Geological Survey (BGS)/Ministry of Energy and Regional Development (MERD) contribution to the Kenya Rift Valley Geothermal Project. This is a bilateral technical co-operation project between the Government of the United Kingdom - represented by the Overseas Development Administration (ODA) - and the Government of Kenya (GOK). Assistance by the Government of the UK was designed to fit within the framework of a larger United Nations Development Programme (UNDP)/GOK project whose objectives were to explore for geothermal energy in the Rift Valley between the Silali crater in the north and the Tanzanian border in the south.

During the project, which lasted from 1985 to 1988, fieldwork and hydrogeological data record collection were initially carried out by W.G. Burgess of BGS in co-operation with MERD scientists Messrs. Mariita, Nyaga, Odondi and Ouma. Subsequent work in Kenya was undertaken by D.J. Allen and W.G. Darling of BGS, assisted by Mr Ndogo of MERD. Sample analyses were undertaken mainly by staff at the BGS laboratories at Wallingford (and elsewhere as noted in the text). Data interpretations were made by the authors. The work was carried out under the general supervision of Dr. M.C.G. Clarke (Project Leader), and Dr. R.L. Johnson (Regional Geologist, Africa and the Middle East).

The report fully supersedes ten interim reports (listed in the References) which have been issued at intervals since December 1985. All analyses given in the previous reports are presented in this summary document.

In general the physical hydrogeological and hydrogeochemical investigations carried out during the project are described separately in this report (Chapters 4 and 5). However in the cases of the Olkaria and Magadi regions the large quantity of data made it more appropriate to consider the areas individually (Chapters 6 and 7). A summary of the conclusions of the study is presented in Chapter 8.

The work described in this report was carried out on behalf of ODA. The results may be used to aid formulation of Government policy but do not in themselves represent Government policy. They are presented in a format agreed between ODA and BGS. The views and judgements expressed are those of the British Geological Survey and do not necessarily represent those of ODA.

SUMMARY

This report presents the results of hydrogeological and hydrogeochemical studies in the Kenya Rift Valley as part of the British Geological Survey (BGS)/Ministry of Energy and Regional Development (MERD) contribution to the Kenya Rift Valley Geothermal Project.

The objective of these studies was to provide a greater understanding of the location, nature and movement of the thermal waters in the Rift and of the cool ambient waters recharging the thermal fields. In the study the physical hydrogeology of the Rift was investigated to provide basic information concerning regional groundwater occurrence and flow patterns. The chemistry of both thermal and ambient waters was studied in order to understand the nature and origin of the thermal waters and to further explain groundwater mixing patterns.

Physical hydrogeological data were collected over a region of the Rift Valley from the Tanzanian border in the south (Figure 2.1) to Nakuru in the north and extending to the groundwater divides on the bounding rift escarpments. Information from 600 boreholes in this area was abstracted from records and supplemented by data collected in the field. The types of data collected included lithological information, hydraulic data and borehole constuction details.

Analysis of these data has shown that on a regional scale the Rift Valley between Lakes Nakuru and Magadi broadly exhibits the hydrogeological features expected of a Valley-interfluve system, with lateral groundwater flows from the Rift escarpments to discharge areas on the Rift floor and axial groundwater flows away from the Rift floor culmination at Lake Naivasha. This model is modified by the presence of the major Rift faults, which act as barriers to lateral flow, leading to longer, deeper, flow paths, and by the grid faulting in the Rift floor which tends to align flow paths within the Rift along its axis.

The permeabilities of the volcanic rocks underlying the Rift Valley are generally poor. Aquifers are normally found in fractured or reworked volcanics and are usually confined. Aquifer properties at depths exceeding 250 metres are virtually unknown except in the Olkaria geothermal field where low permeabilities (around 5 millidarcies) are found. Preliminary modelling studies carried out during the project suggest that rocks at depth elsewhere in the rift may also have low permeabilities.

Preliminary water balance estimates from the Naivasha catchment suggest that subsurface flow from Lake Naivasha is directed predominantly to the south, and that the quantity of discharge is greatly in excess of the geothermal discharge of the Olkaria power station. It is therefore considered unlikely that geothermal abstraction affects the level of the lake.

Fluid samples for hydrochemical analysis were taken from 129 sites ranging from the Silali area in the north (Figure 2.1) to Lake Magadi in the south. Samples were taken both from thermal sources (geothermal boreholes, fumaroles and thermal springs) and non-thermal sources (water boreholes, springs, lakes and rivers). In addition samples of rainfall were taken for isotopic analysis, and fumarole fluid samples collected by a UNDP project were

analysed.

These analyses have enabled the model of the regional flow systems to be substantially improved. In particular the mixing between subsurface discharge from Lake Naivasha and rift-wall waters has been shown using stable isotope techniques, and Naivasha water has been traced as far south as Suswa volcano and to the north as far as Lake Elmenteita. The analysis of geothermal fluids from Eburru, Olkaria, Longonot and Suswa has led to the conclusion that all the fluids can be explained in terms of a mixing series between Rift wall water and water from Lake Naivasha, and there is no evidence of a unique deep thermal water.

Two thermal areas - Olkaria and Magadi - were examined in some detail during the study. At Olkaria the results support the conclusion of other workers that the present wellfield is situated somewhat to the south of a thermal upflow. Other thermal upflows at Eburru and Longonot are implied from gas analyses. There are indications at Olkaria that short flow paths may be involved, and that the system may be quite old. At Magadi it is concluded that the thermal springs are formed by a two-component mixing series, probably with a local heat source, and that the hot end member is at a temperature of 100-130°C.

The main conclusions of this study are that the geothermal areas at Eburru, Olkaria-Domes, Longonot, Suswa and Magadi are individual geothermal fields with local heat sources giving rise to separate convective cells in which the geothermal fluids originate as mixtures of ambient groundwaters and lakewater (or groundwater and river water in the case of Magadi). It is recommended that further investigation concentrates on the main areas of upflow, at Olkaria-Domes, Eburru and Longonot.

ACKNOWLEDGEMENTS

The authors wish to express their thanks for the assistance provided by the following: Martin Clarke and Derek Woodhall (resident BGS geothermal team in Nairobi) for their help and patience during our visits; MERD staff, in particular Mr J. Kinyariro (Project Leader) and MERD scientists Messrs. Mariita, Ndogo, Nyaga, Odondi and Ouma; UNDP Geothermal Project members, and BHC staff in Nairobi. We are also grateful to the Ministry of Water Development for permission to use groundwater data.

This report is published with the permission of the Director, BGS (NERC).

CONTENTS

References

Appendix 1 - General Borehole Data

Appendix 2 - Borehole Completion Data

Appendix 3 - Borehole Water Strikes and Levels

Appendix 4 - Borehole Productivity

Appendix 5 - Borehole Location List

Appendix 6 - Estimated Hydraulic Properties of Boreholes

Appendix 7 - List of Geochemical Sampling Sites (BGS and UNDP) including Grid Reference and Sample Source

LIST OF FIGURES

LIST OF TABLES

1 INTRODUCTION

The purpose of this study was to investigate the hydrogeology of a section of the Rift Valley with particular reference to its geothermal character. The study examined in detail an area between Lake Nakuru in the north and Lake Magadi in the south (Figure 2.1), with emphasis on the Naivasha catchment. In addition chemical sampling was undertaken as far north as Silali and as far west as Homa Bay, and rainfall samples were collected over an even larger area.

The ultimate objective of a study such as this is the production of a conceptual model of the major systems of groundwater flow in the Rift Valley. These can broadly be classified as cold or ambient water systems, which are driven by topographic head gradients, and hot water systems, driven principally by head gradients resulting from the density differences between hot and cold fluids.

The cold water systems can be studied by standard hydrogeological techniques which involve the construction of piezometric maps from water level data (mainly derived from boreholes), and the assessment of the hydraulic properties of the aquifer (normally obtained from pumping tests). In the Rift Valley these techniques are restricted by the lack and poor quality of such data, but by making certain assumptions valuable insight can be obtained into directions and likely amounts of flow. In addition to the physical data, chemical and isotopic data are important in helping to identify possible recharge areas, mixing patterns and residence times of groundwaters, which in turn are used to correct and improve the physical model.

Geothermal systems are unlikely to be penetrated by boreholes (unless geothermal exploration boreholes have been drilled) and the geochemical investigation of the thermal fluids therefore assumes a greater importance. Indeed in the reconnaissance stage of exploration (before surface geophysical techniques are employed) geochemistry is by far the most valuable tool in determining the hydrodynamic nature of a geothermal system, providing information such as the nature of the geothermal fluid, temperatures at depth, mixing processes and likely areas of upflow.

By combining the model of the cold water systems (derived mainly from physical data) with that of the geothermal systems (deduced essentially from chemical data) the relationship between the two can be studied. This enables questions about the origin of the geothermal fluids, areas of recharge to and discharge from the geothermal fields, and availability of recharge to the exploited fields to be addressed.

The structure of the report reflects the above approach. The initial sections are concerned with the physical hydrogeology of the study area, and in the main these are concerned with ambient water flows. The section on geochemistry deals in detail with geothermal manifestations, as well as ambient water chemistry. The geothermal field at Olkaria and the geothermal manifestations at Magadi have warranted detailed investigations and accordingly are treated separately.

The concluding discussion is essentially a broad summary of the conclusions reached in the preceding sections of the report.

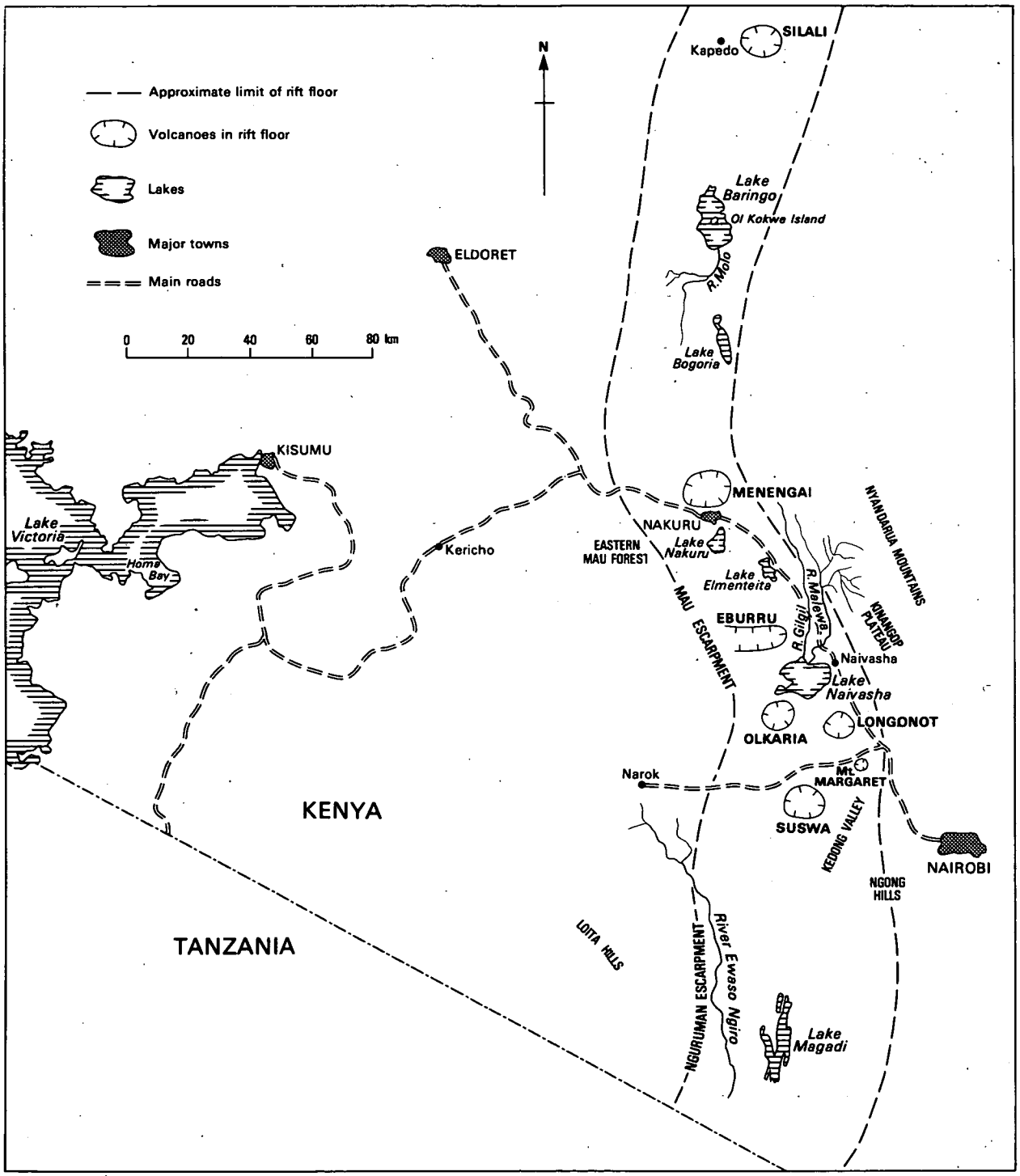

Figure 2.1 Location map

2 PHYSIOGRAPHY AND SURFACE HYDROLOGY

2.1 Nakuru - Longonot

The Rift Valley in the area between Lake Nakuru and Longonot volcano (Figures 2.1 and 4.1) is bounded by the Mau Escarpment in the west, rising to 3000 m, and the Nyandarua - Kikuyu Escarpment in the east with a maximum elevation of 3999 m. The central Rift is further bounded by relatively high fault scarps and intervening plateaux on either side, notably the Rongai Plain (1800 to 2000 m) and the Eburru Forest (2400 to 2670 m) in the west and the Bahati Escarpment (2100 to 2400 m) and the Kinangop Plateau (2100 m) in the east, (although the Kinangop Plateau is strictly speaking a shelf rather than a plateau). The Ol Bolossat Plain (2300 m) lies between the Nyandarua Mountains and the Bahati Escarpment and forms a northward extension of the Kinangop Plateau.

The floor of the Rift Valley culminates near Lake Naivasha (1880 m). To the north are Lakes Elmenteita (1780 m) and Nakuru (1760 m). All three lakes lie in basins of internal drainage. To the south of Lake Naivasha Longonot volcano rises to 2780 m and Menengai crater (2280 m) lies to the north of Lake Nakuru. A series of smaller volcanic hills further disrupts the valley floor between Olkaria (2434 m) south-west of Lake Naivasha, and Lake Elmenteita, either side of Eburru mountain. A prominent gorge, Ol Njorowa (Hell's Gate) runs south from Lake Naivasha separating Olkaria from the lower slopes of Longonot.

In terms of surface water hydrology the area containing Lakes Nakuru and Elmenteita can be considered separately from that occupied by Lake Naivasha.

2.1.1 Nakuru - Elmenteita Area

Lake Nakuru (which is separated from Lake Elmenteita by a low topographic divide) lies at the northern boundary of the study area, in a graben between Isirkon (2097 m) to the east and the Mau Escarpment to the west. Menengai rises to the north of the lake, and the high ground of the Mau and Eburru Forests lies to the south. The lake is alkaline and saline (sodium - bicarbonate type) as a result of evaporation and is recharged by rainfall, surface runoff and groundwater.

The rivers Njoro, Larmudiac, Makalia, and Nderit drain from the Mau Escarpment towards Lake Nakuru, but most of the flow is lost as groundwater recharge before the lake is reached. Of these rivers the Makalia and Njoro are normally perennial (McCann, 1972). The Ngosur (a permanent stream) and several minor streams flow from the Bahati uplands westwards towards Lake Nakuru, although none of them reaches the lake.

Lake Elmenteita is, like Lake Nakuru, recharged by direct precipitation, from shallow aquifers and by surface runoff. The Meroni, Mbaruk and Kariandusi streams (which flow from the Bahati Escarpment) reach the lake, but only after most of their discharge has been lost to shallow aquifers.

2.1.2 Naivasha Area

The Naivasha catchment is separated from the Nakuru - Elmenteita catchment mainly by the Eburru volcanic pile which is linked to the Mau Escarpment by a ridge at an altitude of around 2600 m. Between Eburru and the Bahati Escarpment the surface drainage divide runs via Gilgil along a culmination of the Rift floor at an altitude of approximately 2000 m.

South-west of the drainage divide the Gilgil and Malewa Rivers, both of which are perennial, provide much of the recharge to Lake Naivasha. The Gilgil River has its headwaters high in the Bahati Forest and drains parts of the eastern slopes of the Bahati Escarpment. These slopes also provide some of the tributaries of the much larger Malewa River. Most of the discharge of the Malewa River however, at least in its upper reaches, derives from the western slopes of the high Nyandarua Range from tributaries which initially flow north-west, and then turn south-west as they drain the Ol Bolossat Plain (a shallow asymmetrical graben lying to the east of the Bahati Escarpment). Further downstream the Malewa is joined by the Turasha River which is also perennial and drains the north Kinangop Plateau via deeply-incised tributaries.

On the west side of the Naivasha catchment the main river draining the Mau Escarpment is the Marmonet, which flows towards the lake but fails to reach it, instead recharging the alluvium of the Ndabibi Plain. Similarly none of the numerous seasonal streams which incise the Eburru Ridge reaches Lake Naivasha.

To the south of Lake Naivasha the surface water divide runs from the Mau Escarpment in the west, via Olkaria and Longonot to the Kinangop Plateau and finally to the Nyandarua Mountains. Surface drainage in this region (at least at the lower altitudes) is limited, only the River Karati providing perennial flow in its upper reaches.

2.2 Longonot - Magadi

The southern part of the Rift Valley is bounded in the west by the Nguruman and Mau escarpments. In the south-east a series of scarps eastwards from the Nkama Plain mark the boundary of the Rift, which is more clearly defined by the Kikuyu Escarpment at the latitude of Mt. Suswa. The Nguruman Escarpment descends from a height of 1950 m via the Kirikiti Platform at 1350 m to the Rift Valley floor at 900 m in the extreme west, from where the valley floor descends by a series of ridge and trough faulted escarpments to 590 m at Lake Magadi in the centre of the Rift. The Mau Escarpment reaches a height of 2375 m to the north-west of Suswa, and the Kikuyu Escarpment 2400 m to the east.

The Rift Valley floor is divided into many sub-parallel ridges and troughs trending approximately NNE, a physiographic expression of the recent grid faulting. The valley floor slopes southwards with a gradient of approximately 1:100 from Lake Naivasha to Lake Magadi and the surfaces of the fault blocks dip similarly gently southwards. At the latitude of Lake Magadi there are six main troughs: the Ewaso Ngiro Plain, the Embaash (Koordiya) plain, the Magadi central trough, the Olkeri Plain, the Koora Plain, and the Nkama (Kuenia) Plain.

The only perennial river in the Rift in this sector is the Ewaso Ngiro River, which has built out an extensive alluvial fan several kilometres onto the Ewaso Ngiro Plain. The river rises in the Ol Pusimoru Forest to the west of the Mau Escarpment and its tributaries drain the south-western slopes of the escarpment, from around the latitude of lake Naivasha southwards. The river initially flows south-east, then turns south, passing to the west of Lake Magadi and to the east of the Nguruman Escarpment, where it is joined by tributary streams draining the escarpment. The Ewaso Ngiro River finally discharges into the Engare Ngiro swamp at the north end of Lake Natron, to the south of the present project area.

All the troughs are bounded by fault escarpments and are generally alluvium-filled discrete basins of internal surface drainage. The Magadi trough at its southern, deepest, end is filled by the alkaline Lakes Magadi and Little Magadi. The Toroka River drains the Kajiado Escarpment in the east into the Nkama depression, and Olkeju Ngiro drains the Koora trough via Oltepesi and the northern slopes of Olorgasailie. Further north the Ewaso Kedong drains from the Kikuyu Escarpment to the east of Suswa volcano.

There is no surface drainage to, nor any outlet from, Lake Magadi. A number of springs and seepages which feed the lake occur around its margin, some of which have a significantly elevated temperature (maximum 86°C at the northern extremity of Little Magadi). As a result of extreme evaporation Lake Magadi has developed some of the most concentrated brines to be found in the alkaline saline lakes of the Rift Valley, and a layer of Trona (crystalline carbonates of sodium) covers the surface.

A number of isolated volcanic centres are located in this area of the Rift, notably Ol Doinyo Nyoke (1169 m), Olorgasailie (1760 m), Ol Esayeti (1950 m) and Suswa (2356 m). Of these the youngest and least eroded are Ol Doinyo Nyoke in the south and Suswa in the north.

2.3 Rainfall

Rainfall in the study area is concentrated into the two rainy seasons of October-November and March-May. Within the Rift mean annual rainfall is low, ranging from 430 mm at Magadi through 627 mm at Naivasha to 981 mm at Nakuru, with most of the region experiencing an average of about 750 mm (Met. Dept. data 1931-1980). The average maximum daily temperature at Magadi is 35°C (minimum 23°C), while at Naivasha, near the culmination of the Rift, it is 25°C (minimum 9°C).

Relative humidity is low throughout the Rift (less than 75% at Naivasha, less than 60% at Magadi) and potential evaporation (1600 to 1800 mm) greatly exceeds annual rainfall. Monthly averaged potential evaporation at Naivasha exceeds rainfall by a factor of 2 to 8 for every month except April when potential evaporation still exceeds rainfall except in the wettest of years. The same figures are not recorded for Magadi where the excess of evaporation over rainfall must be considerably greater. However individual storms in the two rainy seasons can be extremely heavy and in areas of permeable material some recharge is probable.

On the Rift escarpments rainfall values are much higher ranging up to around 1250 to 1500 mm annually (McCann 1974). Also evapotranspiration rates at these altitudes are lower at about 1400 mm per year, and much less during the rainy seasons.

2.4 Geothermal Manifestations

Geothermal manifestations in the area between Lake Nakuru and Lake Magadi consist of hot and altered ground, fumaroles and hot springs. The most active thermal areas are mainly those associated with the volcanic centres at Eburru, Olkaria, Longonot and Suswa. In these areas fumaroles - often lying on fault lines - are common, although thermal springs are rare. This is in part because the volcanic centres occupy high ground and are therefore in hydrological recharge areas. Hot springs associated with these areas are found (though infrequently) in topographically lower regions such as to the north of Eburru and in Njorowa Gorge to the south-east of Olkaria. The

natural heat discharge from Olkaria has been estimated as 376 MW, and from Eburru as 130 MW (Glover, 1972).

The only important thermal area which is not associated with a volcanic centre (and where there are no fumaroles) is at Lake Magadi. Here the hot and warm springs surrounding the Lake discharge an estimated 250 MW (Crane, 1981). Elsewhere thermal springs are infrequent and usually occur near the Rift margins. These springs are often associated with faulting and do not reach elevated temperatures.

3 GEOLOGY

In the study area the Rift Valley is mainly composed of a succession of late Tertiary and Quaternary volcanics with, in some areas, intervening lacustrine beds and alluvium principally of reworked volcanic debris. Pre-Cambrian Basement rocks are postulated to underlie this volcano-sedimentary succession at or below sea-level. The topography of the basement is uncertain and is the subject of continuing geophysical research.

The Rift is defined by the major Pliocene boundary faults of the Nguruman and Mau Escarpments in the west, and the Kikuyu, Nyandarua and Bahati Escarpments in the east. In the south-east the boundary of the Rift is less well defined, there being a succession of smaller escarpment faults with intermediate faults between them. The main fault scarps range from 300 to 1600 m in height, are en echelon in plan, and form a complex graben 60 to 70 km wide, reducing to 17 to 35 km by fault offsets and steps. The volcanic succession on the flanks of the Rift Valley is over 2000 m thick in places, and the succession in the Rift floor is considered to be significantly thicker than this, perhaps reaching 3000 to 4000 m (Baker, Mohr and Williams, 1972).

A dense system of Middle and Upper Pleistocene grid faulting within the Rift dissects the graben floor and step-fault platforms. These faults are sub-parallel to the main Rift faults, reach densities of two or three per kilometre and normally have throws of less than 150 m (Baker, Mohr and Williams, 1972). The Rift floor faults are locally obscured by late Quaternary volcanic piles, such as Longonot and Suswa, and by lower and middle Pleistocene sediments around Magadi and between Naivasha and Nakuru.

The oldest rocks found in the study area are Archean Basement gneisses which outcrop near to the summit of the Nguruman Escarpment in the south-west (Baker, 1958). These are overlain by Pliocene basalts, which also occur beneath a cover of younger volcanics along parts of the rift floor. Several volcanoes of Pliocene age appeared along the sides and floor of the developing Rift and examples in the project area are; the Nyandarua (Aberdare) Range, composed of basalts, phonolites, trachytes and mugearites, and the Olorgesailie, Ol Esayeti and Ol Esakut volcanoes to the south-west of Nairobi which are composed of basalts, trachytes, phonolites and nephelinites. The Ngong volcano, also to to south-west of Nairobi contains melanephelinites, basanites and phonolites (Baker, Williams, Miller and Fitch, 1971).

Plio-Pleistocene trachyte lavas and ignimbrites occupy nearly all the floor of the central and southern Rift in Kenya and occur in places on the marginal plateaux. The lower part of the group consists of trachytic tuffs with prominent ignimbrite units which are best exposed on the Bahati and Kinangop Escarpments on the eastern side of the Rift (Thompson and Dodson, 1963). Further east ash flows of this age are found on the flanks of the Nyandarua Range and elsewhere.

West of the Rift Plio-Pleistocene ignimbrites form most of the Mau Range and extend northward (Baker, Williams, Miller and Fitch, 1971). On the Rift floor trachyte and some basalt occur within the ignimbrite succession.

In the Magadi area the extensive plateau trachytes represent the upper part of the group (Baker, 1958), and these extend onto the eastern side of the Rift to form the Limuru trachytes west of Nairobi. On the Kikuyu Escarpment and in the Kijabe area trachytic flows and pyroclastics are interbedded (Thompson, 1964).

A late Quaternary phase of mainly trachyte caldera eruptions occurred along the floor of the Rift Valley and is represented in the study area by the large central volcanoes of Suswa and Longonot, which date from the middle Pleistocene and comprise phonolite, alkaline trachyte and rhyolite lavas and extensive pyroclastics. Also included in this phase of activity are the basaltic cinder cones, rubbly lavas and tuff rings of the Elmenteita region, the Eburru volcanic pile (heavily mantled with pyroclastics but with phonolite and trachyte reported [Thompson and Dodson, 1963]) and the highly comenditic lavas of the Olkaria area.

Sedimentary deposits are mainly found in the central southern and northern parts of the project area. In the south a thin layer of lake beds (the Oloronga beds), mainly reworked volcanic debris with thicknesses of up to 15 m, overlie the plateau trachytes and preceded the extensive grid faulting which determines the present day topography. Succeeding Middle Pleistocene sediments include the Olorgasailie lake beds of diatomaceous clays and the fine silts and clays of the Ewaso Ngiro basin, sediments of the Kedong Valley (predominantly clays and fine sandstones with poorly sorted conglomerate), and the silicified clays of the earliest Magadi lake. Subsequent minor faulting disturbed these sediments and was followed in the Magadi area by extensive lacustrine deposition (the High Magadi beds) to a level 12 m above the present lake surface, and by further sedimentation in the Ewaso Ngiro basin (Baker, 1958). At Magadi deposition of the Evaporite Series is thought to mark the onset of alkaline spring activity, which continues to the present day.

In the northern part of the project area Lower Middle Pleistocene sediments (mainly subaqueously deposited pyroclastics) have been found in the Kinangop scarp and in the Njorowa Gorge (Thompson and Dodson, 1963). There are also diatomaceous sediments of Upper Middle Pleistocene age east of Lake Elmenteita. However the most widespread sediments were deposited during the Gamblian Pluvial period towards the end of the Pleistocene and cover much of the Rift floor between Lake Naivasha and the northern boundary of the project area.

During this period relatively stable conditions existed in the area and extensive lacustrine deposits were laid down and subsequently partly eroded. Three lake levels have been recorded and it was only during the first maximum of the Gamblian Pluvial that the lake occupying the Naivasha basin joined that occupying the Nakuru basin , when the respective lake levels were 122 m and 220 m higher than at present. The Gamblian lake deposits are composed of volcanic ash, silts, clays and a few bands of diatomite. They are tectonically relatively undisturbed and have a maximum recorded thickness of 33 m (Thompson and Dodson, 1963).

4 HYDROGEOLOGY

4.1 Introduction

4.1.1 Scope of the Study

In general the permeability of rocks in the Rift Valley is low, although there is considerable local variation. Aquifers are normally found in fractured volcanics, or along the weathered contacts between different lithological units. These aquifers are often confined or semi-confined and storage coefficients are likely to be low. In addition aquifers with relatively high permeabilities are found in sediments covering parts of the Rift floor (particularly around Lake Naivasha). Such aquifers are often unconfined and will have relatively high specific yields. Tectonic movements of the Rift Valley have important effects on aquifer properties, both on a small scale by creating the local fracture systems which comprise many aquifers, and on the large scale by forming regional hydraulic barriers or shatter zones of enhanced permeability.

Knowledge of the hydrogeology of the Rift Valley varies considerably over the project area (between Lake Nakuru and Lake Magadi) and depends primarily on the distribution of water supply boreholes. Around Lake Naivasha for example over 100 boreholes have been drilled since the 1930's, whereas less than 20 boreholes have been drilled in the Rift floor between Longonot volcano and Lake Magadi - a distance of nearly 100 km.

Another limitation is that boreholes can strictly only provide information concerning groundwater conditions within the drilled depth of the borehole, and in the case of the Rift Valley boreholes this usually implies depths of less than 250 m (an important exception is the Olkaria geothermal field where borehole depths exceed 1 km). This means that to a large extent the hydrogeology of the Rift Valley at depths relevant to the recharge of geothermal fields (several kilometres) has to be inferred from information such as piezometric and chemical data. In particular the degree of connection between aquifers intercepted by boreholes on the Rift sides, and those at depth beneath the Rift is poorly known

In this study borehole data have been used in two main ways. Firstly they have been used to construct a piezometric map of the Rift Valley - vital in attempting to examine regional flow systems. Secondly an attempt has been made to identify variations in aquifer properties with rock type, and with depth. After examining the effects of structure, a semi-quantitative assessment of the regional flows which may contribute to the deep geothermal systems has been made.

4.1.2 Previous Work

General accounts of the hydrogeology of the project area are given in the reports of the Geological Survey of Kenya. Particularly relevant reports are; No. 78 covering the area from Gilgil to beyond the northern boundary of the area (McCall, 1967), No. 55 covering the Longonot-Gilgil area (Thompson and Dodson, 1963), No. 43 covering the Kijabe and Kinangop areas (Thompson, 1964), and No. 42 covering the Magadi area (Baker, 1958). In addition Ministry of Works Technical Report No. 3 discusses groundwater conditions in the Nakuru area (McCall, 1957).

Hydrogeological reports with specific reference to geothermal energy studies in the Rift Valley in areas north of Longonot were prepared as part of a

previous UN study (McCann, 1972 and 1974), and similar investigations have recently been completed to the north of the present project area (Geotermica Italiana, 1987). Several papers and reports have been published which are relevant to the hydrogeology of the Rift Valley in the project area, and these are mentioned in the appropriate sections of this report.

4.2 Data Collection and Data Base Construction

The geological and topographic variations of the Rift Valley both have important consequences for water occurrence and movement. Water flows in the direction of decreasing head, and in general this implies flow down a topographic gradient. Therefore given the overall surface geometry of the Rift in the project area as a wide trough, sloping axially to the north and south away from a culmination at Naivasha, groundwater may be expected to flow from the sides of the Rift towards the centre and axially towards the north and south, away from Naivasha. However the geological complexity of the area, both in terms of lithology and structure, influences this simple intuitive picture substantially, and in order to attempt any quantitative assessments about groundwater location and flow, data concerning head gradients, permeabilities, porosities and flow boundaries must be obtained.

In the Rift such data can only be obtained from boreholes (and from infrequent springs) and must be collected over the area which influences the groundwater systems. In practice this means examining an area bounded by the groundwater divides of the Nguruman and Mau Escarpments to the west, and the Nyandarua, Kikuyu and minor escarpments to the east.

The resulting survey of borehole data covers 32 sheets of the 1:50,000 scale topographic map series, and extends from Lake Nakuru in the north to Lake Magadi in the south, and from Njoro in the west to the outskirts of Nairobi in the east.

All borehole data were obtained from the Ministry of water development (MWD) in Nairobi. At MWD borehole positions and numbers are marked on 1:50,000 scale maps. Details of lithology, well construction, water strikes and levels, and pumping test data are held on file.

Data for 596 boreholes were abstracted from MWD records. The density of borehole data varies considerably; most boreholes are in the north and east of the project area, with very few in the south and west. Data for most boreholes in the Nakuru-Magadi region of the Rift were abstracted; the exceptions were generally where borehole density was high, when a representative sample was taken.

Data were initially copied from the files and were subsequently entered into a computer data base at Wallingford, listings of which are given in Appendices 1 to 5.

Appendix 1 shows basic borehole data. The boreholes are listed in order of borehole number (for the majority of boreholes which have a "C" prefix this is also, in general, a chronological listing). The grid reference and borehole altitude were obtained by reference to the borehole position marked on the relevant 1:50,000 scale map held at MWD (this information is not normally given in the MWD files). Where the borehole was dry the rest water altitude is shown as a maximum value.

Appendix 2 lists borehole completion data such as depth, diameter and the depth to which plain casing extends below ground level. Aquifer lithology, where known,is taken from the driller's log.

Appendix 3 gives water strikes and water levels. Normally one water strike and a final rest water level were recorded, but multiple strikes and levels are not uncommon.

Appendix 4 shows borehole productivity data. Most boreholes which struck water were pumped and a borehole yield noted. Often (particularly recently) data concerning discharge rate and drawdown are recorded in the MWD files, enabling specific capacity to be calculated, and values are given in the Appendix. Also included are notes concerning features of borehole productivity such as high temperature, production of steam, or whether the borehole was dry.

Appendix 5 is included as an aid to locating particular boreholes. Boreholes are listed in order of increasing values of Grid Easting, and for a particular value of Easting are arranged in order of increasing values of Northing.

4.3 Water Level Data and the Piezometric Map

4.3.1 Data Reliability and Map Construction

A problem with collecting hydrogeological data in the Rift Valley is that so few wells have access for water level measurements, either because a piston pump is installed or because the borehole is blocked. Therefore water levels are taken from borehole records. These data refer to the levels at the time of well completion, which is a period spanning over 50 years for boreholes in the project area. This introduces errors in defining piezometric contours, because of the seasonal and longer term variations in groundwater levels.

The scale of such errors may be found by comparing borehole water levels at the time of completion with levels measured recently. Table 4.1 shows this for boreholes of various ages in the project area. The recent values were measured as part of a thermal gradient survey carried out by G. Batticci as part of the recent UN Geothermal Project (G. Batticci, pers. comm.).

Table 4.1 indicates differences in water level between original and recently-measured levels ranging from zero to 107 and 124 m. However the higher figures are unreliable, the first (borehole C2388) because the 1955 level does not take into account a perched water level (given in brackets), and the second (borehole C1726) because both the original and recent water levels are uncertain. The remaining twelve values range between zero and 39 m with all but one value below 20 m. While these differences are not insignificant, such temporal variations are small when compared with the large spatial variation in surface topography and water table geometry encountered in the Rift, and can therefore be ignored when groundwater movement on the scale of the Rift is considered. They cannot however be ignored if local small-scale effects are examined.

Other errors are introduced into piezometric map construction by using borehole rest water levels which may represent a local averaging of several piezometric surfaces where different aquifers are intersected by a borehole. Again the importance of such errors depends on the scale considered.

The scale chosen for the piezometric map of the project area (Figure 4.1) was

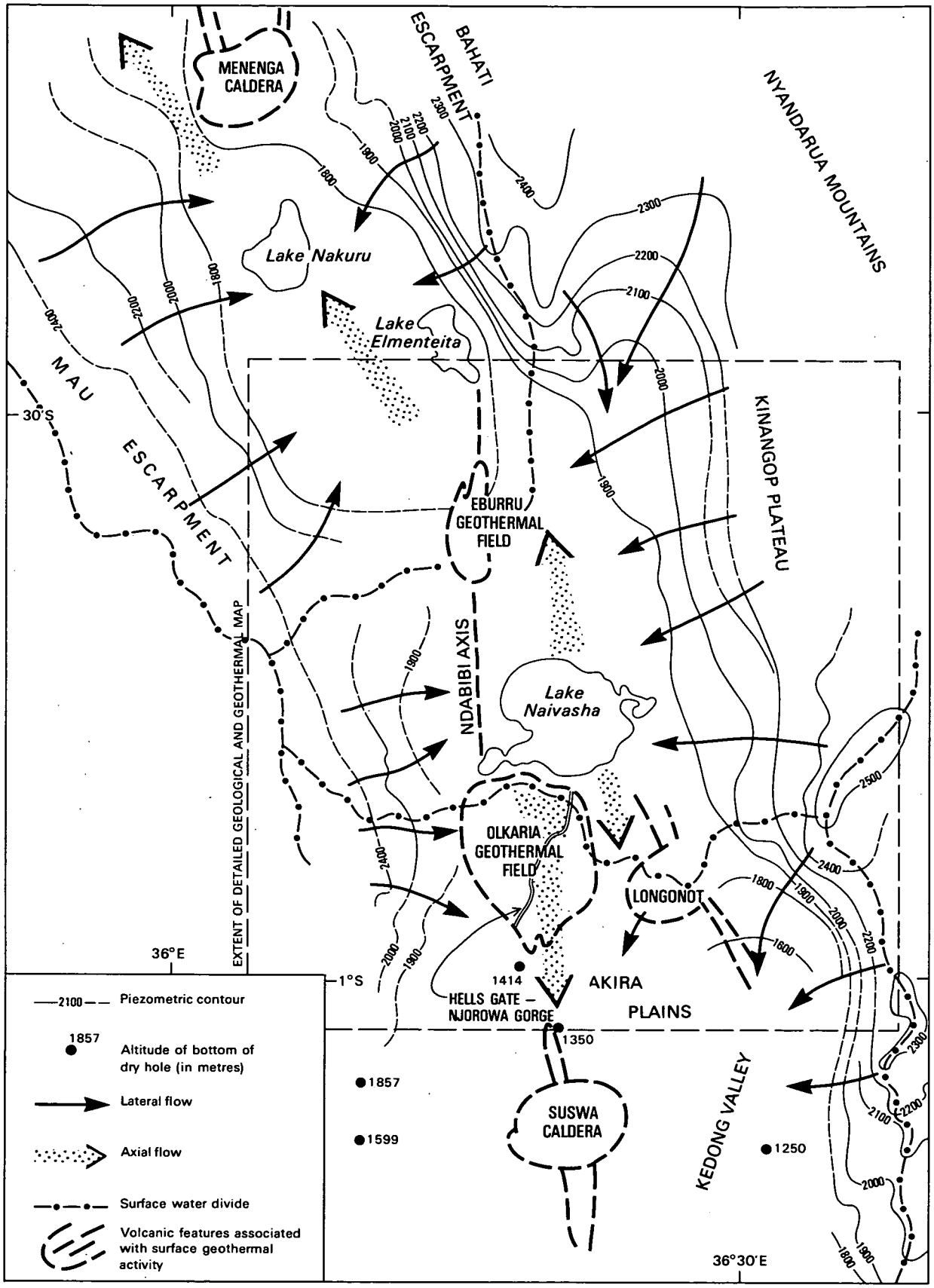

Figure 4.1 Piezometric Map of the Project Area.

Table 4.1 Borehole water level comparisons.

Well No.	ORIGINAL WATER LEVEL		RECENT WATER LEVEL*		
	Borehole completion date	Borehole rest water level (m)	Date	Borehole rest water level (m)	Water level change (recent-original) (m)
C1391	31/3/51	111.0	29/1/86	95	- 15.0
C1726	31/3/51	?259.2	26/9/85	?135	?-124.2
C2109	16/12/53	42.0	11/9/85	43.9	1.9
C2358	25/3/55	265.0	12/10/85	225.6	- 39.4
C2388	4/6/55	?241.7	10/9/85	134.5	?-107.2
C2813	14/4/58	41.5	13/9/85	24.4	- 17.1
C3397	23/8/66	108.0	1/2/86	107.7	- 0.3
C3677	25/2/68	15.2	13/2/86	19.7	4.5
C4143	-/-/76	172.0	25/3/86	173.0	1.0
C6271	-/-/84	34.6	1/2/86	34.6	0
C6056	29/1/85	13.8	31/1/86	14	0.2
C6290		197	20/9/85	197	0
C6300	9/3/83	132.9	25/9/85	133.4	0.5
M001	-/-/85?	155	14/2/86	155	0

* Recent water levels measured by G Battici, UN Geothermal Project.

1:250,000 with a contour interval of 100 m (with variations depending on the data quality). At this scale the regional flow systems which may contribute to geothermal recharge can be well represented, while the effects of errors such as those discussed above can be minimised. Piezometric contours have been drawn using the borehole water level data, and spring data obtained from the 1:50,000 and 1:250,000 topographic map series. Where such data are scarce local topographic variations have been used as a guide to contour geometry. Surface water divides have been drawn with reference to the topographic maps.

4.3.2 Analysis of the Piezometric Map

In general the map shows the features expected of a valley/interfluve system, with groundwater flowing from elevated recharge areas to low-lying discharge areas, the flow occurring both laterally and longitudinally according to the Rift geometry. In the following discussion the different sub-catchments are considered separately.

Nakuru-Elmenteita

Lakes Nakuru and Elmenteita lie a little to the north-west of the culmination of the Rift floor (between Naivasha and Gilgil). Groundwater gradients and therefore flows in this area are generally directed towards the lakes, with some flow away from the area to the north-west. In more detail, groundwater flows north-east from the Mau Escarpment, south-west from the Bahati Escarpment and northwards from Eburru. It is also probable that there is some southerly flow from Menengai towards Lake Nakuru. However at depth it is likely that flow occurs to the north-west away from the Nakuru-Elmenteita catchment towards the lower-lying area around Lake Bogoria.

Naivasha

This is the most important catchment in the project area in terms of present and near-future geothermal development. It is also the most complex hydrogeologically, because while it is lower than the Rift escarpments it is at a culmination of the Rift floor.

Flows towards Lake Naivasha from the Mau Escarpment and the Kinangop Plateau are unambiguous and some of the groundwater from the western side of the Rift must eventually form part of the discharges at Olkaria and Eburru. However the longitudinal flows in this area are more difficult to assess.

To the north of Naivasha the surface water divide runs approximately east-west through Eburru, and then north through Gilgil. However there is no evidence that a groundwater divide follows this route, because the piezometric surface has an uninterrupted fall from Lake Naivasha, around the east side of Eburru, towards Lake Elmenteita, indicating flow in this direction.

The configuration of groundwater contours around Eburru is uncertain because boreholes drilled at Eburru have encountered steam. It is probable that while shallow groundwaters on the south side of Eburru move locally towards Naivasha, deeper flows are substantially northwards.

Around Lake Naivasha itself the groundwater level is between approximately 1880 and 1890 m, i.e. roughly that of the lake itself. East and west of the lake the groundwater contours rise, indicating flow towards the lake, while to the south they remain at about the same level as far as the latitude of

the Longonot/Olkaria complex.

South of this region the piezometric surface drops by several hundreds of metres. Indeed its position is unknown because the few boreholes drilled between Longonot and Suswa have all proved to be dry, or have produced steam. The data do indicate a fall of at least 450 m in piezometric level over a distance of around 10 km (i.e. a gradient of at least 0.05 m/m). At depth a north-south pressure gradient of 11 bars/km has been reported in the Olkaria geothermal field (Bodvarsson and others, 1987) which corresponds to a freshwater head gradient of 0.1 m/m.

Groundwater certainly flows away from Lake Naivasha because the lake water is fresh, even though the lake has no outlet and lies in an area of high evaporation. The position of the lake, at a culmination of the Rift floor, suggests flow both to the north and to the south (i.e. a groundwater divide runs east-west in the vicinity of the lake). As discussed above, northerly flow may occur both via Gilgil and under Eburru (but see Section 5.3). Southerly flow must also occur, following the hydraulic gradient, but the high values of the gradient suggest that values of permeability in the Olkaria-Longonot region are low. Values for subsurface discharge in the Naivasha area are discussed in Section 4.6.

Longonot-Magadi

A surface water divide runs east-west through Olkaria and Longonot but appears to have little effect on the southerly flow of groundwater from Naivasha. Between Longonot and Lake Magadi groundwater flows from the sides of the Rift towards the centre, and southwards along the Rift towards Magadi. The unknown, but very deep position of the piezometric surface in the Suswa area suggests that flow from the sides of the Rift in this area is limited, and it is very likely that the major Rift faults act as low permeability barriers to flow across the Rift. For example borehole C4971 in the Rift to the east of Suswa encountered no water at a depth of 300 m, corresponding to a maximum water level altitude of 1250 m, whereas less than 10 km to the east, on the side of the Rift, the piezometric surface is between 100 m and 200 m below the surface, at an altitude of 1900-2000 m.

Between Suswa and Lake Magadi water level data are very sparse, but the limited evidence indicates the expected flow down the topographic gradient, i.e. southwards from Suswa, south-east from Narok, south-west from the Ngong area and east from the Nguruman Escarpment, with all flows eventually coinciding in the topographic low around Lake Magadi. From hydraulic evidence there is no way of distinguishing which of these flows contributes the most to the thermal springs at Lake Magadi, but the nearby Nguruman Escarpment would seem to be a likely source because of the substantial hydraulic head gradient which it could provide.

4.4 Aquifer Properties

4.4.1 Specific Capacity, Transmissivity and Hydraulic Conductivity

Very little information is available concerning the variation in aquifer properties between the various rock types of the Rift Valley. The main reason for this is that the standard hydrogeological field test to determine aquifer transmissivity - a carefully monitored pumping test with observation wells - has not been undertaken when water wells have been drilled. (The Olkaria wells form a special case and will be considered later). In general, after water wells have been drilled they have been test-pumped for a few hours in

order to obtain a well yield. In some cases recovery data have been recorded, but for the majority of wells only a yield, or a yield and a pumped water level at equilibrium have been noted. (While theoretically equilibrium conditions are never attained in confined conditions,in practical terms drawdowns often increase at very low rates after a short period of pumping). Where yield and equilibrium drawdown data are available then specific capacities (yield/drawdown) can be calculated, and these are given in Appendix 4. Where drawdowns were too small to be registered a nominal maximum value of 0.2 m has been used (it is assumed that drawdowns greater than this would have been noticed). The calculated values of specific capacities in these cases are therefore probably minima.

The specific capacity of a well depends primarily on the transmissivity of the aquifer. Other factors which influence specific capacity are well losses and partial penetration, but in general, variations in specific capacity are paralleled by variations in transmissivity. In certain circumstances, namely if the pumped well has no well losses and fully penetrates an extensive confined aquifer which is homogeneous and isotropic then transmissivity can be derived from specific capacity by using the Thiem equation (Thiem, 1906) with the extra assumption that the radius of influence of the well is 300 m. (This value need not be exact because it appears as a logarithm in the equation).

Thus

$$T = \frac{43.2Q}{\pi s} \ln[300/r_w] \qquad (1)$$

Where T = Transmissivity (m^2/d)
Q = Discharge rate (l/s)
s = Drawdown at equilibrium (m)
r_w = Well radius (m)

Equation 1 has been applied to all cases where the specific capacity and the well radius are known. In a few cases the well radius is unknown and for these the Logan approximation has been used (Logan, 1964).

$$T = 105.4Q/s \qquad (2)$$

where all symbols have the same meaning as before

Naturally the strict validity of equation 1 is questionable for many if not most of the boreholes for which specific capacity data are available (and this is true to an even greater extent for equation 2). While most of the boreholes are at least partially confined (water strikes and rest water levels often differ greatly), factors such as partial penetration and anisotropy are likely to be common. Some idea of the validity of the equation may be obtained by comparing the predicted variation of transmissivity with specific capacity with values derived from carefully monitored (albeit single well) pumping tests. Figure 4.2, using data from McCann (1974) indicates that the correlation is, in general, good.

Transmissivity values may be converted to values of hydraulic conductivity if the thickness of the producing interval is known. An estimate of this thickness may be obtained by assuming that it corresponds to the distance between the main water strike and the bottom of the borehole. This estimate

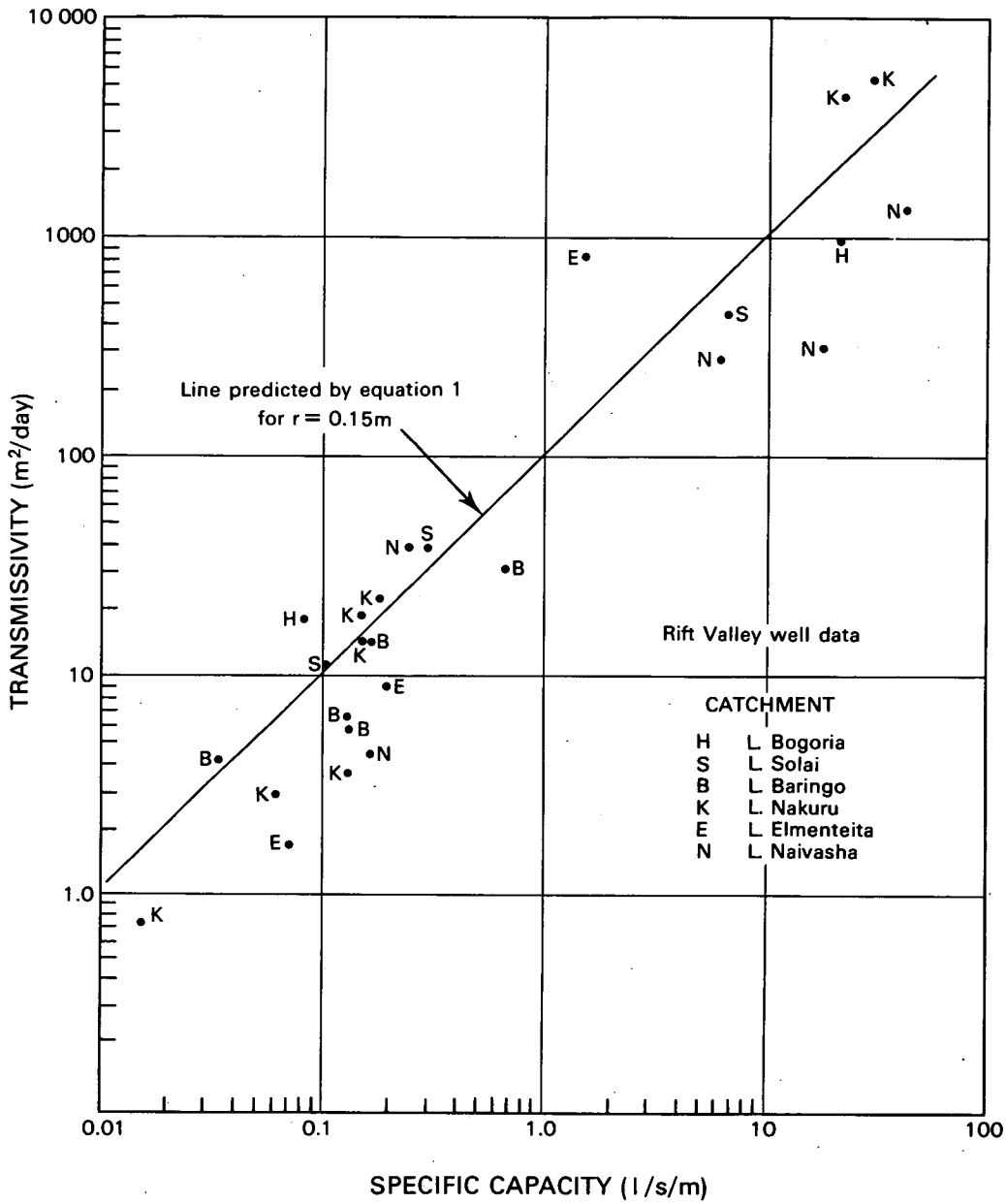

Figure 4.2 Variation of Transmissivity with Specific Capacity.

of aquifer thickness will tend to be an over-estimate, because it takes no account of the non-producing intervals within the aquifer, and therefore it will tend to lead to an under-estimate of hydraulic conductivity.

Values of estimated transmissivity and hydraulic conductivity are given in Appendix 6. It must be stressed that these values - particularly the hydraulic conductivities - should be regarded as semi-quantitative only, because of the assumptions on which they are based. They are useful because they enable the hydraulic properties of one area to be compared to another, providing an insight into the relative merits of different rock types as aquifers.

4.4.2 Variations in Aquifer Properties over the Rift

Introduction

Borehole data taken from areas of the Rift which can be represented by particular rock types have been examined using the search facility of the data base and the results are detailed below.

The Rift Floor in the Naivasha-Nakuru Area

The sediments of the Naivasha-Nakuru region are penetrated by numerous wells which provide water to the various towns and settlements in the region. The relatively large amount of data available therefore enables the hydrogeological properties of the Lake deposits to be examined in a series of small areas.

Lake Naivasha Area

Details of 100 boreholes around Lake Naivasha have been used in the data base. These penetrate Gamblian sediments and underlying Middle Pleistocene volcanics and sediments. Boreholes within an area bounded by Eastings 1900 and 2150 and between Northings 99050 and 99300 are considered, and this area is further subdivided into four quadrants termed NW Naivasha, NE Naivasha, SW Naivasha, and SE Naivasha by Easting 2050 and Northing 99150.

N.W Naivasha

This area extends from the west bank of the Gilgil River around the lower slopes of Eburru to the Ndabibi Plain and the western shore of Lake Naivasha to a point approximately 1 km north of Crater Lake. Details of 26 boreholes are held on the data base, of which the majority lie within 5 km of the lake shore. Borehole depths range between 10 m (C2356) and 213 m (C4499) and drilling logs indicate that aquifers are composed predominantly of fractured lavas and pyroclastics.

The average values of yield, specific capacity, estimated transmissivity and estimated permeability for this area are given in Table 4.2. While there is no universally accepted method of averaging permeability data many workers prefer the geometric mean where aquifer permeability varies laterally (Warren and Price, 1961; Bennion and Griffiths, 1966) and this mean has therefore been used for specific capacity, estimated transmissivity and estimated permeability data, with the arithmetic average shown in brackets. In the following discussion "mean" refers to the geometric mean and "average" refers to the arithmetic mean.

The data show this region to have good aquifer properties. Only one well in

Table 4.2 Average aquifer characteristics of selected areas and lithologies from borehole data. (Figures in brackets are arithmetic means)

Area	Lithology	Arithmetic mean borehole yield l/s	Geometric mean specific capacity l/s/m	Geometric mean estimated transmissivity m^2/d	Geometric mean estimated permeability m/d	No. dry boreholes	Total No. boreholes
NE Naivasha	Sediments + volcanics	9.3	2.8(11.6)	307(1170)	12(33)	0	35
SE Naivasha	"	4.4	4.6(29.2)	502(3082)	20(114)	0	22
SW Naivasha	"	5.4	2.7(8.7)	297(940)	63(196)	0	17
NW Naivasha	"	6.4	14.9(52.6)	1601(5308)	148(818)	0	26
Naivasha-Elmenteita	"	2.6	0.7(1.3)	78(143)	1.4(3.9)	1	12
Elmenteita-Nakuru	"	1.9	0.3(2.4)	32(261)	2(7)	2	31
Bahati Escarpment	Tuffs	3.4	0.1(0.4)	14(47)	1.2(3.7)	1	25
Kinangop Plateau	"	1.8	0.2(0.9)	14(106)	0.8(5)	5	32
S Kinangop	Pyroclastics	1.9	0.03(0.04)	4(5)	0.1(0.2)	3	11
E Suswa Rift Escarpment	Trachyte	2.1	0.2(2.6)	20(325)	1.1(35)	4	48
Mau Escarpment	Pyroclastics	1.3	0.2(1.6)	22(174)	1(10)	5	23
Mau Forest (W Nakuru)	"	1.7	0.2(1.1)	20(119)	1.1(22)	4	43

the area was found to be dry - C4499, which is not included in the averaging procedure - and the average yield is 6 l/s. The mean specific capacity of 14.9 l/s/m is the highest of any region examined in the study area and this is reflected in the high values for estimated transmissivity and hydraulic conductivity.

N.E Naivasha

This area stretches from the right bank of the Gilgil River around the north-eastern shore of Lake Naivasha to Crescent Island, and includes Naivasha Township, where most of the boreholes are situated. Thirty-five borehole records in the area were examined, ranging in depth from 26 m (C2117) to 128 m (C4155). Drillers'logs commonly show the aquifer as consisting of 'sand and gravel' (reworked volcanics) or 'lake sediments'with a few references to pyroclastics. None of the boreholes are dry and productivities are generally good with yields averaging 9 l/s and specific capacities averaging 3 l/s/m (Table 4.2). The estimated mean transmissivities and hydraulic conductivities are less than in the N.W Naivasha area, but are nevertheless high when compared with other areas of the Rift. The permeability estimate for this area of 12 m/d is of the order which would be expected for clean sands (Freeze and Cherry, 1979).

S.E Naivasha and S.W Naivasha

The S.E Naivasha area extends from Crescent Island around the S.E shore of Lake Naivasha between the lake shore and the lower slopes of Longonot to the southernmost point of the lake. The S.W Naivasha area lies to the west and includes the Kongoni settlement, part of the Ndabibi plain and Crater Lake. Details of 22 boreholes in the S.E Naivasha area and 17 boreholes in the S.W Naivasha area are included in the data base, with most of the boreholes clustered around the lake shore. Borehole depths in the S.E area range from 25 m (C4989) to 183 m (C1279), and in the S.W area from 31 m (C2636) to 152 m (C2863). In both areas boreholes penetrate lake sediments and volcanics. Average borehole yields for both areas are similar at around 5 l/s, and slightly lower than those for the N.W and N.E Naivasha areas and there are no dry wells. There is some evidence that specific yields and transmissivities are higher in the S.E area than in the S.W (Table 4.2) but the data are too few to permit further interpretation.

Boreholes around Lake Naivasha are on average the most productive in the project area - a fact noted by Thompson and Dodson (1963) who suggested that the cause was the shallow water table and the use of more efficient pumps in these boreholes. That this is not the case is shown by the high values of specific capacity (a factor independent of rest water level or pump efficiency) which are found in the Naivasha area (Table 4.2). It is likely however that the proximity of a recharge boundary in the form of the lake accounts to some extent for the high specific capacities, but only for those wells in the immediate vicinity of the lake, because production tests normally last for less than one day. In the N.W Naivasha area, for example, which is characterised by the highest values of specific capacity, many of the boreholes are close to the lake and may therefore be affected by a recharge boundary. However boreholes at some distance from the lake also have high specific capacities (e.g. boreholes C2522, C2706, C2813 and C4499 which has the highest value in the area) and it is concluded that the permeability of the Lake Naivasha area is higher than that of the rest of the Rift in the project area.

Naivasha-Elmenteita

Twelve boreholes have been drilled in the Rift Valley floor between Naivasha township and Elmenteita, in an area defined by Eastings 1950-2130 and Northings 99300-99470. Borehole depths vary between 61 m (C3929) and 264 m (C2388) with aquifers mainly occurring in sand and silt deposits. (One borehole near to the eastern margin of the Rift (C2076), to the north of Gilgil encountered water at 65.5°C). Table 4.2 shows that the average yield of these boreholes, at around 2.5 l/s, is approximately half of boreholes further south, and specific capacities are greatly reduced - although only four values can be determined. It is likely that the lower permeability is due to the smaller grain size of these deposits.

Elmenteita-Nakuru

Thirty-one boreholes have been drilled in the floor of the Rift Valley between Lake Nakuru and Lake Elmenteita (in an area defined by Eastings 1700-1950 and Northings 99350-99600). Water bearing rocks in this region include surface sediments, pyroclastics and lavas. Borehole yields are similar to those of the Naivasha-Elmenteita region (c. 2 l/s) and specific capacities are also comparable, of the order of 1 l/s/m. Two dry wells were drilled in the area, corresponding to a failure rate of 7%.

Rift Margins

Bahati Escarpment

Data from 25 boreholes (one of which was dry) drilled in the Pliocene Tuffs forming the Bahati Escarpment, between Eastings 1854-2049 and Northings 99600-99800, shows them to be less permeable than the Rift Floor deposits. The mean specific capacity is only 0.1 l/s/m (Table 4.2) and estimated mean transmissivities and permeabilities are about half those determined for the Rift Valley floor to the west.(Borehole yields are similar to those in the Rift Valley Floor between Lakes Nakuru and Elmenteita, but the comparison is misleading because larger drawdowns are incurred on the escarpment). Limited data suggest that aquifers are often found where the tuffs are fractured and weathered.

Kinangop Plateau and Kikuyu Escarpment

Details have been obtained of 32 boreholes drilled in the Kinangop Tuffs forming the Kinangop Plateau, in an area defined by Eastings 2175-2400 and Northings 99150-99300. Table 4.2 indicates that the aquifer properties of these tuffs are similar to those of the Bahati Tuffs to the north, with low values of specific capacity, estimated transmissivity and estimated hydraulic conductivity. Borehole yields are low and a significant proportion of boreholes (16%) proved to be dry. Most water-bearing material comprises weathered tuffs and sediments.

To the south of this area, details of 27 boreholes on the south Kinangop Plateau and the Kikuyu Escarpment (in an area defined by Eastings 2225-2400 and Northings 99040-99150) have been examined. These boreholes which mainly penetrate pyroclastics generally have poor aquifer properties, with specific capacities normally less than 0.05 l/s/m, and the estimated mean hydraulic conductivity is around 0.1 m/d. Three dry wells are recorded in this area, corresponding to 11% of the total.

Rift Escarpment east of Suswa

An area defined by Northings 98550-98850 and Eastings 2300-2400 (and Easting 2450 north of Northing 98650) was selected to examine boreholes drilled in the Limuru Trachyte. Records of 48 boreholes in this area are held on the data base, and these indicate the aquifer properties to be similar to those of the Kinangop tuffs and Bahati tuffs, with a mean specific capacity of 0.2 l/s/m and with a mean estimated hydraulic conductivity of around 1 m/d. Four boreholes (8%) were dry. Drillers logs indicate that the main aquifer potential lies in weathered zones and fractures.

Mau Escarpment

Data from 23 boreholes drilled in the Mau Pyroclastics, in an area to the west of Naivasha defined by Eastings 1500-1900 and Northings 99100-99350, have been examined. Five (22%) of the boreholes were dry when drilled and the remainder have in general low specific capacities and estimated transmissivities and hydraulic conductivities (Table 4.2). In fact the aquifer properties shown by these rocks are very similar indeed to those of the Kinangop Tuffs across the Rift Valley. This is not unexpected because both formations are of similar age and lithology (Thompson and Dodson, 1963).

Mau Forest slopes

To the west of Lake Nakuru the lower slopes of the Mau Escarpment comprise mainly Recent and Quaternary pyroclastics and pumice. The aquifer properties of these materials were investigated in an area bounded by Eastings 1500-1660 and Northings 99550-99700. Table 4.2 indicates that the aquifer characteristics of these formations are similar to those of the Mau pyroclastics, with aquifers mainly consisting of weathered volcanics. Four boreholes (9% of the total) were dry.

Conclusions

The above survey is necessarily confined to areas where enough boreholes have been drilled to enable a reasonable estimate of average aquifer properties to be obtained. In practice this has meant that most of the Rift margins south of Suswa, and all the Rift floor south of Longonot cannot be examined because of poor data coverage. The best-known area is the Rift floor around Lake Naivasha, and it is here that the most productive wells are found. Borehole yields in this area are usually in excess of 3 l/s and mean specific capacities are around 3 l/s/m. The highest permeabilities in the area are to the north-west of the lake where the geometric mean specific capacity is 15 l/s/m. While to some extent these values may be attributed to recharge from the lake it is evident that the sediments and volcanics which underlie this region have a substantially higher permeability than elsewhere in the project area.

Further north permeability falls, probably as a result of a decrease in sediment size, and in the area between lakes Nakuru and Elmenteita borehole yields fall to around 2 l/s and the mean specific capacity is only 0.3 l/s/m.

On the sides of the Rift the permeability is in general lower than that of the Rift floor. There is a fair degree of regional uniformity in the aquifer properties of the various rock types, although those obtained from individual boreholes may vary greatly. In particular the pyroclastics covering the Mau Escarpment and the north Kinangop Plateau have very similar properties with borehole yields of around 1 l/s and geometric mean specific capacities of

0.2 l/s/m. The Bahati Escarpment tuffs and Limuru trachytes also appear to have similar hydraulic properties to the Mau pyroclastics. Only the pyroclastics of the south Kinangop Plateau and the Kikuyu Escarpment differ markedly, with lower specific capacities.

The estimated values of transmissivity shown in Table 4.2 mimic the variations in specific capacity from which they were calculated. Estimates of hydraulic conductivity are more variable, but support the conclusions reached from the specific capacity variations, and in addition suggest values for use in regional modelling. The geometric mean hydraulic conductivity of rocks bordering the Rift is estimated to be of the order of 1 m/d on the basis of the estimates in Table 4.2. This increases slightly for the Rift floor between Naivasha and Nakuru, and is approximately one order of magnitude greater for the sediments and volcanics around Lake Naivasha, and up to two orders of magnitude greater to the north-west of the lake (with some of the increase being apparent and caused by the proximity of the lake). The very large estimated permeability of the north-west Naivasha area suggests that grid faults may significantly contribute to flows in this area.

These values of hydraulic conductivity are only rough estimates, but they are reasonable for large volumes of fractured, partly-weathered rock (Freeze and Cherry, 1979). However they are only valid for the depth of rock penetrated by the boreholes, which is typically less than 200 m. At depth, where weathering ceases and where fissure apertures are reduced by overburden stress the hydraulic conductivity will be less, as discussed below.

4.4.3 Aquifer Properties of rocks at depth

The only deep boreholes drilled in the Rift are those in the Olkaria geothermal field, (the hydrogeology of which is discussed in Section 6.1). The permeability of the reservoir rocks at Olkaria is low, and recent modelling of the Eastern Olkaria borefield has produced values of intrinsic permeability of 7.5×10^{-15} m^2 for the steam zone (700-800 m approximately) and 4×10^{-15} m^2 for the underlying liquid-dominated zone (Bodvarsson and others, 1987). In the commonly-used oil industry notation these values correspond to 7.5 millidarcies (mD) and 4 mD respectively. The average value of intrinsic transmissivity of the reservoir is also low, with values ranging between 1 and 5×10^{-12} m^3. The effective porosity of the liquid-dominated zone is estimated to be 2% on average, with spatial variations of 0.25-5%. In terms of well response the reservoir behaves as a dual porosity system, with both fracture and matrix porosity and permeability.

As a result of the poor transmissivity the flow rates from the Olkaria wells are low, with the average well producing only 6 kg/s of steam, which is the equivalent of 2.5 MW_e (Bodvarsson and others, 1987).

Translated into cold water (20°C) terms for comparison with the water borehole values these figures indicate hydraulic conductivity and transmissivity values of around 3×10^{-3} m/d and 1-4 m^2/d respectively.

The values are significantly lower than those obtained for most water boreholes throughout the Rift, which is expected in view of the depth of the geothermal reservoir. However it is not known how representative these values are of permeabilities elsewhere in the Rift because the geothermal reservoir is in an unusual environment where mineral alteration, dissolution or deposition can enhance or reduce rock permeability.

In the absence of other deep wells in the Rift a preliminary estimate of

permeability at depth has been made by calculating the transit times of groundwater flows for a range of permeabilities and comparing these with age data from groundwater samples obtained by radioisotope analysis.

An analytical model has been used (developed by J.Barker of B.G.S) which considers steady state flow below an irregular water table in a two-dimensional vertical section of an aquifer between vertical no-flow boundaries (interfluves or valley bottoms) and above a horizontal no-flow boundary. In addition to the geometry of the water table and the positions of the boundaries the model requires that the hydraulic conductivity (horizontal and vertical) and the porosity be known and constant throughout the section. The model calculates the heads around the boundaries and at any point within the section, and fluxes at the water table, using a 'Biem' analytical technique. In this study the model was also used to trace flow paths within the section and to calculate transit times.

The section chosen lies across the Rift north of Naivasha (Figure 4.3). The line was selected to pass through boreholes C1404 and C4178 from which ^{14}C ages have been obtained. The uncorrected ^{14}C ages of waters from these boreholes are of the order of 1000 years, but these are upper limits (Section 5.5) and the average ages are considered to be much less, possibly only of the order of 100 years.

Head data from the model were obtained from the piezometric map and various combinations of hydraulic conductivity and porosity data were used. Figure 4.3 shows flow paths which are relevant to the two boreholes for an isotropic system. The model results indicate that if a porosity of 2% is chosen (similar to that found at Olkaria) then, to obtain an age of around 100 years a hydraulic conductivity of 0.15 m/d must be used, whereas for an age of 1000 years the relevant value is 0.015 m/d.

These estimated values of hydraulic conductivity values are 5-50 times larger than the value obtained for the Olkaria geothermal field, but they should be regarded as maxima. This is because the model assumes that the waters found in the boreholes originate on the sides of the Rift; whereas there are several chemical indications (discussed in Section 5) that these waters have an essentially local origin. If the well-waters indeed have a mainly local origin then the small component of Rift-wall groundwater which reaches the wells is presumably significantly older than the local waters (for it is unlikely that Rift-wall waters could move via deep flowpaths to the Rift centre so rapidly as to be younger than local groudwaters and yet arrive in undetectably small quantities). Hence the modelled hydraulic conductivities of the deep aquifers are likely to be be less than the range given above. In conclusion, this simple model therefore suggests that the average hydraulic conductivity of rocks at depth under the Rift in the Naivasha area is probably much less than 0.1 m/d and may in fact be of the order of 0.001 m/d as at Olkaria (although this is speculative).

4.5 Structure

The structure of the Rift Valley and in particular the major marginal Rift faults and the system of grid faulting on the Rift floor undoubtedly have a substantial effect on the groundwater flow systems of the area.

In general faults are considered to have two effects on fluid flow. They may facilitate flow by providing channels of high permeability, or they may prove to be barriers to flow by offsetting zones of relatively high permeability. The hydraulic role of faults is a subject which is poorly understood because

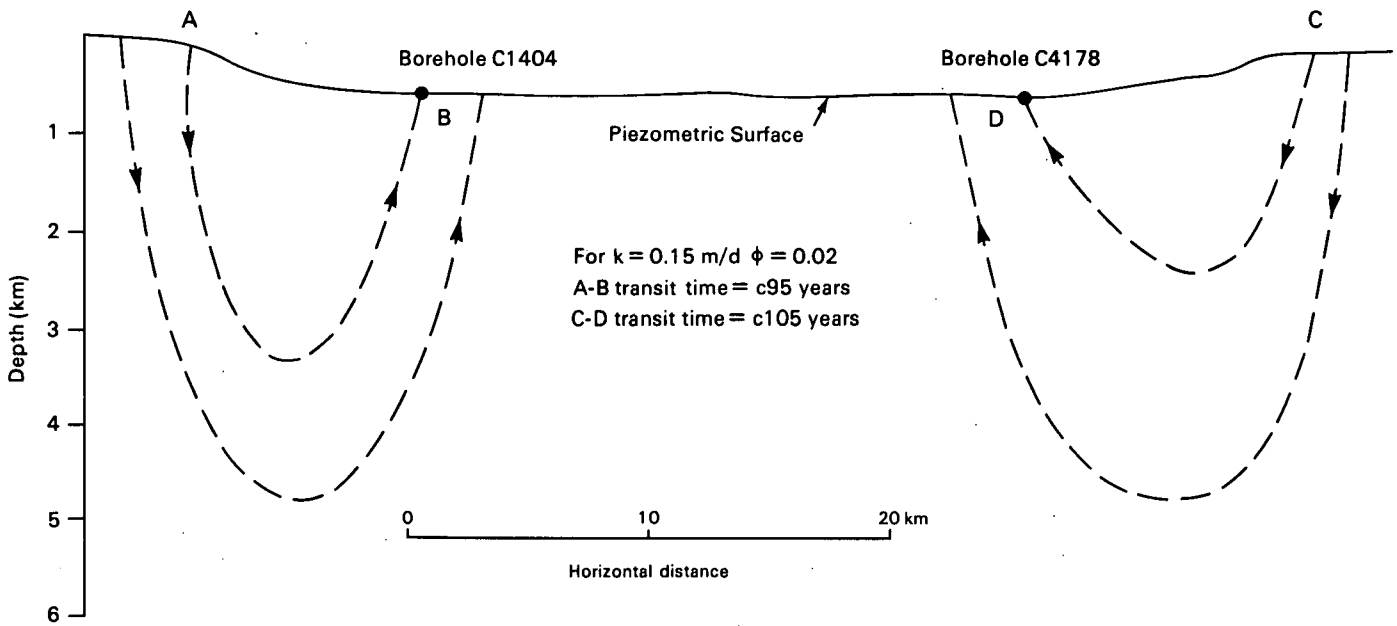

Figure 4.3 Section across the Rift showing possible flow paths.

there is often little direct evidence that a particular fault behaves in a particular way. On the whole faults are more commonly thought of as hydraulic barriers in cold groundwater systems where horizontal flows predominate, whereas in geothermal systems where vertical flows are more important they are often considered to provide conduits for flow. However care is needed to avoid invoking either property without evidence.

In the Rift Valley the main direction of faulting is along the axis of the Rift, and this has a significant effect on flows across the Rift. It is apparent from the high hydraulic gradients which are developed across the Rift escarpments that the effect of the major faults is to act as zones of low permeability. This is particularly true of the Bahati Escarpment and the escarpment to the east of Suswa. Water flowing in the weathered zones (which are often old land surfaces and therefore sub-horizontal) and fractures of the pyroclastics and lavas forming these Rift escarpments is forced to flow downwards by the faults, and in the case of the escarpment east of Suswa the fault permeability is so low that the piezometric surface in the Rift Valley is considerably below the Rift floor.

The effects of Rift faulting appear to be less in the Kinangop Plateau area where the piezometric contours are more widely spaced, and limited borehole evidence from the Mau Escarpment to the west of Naivasha suggests that flows towards the lake are not greatly affected. Borehole data are very limited on the west side of the Rift south of Longonot, but dry boreholes to the west of Suswa indicate that Rift faulting may inhibit lateral flows in this area.

Flows along the Rift are likely to be strongly affected by the substantial amount of grid faulting of the Rift floor. The effect of these faults is to channel flow along the axis of the Rift, either because the faults are open and act as conduits, or if they are infilled because they provide permeability barriers to lateral flow. A microseismic study of the Rift valley concluded that the grid faults, unlike the escarpment faults, are quite active (Tobin, Ward and Drake, 1969) which suggests that they are open. Alternatively in a recent study of the Olkaria area (Ogoso-Odongo, 1986) it was stated that faults in the Olkaria region acted as barriers, diverting southerly flow from Eburru to the south-west, towards Suswa; however the evidence for such behaviour is slim. Within the Olkaria geothermal field no evidence has been found of hydraulic barriers (Bodvarsson and others, 1987).

In summary the effect of faulting is to cause groundwater flows from the sides of the Rift towards the centre to follow longer flow paths reaching greater depths, and to align flows within the Rift along its axis.

4.6 Regional Groundwater Flows in the Longonot-Eburru Area

4.6.1 Introduction

The Naivasha catchment between Longonot and Eburru is in a hydrogeologically complex environment (as noted in Section 4.3.2), receiving water from direct precipitation and from the Rift flanks - either as stream flow or subsurface flow - and discharging groundwater to the north and south. The geothermal fields at Olkaria and Eburru lie at the southern and northern edges of the Naivasha catchment and the recharge of these fields is therefore intimately connected with subsurface flows within (or more precisely out of) the catchment.

Attempts to quantify groundwater flows in the Naivasha catchment comprise two

types; water balance studies, and applications of Darcy's Law of groundwater flow on a regional scale. These are considered below.

4.6.2 Water Balance Studies

A water balance approach has been used by McCann (McCann, 1972 and 1974) in an attempt to assess the water available for recharging deep aquifers and geothermal systems in several of the Rift catchments. McCann's method involved the determination of the ratio of orographic precipitation to potential evapotranspiration. A correlation (based on studies of semi-arid basins in the United States) between this ratio and the ratio of recoverable water to potential evapotranspiration, was then assumed, which enabled the quantity of recoverable water to be calculated.

For the Naivasha catchment McCann calculated a total precipitation of 2761×10^6 m^3/y. Of this he calculated that 2507×10^6 m^3/y evaporated (from Lake Naivasha, swamps and the surrounding catchment) leaving 254×10^6 m^3/y as outflow from the catchment.

The problem with this type of calculation is that the evaporation rate is so high in the Rift valley that any errors in its estimation or in the estimation of rainfall result in large errors in the calculated value of recharge. For example, in the above calculation the resulting value of recharge is only 9% of the initial precipitation, and combined errors in estimated precipitation and evaporation could easily equal this amount. In the case of recharge from Lake Naivasha alone however different methods can be used to assess the water balance in order to provide a comparison.
Subsurface flow from Lake Naivasha

It has long been recognised that subsurface flow from Lake Naivasha must occur, because the lake water is fresh even though the lake has no surface outlet and lies in an area of high evaporation. Examples of attempts to quantify discharge from the lake are given below.

Physical model

McCann (1974) used a water balance method to estimate groundwater recharge from the lake. Water inflows to a combined lake and swamp area of 203 km^2 were assumed to comprise direct precipitation of 132×10^6 m^3/y and gauged streamflow of 248×10^6 m^3/y. Output from the lake was considered to take the form of evaporation of 346×10^6 m^3/y (at a potential rate of 1700 mm/y) and groundwater recharge, which was therefore calculated to be 34×10^6 m^3/y. This figure for recharge is likely to be an under-estimate, as McCann points out, because the stream inflow is a minimum value (some flows were not gauged). McCann's recharge value agrees well with that previously obtained by Sikes (1935), who determined a figure of 43×10^6 m^3/y using a similar water balance method.

Isotopic model

Panichi and Tongiorgi (1974) used isotopic data from influent waters and lake water to model the groundwater recharge from the lake. The method relates the (oxygen) stable isotopic composition of the lake to that of influent water for a given ratio between inflow and evaporation rates and for a given value of relative humidity. The model also requires knowledge of the fractionation factor between liquid and vapour and the isotopic composition of atmospheric vapour; the relationship between these quantities and humidity was determined

by the authors by reference to Lake Elmenteita.

Therefore if the isotopic compositions of the influent waters and the lake are known, and if the evaporation rate is known, then the inflow rate to the lake can be calculated for a given humidity. The difference between inflow and evaporation rates is therefore presumed to be equal to the recharge from the lake.

Panichi and Tongiorgi derive a value of 250×10^6 m^3/y for groundwater recharge by this method. They argue that this figure agrees well with McCann's but this is based on a misreading of his work; McCann arrives at a similar value of 254×10^6 m^3/y, but for the entire catchment, his figure for lake recharge alone is 34×10^6 m^3/y as discussed above.

If however the isotopic balance method is used with isotopic data obtained during the present project different values are found. Panichi and Tongiorgi used a $\delta^{18}O$ value of +4.6‰ for Lake Naivasha water, whereas an average value of +6.1‰ was obtained in the present study (samples 24,76). Also they used a $\delta^{18}O$ value of -4‰ for water influent to the lake. While this does appear to be appropriate for the precipitation in the area, the volume of precipitation over the lake is only around 35% of the total inflow (McCann, 1974). Most of the inflow to the lake is in fact provided by the Rivers Gilgil and Malewa, which, arising in the high Rift Escarpments to the east, have a much lighter isotopic composition (a $\delta^{18}O$ value of -9‰ was determined for the River Malewa [sample 79]). it is therefore estimated that an average $\delta^{18}O$ value of -7‰ should be used to represent all waters influent to the lake.

Using these new stable isotope values, and the humidity range of 0.7-0.8 suggested by Panichi and Tongiorgi, values of 1.01-1.15 are obtained for the ratio of inflow to evaporation. For an evaporation of 346×10^6 m^3/y from the lake and marginal swamps (McCann, 1974) this corresponds to a recharge range of $4\text{-}52 \times 10^6$ m^3/y, a value which encompasses the McCann, and Sikes, estimates.

Chloride balance

A third approach to the problem is a chemical balance using an ion such as chloride which is conserved in the groundwater system. Chloride values of the lakewater are recorded as varying between 7 ppm and 28 ppm (Glover, 1972) but the upper values were found only in the small south-western bay; most values vary between 7 ppm and 10 ppm, with an average of 8.6 ppm (5 values). For the whole lake, including the SW bay, a mean value of 10 ppm is assumed.

The inflow from the Malewa and Gilgil rivers has an estimated chloride concentration of 2-3 ppm (Glover, 1972) and an average of 2.5 ppm is assumed. The chloride concentration of rainfall in the area is unknown, but is unlikely to exceed 1 ppm. The total annual chloride input to the lake is therefore estimated to be 7.5×10^8 grams of chloride (using McCann's figures for precipitation and river flow) and the recharge necessary to remove this amount is 7.5×10^7 m^3/y.

Discussion

All three of these methods rely on assumptions in which there may be significant errors; for example they all assume that the volume of the lake is essentially unchanging when this is known to be untrue - although such changes occur only slowly. Also the methods all rely on McCann's calculations of evaporation or inflow, or both, and none of them takes into account the unknown groundwater additions to the lake from the sides of the Rift. However

the range of estimates is small enough to suggest that a mean value of $50x10^6$ m^3/y may be taken for the subsurface recharge from Lake Naivasha, with an estimated error of $\pm 40x10^6$ m^3/y.

The significance of this figure is that it sets a minimum value for the total recharge to aquifers over the whole of the Naivasha catchment. Thus while McCann's figure of $254x10^6$ m^3/y cannot be accepted with any confidence, the total recharge value must be at least that from the lake alone i.e. of the order of $50x10^6$ m^3/y.

4.6.3 Regional flows

Estimates of the quantities of flow on a regional scale out of the Naivasha catchment can be attempted if certain assumptions are made concerning regional head gradients and permeabilities.

Southward flows from the Naivasha area

In Section 4.3.1 it was established that a north-south groundwater gradient of at least 0.05 m/m exists over the Olkaria-Longonot area, and over the Olkaria field itself the gradient has been measured as 0.1 m/m. If the latter gradient is accepted and if the estimated hydraulic conductivity of the Olkaria geothermal field ($3x10^{-3}$ m/d - Section 4.4.3) is taken to represent that across the Rift (with a width of25 km), and assuming flow to occur to a depth of 5 km (below which depth fissures are unlikely to be open) then the southerly flow at depth from the Naivasha catchment is estimated to be $14x10^6$ m^3/y. To this figure must be added the amount of southerly flow in shallow aquifers. The hydraulic conductivity of rocks at relatively shallow depths (to around 500 m - the depth of the caprock) in the Olkaria-Longonot area is unknown, but if it is taken to be between 0.1 m/d and 1 m/d i.e. similar to the Rift-wall rocks then, assuming the same hydraulic gradient and a saturated thickness of 300 m (that is, assuming the average depth to the water table to be 200 m) then the shallow component of southerly flow is estimated to be between $27x10^6$ m^3/y and $270x10^6$ m^3/y.

The above figures are very crude, being based on very rudimentary data, but they do indicate the order of magnitude of southerly flows from the Naivasha catchment, and suggest that the shallower aquifers may form a significant conduit for southerly flow.

Northerly flows from the Naivasha area.

McCann (1974) estimated a northerly flow of $39x10^6$ m^3/y from the Naivasha catchment towards the Elmenteita catchment (on the basis of a transmissivity of 1000 m^2/d). Data from the present study (Table 4.2) suggest values of transmissivity of less than 100 m^2/d to the drilled depth of boreholes between Naivasha and Elmenteita, suggesting transmissivities of the order of 500 m^2/d for shallow aquifers (to around 500 m, assuming water tables to be near the surface). If a mean groundwater gradient of 0.004 m/m is taken (from the piezometric map) and assuming the width of the Rift to be 15 km an estimate of $11x10^6$ m^3/y is obtained for shallow northerly flow. Deep northerly flow (i.e between 500 m and 5 km) over the same cross-section is estimated as $0.3x10^6$ m^3/y, assuming the same permeability as at Olkaria.

4.6.3 Discussion

The implication of the above rough analysis is that much of the subsurface outflow from the Naivasha catchment flows to the south, via Olkaria-Longonot

towards Suswa, and eventually towards Magadi (although there is little evidence that such water ever reaches Magadi in an identifiable form).

In terms of relative flow amounts to the north and south, the most important, and least known value is the hydraulic conductivity of relatively shallow material beween Longonot and Suswa. If the higher value of the range given above is taken, the the total flow out of the Naivasha catchment is estimated to be around 295×10^6 m^3/y - a figure which agrees reasonably well with McCann's estimate of 250×10^6 m^3/y - of which around 20% is lake recharge. Less than 5% of this total would flow north, and of the southerly flow only 5% would occur at depth.

If the lower estimate of hydraulic conductivity is taken, then the total estimated recharge value is 52×10^6 m^3/y, virtually all of which could be lake recharge. Here northerly flow would account for about 20% of the flow from the catchment, and of the southerly flow around 25% would be at significant depths.

Concern has been expressed about the possible effect of geothermal production on the level of Lake Naivasha. According to Bodvarsson and others (1987) the average well at Olkaria produces about 6 kg/s of steam, equivalent to around 2.5 MW_e. Therefore in order to produce 45 MW_e the present wellfield discharges approximately 100 kg/s of steam, equivalent to a liquid discharge rate of 3×10^6 m^3/y. This is only a small proportion of even the minimum estimated total natural southerly flow from the Naivasha area (41×10^6 m^3/y). It is therefore considered that any effect of present or proposed geothermal production on lake levels is likely to be masked by the effects of natural rainfall variations over the catchment.

5 GEOCHEMISTRY

5.1 Geochemical Sampling and Analysis

5.1.1 Sampling

The locations of all BGS - sampled sites are given in Appendix 7, which provides additional information on these and various UNDP sites. Water samples intended for chemical analysis were filtered through a 0.45µ Millipore filter under wellhead or hand pump pressure. Two 30ml Sterilin sample tubes were filled at each site, one being acidified with a drop of concentrated HCl (primarily to stabilise cations) and the other left unacidified to preserve original chloride and bicarbonate as far as possible. When hot springs were sampled a third 30ml water sample was collected, diluted ten times by distilled water to prevent silica from precipitating.

Samples for O and H stable isotope analysis were collected in 30ml glass bottles with neoprene-lined caps (McCartney type). Waters for $\delta^{13}C$ measurement of dissolved inorganic carbon (DIC) were collected in 250ml glass bottles and usually precipitated in the field with alkaline $BaCl_2$ solution.

Samples for tritium analysis were collected in 500ml glass bottles. Radiocarbon analysis entailed the collection of two 60 litre water samples in aspirators at most sites except those with high bicarbonate, when one was sufficient. Field precipitation with alkaline $BaCl_2$ was carried out with $FeSO_4$ added to speed up flocculation where necessary. The resulting pairs of carbonate precipitates were eventually bulked in 2.5 litre polythene bottles.

Gas samples for chemical and isotopic analyses were collected from geothermal wells, fumaroles and one water well in 125ml glass bulbs with side septa. Steam from the geothermal wells and fumaroles was condensed through a stainless steel coil immersed in cold water to permit the collection of these samples.

Samples for inert gas ratio and helium isotope ratio measurement were collected in copper tubes clamped at each end. Samples were collected in dissolved or gaseous form, the latter with or without a condensing coil, depending on the sampling technique used.

5.1.2 Measurement

Measurements of pH, temperature and sometimes Eh and alkalinity were made at the time of sampling. Eh measurements require flowing, air-free water, and these conditions were not always possible to fulfil. All other measurements were carried out in the UK. Chemical analysis (at BGS Wallingford) was by plasma emission spectrophotometry for cations and non-halides, and automated colorimetry for halides.

Stable isotope analysis was carried out at BGS Wallingford by mass spectrometry of H_2 produced by reduction of water by zinc (for δ^2H), and of CO_2 produced by equilibration with water (for $\delta^{18}O$), acid decomposition of precipitated bicarbonate ($\delta^{13}C$ DIC) or from geothermal sources after cryoseparation and drying ($\delta^{13}C$ CO_2). Gas ratio measurements were made by gas chromatography using thermal conductivity and flame ionisation detectors.

Tritium measurements were made by the DSIR Institute of Nuclear Sciences, New Zealand employing pre-distillation, electrolytic enrichment and liquid scintillation counting. Radiocarbon was measured by the NERC Radiocarbon

Laboratory by counting benzene after conversion from CO_2 liberated by acid from $BaCO_3$ precipitated in the field (see above); this work was supervised by Dr D D Harkness.

Inert gas samples were measured at the University of Bath by static mass spectrometry. Helium isotope ratios were also determined by mass spectrometry after suitable preparation; this work was carried out at the University of Cambridge. We are grateful to Mr M J Youngman and Dr J N Andrews (Bath) and Ms E Griesshaber and Prof. R K O'Nions (Cambridge), both for measuring the samples and for discussing interpretation of the results.

5.2 Water Chemistry

5.2.1 Non-thermal and Slightly Thermal Waters: Suswa to Nakuru.

This section deals with most of the waters sampled between Suswa and Nakuru. The only high-temperature waters in this area were collected from the Olkaria area, and these, together with samples from the Ol Njorowa (Hell's Gate) Gorge, are treated in Section 6 of this report.

The waters sampled fall into two main classes: modified and unmodified. The latter category includes waters whose chemical composition is derived from normal water-rock interaction at moderate temperatures, while the former comprises waters which possess evaporated or thermal components.

Results are reported in Table 5.1 and their areal distribution plotted in Figures 5.1a to 5.1g. Most unmodified groundwaters tend to be associated with the eastern and western Rift walls, i.e. sites 25-27, 85, 87, 90-92, 96, 100 and 101. The major element chemistry of these waters is summarised in Table 5.2, from which it is apparent that the waters are of sodium bicarbonate type with a relatively high silica content. The analyses are typical of igneous terrains, where dissolution of minor carbonate provides the main anion, HCO_3^- . Table 5.15 shows that all waters are oversaturated with respect to SiO_2, but most have not yet reached calcite saturation. Only trace amounts of chloride and sulphate minerals are present in these rocks, hence the low amounts of these ions, and the relatively low total dissolved solids (TDS), averaging 365 mg/l. While much lower TDS values are known from groundwater in igneous rocks in temperate climates, the higher TDS in these waters is attributed in most cases to the high ambient temperature obtaining in the Rift Valley rather than to long residence time or particularly deep circulation.

Waters of similar composition are seen in some wells on the Rift floor - for example sites 37, 39, 82, 95 and 118, and it is considered that these waters too are the product of rainfall followed by limited water-rock interaction. When the major constituents of both categories are plotted against chloride, reasonably linear relationships are seen (Figures 5.2a to 5.2g), leading to the conclusion that simple dissolution of rock is proceeding except for Si, which reaches early saturation. There is no evidence that waters are mixing with those from another hydrochemical 'facies', for example a chloride-rich, calcium-depleted thermal water. Even in the case of the slightly thermal springs and boreholes this seems to be the case; a plot of Na against temperature maintains a basic relationship (Figure 5.3a) though Si varies little (Figure 5.3b) for the reasons given above. Simple increases in solutes are observed to take place with rise in temperature, presumably both because of the increased temperature and because these waters have taken more time to circulate, though radioisotope data suggests that these time differences are not great (Section 5.5).

Table 5.1 Chemical and stable isotope data for all water samples collected in the Rift Valley during the present study.

Site No.	Na	K	Ca	Mg	HCO3	Cl	SO4	Si	Li	B	F	D2H	D18O
1	10000	186	0.6	<.4	18900	5250	163	37.3	1.17	7.71	150	-4	-1.2
2	11500	197	0.5	<.4	21800	5950	159	40.2	1.2	8.53	180	-4	-1.0
3	10900	185	0.5	<.4	20400	5550	160	39.4	0.13	8.04	170	-6	-0.9
4	11400	195	0.6	<.4		5950	159	40.2	1.18	8.67	170	-4	-0.5
5	10300	174	0.5	<.4		5200	162	36.8	1.15	7.48	150	-7	-1.1
6	11400	176	0.5	<.4	20700	5600	155	41.4	0.98	8.26	170	-6	-1.1
7	10300	158	0.6	<.4	19900	5300	153	41.2	0.84	7.6	160	-6	-1.2
8	10500	165	0.4	<.4	23000	5350	141	40.2	0.91	7.77	160	-5	-1.2
9	9640	112	0.7	<.4	16700	4900	204	49.2	0.45	7.7	80	-17	-3.1
10	9120	105	1.2	<.4	16800	5100	194	47.3	0.41	6.89	90	-20	-3.2
11	11100	157	0.6	<.4	20900	5850	134	39.0	0.78	7.83	130	-7	-1.0
12	12500	173	0.6	<.4	23600	6900	129	40.6	0.8	9.0	180	-4	-0.6
13	12200	100	0.6	<.4	23100	6400	160	23.8	0.16	6.83		-16	-2.4
14	12000	96.8	0.6	<.4	22900	6550	157	22.6	0.16	6.96	140	-16	-2.5
15	7000	75.4	0.6	<.4	13000	3550	52.4	16.7	0.15	2.69	70	-16	-1.8
16	12700	109	0.7	<.4	23800	6450	169	25.6	0.17	7.42	140	-14	-2.4
17	12600	109	0.6	<.4		6850	169	25.0	0.17	7.22	130	-15	-2.5
18	12300	115	0.6	<.4	23400	6450	189	32.0	0.16	7.44	130	-23	-2.5
19												-17	10.4
20	59.1	16.2	16.9	3.96	193	15	10.6	49.2	<.01	<.035	2.3	-6	-1.5
21	5.5	2.6	6.2	3.89	46	4.4	2.5	7.8	<.01	<.035		-22	-4.2
22	162	15.8	8.8	1.8	390	26	10.5	38.7	0.11	0.08	20	-25	-4.2
23											0.14	23	2.5
24	40.7	23.8	22.3	7.8	195	13	0.9	4.4	0.01	<.035	0.8	34	5.6
25	100	7.1	0.9	0.2	251	5.0	2.1	36.2	.011	<.035	30	-20	-5.3
26	82.5	1.4	0.2	<.15	240	53.5	1.7	19.0	<.01	<.035	30	-19	-4.2
27	38.9	8.0	3.6	1.3	106	10.5	5.8	31.4	<.01	<.035		-18	-4.3
28	31.5	8.4	10.0	2.8	201	21	4.1	30.8	.012	<.035	0.7	-28	-4.8
29												-36	-3.9
30	5.1	13.4	4.6	1.3	62	6.7	2.6	6.5	<.01	0.05		8	0.6
31	<.1	<.75	<.03	<.15		<.4	<.5		<.01	<.035		-14	-2.2
32	23.7	11.8	8.5	1.5	78	6.9	4.6	24.8	<.01	<.035	1.4	-12	-2.9
33	35.6	13.6	20.9	8.6	143	15	24.2	20.7	<.01	<.035	0.8	-31	-5.2
34	33.1	13.2	21.8	8.8	135	13.5	25.1	24.3	<.01	<.035	0.14	-27	-5.2
35												-14	-3.7
36												-24	-3.7
37	58	20	10.5	2.7	156	50	3.4	43.8	0.02	0.02		-19	-3.7
38												-18	-4.5
39	29	13	5.09	0.7	90	5.5	4.9	45.2	0.02	0.02		-20	-4.5
40												-16	-4.6
41	1050	35	0.46	<.1	1450	490	82	58.3	0.21	0.92		-7	-1.1
42	773	31	0.54	<.1	1080	360	68	57.0	0.21	0.71		-10	-1.5
43												-32	-5.8
44	2180	57	3.0	0.2	4830	290	199	36.5	0.98	0.88		-20	-4.4
45	2150	57	2.95	0.2	4710	295	197	35.7	0.96	0.87		-23	-3.1
46	2100	53	2.53	0.2	4440	295	195	35.5	0.95	0.87		20	-3.3
47	2100	55	2.58	0.2	4840	295	196	35.5	0.94	0.87		-19	-2.9
48	988	22	1.58	0.6	2000	215	80	35.6	0.06	0.87		-7	-3.5
49	1000	22	1.55	0.5	1930	205	79	35.2	0.05	0.87		-11	-2.9
50	1100	23	2.82	0.9	2230	210	80	31.8	0.05	0.9		-6	0.1
51	994	23	2.48	0.6	1940	210	81	36.8	0.06	0.89		-6	-0.2
52												-13	-2.4

Table 5.1 (contd) Chemical and stable isotope data for all water samples collected in the Rift Valley during the present study.

Site No.	Na	K	Ca	Mg	HCO3	Cl	SO4	Si	Li	B	F	D2H	D18O
53	6430	108	160	0.4	12200	1800	1630	29.7	0.47	2.28		-16	-3.0
54	8210	138	2.29	0.3	19000	2550	2060	31.7	0.62	2.93		-5	-1.3
55	7140	119	2.34	0.45	13100	1950	1780	32.0	0.52	0.45		-18	-2.5
56	6430	74	1.49	0.3	12200	1750	1590	29.9	0.47	2.25		-14	-3.7
57	6130	92	3.75	1.6	11400	1800	1560	28.1	0.44	2.1		-17	-3.6
58	16.9	4.7	6.38	3.3	103	11.5	1.9	4.8	0.01	0.02		26	4.2
59	6360	74	4.68	1.0	15384	1060	152	59.2	<.01	0.62		37	7.8
60	17.0	4.7	6.15	3.1	76	5.8	1.5	3.13	0.01	0.02		23	4.1
61												1	0.6
62												-12	-2.8
63												-13	-3.2
64												-7	-3.5
65												36	20.0
66												24	15.4
67												41	13.5
68												-3	-1.2
69												-2	-1.0
70	241	18.8	11.2	5.2	546	65	23	14.5	<.01	0.15		47	8.8
71	832	36	0.54	<.7	1960	260	40	87.0	0.56	1.04		7	1.3
72	544	10.7	10.9	5.9	1210	25	207	16.4	0.6	0.11		-24	-4.8
73	13300	240	0.5	<.7	24900	6600	132	35.2	1.17	9.24		-2	0.1
74													
75													
76												36	6.6
77												-29	-5.0
78												-38	-6.9
79												-62	-9.0
80	56	38	46.3	10.0	41	20	0.8	36.4	0.02	0.04		18	3.7
81	212	18.7	27.5	8.3	66	30	4.9	28.3	0.03	0.06		22	4.5
82	75	14.0	19.1	2.1	241	7.5	4.8	37.5	0.02	0.03		-24	-4.1
83	186	26	23.1	10.6	56	27	<.5	30.4	0.07	0.09		32	5.6
84	275	17.0	11.2	108	58	60	45	31.9	0.03	0.06		-11	-1.9
85	80	15.0	13.8	1.8	24	8.2	8.7	32.4	0.02	0.02		-22	-4.4
86	122	36	52	28	62	30.5	5.8	46.5	0.05	0.06		19	3.7
87	177	29	10.0	0.6	45	16.8	12	36.3	0.01	0.04		-29	-3.7
88	264	18.2	13.4	1.7	65	59	48	29.1	0.03	0.06		-11	-1.9
89	341	17.7	18.2	2.1	81	100	22	29.0	0.07	0.08		6	0.3
90	113	14.2	8.8	0.6	30	10.6	9.0	34.0	0.02	0.03		-20	-4.2
91	23	9.0	3.67	0.7	8.4	2.2	1.5	38.2	0.01	0.02		-13	-3.9
92	24	9.4	4.02	0.7	8.5	2.2	1.6	38.6	0.01	0.02		-17	-4.7
93	81	29	26.3	6.1	23	39	35	44.5	0.02	0.02		-17	-3.5
94	797	38	4.51	<.7	149	390	58	29.2	0.06	0.11		-8	-1.1
95	109	8.6	3.22	0.3	28	29.0	14	20.2	<.01	<.02		-16	-3.6
96	10.9	5.9	1.71	0.6	6.0	0.6	1.1	34.1	0.01	0.16		-24	-4.7
97	37	17.0	6.1	1.6	16	6.8	2.3	47.6	0.01	0.02		-18	-4.0
99	98	4.6	120	48	67	100	31	29.7	<.01			-24	-4.1
100	64	16.0	5.7	0.9	151	13.0	12.6	47.0	0.04	<.02	8	-28	-4.6
101	26	18.0	9.6	2.7	90	14.0	16	36.0	.021	<.02	3	-35	-5.3
102												8	16.6
103												1	4.0
104	197	7.1	0.5	0.1	305	33	22	57.0	0.11	0.04	38	7	4.1

Table 5.1 (contd) Chemical and stable isotope data for all water samples collected in the Rift Valley during the present study.

Site No.	Na	K	Ca	Mg	HCO3	Cl	SO4	Si	Li	B	F	D2H	D18O
105												8	2.5
106	97	49	5.4	0.5	0	4.3	262	95	0.16	0.018	3.4	10	3.2
107	957	31	11	0.2		900	419	78	1.02	0.93			
108	379	27	10.8	1.8	713	86	64	40	0.24	0.95	48	2	3.5
109	489	6.1	3.4	<.1	183	370	299	68	0.33	0.3	52	11	3.9
110	584	118	0.8	<.1	57	800	30	55.1	1.09	7.14		3	2.1
111	265	40	0.5	<.1	108	240	23	250	0.66	2.53		11	2.6
112	398	37	0.3	<.1	334	236	86	212	0.52	2.06		13	2.7
113	486	74	0.4	<.1		624	20.2	248	1.16	7.12		10	3.1
114	311	42	0.4	<.1	183	194	34	247	0.72	2.82		13	3.6
115	386	53	0.2	<.1	172	390	151	262	1.05	4.78		8	2.8
116	3.2	<.7	0.7	<.1	0	3	12.4	2.3	<.01	0.95		18	3.7
118	68	15	12	1.3	187	13	9.5	38	0.016	<.02	3.3	-18	-2.8
119													
120													
121	400	48	40	1.4	1120	14	9.1	59	0.53	0.05	8.9	-27	-5.0
122	199	32	41.6	3.3	653	13	8.6	49.4	0.25	0.05		-28	-4.8
123												-16	-4.0
124	403	64	58	4.9	1100	55	17	61	0.43	0.14	13	-24	-3.8
125	386	30	13	14	989	78	22	31	0.096	0.1	9.4	-23	-3.5
127												-38	-5.5
128												-49	-8.0
129	187	48	38	18	686	12	8.8	43	0.089	0.03	8.4	-28	-4.6

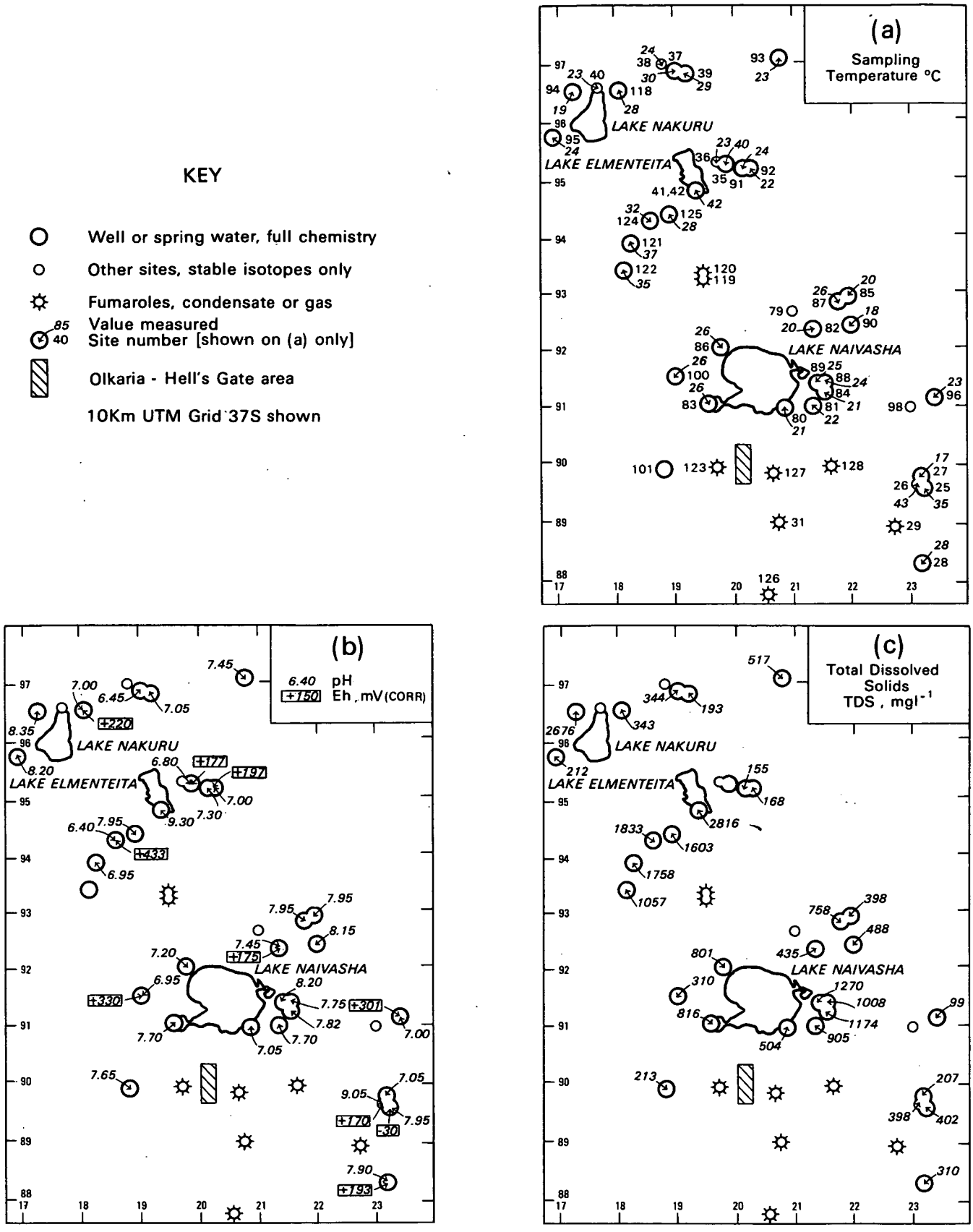

Figure 5.1a-c Maps of sampling, chemical and isotopic data from the Suswa-Nakuru sector.

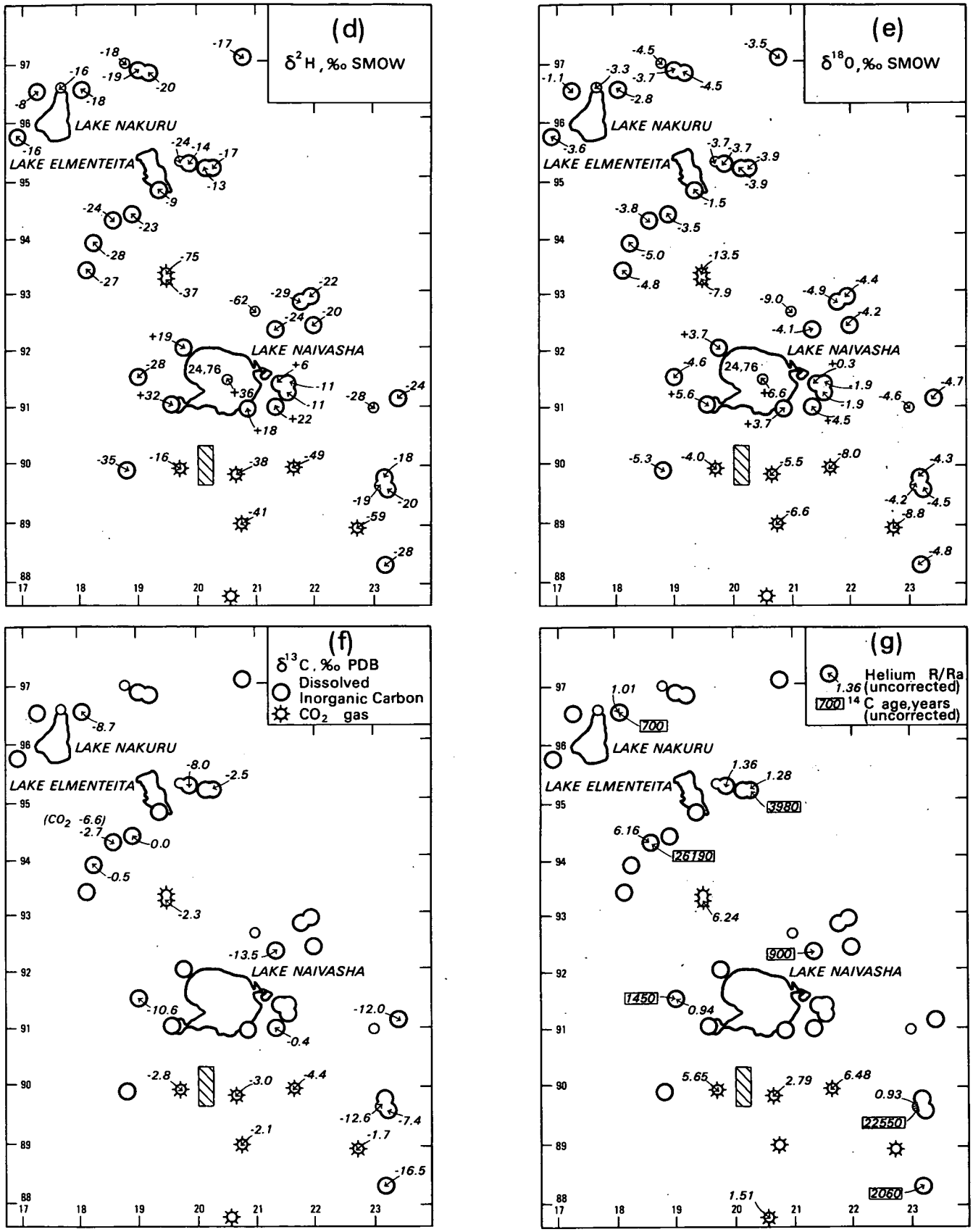

Figure 5.1d-g Maps of sampling, chemical and isotopic data from the Suswa-Nakuru sector.

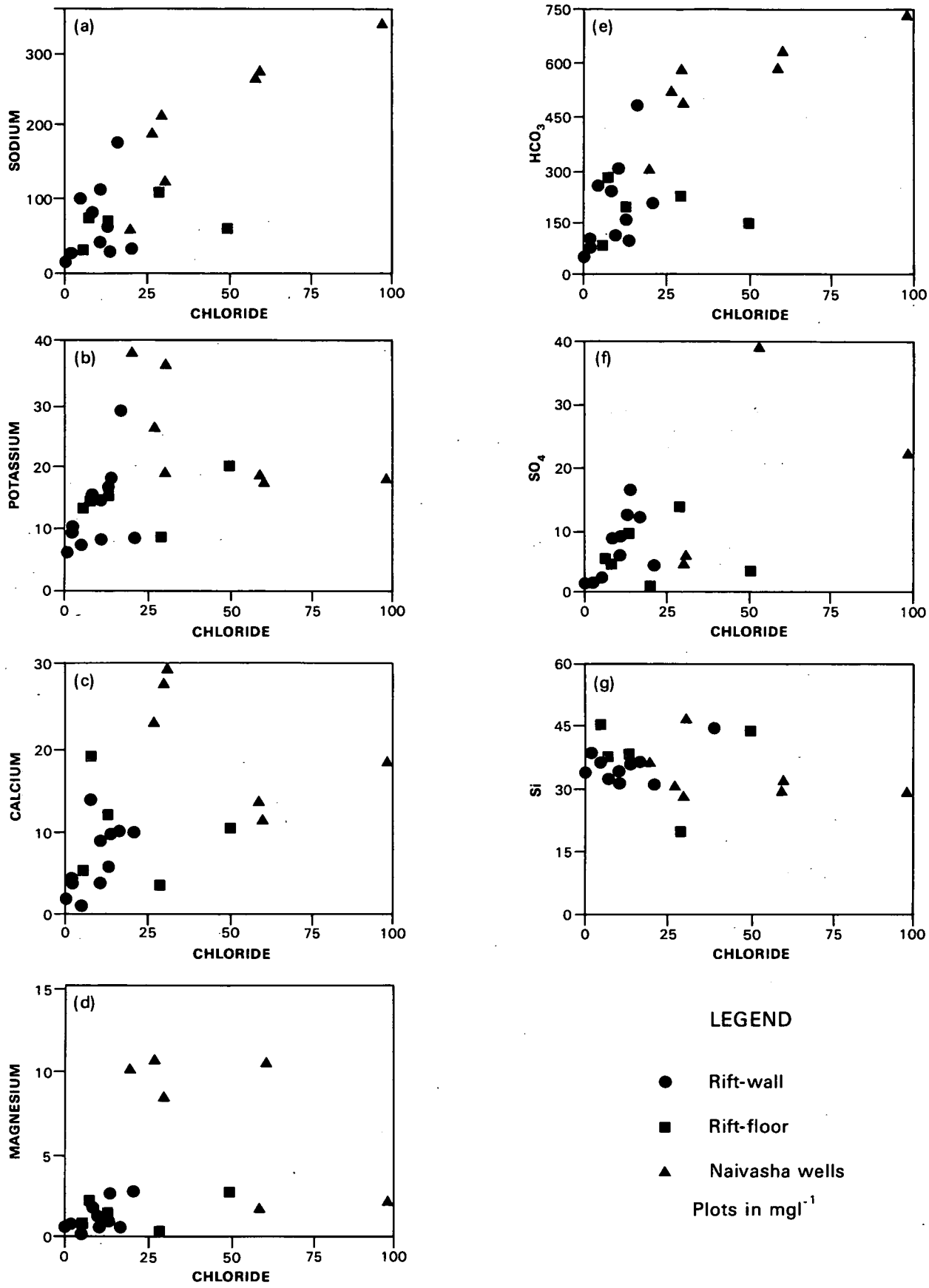

Figure 5.2a-g Plots of major ions versus chloride for unmodified Rift-wall and Rift-floor groundwater, and for wells with a large proportion of water from Lake Naivasha.

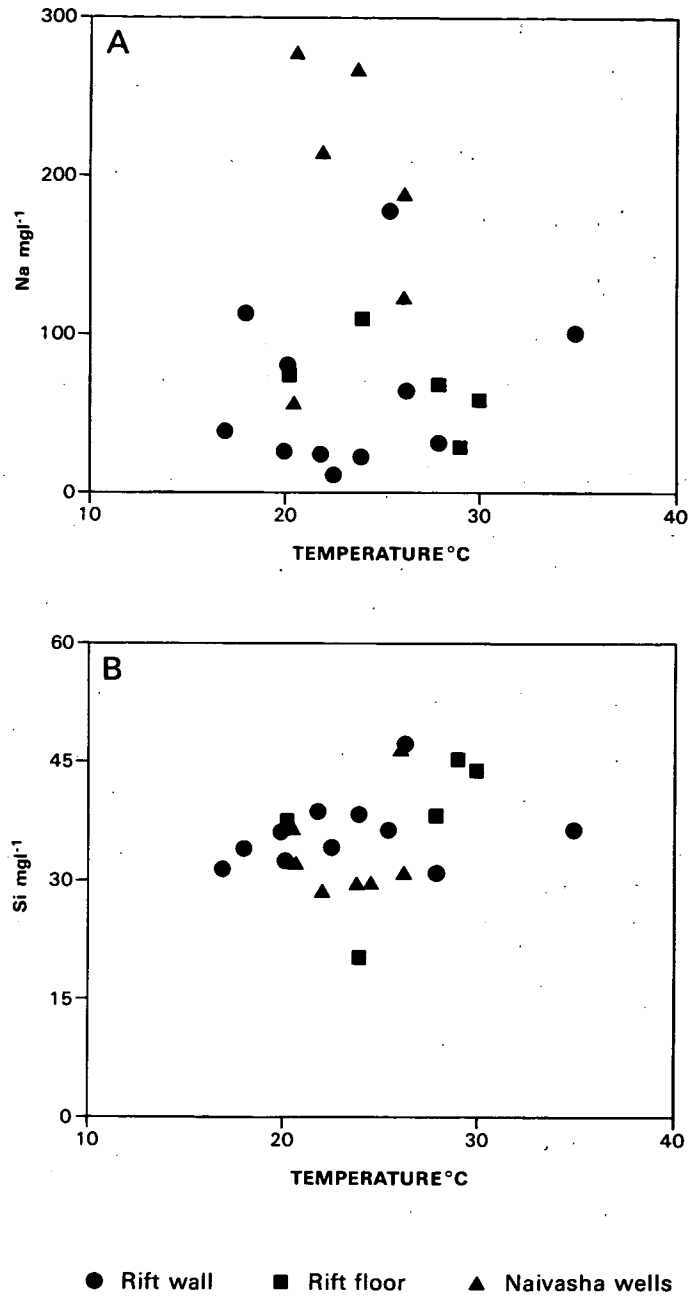

Figure 5.3a-b Plots of sodium and silica versus sampling temperature for unmodified Rift-wall and Rift-floor groundwater, and for wells with a large proportion of water from Lake Naivasha.

Other properties of these waters, such as pH and Eh (oxidation potential) measurements, do not conflict with the picture of unevolved groundwater obtained from the solutes. Figure 5.1b shows that pH is similar for most of these waters, with a very few exceptions such as the alkaline Kijabe springs (27), and averages 7.5 pH units which is typical of dilute bicarbonate waters. Eh values were recorded at comparatively few sites (Figure 5.1b), but they all indicate that the waters are oxidising in character. Temperatures range from 18°C (90) to 43°C (27), but (as already stated) there are no grounds on the basis of water chemistry for believing that the warmer waters are cooled or diluted high temperature waters.

It is likely that the compositional range of the waters described above (Table 5.2) is typical of shallow waters from the Rift wall and floor for considerable distances north and south of the Suswa-Nakuru sector. Supporting evidence comes from the BGS data in the Magadi area and from the MERD data in the Bogoria area.

Modified waters can be divided into those north and south of the Eburru massif. The southern group are all relatively close to Lake Naivasha; the furthest is some 6 km away. Seven wells were sampled (80, 81, 83, 84, 86, 88 and 89) and the average and range of analyses for major elements are given in Table 5.3. If the average analysis is compared with the mean for Rift-wall groundwaters it can be calculated that the average concentration increase is by a factor of 3.4, and that most of the ions have a similar ratio to chloride in both groups (Figures 5.2a to 5.2g). Only silica differs from this pattern, and this can be attributed to its abundance in the rocks: a similar solubility limit has been reached in both groups (Table 5.15).

The rather consistent increase in concentration in the Naivasha wells can plausibly be linked to evaporation in the lake, as Glover (1972) noted. Stable isotope results (Section 5.3) are very diagnostic of this process and confirm that the Naivasha wells contain up to 80% of lakewater. It is assumed that the lake is recharged by a combination of river and groundwater in the northeast, which then undergoes evaporative concentration before eventually discharging to the south and perhaps north of the lake, which lies at the culmination of the Rift floor. Thus mixing between lakewater and shallow groundwater would occur along flowpaths away from the lake, giving rise to the chemical and isotopic properties of the Naivasha group of well waters. There is no evidence that the well waters are linked in any way to possible outflows from Olkaria or Eburru.

Waters sampled to the north of Eburru in the modified category include four wells between the massif and Lake Elmenteita (121, 122, 124 and 125), a warm spring complex at the southern end of Elmenteita (41/42), and a well to the northwest of Lake Nakuru (94). The remainder of sampling points in this area are considered to be unmodified groundwaters.

The sample from site 94 is best explained by considering it to be outflow from the highly saline Lake Nakuru, though much diluted by fresher water from the sides of the Rift (Section 5.3.3). The well has an ambient temperature (Table 5.4) which effectively rules out the possibility that it is some kind of thermal outflow perhaps flowing towards the lake. Although Lake Nakuru is highly saline and therefore typical of a closed basin lake, the possibility of a small amount of flow out to the northwest does exist on piezometric grounds (Section 4.3.2). In the next section it is noted that no traces of Nakuru-type water are seen in wells to the north of Nakuru.

Table 5.2 Range of concentrations and average major ion values for unmodified Rift-wall waters.

Ion	average value mgl^{-1}	range mgl^{-1}
Na	61	11-177
K	13	1-29
Ca	8	1-19
Mg	1.5	0-3
HCO_3	190	44-476
Cl	13	1-50
SO_4	7	1-12
SiO_2	71	22-101

Table 5.3 Range of concentrations and major ion values for wells containing a large proportion of water from Lake Naivasha.

Ion	average value mgl^{-1}	range mgl^{-1}
Na	208	56-275
K	25	17-38
Ca	27	11-52
Mg	9	2-28
HCO_3	543	297-626
Cl	47	20-100
SO_4	18	0-48
SiO_2	71	61-100

Table 5.4 Chemistry and isotopic composition of water from the 'Badlands' wells and warm springs of Lake Elmenteita.

Property	122	121	124	125	41-42
Temperature, °C	35	37	32	28	42
pH	-	7.0	6.4	8.0	9.2
Na, mgl^{-1}	199	400	403	386	917
K, mgl^{-1}	32	48	64	30	33
Ca, mgl^{-1}	42	40	58	13	13
Mg, mgl^{-1}	3	1	5	14	0
HCO_3, mgl^{-1}	653	1120	1100	998	1230
Cl, mgl^{-1}	13	14	55	78	425
SO_4, mgl^{-1}	9	9	17	22	75
SiO_2, mgl^{-1}	106	126	131	66	123
TDS, mgl^{-1}	1057	1758	1833	1603	2816
δ^2H, $^o/_{oo}$	-27	-28	-24	-23	-9
$\delta^{18}O$, $^o/_{oo}$	-4.8	-5.0	-3.8	-3.5	-1.5

	Average Olkaria thermal water	Average Naivasha well water	41-42	Indicated lakewater contribution to 41-42
Na/Cl	0.98	4.4	2.2	35%
HCO_3/Cl	0.36	11.6	2.9	23%
SO_4/Cl	0.14	0.38	0.18	17%

The sequence of sites running northeast from well C431 (122) to the Elmenteita springs (41 and 42) is interesting as it presents the only opportunity (apart from fumaroles) of looking at the remnants of a geothermal outflow in the Suswa to Nakuru sector of the Rift. All the wells exceed the unmodified Rift-wall type of composition in terms of dissolved constituents (Table 5.4), and it is known from $^{3}He/^{4}He$ measurements at site 124 (Section 5.6.2) that a high temperature upflow must ultimately be responsible for the chemistry of much of the water flowing north from Eburru. Because of the curved disposition of these sites in relation to the Eburru volcanic centre, they all lie at about the same distance from the centre (around 13 km). There is an increase in TDS values from about 1000 mg/l in the southwest to nearly 3000 mg/l at the warm springs, with chloride increasing at the expense of bicarbonate and sulphate, though bicarbonate remains the dominant anion.

The increase in TDS to the northeast does not necessarily imply a greater outflow contribution. Taking the average Olkaria thermal water composition to represent that of the Eburru upflow, and the average composition of the wells close to Lake Naivasha to represent northward subsurface flow from Lake Naivasha, it can be seen from comparisons of the ratios of major constituents to chloride that some 30% or so of lakewater mixing with thermal water could be responsible for the compositions seen in the warm springs at the southern end of Lake Elmenteita (Table 5.4). Close support is given by the stable isotopic results (Section 5.3.3) which imply a lakewater contribution of between 30-35%.

To the southwest of the springs the wells suggest a much smaller or totally absent lakewater contribution - indeed the slight increase in heavy isotopes might simply be due to steam loss from the underlying groundwater. However, study of the ratio of constituent ions to chloride for all five sites does imply that a dilution series is involved and that the isotope results can probably be taken at face value.

In view of the low chloride contents measured in the wells it may be doubted that they are truly representative of primary outflow from Eburru. The high bicarbonate values suggest that they may be the result of condensation of CO_2 and associated gases into what is basically a Rift-wall type of water on the basis of stable isotopes. It is shown elsewhere (Section 5.3.4) that Eburru upflow water is probably very similar in isotopic terms to Rift-wall water, and therefore mixing or steam heating involving shallow and thermal waters in the Eburru outflow area is unlikely to show up isotopically. However, the likelihood that the well waters are of secondary composition is not supported by the high SiO_2 and Li results, particularly from sites 121 and 122.

Nevertheless, if the wells are considered to be secondary manifestations of thermal outflow from Eburru, then the low temperatures of the waters and the lack of evidence of secondary steam production in the 'badlands' area is an indication that the quantities of cold, shallow groundwater flowing from the Rift wall are of sufficient volume to 'quench' steam boiling off the thermal outflow. Only where the outflow water itself is ascending towards the southern end of Lake Elmenteita and mixing with water flowing north from Lake Naivasha does the shallow groundwater temperature become higher.

If, however, the SiO_2 and Li results are given weight then it must be assumed that the Eburru upflow water is considerably lower in chloride than the thermal fluid at Olkaria. To some extent this is likely, as the Eburru system is considered on isotopic grounds to derive from the low-chloride

Rift-wall water rather than the higher-chloride lakewater which feeds Olkaria. In this case it must be assumed that there is only a small upward leakage of outflow water on its journey north to Lake Elmenteita. The result appears to be a ternary mixing system between Rift-wall water, thermal outflow and Lake Naivasha water.

Despite the differences between these two models, it is clear that there must be outflow north from Eburru and also underflow from Lake Naivasha. These two sources combine to account for the apparent water supply deficiency in the Elmenteita basin noted by McCann (1972).

5.2.2 Surface, Thermal and Non-Thermal Waters: Nakuru to Silale.

The rather limited number of samples collected and analysed by the BGS-MERD team from this area has been supplemented by 11 samples collected between northern Lake Bogoria and Nakuru by two MERD staff members (Messrs M. Arusei and J. Wambugu) as part of their MSc course work at Leeds University, where the samples received chemical analysis. Isotopic analysis of these samples was performed at BGS Wallingford and the results are considered in Section 5.3.5 of this report.

Water chemistry results are presented in Tables 5.1 and 5.5 and Figures 5.4a to 5.4.d. Major element chemistry is now considered. Between Nakuru and Bogoria concentrations resemble those measured in the Suswa-Nakuru sector for waters believed to have originated as rainfall on the Rift wall or higher floor. In fact stable isotopic measurements suggest that the groundwater in this area is mainly from the Rift floor rather than wall, but otherwise the waters are similar in character with the ranges of Na 37-174, K 4.7-22, Ca 1.0-20, Mg 0.1-3.8, Cl 4.2-13, SO_4 2-20 and HCO_3 187-322 mg/l. Though there is a considerable drop in altitude between Lake Nakuru and Lake Bogoria (some 770 m) there is no geochemical evidence of flow out of Lake Nakuru to the north. Samples collected from wells or springs a few km from Lake Bogoria (i.e. B1, B4 and B7) are generally similar to those further south in their chemistry and suggest that, like these samples, they are derived from local rainfall. It is presumed that groundwater flow in the general area must be directed towards Lake Bogoria, which has the very high salinity associated with closed or almost closed basin lakes. Near the shores of the lake two boiling springs were sampled (B2 and B3). The chemistry of these springs suggests locally-derived groundwater which has been drawn into a CO_2-rich geothermal upflow. The concentration ratios are similar to those measured at the warm spring at the southern end of Lake Elmenteita (see previous section) and the total TDS value is about 1.5 times larger. The Elmenteita springs are some 15 km north of the Eburru upflow, their presumed source, but issue at only about 40°C compared to the boiling temperatures of the Bogoria springs. This suggests that the Bogoria springs are much closer to their upflow and may be rapidly cooling by adiabatic rather than conductive processes; the apparent steam loss identified from stable isotopic measurement supports this (Section 5.3.5). The silica and alkali geothermometers give temperatures of below 150°C for the Bogoria springs; such temperatures at depth seem too low in view of the vigorous boiling of the springs. This implies that upflow is being modified by a cooler inflow at some stage. Isotopic evidence (Section 5.3.5) points to a small amount of lakewater contamination but suggests that steam heating is not involved; on this basis the lakewater could be contributing at various levels in the thermal circulation. Equally, non-thermal 'fresh' groundwater could be responsible for the erroneous performance of the geothermometers, though in view of the relatively high salinity of the boiling springs this is

Table 5.5 Chemistry and isotopic composition of samples collected by MERD personnel in the Lake Bogoria area.

SITE No	Temp °C	pH	Na	K	Ca	Mg	HCO_3	Cl	SO_4	SiO_2	TDS	δ^2H	$\delta^{18}O$
							mgl^{-1}					‰	
B1	37.0	6.8	117	10	4.9	1.7	278	20	11	90	533	-12	-2.8
B2	93.5	8.7	1336	12	1.4	0.40	2645	280	57	111	4443	-3	-0.7
B3	96.4	9.3	1669	37	0.7	0.16	2787	400	52	137	5083	-2	-0.5
B4	34.5	7.6	93	10	8.9	3.8	283	11.8	20	58	489	-15	-3.2
B5	29.4	7.7	121	17	49	40	671	16.5	6	70	991	-14	-3.1
B6	42.9	8.1	169	29	14.3	7.5	542	28	6	51	847	-15	-3.3
B7	37.7	6.3	117	10	4.5	1.0	325	11.8	11	80	560	-10	-2.7
M1	29.2	6.9	91	22	19.6	2.8	322	5.2	11	84	558	-13	-2.5
M2	33.2	7.5	84	10	6.3	1.1	195	21	16	61	394	-19	-2.8
M3	38.5	7.4	37	4.7	11.6	2.5	195	4.2	2	70	327	-16	-2.7
M4	36.9	8.6	174	10	1.0	0.10	283	26	20	98	612	-14	-2.8

NOTE: Chemical analyses carried out at Leeds University by M Arusei and J Wambugu of the M.E.R.D.

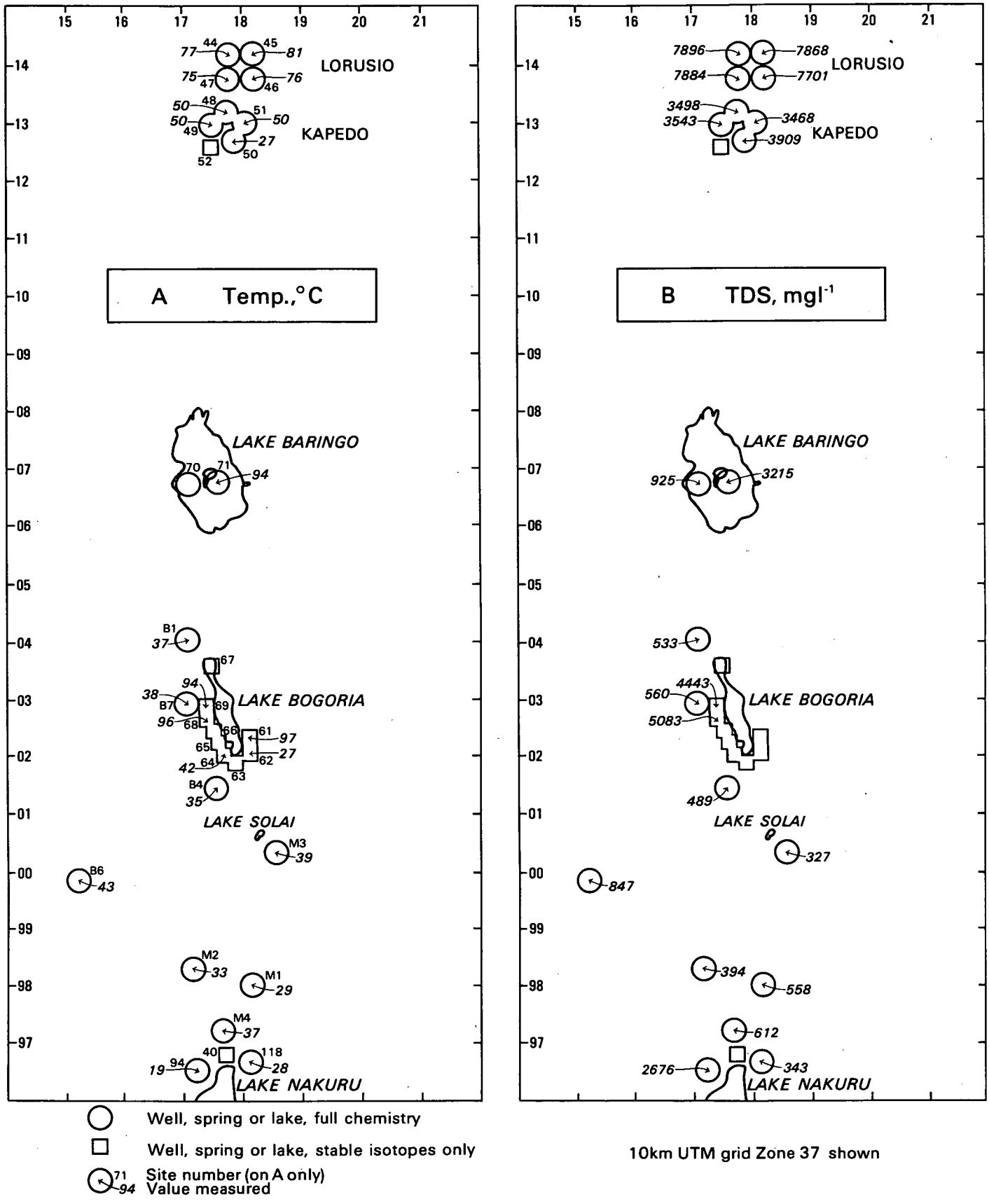

Figure 5.4a- b Maps of chemical and isotopic data for the Nakuru-Silale sector ('M' and 'B' numbers relate to samples collected by MERD).

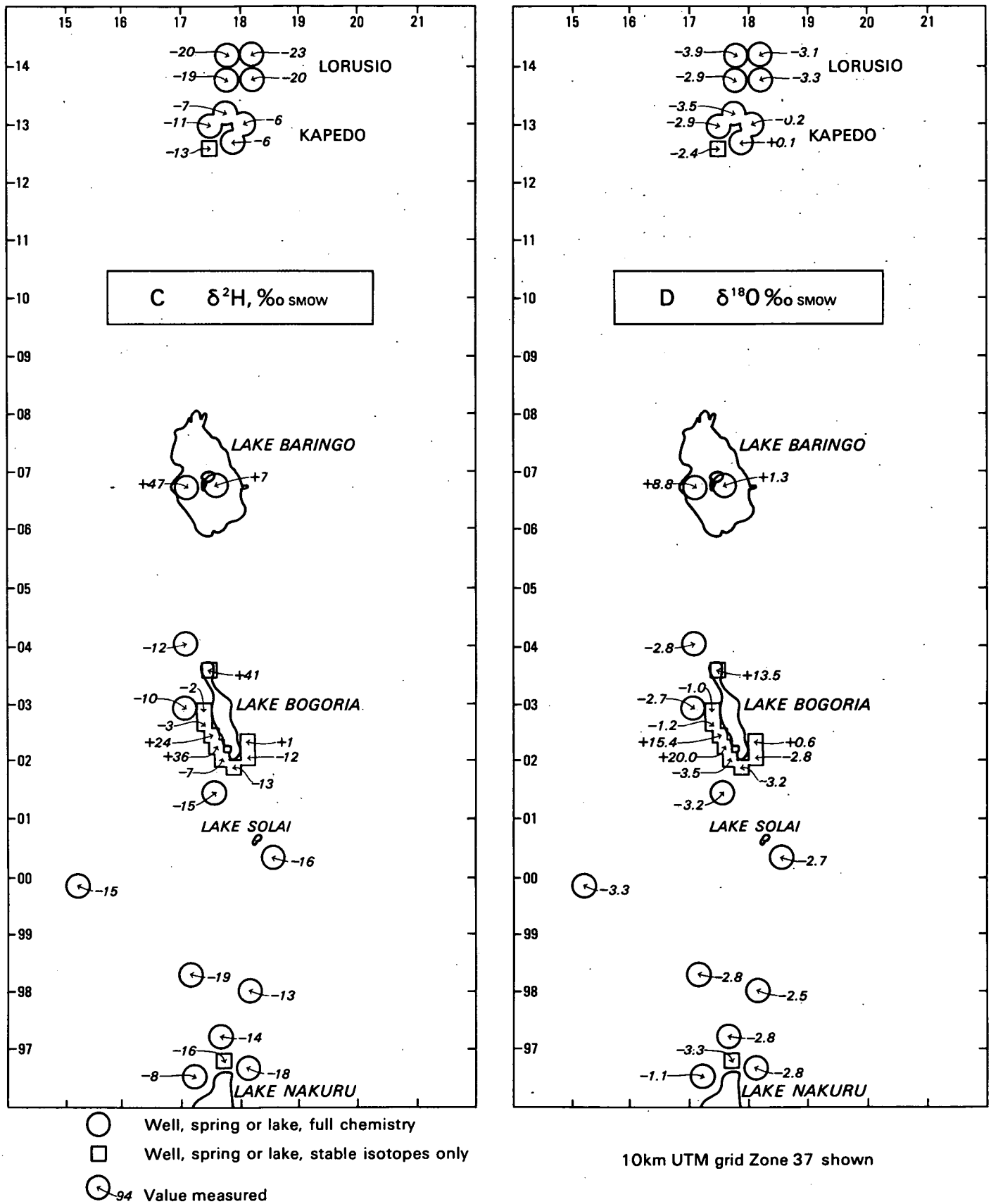

Figure 5.4c-d Maps of chemical and isotopic data for the Nakuru-Silale sector ('M' and 'B' numbers relate to samples collected by MERD).

perhaps less likely. Geotermica Italiana (1987) proposed a ternary mixture of thermal water, lakewater and another water component, the origin of which was not altogether clear from their isotopic evidence. Their mixing models suggested the maximum temperature at depth to be about 190°C, while gas and isotopic geothermometers gave results in excess of 200°C. The few data considered here cannot confirm these results quantitatively, but qualitatively their similarity to the Eburru outflow and to some extent the Olkaria fluid suggests that such temperatures may well be correct.

At Lake Baringo, samples were collected from a boiling spring on the central island of Ol Kokwe, and from the lake. Analyses are given in Table 5.1 and shown in Figures 5.4a to 5.4d. The spring water is almost four times higher in TDS than the lake and therefore, as Glover (1972) pointed out, is most unlikely to be the result of steam heating of lakewater. Its chemistry is typical of other high temperature thermal waters further south in the Rift - for example there is a strong resemblance to the Olkaria fluid (e.g. very similar Cl/SO_4 ratios) except that there is much more bicarbonate, which implies condensation of CO_2 at shallow depths. Stable isotope results indicate that the boiling springs probably contain a proportion of lakewater mixed with the original groundwater presumed to feed the system. Silica and alkali geothermometers (Table 5.14) show temperatures in excess of 175°C, and it is concluded from this that lakewater must be entering the system before or during heating; if lakewater were mixing at shallow depths interference with the geothermometers would tend to result, as is apparently the case at Lake Bogoria.

Two groups of hot springs north of Lake Baringo were sampled. The results (Table 5.1, Figures 5.4a-d) show that the waters are not dissimilar in element ratios, but that the Lorusio group is twice as high in TDS and contains proportionately higher amounts of HCO_3. Silica and alkali geothermometers give rather similar temperatures at depth for each group in the range 120-150°C. Since the Lorusio group is hotter and more concentrated in TDS, it is tempting to consider that the Kapedo group is the result of dilution of the Lorusio water, but isotopic measurements make this explanation inplausible and imply a separate origin (Section 5.3.5).

The Kapedo springs are similar in chemical composition and amount to the Ol Kokwe spring water, though in terms of Na/K ratio and SiO_2 content are different enough to affect geothermometry results. The spread of values of elements between the various springs is probably a consequence of evaporation/steam loss (Section 5.3.5). In spite of the similarity to the Ol Kokwe spring the isotopic signatures are much closer to the meteoric line and do not suggest that Lake Baringo water penetrates this far north in recognisable form, thus contradicting the admittedly tenuous evidence from C_2H_6/CH_4 ratios (Section 5.6.1).

5.2.3 conclusions

The consideration of chemical data, particularly from the relatively well-sampled Naivasha-Nakuru sector of the Rift Valley reveals that on the whole large-scale mixing of high temperature thermal outflow with 'fresh' Rift-wall water does not occur where it can be directly sampled. Few ambient or slightly warm well or spring waters show any evidence of mixing, although the basalt 'badlands' north of Eburru are an exception. Otherwise thermal outflows often appear very close to lakes - i.e. in low-lying discharge areas. (Lake Naivasha is an exception because it is itself recharging, and the outflows from the neighbouring Olkaria-Domes-Longonot area, or the Suswa area, have not been detected). The association of hot or

boiling springs with low-lying lakes has led to the belief that there could be a general body of thermal water underlying the Rift over a large area (Mahon, 1972). Certainly there is a similarity between the chemistry of many of the hotter thermal springs as far north as Lorusio. However stable isotope evidence (Section 5.3.3 et seq.) tends not to support this conclusion. Instead the general chemical resemblance is more likely to be due to separate convective systems in rather similar lithologies (in geochemical terms) aided by the copious flux of CO_2 in the Rift Valley (Bailey, 1980).

5.3 Stable Isotopes - Water.

5.3.1 Introduction

Oxygen ($^{18}O/^{16}O$) and hydrogen ($^{2}H/^{1}H$) isotope ratios are calculated with reference to Vienna Standard Mean Ocean Water (SMOW) and are presented in Table 5.1. They were measured on rainfall, surface water, groundwater and fumarole steam condensates.

5.3.2 Rainfall in the Rift: Magadi to Lodwar.

Counterpart staff distributed sample bottles to 21 rainfall stations throughout the Kenya Rift Valley in January/February 1986. The station locations are given in Appendix 7 and range from Magadi in the south to Lodwar near Lake Turkana in the north.

The stable isotope characteristics of the samples were determined at Wallingford using the methods of Darling et al. (1982). $\delta^{18}O$ and $\delta^{2}H$ values are given in Table 5.6 and are plotted on Figure 5.5. Data from three rainfall samples taken in 1985 are also included in the figure. Least squares linear regression analysis was used to identify the line

$$\delta^{2}H = 5.56\ \delta^{18}O + 2.04 \qquad (r^2 = 0.88) \qquad (3)$$

through the data. In addition lines were fitted separately to data for the smaller and larger rainfall events to check for bias (such as that related to the 'amount effect' (Dansgaard, 1964) or to possible evaporation from rain collectors), but none was found.

Equation 3 has a smaller slope than that of the world meteoric line proposed by Craig (1963) with a slope of 8; this is probably because rain over the Rift Valley evaporates somewhat as it falls. A regression calculated for 80 Rift Valley groundwaters from Magadi to Silale (Figure 5.6) gave a slope very similar to that defined by rainfall:

$$\delta^{2}H = 5.49\ \delta^{18}O + 0.08 \qquad (r^2 = 0.81) \qquad (4)$$

This suggests that the rainfall line, though based on sampling over a limited period of time, is likely to be reasonably accurate. Additional support is provided by studies outside the Rift: in the Chyulu Hills of southeast Kenya the following relationship was observed for 35 samples (BGS unpublished data):

$$\delta^{2}H = 5.68\ \delta^{18}O + 6.04 \qquad (r^2 = 0.89) \qquad (5)$$

This indicates that rather low meteoric gradients are found in southern Kenya as a whole and are not confined to rainfall in the Rift Valley.

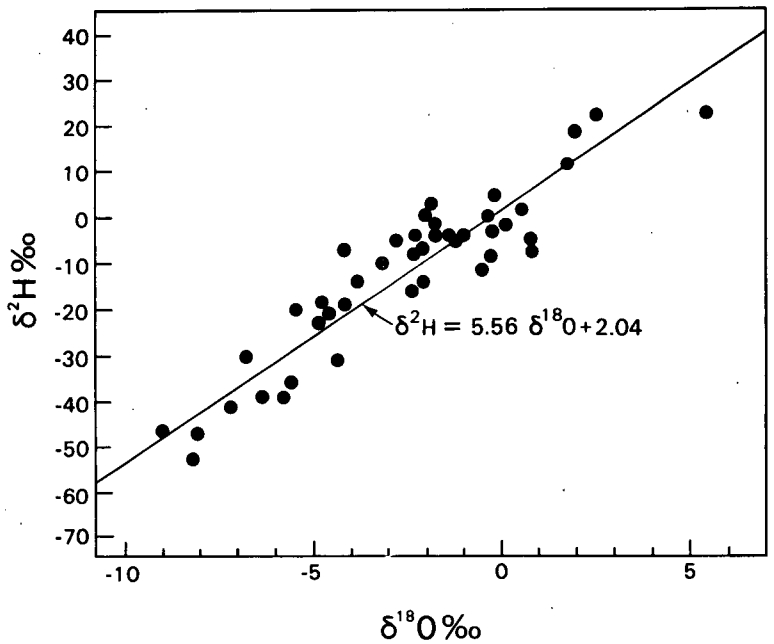

Figure 5.5 Delta-diagram of rainfall stable isotope data from collection stations in the Magadi- Silale sector.

Table 5.6 Stable isotope values of rainfall in the Rift Valley.

STATION	COORDINATES	ALTITUDE (m)	DATE	RAINFALL (mm)	δ^2H ‰ SMOW	$\delta^{18}O$ ‰ SMOW
1	AH 99 91	600	21.3.86	16.3	-7	+0.8
			31.3.86	2.6	+22	+5.4
2	BJ 16 26	600	21.3.86	8.4	-8	-0.3
			7.4.86	11.4	-14	-2.1
3	BJ 37 37	1000	18.3.86	3.2	+12	+1.7
			-	-	-	-
4	ZP 18 30	1800	6.4.86	?	-10	-3.2
			10.4.86	?	-64	-10.2
5	ZP 20 80	1900	5.3.86	14.3	+5	-0.2
			11.4.86	6.6	-30	-6.8
6	ZQ 16 36	2760	18.4.86	21.5	-47	-9.0
			20.4.86	22.2	-18	-4.8
7	BJ 31 98	2200	7.3.86	8.4	-39	-5.8
			23.4.86	7.6	-36	-5.6
8	AK 42 21	2550	10.3.86	8.8	-4	-2.3
			22.4.86	49.0	-23	-4.9
9	BK 14 20	1920	10.3.86	22.2	-7	-4.2
			10.4.86	16.1	-39	-6.4
11	BK 02 45	2000	12.4.86	4.2	-3	-0.3
			23.4.86	34.7	-53	-8.2
12	AK 73 69	1850	20.3.86	2.0	-4	-1.4
			18.4.86	11.0	-5	-1.3
13	BJ 41 79	2340	21.3.86	13.7	-14	-3.9
			23.4.86	18.4	-41	-7.2
14	ZR 04 04	2100	18.3.86	23.3	0	-2.0
			?	?	+3	-1.9
15	AL 72 29	1150	20.3.86	10.7	+2	+0.5
			10.4.86	39.7	-11	-0.5
16	ZR 30 06	1550	18.3.86	8.0	-20	-5.5
			4.7.86	25.0	-5	+0.7
17	AL 76 38	1000	10.4.86	17.0	-19	-4.2
			20.4.86	19.2	-5	-2.8
18	ZR 05 54	2050	7.3.86	10.1	-4	-1.8
			10.4.86	16.8	-47	-8.1
19	AM 69 05	900	7.3.86	16.1	-1	+0.1
			22.3.86	5.4	0	-0.4
20	BM 43 21	2000	18.3.86	4.4	-31	-4.4
			21.4.86	10.2	-16	-2.4
21	35°40'E 2°23'N	880	5.3.86	32.3	-7	-2.2
			7.3.86	23.3	-1	-1.8
22	35°36'E 3°07'N	550	4.3.86	28.9	+19	+1.9
			24.4.86	33.4	-21	-4.6

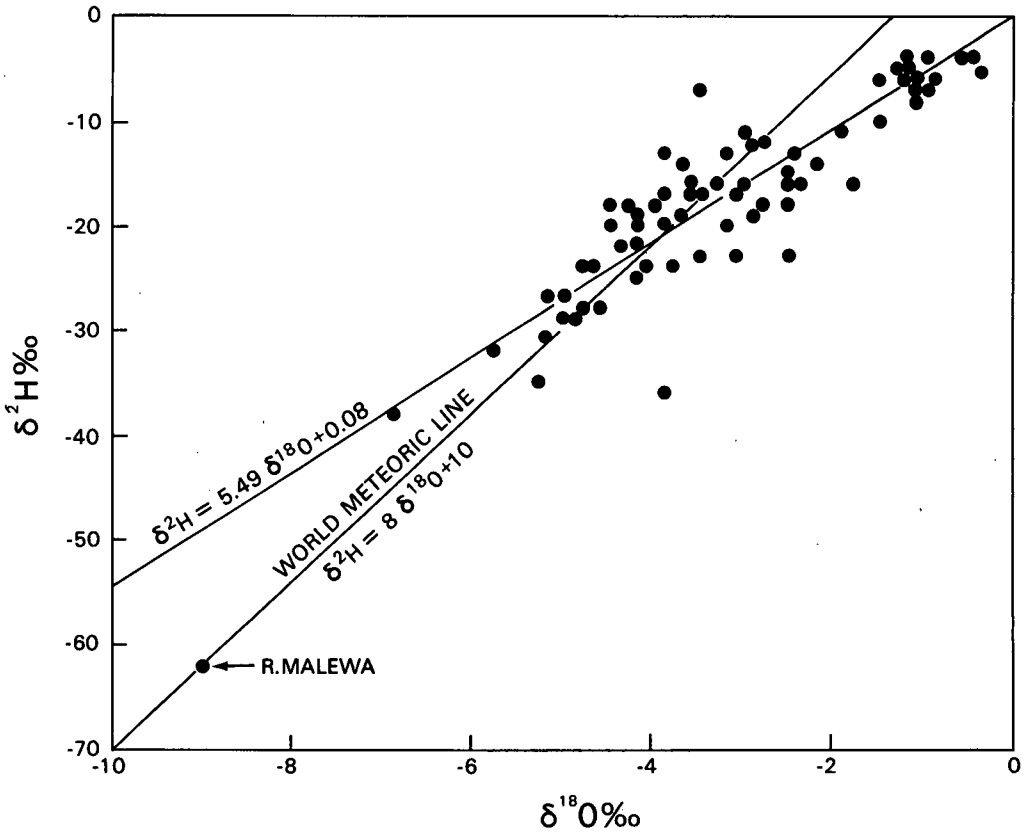

Figure 5.6 Delta-diagram of stable isotope data from unmodified groundwaters in the Magadi-Silale sector.

However, rather depleted water from the Malewa River which rises in the Nyandarna Mountains is seen to fall on the world meteoric line. This implies that the modifying influeces are restricted to lower altitudes, as might be expected.

Altitude and Latitude Effects.

The high topographic relief of the Kenya Rift Valley makes it likely that significant variations with altitude in the mean isotopic composition of rainfall will occur. This was investigated for the rainfall samples by plotting $\delta^{18}O$ vs height and $\delta^{2}H$ against height. Taking height as the controlled variable in each case a least squares regression line was fitted to the data sets giving:

$$\delta^{18}O = -0.0029 \times \text{altitude (m)} + 1.99 \quad (6)$$

$$\delta^{2}H = -0.0148 \times \text{altitude (m)} + 10.82 \quad (7)$$

The values of the coefficients of determination for equations 6 and 7 are 0.32 and 0.24 respectively, indicating significant scatter in the data. It is thought that this is largely caused by the limited number of samples obtained from each station. Individual rainfall events at a given station can give widely differing isotopic results, as shown in Table 5.6, because evaporation and temperature effects will be different for different rainfall events. Many samples from a given station would however be expected to have isotopic compositions which fall around a mean, dependent mainly on the altitude.

The change in $\delta^{18}O$ is estimated as -0.29‰ (i.e. decrease) for every 100 m of ascent from equation 6. This compares favourably with values obtained elsewhere; i.e. -0.2‰ for Sweden, -0.4‰ (French Alps), -0.28‰ (Czechoslovakia), -0.26‰ (Nicaragua), -0.18‰ (Cameroon), -0.16‰ (Greece) (Figures quoted in Darling and Lardner, 1985). Few studies of deuterium variation with height are available but it is assumed that if the figure for oxygen is accepted, then the estimated variation of -1.5‰ per 100 m for $\delta^{2}H$ from equation 7 can also be accepted because of the close correlation between $\delta^{2}H$ and $\delta^{18}O$ described by equation 3.

The possible effect of latitude on the isotopic characteristics of the rainfall samples has been examined by plotting the isotopic variation with height for samples from the southern (Nairobi and Narok 1:250,000 maps), central (Nyeri and Kisumu maps), and northern (Rumuruti, Eldoret, Maralal and Turkana maps) areas respectively. This showed some evidence of a decreasing trend in the amount of isotopic variation with height changes from south to north, with the central area falling most closely on the line described by equations 6 and 7. However the coefficients of determination were low, and the hypothesis of a latitude dependent effect is regarded as inadequately supported by the available data. Also there was no evidence of a systematic variation in isotopic composition from one side of the Rift to the other.

5.3.3 Surface and Low Temperature Groundwater: Suswa to Nakuru.

In this area a typical stable isotope value for groundwater from the side of the Rift is -28‰ $\delta^{2}H$, -4.8‰ $\delta^{18}O$, which is similar to values measured on the Kinangop plateau (Figures 5.1d and 5.1e). Slightly lighter Rift-wall waters were measured (up to -35‰ $\delta^{2}H$, -5.3‰ $\delta^{18}O$) in a few places, but there is no evidence of the highly depleted isotopic compositions presumed to exist in the Nyandarua (Aberdare) Mountains to the northeast and which are measured in

the main river (River Malewa) feeding Lake Naivasha. The implication is that the mountains are drained chiefly by surface water whose depleted composition is masked by the high evaporation acting on Lake Naivasha, the local sump for surface drainage.

The typical Rift-wall composition of -28‰ δ^2H, -4.8‰ $\delta^{18}O$ does not accord particularly well with the isotope-altitude relationships propounded in the previous section, but these are necessarily tentative and probably more important as relative indicators of altitude. In this sector of the Rift unmodified meteoric water appears to range from -35‰ to about -18‰ δ^2H, an altitude difference of some 700 m. The corresponding $\delta^{18}O$ range is -5.3 to -3.5‰ suggesting a difference of 600 m.

In contrast to the well waters on or near the side of the Rift, lakewaters are highly enriched in heavy isotopes owing to the great potential for evaporation. While lakes Elmenteita and Nakuru are discharge areas within an almost closed drainage basin, Lake Naivasha is a source of recharge to the Rift and provides a very effective tracer for axial groundwater movement. The typical Naivasha composition is +35‰ δ^2H, +6.6‰ $\delta^{18}O$, and it is possible to draw contours (where there are sufficient well data) showing the approximate percentage of lakewater in the mixing series between lakewater and groundwater (Figure 5.7). If certain assumptions about the production of fumarole steam are made it is possible to infer groundwater compositions beneath thermal centres; while these data have been added to Figure 5.7 their calculation is explained in the next section.

Most of the groundwater sampled in this part of the Rift can be explained in terms of unmodified rainfall or of rainfall mixed with lakewater. There is no evidence for a third source of water with thermal characteristics (for instance with a pronounced $\delta^{18}O$ shift) underlying the area at depth. The greatest mixing effects are demonstrated in the wells close to Lake Naivasha, which have an obvious lakewater contribution . Since the lake is on the topographic culmination of the Rift floor, discharge to both north and south may be expected. Unfortunately well data are concentrated on the east and west sides of the lake, and the only strong indication of the presence of lakewater elsewhere (apart from high-temperature geothermal sources) comes from the warm springs near the southern end of Lake Elmenteita some 30 km to the north. These suggest a 30% contribution from Lake Naivasha. To the northeast of the lake the River Malewa debouches into a swamp which ultimately must recharge the lake, and there is accordingly no evidence of heavily-evaporated water here. While the influence of the lake is seen up to 6 km away SSE of the lake, data from the western side suggest that there is very little flow to the west.

The warm springs at the southern end of Lake Elmenteita show evidence of water from Naivasha, as already mentioned. A few kilometres to the northeast and southwest of the springs typical Rift-wall water compositions of -24‰ δ^2H are seen (36 and 124). The flow of (already considerably diluted) lakewater to the north therefore passes through a relatively narrow constriction at this point. Beyond this well data are sparse, and the effects of discharge at the northwest end of Lake Elmenteita of considerably enriched water would in any case obliterate evidence of Naivasha water. Although Lake Nakuru is assumed (like Elmenteita) to be extremely enriched in heavy isotopes, there are only limited signs of this in wells to the northwest of the lake. The implication of this is that flow out of this basin is very small and most water is lost by evaporation. Alternatively, if there is a greater flow to the northwest from the lake it is being rapidly diluted by a comparable amount of flow from the sides of the Rift (particularly from the west).

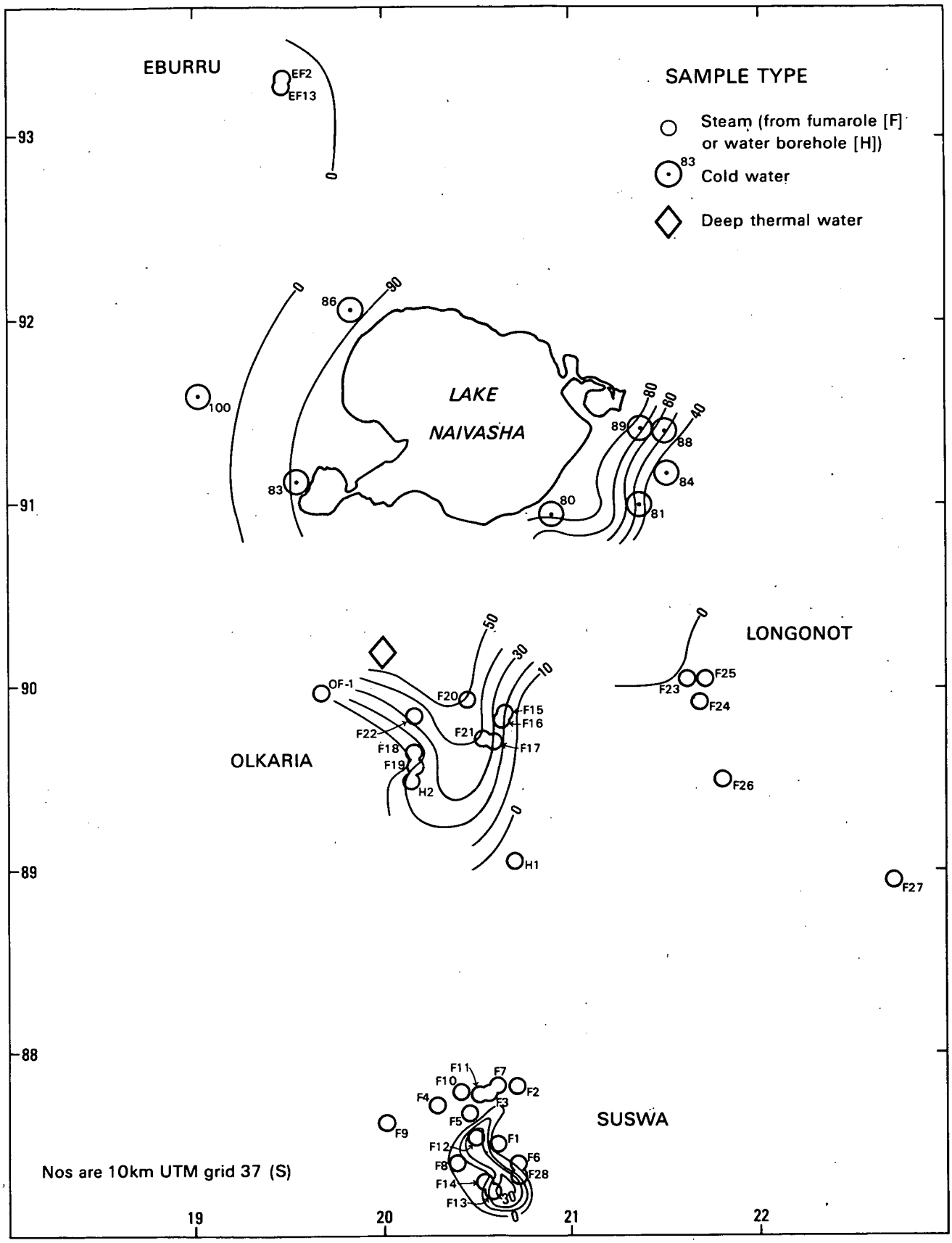

Figure 5.7 Contour map showing the contribution of Naivasha lakewater to groundwater in the Suswa-Eburru sector, based on geochemical evidence from wells, springs and fumaroles. Contours are in percent lakewater.

5.3.4 Thermal Waters: Suswa to Eburru.

Steam condensate from fumarolic discharges on Suswa, Longonot Domes, Olkaria, Eburru and surrounding areas was collected for analysis, much of it by Dr. H. Armannsson of the UNDP. (Site details are provided in Appendix 7) Deep thermal fluid was sampled from some of the wells in the E. Olkaria geothermal field which, although only a small area on the maps in Figures 5.1d and 5.1e, is of extreme importance as the only location in this part of the Rift where the total geothermal fluid can be sampled.

The geochemistry of Olkaria-Hell's Gate area is dealt with in greater detail in Section 6.2, but the total fluid compositions from the wells are plotted together with steam condensates from all fumaroles on Figure 5.8. The steam condensate samples form an elongate group, parallel to the meteoric line for the Rift, and covering a large range, approximately -1 to -15‰ $\delta^{18}O$. There is no sign of a conspicuous $\delta^{18}O$ shift in the fumarole results or the Olkaria thermal fluid.

On the basis of the steam results it is proposed that most, if not all, of the fumarole condensates are products of steam separation from a mixing series between Naivasha lakewater (+36‰ $\delta^{2}H$, +6.6‰ $\delta^{18}O$) and Rift-wall groundwater (-30‰ $\delta^{2}H$, -5.0‰ $\delta^{18}O$). This situation may be slightly complicated by a small $\delta^{18}O$ shift (maximum 1.5‰) suggested by the Olkaria results.

To demonstrate this hypothesis, Figure 5.9 shows a δ- plot of all steam samples together with theoretical lines formed by primary steam separation from various dilutions of lakewater with Rift-wall water allowing for a small (1‰) $\delta^{18}O$-shift. The resulting temperature ranges (100-260°C) form parallel curves with a gradient somewhat steeper than the KRML, and several of the fumarole groups form dispositions sub parallel to these calculated lines - e.g. Longonot, Hell's Gate and Suswa caldera floor - suggesting that the interpretation may be justified. Samples lying outside the primary steam range are likely to be caused by local conditions - for example the fumaroles from the Eastern Olkaria wellfield appear to derive from steam heated groundwater, and the more depleted waters from Suswa may be the result of steam condensation, a process considered by Darling and Armannsson (in prep.). In addition, the primary steam envelope would itself be subject to possible local dilution effects and small variations in $\delta^{18}O$ shift.

The steam data from each region are now considered in terms of the lakewater mixing model. Starting with Eburru, the most northerly high-temperature manifestation in this sector of the Rift, it can be seen on Figure 5.9 that the samples obtained from EF2 lie beyond the influence of lakewater. This implies that water from Naivasha does not flow beneath Eburru during its passage northwards. Eburru EF2 shows some evidence of local dilution effects, but the presence of He and H_2 in the accompanying gases confirm that the steam is basically primary and derived from local Rift-wall groundwater. This is confirmed by the outflow from Eburru which affects the chemistry of wells at sites 121, 122, 124 and 125. These waters have a basic Rift-wall isotopic composition but their chemistry is clearly the result of thermal processes - they contain for example high silica, lithium and bicarbonate, as well as having a high gas content (mainly CO_2) and a $^{3}He/^{4}He$ ratio similar to EF2 (Table 5.11). EF13, on the other hand, is highly depleted in heavy isotopes and can only easily be explained by a large degree of steam condensation below surface. The very low gas content of this fumarole (Z. W. Muna, pers. comm.) tends to confirm that it is not unmodified primary steam.

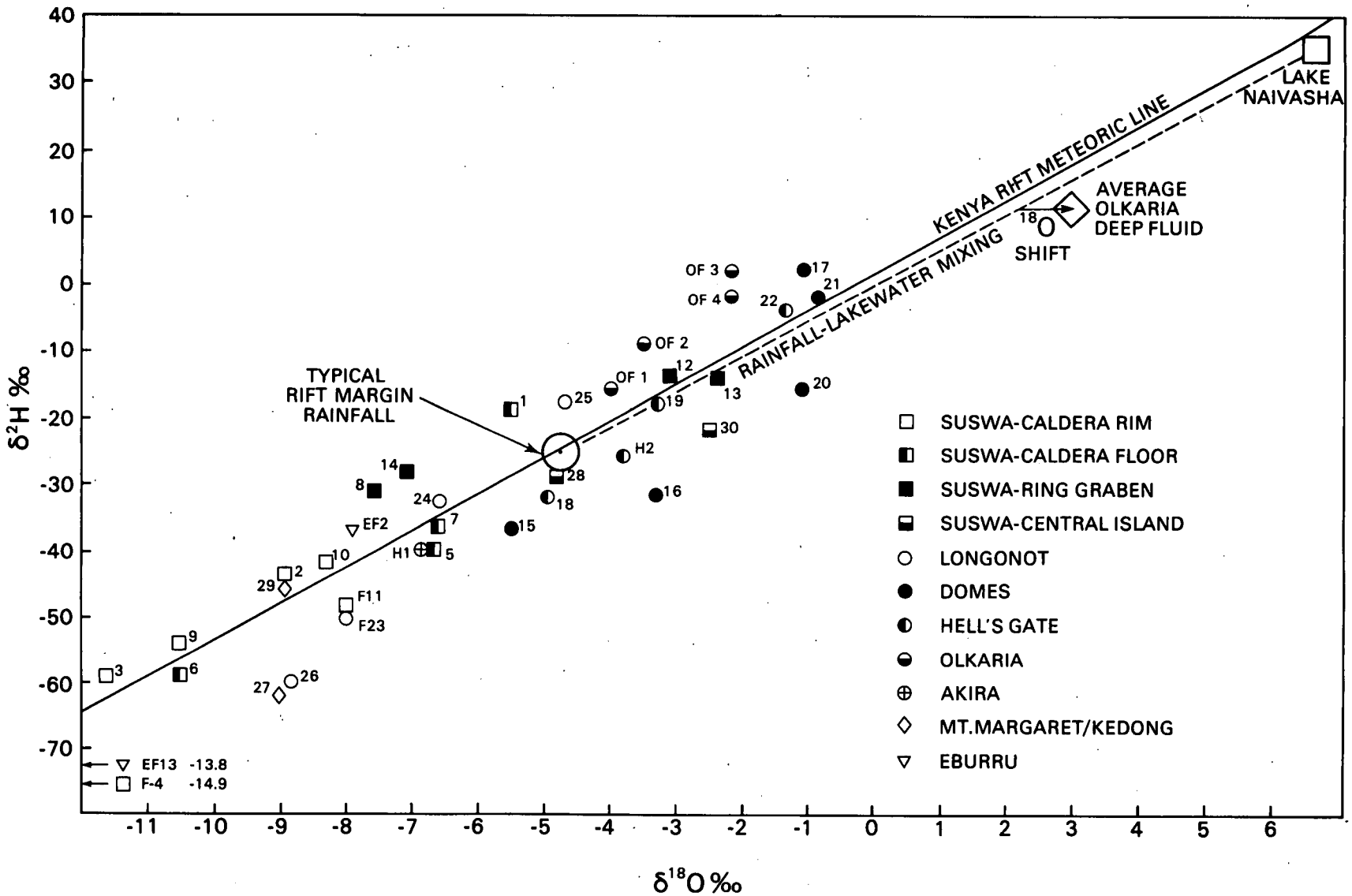

Figure 5.8 Delta-diagram of fumarole condensate stable isotope data from the Suswa-Eburru sector.

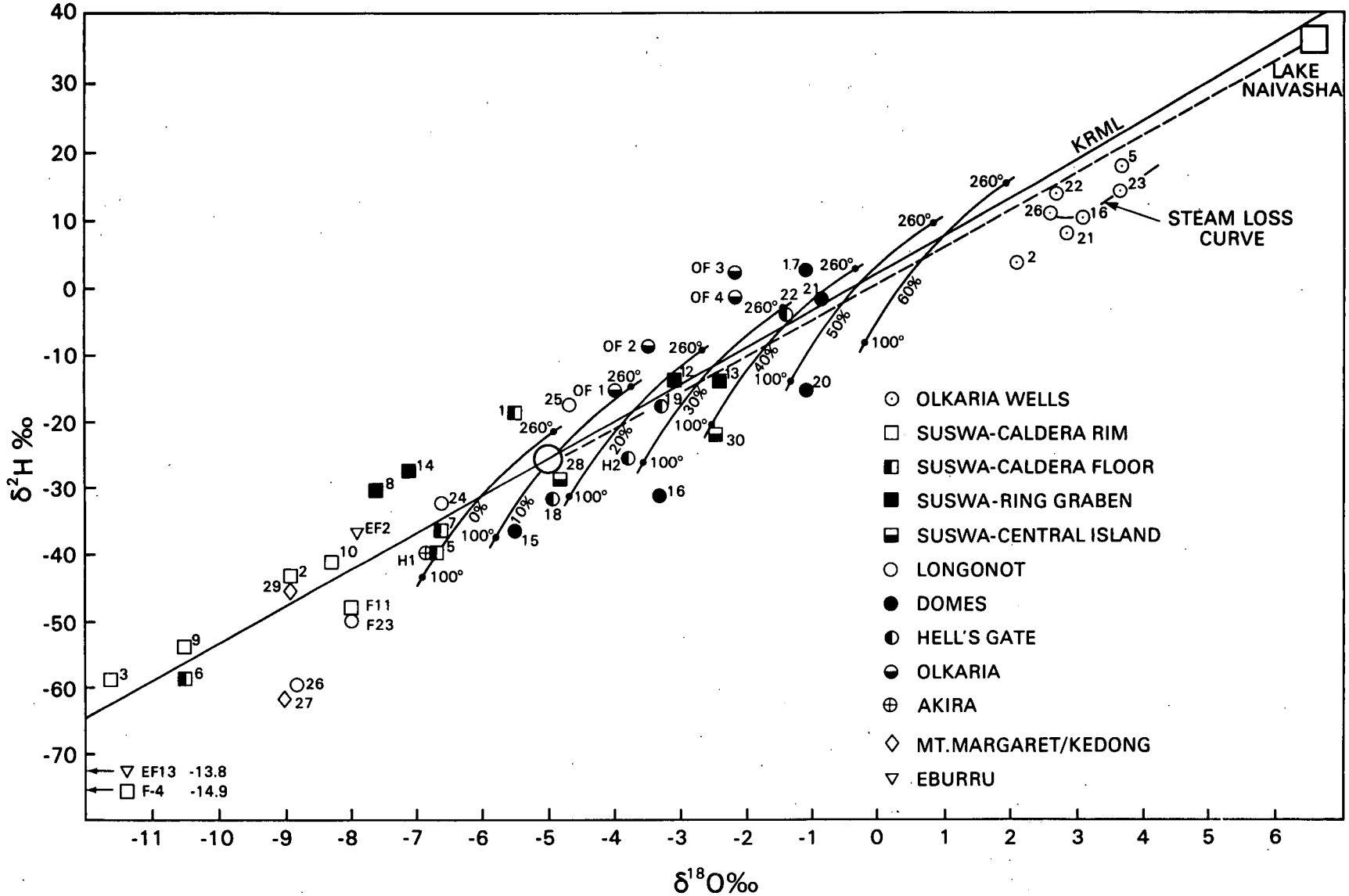

Figure 5.9 Fumarole stable isotope data shown in relation to primary steam production from a groundwater-lakewater mixing series. The curves show the percentage of lakewater contributing to steam.

The fumaroles in the Olkaria and Hell's Gate area are treated in more detail with the Olkaria wellfield in Section 6.2, but all show the influence of lakewater to a greater or lesser extent. In the Domes area east of Hell's Gate, the fumaroles generally show compositions suggesting more than 30% lakewater in the thermal fluid. The Longonot crater fumaroles (F23-25) on the other hand imply little or no lakewater at depth, while the fumarole on the southern slopes of the volcano (F26) and those of the eastern part of the valley beyond, Mt. Margaret (F27) and Kedong (F29) suggest that no lakewater reaches these areas.

The Suswa area has four different zones: caldera rim, caldera floor, ring graben and central island, and this zonation is partly reflected in the condensate stable isotope results (Figure 5.9). In general only samples from the ring graben and central island show evidence of lakewater content, with F8 and F14 showing evidence of steam heating. A small hot spring (56°C) in the ring graben was recently discovered (M C G Clarke, pers. comm.) which yielded a result of -25‰ δ^2H, -4.5‰ $\delta^{18}O$. This composition probably represents the residual water remaining after the steam heating responsible for F8 and F14, and implies that local rainfall on Suswa meets ascending steam as it percolates downwards. Caldera rim and floor samples are in general depleted and are probably the results of local dilution processes and/or (especially in the case of the most depleted samples) condensation processes; it is known from gas analyses (Section 5.6) that at least some of the rim fumaroles contain a component of air.

The fumarole data have been added to the contour map of lakewater dilution based on well water analyses (Figure 5.7). The fumarole data suffer some disadvantages (assumptions of origin, probable large variations in depth and tortuosity of routes to the surface) but by and large provide a plausible picture of southward flow from Lake Naivasha, perhaps largely confined in width to the E. Olkaria-Domes area but large enough in volume to form up to 30% of the water beneath parts of Suswa. The fumaroles of the Suswa caldera floor and rim are on the direct path of this supposed flow to the south, yet show few signs of direct derivation from the flow. Either the steam has been much modified by dilution and/or condensation as discussed above, or perhaps less likely, a strong flow of Rift-wall water is entering the system from the west.

Owing to the lack of opportunities to sample water or steam south of Suswa it is impossible to say how far towards Lake Magadi the influence of Naivasha water may extend. Inasmuch as 30% lakewater could be present 30 km south of Naivasha it may be assumed that recharge from the Rift walls will have diluted lakewater beyond recognition at perhaps 50 km south of the lake, so that it would be impossible to identify the influence of Naivasha water on Lake Magadi, some 100 km away.

In summary, it has been demonstrated that most fumarole isotope ratios can be explained by production of steam (suitably modified in certain cases) from a mixing series between Rift-wall meteoric water and evaporated water from Lake Naivasha. No evidence of any deeper reservoir of singular composition has been seen, and it appears that oxygen shifting of the dimensions commonly seen in other geothermal systems does not exist. It should be remembered that $\delta^{18}O$ shifting is dependent on a combination of residence time, initial rock and water $\delta^{18}O$ values and the porosity of the system(s). Not enough is yet known about rock $^{18}O/^{16}O$ ratios to comment on the rather low $\delta^{18}O$ shifts.

The conclusions of this report regarding the significance of fumarole

isotopes are broadly similar to those of Armannsson (1987b) in that he proposed mixing between unmodified Rift-wall water and a deep thermal water of an evaporated origin. Isotope data reported here (Section 6.2) have shown that Olkaria must be considered to be part of the general hydrothermal system in the area, and that Lake Naivasha is therefore the source of this evaporated water.

5.3.5 Surface, Thermal and Non Thermal Waters: Nakuru to Silale.

Various thermal and associated waters were sampled from the Nakuru area to a point some 170 km further north near the Silale volcanic centre. Stable isotope results are given in Tables 5.1 and 5.5 and are shown in Figures 5.4c and 5.4d.

As discussed in the previous section, there appears to be comparatively little outflow from the almost closed basin of Lake Nakuru. Between this lake and Lake Bogoria to the north, groundwater stable isotope values are similar to those from the valley floor further south and average -16‰ δ^2H, -2.9‰ $\delta^{18}O$. Despite the fact that some of these waters are slightly thermal (up to 43°C, Figure 5.4a) they probably all represent unmodified Rift-floor rainfall with the thermal waters similar in provenance to the Kariandusi warm spring (35).

At Lake Bogoria itself a wide variation in stable isotopes is seen, ranging from unmodified Rift-floor recharge through boiling springs to highly evaporated lakewater. Figure 5.10 shows the various waters plotted on a delta-diagram. Non-thermal or slightly thermal waters cluster round the local Rift meteoric line at about -13‰ δ^2H, -2.8‰ $\delta^{18}O$ and are presumably derived from local recharge in the hills around the lake, The three boiling springs sampled have rather heavier compositions, whereas the lakewater itself is extremely enriched in heavy isotopes due to the large amount of evaporation taking place from the closed basin.

It was suggested by Glover (1972) that slightly thermal water underlying the general area reacts both with ascending steam and with lakewater, while Geotermica Italiana (1987) postulated a ternary mixing model involving local groundwater, thermal water and lakewater. The few data reported here do not support the steam heating model, but neither do they prove the ternary mixing hypothesis. Although the three boiling springs do not lie directly on a dilution between the regional cool springs and the extremely evaporated lakewater, their position is consistent with steam loss from points along this line (Figure 5.10). To this extent the contention that lakewater is involved is likely to be correct (and indeed the situation of the boiling springs on the lakeshore makes this very likely) but there is no evidence that steam with a different isotopic composition is playing a part in the process. It appears from the isotopic evidence that regional shallow groundwater could be suitable as a source for the thermal fluid, and that the somewhat enriched isotopic compositions seen in the boiling springs are due more to steam separation than to a lakewater contribution. There is no isotopic evidence from these results for the slightly heavier thermal water invoked by Geotermica Italiana (1987), which could probably only come from a source like Lake Baringo. While subsurface flow counter to the general dip of the Rift floor to the north in this area cannot be ruled out, it is unlikely. This is not to rule out the possibility of the boiling springs being the product of a complex mixing process between shallow groundwater, thermally modified groundwater and lakewater - Section 5.2.2.

Lake Baringo is a 'freshwater' lake which in view of the lack of surface

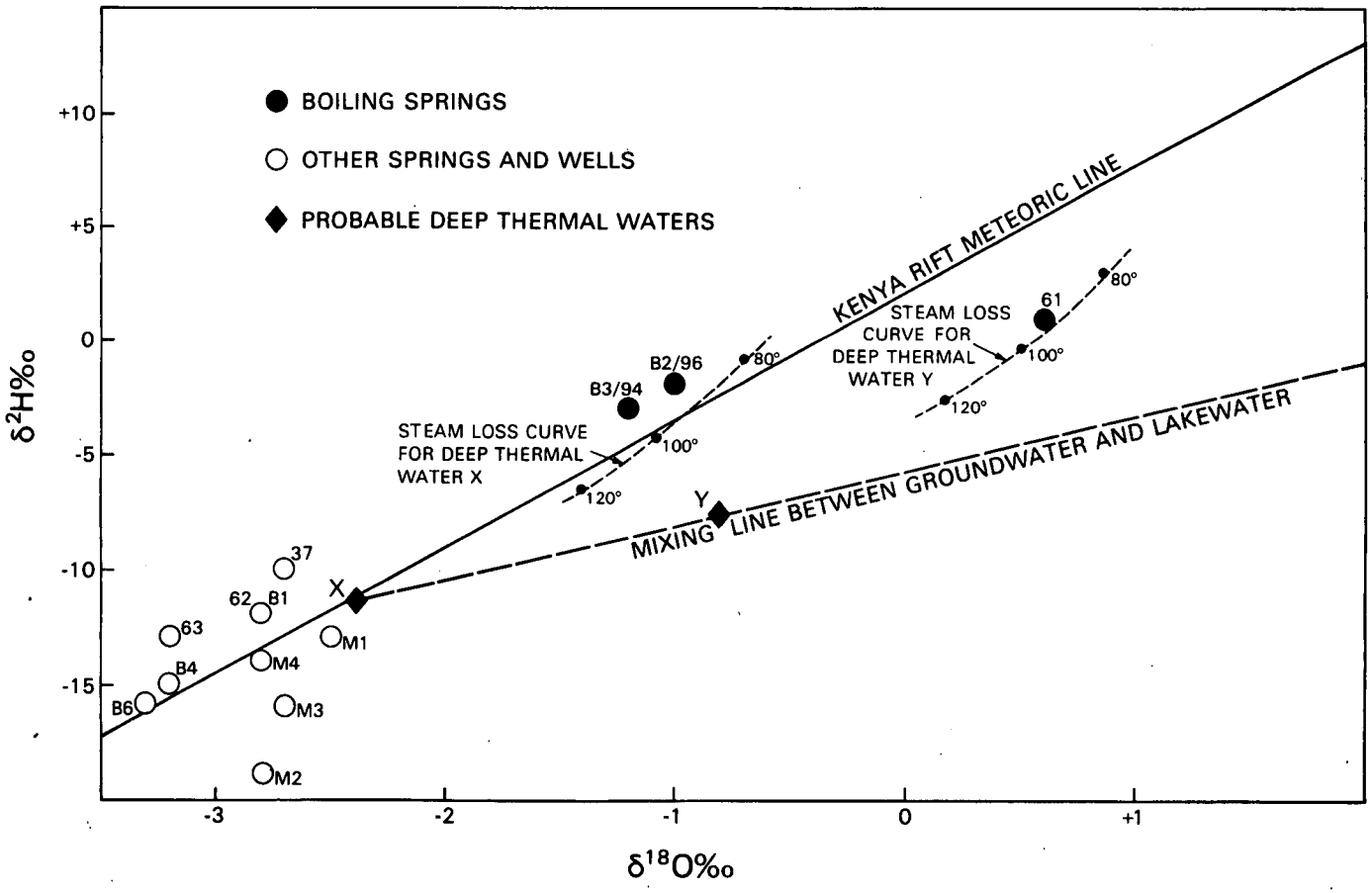

Figure 5.10 Delta-diagram of stable isotope data from groundwaters, thermal waters and lakewater of the Lake Bogoria region.

outflow must have a considerable subsurface egress. In this respect it may be compared to Lake Naivasha, though unlike that lake outflow is likely to be restricted to a northerly direction. Only two sites were sampled at the lake - a boiling spring on the central, remnant volcanic cone island of Ol Kokwe, and the lakewater itself. The results are shown on a delta-diagram in Figure 5.11. It can be seen that the lakewater is highly evaporated, though to a much lesser extent than the stagnant Lake Bogoria. The boiling spring on the central island lies on a direct dilution line between the local shallow groundwater (presumed to be similar to that of the Bogoria area) and the lakewater, and might therefore be assumed to be the product of heating a mixture of both waters by steam. However as demonstrated by the results considered in Section 5.2.2 (and pointed out by Glover, 1972), the boiling spring contains a much higher TDS content than the lakewater and cannot therefore be the result of steam heating of lakewater. In spite of this it seems clear that the boiling spring is related to lakewater in some way: the isotopic content of the spring water is too enriched to be simply the result of steam loss from thermal water derived from shallow Rift-floor recharge. It appears that any mixing between lakewater and shallow groundwater must take place in the deep geothermal system, with the upflow into the central island being largely unaffected by the lakewater, however unlikely this may seem at first sight.

Subsurface discharge from Lake Baringo to the north should be detectable in wells, springs and perhaps fumaroles north of the lake, though only sites at Kapedo and Lorusio were sampled. These sites are some 50 and 60 km away respectively, and by analogy to the Naivasha outflow little evidence of lakewater would be likely to remain. Although two of the Kapedo group of springs show enriched isotope values (Figure 5.11) these are not on the dilution line between presumed local groundwater and lakewater, and instead are more likely to represent evaporative enrichment from the local groundwater.

The Lorusio springs are hotter than the Kapedo springs, and the average isotopic composition is shown in the delta-diagram in Figure 5.11. It is apparent that it is slightly lighter than any of the Kapedo group and may therefore be derived more from the Rift wall than the floor. Though the two groups of springs are relatively close to each other it is unlikely that Kapedo is diluted Lorusio water; not only is it difficult to see what the positive end member could be, but it would also imply a southerly flow, which is contrary to the general flow direction in this part of the Rift. On these grounds therefore it is considered that the two groups are unrelated manifestations.

5.4 Stable isotopes - carbon

Differences in the $^{13}C/^{12}C$ ratio relative to that of the Pee Dee Belemnite (PDB) zero standard were measured on dissolved inorganic carbon (DIC) precipitated from water as $BaCO_3$, or directly on CO_2 gas. Results are reported in Table 5.7.

Most samples were collected from the Suswa-Nakuru sector of the Rift and the distribution of sampling points is shown in Figure 5.1f). In this area quite a large variation in $\delta^{13}C$ DIC is seen, ranging from around 0 to -16.5‰. The isotopic value of DIC depends primarily on the values of soil CO_2, rock carbonate, and amount and temperature of water-rock contact. The interpretation of $\delta^{13}C$ DIC can therefore be complicated in areas such as the Rift where crustal CO_2 is present in considerable amounts (Bailey 1980).

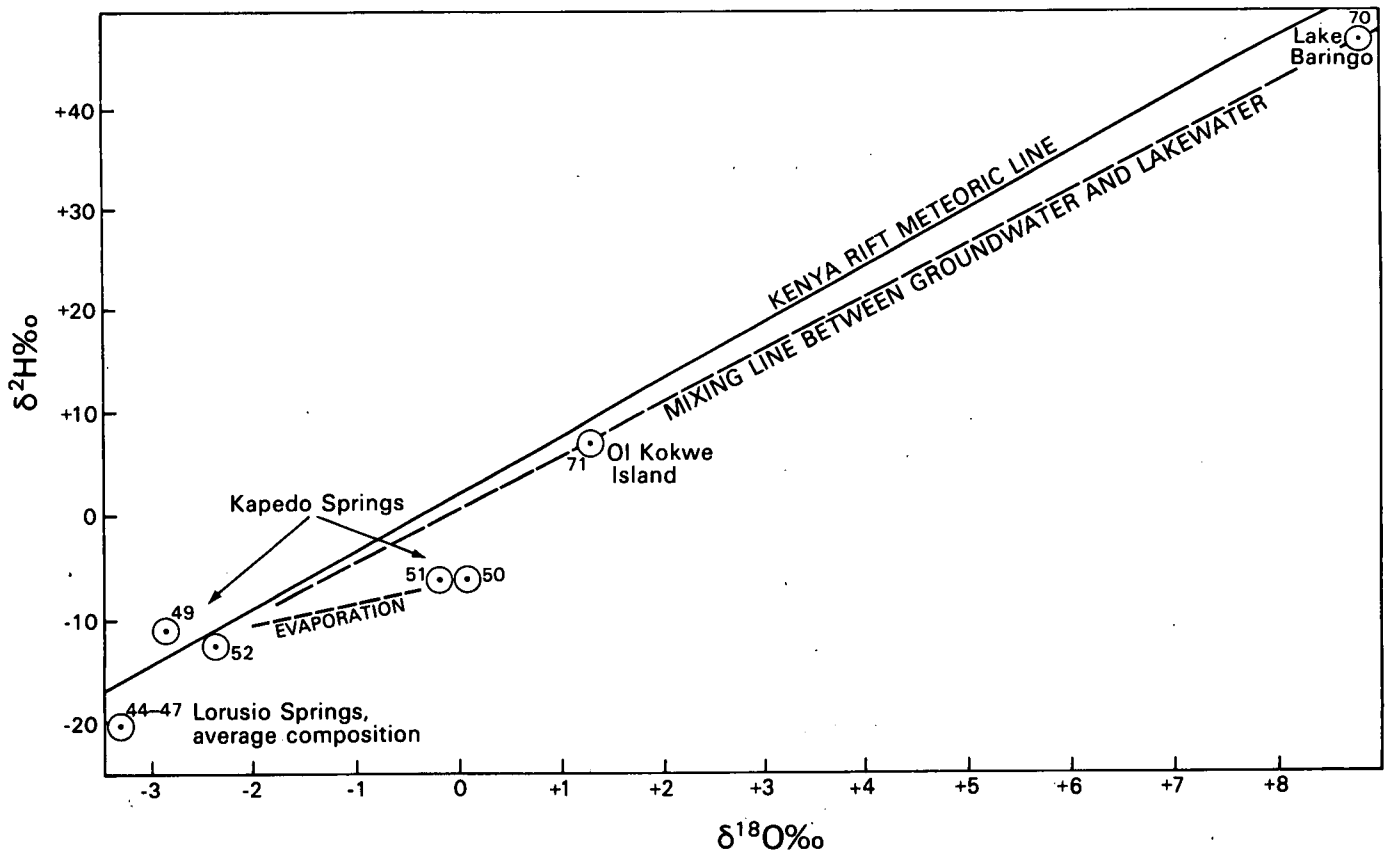

Figure 5.11 Delta-diagram of stable isotope data from thermal waters and lakewater of the Lake Baringo region.

Table 5.7 Carbon stable isotope data for Rift Valley water and gas samples.

Site No.	Site Name	$\delta^{13}C_{DIC}$	$\delta^{13}C_{CO_2}$	$\delta^{18}O_{CO_2}$
		------ ‰ PDB ------		‰ SMOW
25	Kijabe RVA	- 7.4		
26	Kijabe Spr	-12.6		
28	Mayer's Fm	-16.5		
29	Mt Margaret*		-1.7	+34.4
31	Akira H-1*		-2.1	+32.8
35	Kariandusi Spr	- 8.0		
53	Bala Springs	- 1.7		
57	Bala Springs	- 2.3		
74	Magadi NW	+ 0.9		
75	Oltopesi	- 7.4		
81	C567	- 0.4		
82	C4178	-13.5		
92	Kanyamwi Fm	- 2.5		
96	Kinangop P65	-12.0		
100	C1404	-10.6		
104	Hell's Gate seep 2	-11.0		
110	Olkaria OW2	-10.2	-2.7	+41.9
111	Olkaria OW26	- 4.8	-2.4	+42.5
112	Olkaria OW22	- 7.5		
114	Olkaria OW23	- 5.1		
115	Olkaria OW21	- 7.1		
116	Olkaria OW5	-14.6		
118	Nakuru No. 7 (Lanet)	- 8.7		
119	Eburru EF-2		-2.3	+36.3
121	C431	- 0.5		
123	W Olkaria fumarole		-2.8	+37.2
124	Soysambu DEL	- 2.7	-6.6	+37.1
125	C1990	0.0		
127	Domes F-15*		-3.0	+35.7
128	Longonot F-23		-3.5	+29.5
UNDP 51	Longonot F-23		-4.4	+29.5
UNDP 44	Suswa F-28		-3.7	+36.6
UNDP 43	Suswa F-12		-3.2	+37.8

C_{DIC} = dissolved inorganic carbon C and O_{CO_2} = carbon dioxide

* = samples collected by UNDP

In Section 5.5 two possible rock carbonate values are considered for ^{14}C modelling purposes, with a value of -5‰ being chosen as the more likely value owing to the presence of carbonatitic volcanism in the Rift. Three carbonatite samples from the Homa Bay area to the west of the Rift had $\delta^{13}C$ values of -3.0. -4.2 and -8.2‰ respectively, so a figure of -5‰ is a reasonable compromise. Assuming soil zone carbon dioxide to have a value of about -26‰, a minimum $\delta^{13}C$ value after stoichiometric dissolution would be around -15.5‰. One sample, from Mayer's Farm (28) is close to this value at -16.5‰, which tends to confirm the young age of this water. Other samples indicating only small amounts of post-dissolution ^{13}C exchange are seen on the eastern flanks of the Rift (Kijabe warm spring, Kinangop P65 - sites 27 and 96) or in wells which appear to derive their water from the flanks, such as Ndabibi (100) in the west and Naivasha C4178 (82) in the east. Slightly heavier $\delta^{13}C$ DIC values are seen at lower altitudes, perhaps because the waters are slightly warmer and able to exchange ^{13}C more readily (though the Kijabe warm spring on the Rift flank (26) does not show such exchange while the RVA well (25), which is cooler, does).

All these waters could be the product of dissolution of rock carbonate by soil-derived CO_2 followed by isotope exchange or incongruent solution. Other Rift waters are significantly heavier in $\delta^{13}C$ DIC. In the case of a site like C567 (81) this is attributed to the high proportion of lakewater present in the well: $\delta^{13}C$ in lakewater tends to become heavier with the loss of CO_2 accompanying evaporation, which can be seen from Table 5.15 to have caused calcite to rise to saturation level. This may also be the explanation for the positive $\delta^{13}C$ DIC from the Magadi N.W. lagoon springs (74, Section 7). For sites like the 'badlands' wells (121,124 and 125) and the Bala springs of the Homa Bay area (53 and 57) magmatic CO_2 of about -3‰ is probably playing an important role in the carbon isotope systematics, tending to drive $\delta^{13}C$ DIC towards zero or even positive values because of the positive CO_2-DIC fractionation at lower temperatures. In the case of site 124, where both CO and DIC were measured, the amount of fractionation (3.9‰) was exactly as predicted for the sampling temperature (Table 5.8). Site 125 appears to posess the greatest contribution from magmatic CO_2 of the three 'Badlands' wells sampled.

At Olkaria, the only other location where both $\delta^{13}C$ CO_2 and $\delta^{13}C$ DIC were measured, equilibrium between the two phases was not well established according to the calculated separation temperatures (Table 5.8). This may be because of insufficient time for re-equilibration to occur between reservoir and wellhead, though neither OW2 or OW26 appear to be in equilibrium at reservoir temperatures (Section 6).

Carbon dioxide in the Suswa-Nakuru part of the Rift has a $\delta^{13}C$ of -3‰ with a standard deviation of 0.7. These may be typical volcanogenic values, but are not always associated with volcanic centres; cold CO_2 'mofettes' are known from the Rift and beyond - for example two wells at Meru, east of Mt. Kenya, each gave a $\delta^{13}C$ value of -3.5‰. This tends to confirm the idea of a pervasive CO_2 flux having a deep crustal origin over a wide area (Bailey, 1980), and indicates that a $\delta^{13}C$ of around -3‰ is not an infallible indicator of thermal activity. One methane-containing sample (from Eburru) was analysed for its $\delta^{13}C$ content - see Section 5.7.3.

The carbon stable isotope results can be summarised as follows. They provide a measure of the approach to equilibrium, if any, of DIC and rock carbonate, which can be broadly related to a combination of residence time and temperature, and which is essential for radiocarbon modelling purposes. They discriminate between 'normal' waters and those being affected by injection of

Table 5.8 Radiocarbon uncorrected and WATEQF-ISOTOP modelled Rift Valley groundwater ages, with equilibrium $\delta^{13}C$ CO_2 values.

SITE NO	$A^{14}C$	Unc. Age	$\delta^{13}C_{DIC}$	$\delta^{13}C_{CO_2}$	$\delta^{13}C_{CO_2}eq$	^{14}C CORRECTED AGES IN YEARS			
						$\delta^{13}C_r = 0$	$\delta^{13}C_r = -5$	$\delta^{13}C_r = 0$	$\delta^{13}C_r = -5$
	PMC	Yrs	———	$^{o}/_{oo}$ PDB	———	——— $pH_I = 5$ ———		——— $pH_I = 8$ ———	
16	-	-	-12.6	-	-18.2	-	-	-	-
25	6.2	22500	-7.4	-	-14.2	9136	4823	16405	8249
27	-	-	-12.6	-	-18.8	-	-	-	-
28	78.6	2060	-16.5	-	-23.7	——— MODERN ———		——— MODERN ———	
35	-	-	-8.0	-	-15.9	-	-	-	-
53	-	-	-1.7	-	-6.2	-	-	-	-
56	-	-	-2.3	-	-6.6	-	-	-	-
74	-	-	+0.9	-	-8.2	-	-	-	-
75	-	-	-7.4	-	-16.5	-	-	-	-
81	-	-	-0.4	-	-6.8	-	-	-	-
82	91.4	900	-13.5	-	-20.9	——— MODERN ———		——— MODERN ———	
92	62.8	3980	-2.5	-	-8.9	——— MODERN ———		——— MODERN ———	
100	86.0	1450	-10.6	-	-16.6	——— MODERN ———		——— MODERN ———	
104	-	-	-11.0	-	-17.6	-	-	-	-
110	-	-	-10.2	-2.7	-9.7	-	-	-	-
111	-	-	-4.8	-2.4	-4.1	-	-	-	-
112	-	-	-7.5	-	-6.9	-	-	-	-
114	-	-	-5.1	-	-4.5	-	-	-	-
115	-	-	-7.1	-	-6.5	-	-	-	-
116	-	-	-14.6	-	-14.0	-	-	-	-
118	94.7	700	-8.7	-	-14.8	700	MODERN	——— MODERN ———	
121	-	-	-0.5	-	-6.1	-	-	-	-
124	4.0	26190	-2.7	-6.6	-6.6	26190	8388	——— MODERN ———	
125	-	-	0.0		-6.4				

A = activity

PMC = percent modern carbon

Unc = uncorrected

pH_I = initial open system pH

$\delta^{13}C_{DIC}$ = dissolved inorganic carbon

$\delta^{13}C_{CO_2}$ = measured CO_2 value

$\delta^{13}C_{CO_2}eq$ = calculated equilibrium CO_2 value

$\delta^{13}C_r$ = rock carbonate value

crustal CO_2 or evaporation. Fractionations between the various carbon species are potential geothermometers, but their use appears to be rather circumscribed.

5.5 Radioisotopes

5.5.1 Carbon-14

The radiocarbon content of groundwater was measured at 7 representative sites (Figure 5.1g). It was considered that an indication of groundwater age would be of use as a check on the flow rates deduced from physical modelling of groundwater movement. The uncorrected ages shown on Figure 5.1g are calculated on the basis of simple ^{14}C decay and take no account of addition of 'dead' carbon to the system. In general this addition comes from the dissolution of 'dead' rock carbonate phases by 'active' carbon dioxide produced in the soil zone; if rock and dissolved inorganic carbon $\delta^{13}C$ values are known or assumed, corrections to the groundwater 'age' can be attempted. Several correcting methods are available - in this case WATEQF-ISOTOP was used.

Table 5.8 shows the results of running WATEQF-ISOTOP with two initial pH values, 5 and 8, and using two different rock carbonate $\delta^{13}C$ values. In each case soil zone CO_2 is assumed to have been -25‰ PDB. Normally rock carbonate is assumed to be marine-derived and to have a $\delta^{13}C$ of about 0‰. This was used as a starting point to run the ISOTOP model, but in the Rift Valley a marine derivation for carbonate phases is unlikely. In view of the carbonatitic volcanism associated with the Rift, the model was run with a rock carbonate value of -5‰ PDB, a typical carbonatite value. In most cases the resulting ages are modern, irrespective of starting conditions. The two exceptions to this are from the DEL well on the Soysambu Estate and the Rift Valley Academy (124 and 25). Both these wells have a high bicarbonate content, especially the DEL well, and it is probable that the apparent ages are an artefact caused by the addition to the carbonate system of large amounts of crustal CO_2. Dissolved CO_2 from the DEL well was measured for ^{13}C content and the value, -6.6‰ PDB, was in exact agreement with the ISOTOP calculated equilibrium for the measured DIC $\delta^{13}C$ of -2.7‰ PDB. In reality these two waters are likely to be very much younger than the modelled ages, and by analogy with wells in similar positions within the Rift, e.g. Ndabibi C1404 (100) and Mayers Farm (28), are probably largely modern.

5.5.2 Tritium

The tritium content of representative groundwater was determined at Rift Valley sites (Table 5.9). In all cases except Lanet (Nakuru No. 7 W.S. well, site 118) values were well below 1 TR, suggesting that there is a negligible contribution from thermonuclear tritium and that accordingly the waters must be at least 25 years old. The slightly higher ^{3}H figure for Lanet can be compared with the ^{14}C value which gave the youngest uncorrected age of any of the Rift samples.

5.5.3 Implications of the radioisotope data

Sites where radiocarbon and/or tritium were measured were selected on the basis of their value in identifying groundwater flow paths. Thus radiocarbon samples were taken in the western side of the Rift floor at the Ndabibi and Soysambu estates (100 and 124), the central part of the Rift at Naivasha C4178 and Nakuru No. 7 (82 and 118) and the eastern flanks at Mayers Farm, Kijabe RVA and Kanyamwi Farm (28, 25 and 92). Mayers Farm and Kijabe RVA

Table 5.9 Tritium content of groundwaters from the Suswa-Nakuru sector of the Rift Valley.

Site No.	Site Name	Temp, ^{o}C	pH	TR	± σ
25	Kijabe RVA	35	7.95	0.09	0.14
28	Mayer's Fm	28	7.90	0.00	0.17
35	Kariandusi	39	6.6	0.34	0.16
82	Naivasha C4178	20	7.45	0.05	0.15
92	Kanyamwi Fm	24	7.30	0.34	0.16
96	Kinangop P65	23	7.00	-0.01	0.14
100	Ndabibi C1404	26	6.95	0.34	0.17
101	Kokot, Maiella	-	7.65	0.42	0.15
110	Olkaria OW2	34*	6.23*	0.19	0.14
111	Oklaria OW26	34*	6.05*	0.27	0.16
118	Nakuru No. 7, Lanet	28	7.00	1.64	0.16
124	Soysambu DEL	32	6.40	0.15	0.15

TR = tritium ratio (1 TR ≡ 1 atom of ^{3}H in 10^{18} atoms ^{1}H)

* = cooled water phase from wellhead separator

might particularly be expected to be associated with deep seated faults, and Nakuru No. 7 is situated on a prominent N-S lineation on the valley floor, but none of these sites indicates long residence times (except perhaps for a small component) once radiocarbon corrections have been made. Conversely, tritium measurements show that in places where rapid flow might have been expected, especially perhaps at the Kokot water collection gallery (101), water was of pre-thermonuclear age.

The radioisotope measurements therefore suggest that there are no slow, deeply circulating groundwater flow paths playing a significant role in the hydrogeology of this part of the Rift Valley. A small contribution from deeper groundwater cannot however be entirely ruled out by the radioisotope evidence.

5.6 Gases

5.6.1 CO_2 and permanent gases (excluding inert gases)

During the investigations in the Rift Valley, gas samples were collected for $\delta^{13}C$ analysis. Most of these samples were taken from fumaroles and wells between Suswa and Nakuru, though samples were also drawn from gaseous springs at Bala (on the Lake Victoria arm of the Rift), Lorusio (in the Rift Valley north of Lake Baringo), and the Meru area ESE of Mt. Kenya. While the isotopic results are discussed elsewhere in this report, the opportunity to carry out permanent gas analysis was taken and the results are presented in Table 5.10.

Excluding gases derived from the atmosphere, either originally or by entrainment or contamination, crustally-derived CO_2 dominates all samples, usually with CH_4 in second place, albeit at a much lower level. When H_2 and/or He are present, methane lies in third place. The low molecular weight gases diffuse very easily; the detection of both H_2 and He is taken as evidence of close proximity to a strong upflow, as at Eburru and Longonot, where the volcanic origins of the gas are confirmed by the helium isotope ratios. In the case of the Lorusio spring only H_2 is present; as a very similar H_2/CO_2 ratio to those of Eburru and Longonot is observed it may be that the springs are close to an upflow, though at a distance which allows escape of helium. The $^3He/^4He$ ratio was not measured for Lorusio and therefore cannot offer confirmation. At Bala He rather than H_2 was present - the He R/Ra value (next section) was not elevated much above the atmospheric level though total He was very high.

In the absence of H_2, He and H_2S (which was not measured) methane may be the best evidence of proximity to upflow (Armannsson, 1987a) and, by implication, deep fluid temperature. The results support this in a qualitative way, with for example Mt. Margaret (29), a relatively cool thermal area, having a much lower CH_4/CO_2 ratio than Eburru (119), which most other data suggest is a high temperature area. The shortcomings of CH_4/CO_2 as a geothermometer are however apparent (Section 5.7.2).

The ratio C_2H_6/CH_4 may be an index of a lakewater contribution, as discussed elsewhere in this report with relevance to the Olkaria area. In the Naivasha area the decline in C_2H_6/CH_4 is roughly in the order northern East Olkaria > West Olkaria > Domes > southern East Olkaria > Eburru > Longonot > Suswa, i.e. fairly consistent with increasing distance from the lake. The high ratio for the DEL well water (site 124) is likely to be an artefact of measurement at low concentrations, but Lorusio and Bala have apparently genuinely high C_2H_6/CH_4 ratios and it may be worth noting that Lorusio has

Table 5.10 Composition of fumarole, well and spring gas samples, excluding inert gases.

	gas composition						ratios by weight		
SITE NO	CO_2	CH_4	C_2H_6	H_2	He	R	CH_4/CO_2	H_2/CO_2	C_2H_6/CH_4
	%	%	vpm	%	%	%		x 10^{-3}	
29/F-27	57.7	0.092	0.5	nd	nd	42.2	0.58	-	10
31/H-1	27.9	0.20	7.5	nd	nd	71.9	2.6	-	7.0
44-47	66.6	0.051	4.0	0.63	nd	33.4	0.28	0.43	15.
53-54	44.0	0.32	15 *	nd	0.93	54.8	2.6	-	8.8
110	40.3	0.67	7.0	nd	nd	59.0	6.0	-	2.0
111	48.0	0.18	9.5	nd	nd	51.8	1.4	-	9.9
119	78.9	4.6	5.0	1.7	0.5	14.3	21.	0.98	0.20
123	74.4	0.37	11	nd	nd	25.3	1.8	-	5.6
124	74.3	0.001	0.5	nd	nd	25.7	0.01	-	94.
126	10.2	3 vpm	nd	nd	nd	89.8	0.01	-	-
127	17.4	0.13	2.5	nd	nd	82.5	2.7	-	3.6
127/F15	12.6	0.06	1.0	nd	nd	87.4	1.7	-	3.1
128	77.4	0.75	1.0	1.7	0.5	19.6	3.5	1.0	0.25
128/F-23	44.4	0.30	0.5	0.90	0.34	54.0	2.5	0.92	0.31
F-7	24.6	0.45	0.5	nd	nd	75.0	6.7	-	0.21
F-12	25.9	0.085	nd	nd	nd	74.0	1.2	-	-
F-28	66.0	0.41	1.0	nd	nd	33.6	2.3	-	0.46
K-1	35.8	0.010	nd	nd	nd	64.2	0.10	-	-
K-2	39.2	12 vpm	nd	nd	nd	60;8	0.01	-	-

* Sample also contained 3 vpm C_3H_8

R = residual gases including N_2, Ar, H_2S and possibly O_2 nd = not detected

Samples with F, H and K prefixes collected by Dr H Armannsson of the UNDP.

been believed to derive its water ultimately from Lake Baringo (though see Sections 5.2.2 and 5.3.5), while Bala is close to the edge of Lake Victoria. By contrast the Meru (Chogoria) springs which cannot be supplied by lakewater have very low CH_4 values and undetectable C_2H_6.

5.6.2 Helium and Inert Gases

Helium isotope ratios

The ratio $^3He/^4He$ was measured for 13 samples from the Suswa-Nakuru sector of the Rift and on one sample from the Bala springs on the edge of Lake Victoria. This latter sampling point had been chosen because a gas sample collected in 1985 indicated a high total helium content. Results are reported (Figure 5.1g, Table 5.11) in the conventional form of R/Ra, where R denotes the $^3He/^4He$ ratio of the sample and Ra the $^3He/^4He$ of air which effectively remains constant. Also shown in Table 5.11 are the He and Ne contents of each sample: He/Ne is a sensitive indicator of air contamination because the level of crustal neon is very much lower than that of air. Providing the amount of air contamination is small, a correction can be made to the original R/Ra value (Table 5.11). This was first proposed by Craig et al (1977) and takes the form:

$$(R/Ra)c = \frac{(R/Ra)(x-1)}{x-1}$$

where

$$x = \frac{He/Ne(sample)\beta Ne}{He/Ne(air)\beta Ne}$$

$(R/Ra)c$ = corrected R/Ra

βNe and βHe = Solubility coefficients for appropriate temperature

The results show that two samples possess helium contents essentially derived from air (Ndabibi C1404 and Nakuru No. 7, sites 100 and 118). While sampling procedures cannot be ruled out as causing this, other samples appear to have been satisfactorily collected using identical techniques. If accepted as genuine, the results tend to support the radioisotopic indications that these samples are very young waters which have largely conserved atmospheric inert gas ratios.

The remaining samples mostly have R/Ra values >1, indicating the presence of excess mantle helium to a greater or lesser extent. Samples collected as gas from fumaroles and geothermal wells tend to have the highest levels (corrected R/Ra values of 5.6-6.7 for Eburru, Longonot and Olkaria) but one water well (Soysambu DEL site 124) possesses a value in this range. Conversely two fumaroles, Suswa F3 and Domes F15 (126 and 127), have lower R/Ra values, though gas analyses suggest that these fumaroles have substantial amounts of entrained atmospheric gases which may be diluting any ^3He component.

The main significance of $^3He/^4He$ ratios within this sector of the Rift is that they do not show much evidence of transport of mantle helium up the deep faults presumed to exist at the sides of the Rift; for example Kanyamwi Farm well C570 and Kijabe Warm Spring (92 and 27) have values close to atmospheric, though the Kariandusi warm spring (35) does have an elevated level (but see next section for further comments on Kijabe). Instead the high levels are all associated with volcanic centres except for the Soysambu

Table 5.11 Helium isotope ratios in groundwaters and gases of the Rift Valley.

Site No.	Site Name	Sample Type	R/Ra	X	(R/Ra)c	He content ------ cm^3 STP/cm^3 or cm^3 STP/g	Ne content -------
26	Kijabe RVA	W	0.928	5	0.896	5.43×10^{-8}	4.52×10^{-8}
35	Kariandusi Spr	W	1.359	1.2	2.947	1.20×10^{-7}	4.28×10^{-7}
53	Bala Springs	W	1.446	85	1.434	2.86×10^{-3}	1.45×10^{-4}
92	Kanyamwi Fm	W	1.281	8.6	1.323	1.08×10^{-7}	5.45×10^{-8}
100	Ndabibi C1404	W	0.938	1.6	0.871	8.13×10^{-8}	2.09×10^{-7}
110	Olkaria OW2	G	5.682	383	5.694	2.67×10^{-5}	3.03×10^{-7}
111	Olkaria OW26	G	5.711	429	5.825	2.26×10^{-5}	2.29×10^{-7}
118	Nakuru No. 7, Lanet	W	1.005	0.9	1.040	3.48×10^{-8}	1.59×10^{-7}
119	Eburru EF-2	G	6.243	282	6.262	1.22×10^{-5}	1.88×10^{-7}
123	Olkaria W. field	G	5.651	881	5.623	4.12×10^{-6}	2.03×10^{-8}
124	Soysambu DEL	W	6.156	14	6.521	2.94×10^{-6}	8.96×10^{-7}
126	Suswa F-3	G	1.510	5	1.610	7.33×10^{-6}	5.80×10^{-6}
127	Domes F-15	G	2.789	17	2.921	5.16×10^{-7}	1.26×10^{-7}
128	Longonot F-23	G	6.482	32	6.656	2.96×10^{-5}	3.98×10^{-6}

W = water (well or spring) G = gas (fumarole or geothermal well) $R/Ra = \frac{^3H/^4H \text{ sample}}{^3H/^4H \text{ air}}$

X = correction factor (see text) (R/Ra)c = R/Ra corrected for air contamination

(samples measured at the University of Cambridge by Ms E Griesshaber)

DEL well (124), which on various grounds can be linked to outflow from the Eburru centre.

On a wider scale the He isotope ratios indicate an approach to a mid-ocean ridge basalt (MORB) type composition with R/Ra values typically of 8-9. Such values and higher have been measured in Ethiopia and a hot-spot origin attributed to the values in excess of 9 (Craig et al, 1977). The R/Ra values associated with Eburru, Longonot and Olkaria are consistent at around 6, suggesting that they share the same local crustal reservoir; whether or not there is a gradual enrichment northwards along the Rift towards MORB values may be answered by the next phase of the Geothermal Project.

As already mentioned, the total helium content of the Bala spring on the edge of Lake Victoria is very high (2.86×10^{-3} cc He/cc total gases). The R/Ra value of 1.446 indicates that there has either been some concentration of air-derived inert gases containing minor enrichment in ^{3}He (and the Ne content is high) or, that any radiogenic (^{4}He) and mantle (^{3}He) additions are largely balancing out in proportional terms. Similar gas compositions and concentrations are known from southern Africa (K O'Nions, pers. comm.).

Inert gases

Measurement of concentrations of inert gases were made on seven well waters, two warm spring waters and seven fumaroles. Results are presented in Tables 5.12(a) and (b) as volumes (STP) of gas per volume of water or gas as appropriate and in Table 5.13 as various ratios.

When the dissolved gas results are plotted in the form of argon versus neon content and xenon versus krypton content (Figure 5.12a), it can be seen that the inert gas ratios are wholly consistent with an atmospheric origin and, apart from one sample showing depletion, can be used to attempt estimates of recharge temperature. As with other gases, the amount of each inert gas in solution is controlled by the air temperature at the point of recharge. Providing water does not undergo significant heating below surface, amounts of inert gas in solution should be preserved at the sampling point, enabling calculation of recharge temperature (Mazor, 1977). However, amounts of gas in solution also depend on air pressure, and this will vary with recharge altitude. Because in the present case this is not known, a gas ratio rather than volume approach has been used here. Gas partition coefficients (Wilhelm et al., 1977) are independent of pressure and in theory permit calculation of recharge temperatures without knowing initial pressures, which in turn allows some conclusions about recharge altitude to be drawn.

Using neon as a reference, tentative temperatures for argon, krypton and xenon have been calculated (Table 5.12a) for all sites except 124 (DEL), where original gas ratios have been disturbed by the influx of geothermal gases (Table 5.13). As the ratio approach is cruder than the volume method, agreement between the three temperature sets is not good, but when the averaged figures are considered they serve as an indicator of relative if not absolute average recharge heights. Of the five sites giving plausible temperatures (25, 28, 91, 96 and 118), the temperature range is about 7°C. With a maximum temperature lapse rate of 0.6°C per 100 m, this would correspond to an altitude range of the order of 1200 m. Altitudes based on the premise of essentially local recharge to Nakuru No. 7 (118) are shown in Figure 5.13 and suggest that the highest sampling point, Kinangop P65 (96), obtains its water from an average altitude of 3200 m. Intermediate wells obtain water from between 150 to 400 m above the sampling point. The results from Naivasha 4178, Ndabibi C1404 and Kariandusi warm spring cannot be

Table 5.12a Inert gas contents (cm^3/cm^3 H_2O at STP) and calculated recharge temperatures for selected groundwaters.

Site No.	Site Name Temp Altitude	He x 10^{-8}	Ne x 10^{-7}	Ar x 10^{-8} Ar/Ne x 10^{-3} t_r	Kr x 10^{-8} Kr/Ne t_r	Xe x 10^{-8} Xe/Ne t_r
25	Kijabe RVA 35°C 2500 m	64.3	1.64	2.60 1.59 21.8	5.98 0.365 16.2	0.86 0.053 13.7
28	Mayer's Farm 28°C 2100 m	3.67	1.47	2.25 1.53 24.0	4.97 0.338 19.9	0.70 0.048 17.5
35	Kariandusi Spring 39°C 2300 m	5.47	1.43	1.94 1.35 >30	4.16 0.291 28.1	0.58 0.041 24.1
82	Naivasha 4178 21°C 1900 m	6.18	2.47	3.38 1.37 >30	7.09 0.287 >30	0.97 0.039 25.6
92	Kanyamwi Farm 27°C 2300 m	5.16	1.64	2.60 1.59 21.8	5.87 0.358 17.1	0.84 0.051 14.6
96	Kinangop P65 21°C 2600 m	5.69	1.67	2.83 1.70 17.9	6.42 0.384 13.9	0.91 0.055 12.4
100	Ndabibi C1404 21°C 2100 m	3.61	1.47	2.11 1.44 28.4	4.53 0.308 25.1	0.62 0.042 22.4
118	Nakuru No. 7 28°C 2000 m	3.34	1.53	2.29 1.50 25.4	5.03 0.329 21.2	0.69 0.045 19.5
124	Soysambu DEL 32°C 1900 m	143	0.87	1.05 - -	2.12 - -	0.30 - -

t_r = calculated recharge temperature, °C

5.12b Inert gas contents (cm^3/cm^3 gas) of selected fumaroles.

Site No.	Site Name	He x 10^{-5}	Ne x 10^{-7}	Ar x 10^{-4}	Kr x 10^{-8}	Xe x 10^{-8}
53	Bala Spring	1270	3.65	30.9	22.4	3.09
110	Olkaria OW2	4.07	0.15	0.10	0.15	-
111	Olkaria OW26	3.07	122	56.4	69.8	7.09
119	Eburru EF-2	5.52	0.30	0.35	0.73	0.11
123	Olkaria West	2.00	0.21	0.26	0.53	0.10
126	Suswa F-3	2.58	74.9	34.5	43.1	3.64
127	Domes F-15	2.57	61.8	30.9	35.6	3.27
128	Longonot F-23	0.75	28.4	12.0	14.0	1.45

(Samples measured at the University of Bath by Mr M J Youngman)

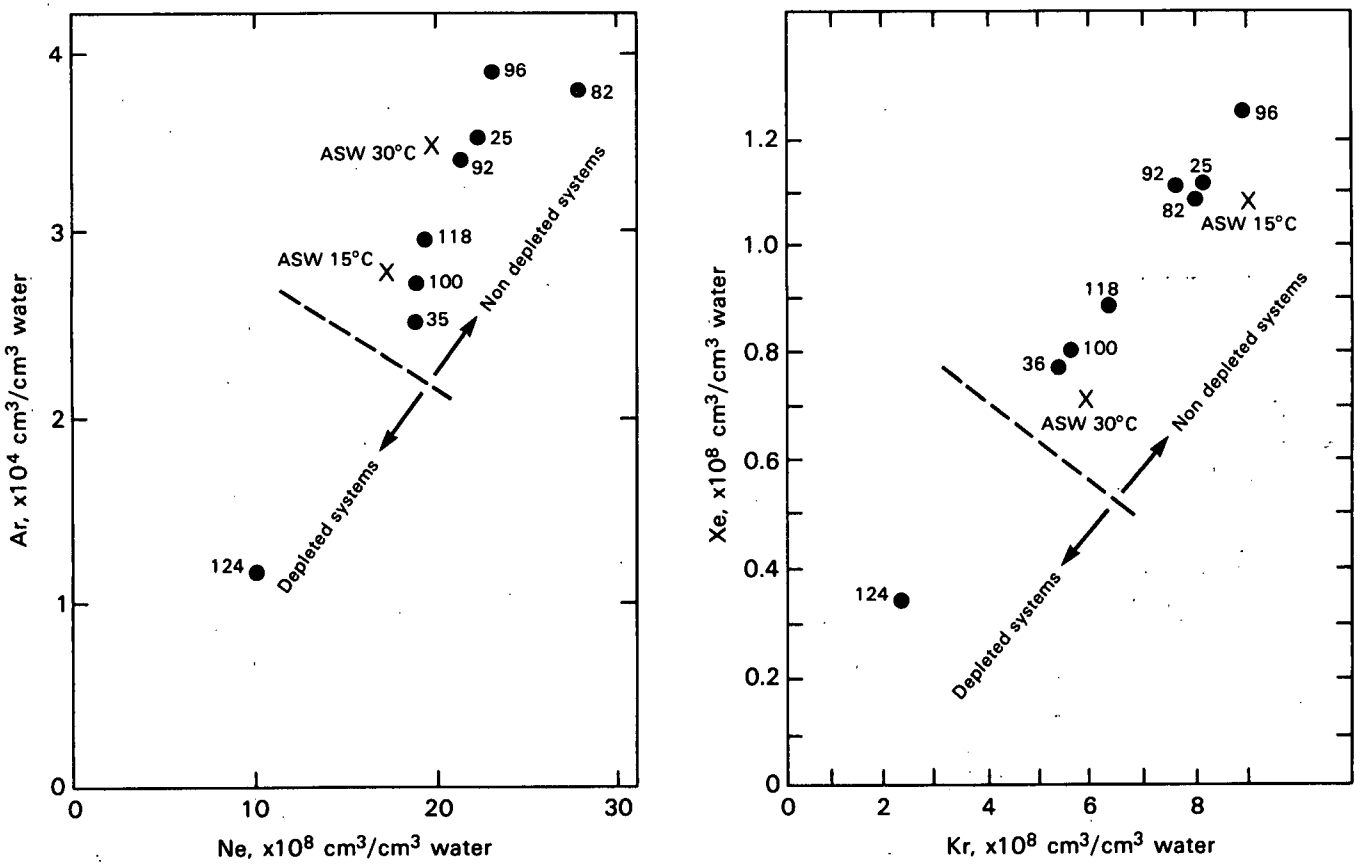

Figure 5.12a Plots of argon versus neon and xenon versus krypton contents of selected groundwaters in the Suswa-Nakuru sector. ASW - air saturated water. (Diagram after Mazor, 1977).

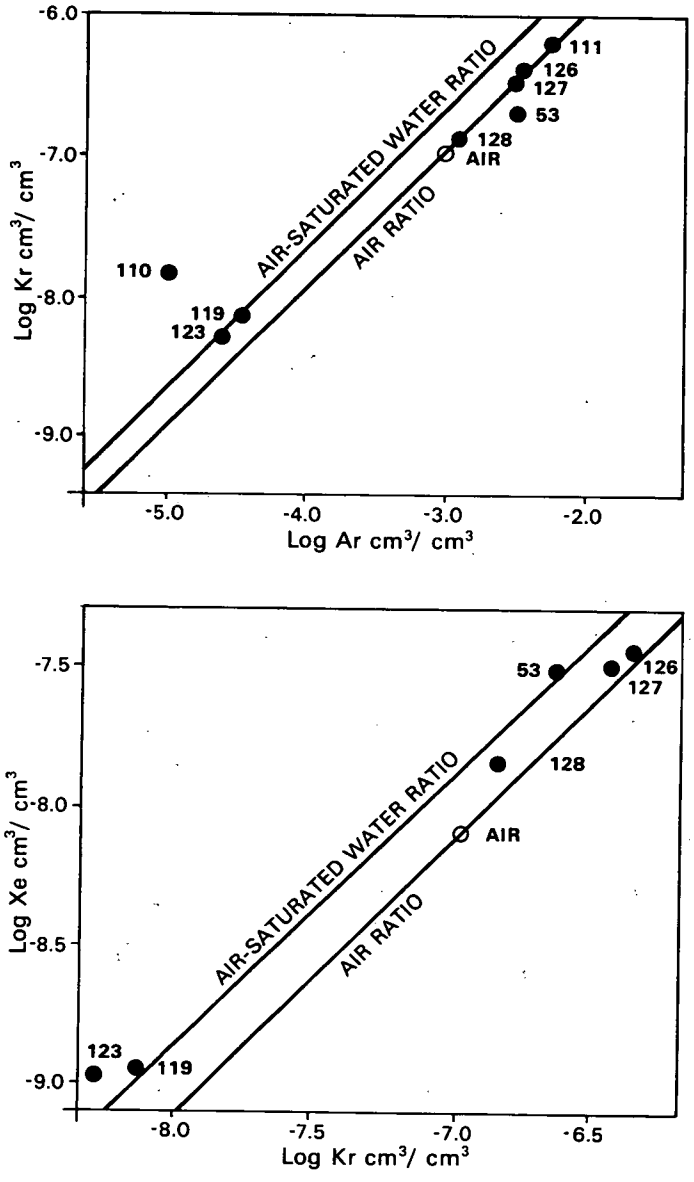

Figure 5.12b Plots of krypton versus argon and xenon versus krypton contents of gases mainly collected from fumaroles.

Table 5.13 Dissolved gas ratios from mass spectrometric measurement of selected groundwaters.

Site No.	Site Name	Sample Type	$^{40}Ar/^{36}Ar$ ratio	±	N_2/Ar ratio	±	CO_2/Ar ratio	±
25	Kijabe RVA	Water	294.1	1.3	37.8	0.2	20.9	1.5
28	Mayer's Farm	Water	294.1	1.0	39.9	0.2	97.3	1.3
35	Kariandusi Spr	Water	295.4	0.5	49.8	0.7	93.3	1.2
53	Bala Spring	Gas	846.0	35.3	22.5	0.7	155.0	1.0
82	Naivasha C4178	Water	296.4	2.2	42.4	0.2	62.5	1.1
92	Kanyamwi Farm	Water	294.9	2.0	39.3	0.2	41.3	1.5
96	Kinangop P65	Water	296.8	0.9	39.1	1.0	61.0	3.7
100	Ndabibi C1404	Water	297.6	0.8	57.9	0.4	39.2	0.9
110	Olkaria OW2	Gas	304.4	7.7	43.2	8.2	86.0	7.0
111	Olkaria OW26	Gas	247.1	21.0	66.9	4.8	60.0	5.0
118	Nakuru No. 7	Water	293.7	1.3	40.2	1.3	35.5	0.7
119	Eburru EF-2	Gas	303.4	3.5	23.2	2.0	40.0	7.0
123	Olkaria West	Gas	261.4	26.5	35.2	6.4	223.0	15.0
124	Soysambu DEL	Water	297.0	2.7	35.2	0.3	972.0	87.0
126	Suswa F-3	Gas	293.1	2.9	87.8	2.5	11.0	1.0
127	Domes F-15	Gas	291.3	0.3	88.0	0.7	16.0	1.0
128	Longonot F-23	Gas	278.7	0.7	77.8	0.4	10.0	1.0

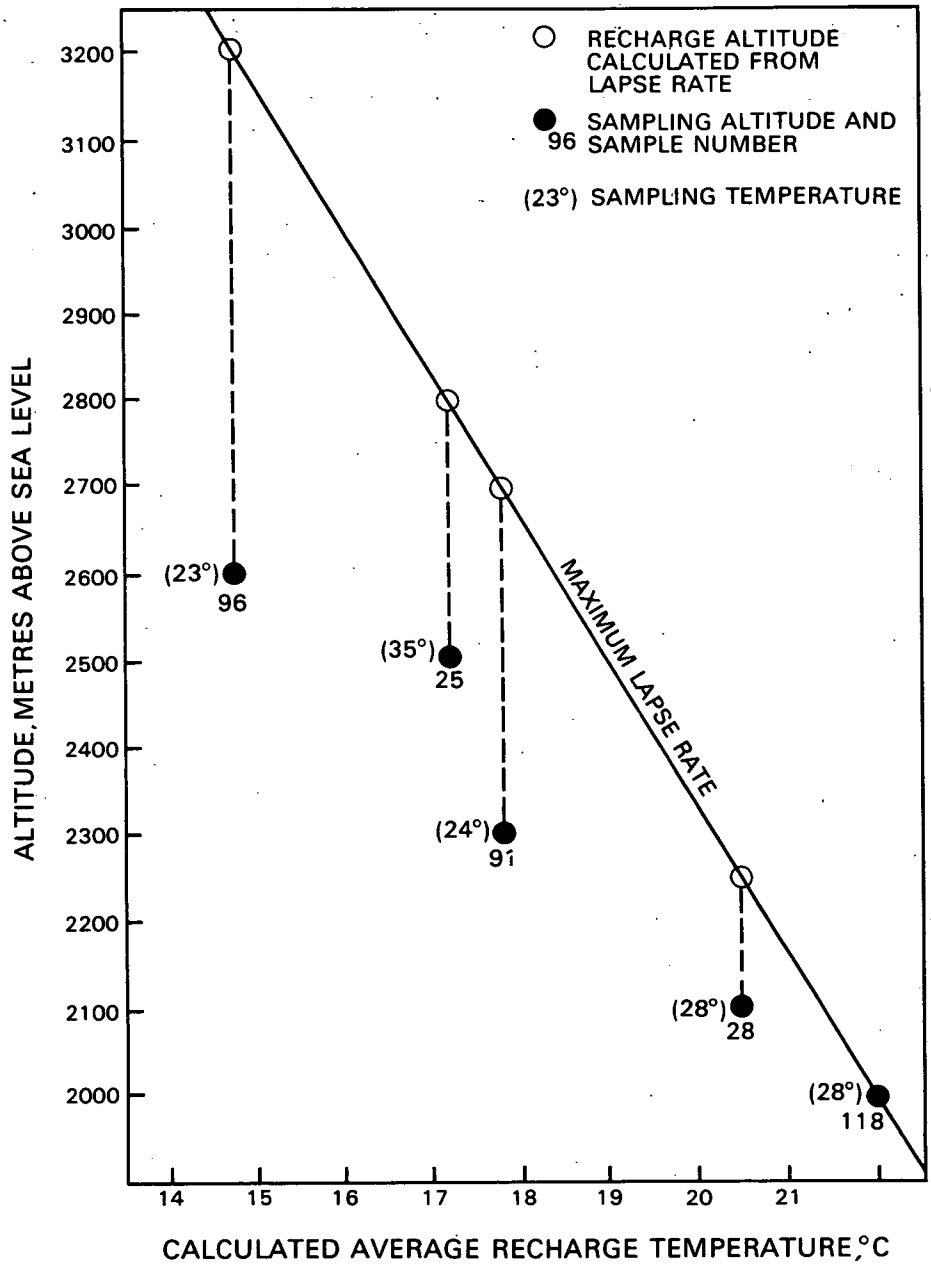

Figure 5.13 Plot of inert gas-derived recharge temperatures versus sampling altitude for selected groundwaters in the Suswa-Nakuru sector compared to temperature lapse rate.

interpreted in the same way. In the case of Kariandusi subsurface heating may have disturbed the ratios of the inert gases, otherwise sampling problems are likely to be responsible for the dubious results.

For free gas samples, plots of Kr content vs Ar content and Xe content versus Kr content are shown in Figure 5.12(b). They indicate that the gases were probably all originally derived from meteoric water, but that air contamination has affected some samples (111, 126-128). In the case of OW 26 and F 23 (111, 128) this probably occurred during sampling or storage, but there is other evidence from gas measurements (see above) that the Suswa and Domes fumaroles F-3 and F-15 (126 and 127) may already have had air entrained. The Bala sample was collected from a bubbling pool, where it is sometimes difficult to avoid some air contamination (cf Kariandusi spring, 35). However, N_2/Ar at Bala is lower than water (Table 13), presumably due to high ^{40}Ar (see below), which indicates that this alone is responsible for the shift from the ASW (air saturated water) line. This is confirmed by the Xe vs Kr plot which shows that the Bala sample is consistent with an ASW origin. The ratio Kr/Xe suggests a recharge temperature of 10°C, and while this ratio seems liable to underestimate temperatures by 10° or so, it does imply that this water has not been subjected to boiling at any stage, and is unlikely to be coooled outflow from a high-temperature geothermal system. This is in agreement with the chemical geothermometers (5.7.1).

The inert gas results also provide other information. They confirm that the Soysambu DEL well (124) has large amounts of helium and carbon dioxide in solution and also indicate that helium is enhanced in the Kijabe RVA well (25). A warm spring near to this particular well had a $^3He/^4He$ index close to that of air, so possibly radiogenic ^4He is offsetting a ^3He contribution. However, examination of the $^{40}Ar/^{36}Ar$ ratio (Table 5.13) indicates that in every case but one the value is comparable to that in air, 295.6 (Nier, 1950), and that therefore there is very little production of the radiogenic ^{40}Ar isotope which usually accompanies ^4He production. The exception, Bala (53), is high in ^{40}Ar which implies that radiogenic He is offsetting an otherwise high R/Ra value to result in the observed R/Ra of 1.4 (5.6.2).

5.6.3 Implications of the gas data

The non-inert gas data in this report are all collected from thermal manifestations and are only interpreted in a qualitative way: presence of He and H_2 is indicative of proximity to an upflow, while the ratio C_2H_6/CH_4 may be a measure of lakewater input to a hydrothermal system. Quantitative interpretation of gas data from the Suswa, Longonot and Domes areas has been provided by Armannsson (1987b)

The inert gas and helium isotope data however have relevance to both thermal and non-thermal hydrogeology. There appears to be little evidence of the enhancement of radiogenic He and Ar isotopes which usually occurs in waters with long residence times. In this respect the data support the conclusion of ^{14}C measurement. Where high helium is encountered it appears to be due to close association with volcanic centres. There is from the work so far no clear indication that mantle helium is encountered in association with deep faulting. The recharge temperatures gained from consideration of amounts of inert gases in solution show a tendency for recharge to be more local at lower altitudes, the reverse of what might be expected. It is unlikely (at least in the cases where inert gases indicate sensible temperatures) that waters have circulated to great depths and have then cooled again during travel to the surface as this would have upset the inert gas ratios.

Table 5.14 Various SiO_2 and alkali cation geothermometers calculated for all Rift Valley water samples.

SITE NO.	MEASURED DATA TEMP DEGC	PH	TDS MG/L	SIO2 MG/L	LOG PCO2	AMPHS	GEOTHERMOMETERS, IN DEG C SILICA QZ	CHALC	CRIST	NA/K/CA B=4/3	B=1/3	PACES	MGCOR	NA/K B=0
1	84.6	8.85	34499	79.8	-1.2	7.7	126.8	97.6	76.1	857.1	195.3	382.5		57.7
2	80.7	9.07	39606	86.0	-1.4	11.5	131.1	102.4	80.4	939.9	195.1	424.3		53.2
3	85.3	0.00	37195	84.3		10.4	129.9	101.0	79.2	908.8	193.5			52.7
4	81.3	0.00	17704	86.0		10.4	129.9	101.0	79.2	884.5	192.8			53.1
5	78.6	0.00	15836	78.7		6.2	125.1	95.7	74.4	874.9	191.9			52.4
6	72.4	0.00	32431	88.6		12.6	132.3	103.7	81.6	894.9	188.9			47.6
7	82.0	9.18	30512	88.1	-1.5	12.2	131.9	103.3	81.3	806.9	184.9	386.5	183.5	47.3
8	82.6	9.13	39156	86.0	-1.4	11.5	131.1	102.3	80.4	917.4	190.5	418.0		48.6
9	45.0	8.82	31556	105.2	-1.6	21.1	141.8	114.4	91.3	679.8	167.6	339.4		33.5
10	43.5	8.81	31321	101.2	-1.6	19.1	139.6	111.9	89.0	584.5	161.7	298.4		33.0
11	66.6	8.96	38141	83.4	-1.4	10.0	129.4	100.4	78.7	814.2	181.9	383.4		43.1
12	60.2	9.13	43302	86.8	-1.6	12.2	131.8	103.2	81.2	859.8	182.9	412.4		42.0
13	39.5	9.56	41960	50.9	-2.2	-11.6	104.8	73.3	54.2	698.1	155.5	387.8		17.7
14	38.5	9.56	41704	48.3	-2.2	-13.7	102.3	70.7	51.8	688.7	154.5	384.1		17.0
15	34.0	9.86	23678	35.7	-2.8	-25.9	87.9	55.2	37.7	591.8	159.7	371.1		29.9
16	40.8	9.58	43228	54.8	-2.2	-8.5	108.3	77.2	57.7	697.6	157.2	387.4		19.7
17	40.5		19728	53.5		-10.5	106.0	74.7	55.4	718.9	158.5			20.0
18	45.3	9.57	42454	68.4	-2.2	1.1	119.3	89.2	68.6	735.0	162.1	401.9		23.4
19														
20	25.7	8.20	315	105.2	-2.9	19.5	140.0	112.4	89.5	115.7	221.0	65.8	96.2	330.1
21	21.5	8.00	71	16.7	-3.3	-51.5	57.0	22.5	7.9	50.8	215.9	21.1		450.8
22		8.80	615	82.8	-3.3	7.8	126.9	97.7	76.3	147.9	185.7	98.9	112.2	185.1
23														
24		7.90	303	9.4	-2.7	-67.0	37.6	2.6	-10.4	118.7	261.9	65.0	82.7	512.2
25	35.0	7.95	366	77.4	-2.5	4.7	123.4	93.8	72.7	175.8	180.3	101.1	155.3	153.6
26	43.3	9.05	379	40.6	-3.5	-22.0	92.5	60.1	42.2	142.1	121.6	98.6		52.7
27	16.9	7.05	174	67.2	-2.1	-1.7	116.2	85.8	65.5	123.2	210.3	56.7	88.0	281.3
28	27.9	7.90	279	65.9	-2.6	-2.5	115.2	84.7	64.5	96.1	211.5	45.5	75.5	325.0
29	87.2													
30		7.91	96	13.9	-3.2	-56.7	50.6	15.9	1.8	110.2	357.4	67.2	190.6	1683.6
31														
32	22.2	7.85	135	53.0	-3.0	-11.6	104.7	73.2	54.1	109.3	248.6	61.8	139.0	464.9
33	51.2	7.25	261	44.3	-1.9	-18.8	96.4	64.2	46.0	97.3	229.3	36.2	53.9	398.3
34	52.5	7.07	251	52.0	-1.7	-12.5	103.7	72.2	53.2	94.3	230.1	31.7	55.0	408.2
35	23.0	6.78												
36	23.0													
37	30.0	6.46	301	93.7	-1.2	13.7	133.6	105.1	82.9	137.7	241.2	52.5	117.6	375.6
38	24.0													
39	29.0	7.03	148	96.7	-2.0	15.2	135.3	107.1	84.7	129.8	252.1	60.9	181.2	437.0
40	23.0													
41	45.0	9.29	3107	124.7	-3.0	28.6	150.0	123.7	99.6	401.6	188.0	269.9		93.6
42	38.0	9.13	2312	121.9	-3.0	27.3	148.6	122.1	98.2	364.1	191.2	245.8		106.7
43	92.0													
44	77.0	7.75	7559	78.1	-0.7	5.4	124.2	94.7	73.6	344.9	171.2	155.4		77.7
45	81.0	7.67	7412	76.4	-0.6	4.4	123.1	93.4	72.4	345.5	171.8	152.7		78.6
46	75.5	7.50	7086	75.9	-0.5	4.1	122.8	93.1	72.1	347.7	170.2	151.2		75.5
47	75.0	7.95	7489	75.9	-0.9	4.1	122.8	93.1	72.1	350.2	172.0	164.3		77.8
48	50.0	8.25	3307	76.1	-1.8	4.1	122.7	93.0	72.0	274.3	155.2	148.2	140.3	68.0
49	50.0	8.13	3238	75.3	-1.7	3.5	122.1	92.4	71.4	275.6	155.0	146.1	145.1	67.3
50	27.0	8.09	3647	68.0	-1.8	-1.0	117.0	86.7	66.3	251.2	149.3	133.3	128.4	64.3

Table 5.14(contd) Various SiO_2 and alkali cation geothermometers calculated for all Rift Valley water samples.

	MEASURED DATA			GEOTHERMOMETERS, IN DEG C										
	TEMP	PH	TDS	SIO2	LOG		SILICA			NA/K/CA				NA/K
	DEGC		MG/L	MG/L	PCO2	AMPHS	QZ	CHALC	CRIST	B=4/3	B=1/3	PACES	MGCOR	B=0
51	50.0	8.12	3251	78.7	-1.7	5.6	124.4	94.9	73.8	254.9	153.6	133.6	142.4	70.3
52														
53	72.0	8.06	22328	63.5	-0.7	-3.1	114.5	84.0	63.9	214.5	135.7	88.3		52.1
54	35.0	7.98	31961	67.8	-0.8	0.1	118.3	88.1	67.6	548.8	173.8	246.0	168.9	52.1
55	58.3	8.36	24092	68.4	-1.1	0.2	118.3	88.2	67.7	512.3	170.6	245.3		51.7
56	74.7	8.15	22046	64.0	-0.8	-2.9	114.8	84.3	64.2	479.5	154.1	218.3		33.0
57	36.3	8.16	20987	60.1	-1.1	-5.6	111.7	80.9	61.1	422.3	158.8	205.5	151.5	46.2
58	25.0	7.00	148	10.3	-2.0	-64.8	40.4	5.4	-7.8	79.4	206.0	24.6	52.0	332.7
59	25.0	7.00	23036	126.6	0.1	30.5	152.1	126.1	101.7	380.2	145.5	149.0		33.5
60	25.0	7.00	799	6.7	-1.1	-75.3	27.2	-8.1	-20.2	80.2	206.1	14.0	53.2	331.6
61	97.0	0.00												
62	28.6	6.50												
63														
64	41.5	6.00												
65														
66														
67														
68														
69														
70	25.0	8.94	910	31.0	-3.2	-31.7	81.0	47.7	31.0	154.8	178.6	101.6	57.0	162.5
71	93.7	7.00	3128	186.1	-0.2	51.9	175.1	152.6	125.4	383.3	197.0	157.3		112.3
72	36.5		2013	35.1		-27.4	86.2	53.3	36.0	142.0	126.2		40.1	60.8
73	62.8		45172	75.3		5.5	124.3	94.8	73.7	1045.2	201.0			56.0
74														
75														
76														
77														
78														
79														
80	20.5	7.04	212	77.9	-2.5	4.9	123.7	94.1	73.0	122.3	272.2	62.7	118.1	561.6
81	22.1	7.70	367	60.5	-2.9	-6.2	111.0	80.2	60.4	125.7	174.9	73.3	63.2	174.7
82	20.3	7.45	363	80.2	-2.1	6.3	125.3	95.9	74.6	109.9	200.9	47.9	135.6	266.6
83	26.3	7.71	328	65.0	-3.0	-3.1	114.6	84.0	63.9	143.3	199.8	87.5	50.6	227.0
84	20.8	7.82	574	68.2	-3.1	-1.0	117.0	86.7	66.3	152.1	168.6	97.1		141.2
85	20.2	7.95	151	69.3	-3.6	-0.3	117.7	87.5	67.1	122.1	205.7	83.5	134.6	267.3
86	26.2	7.18	336	99.5	-2.4	16.7	136.9	108.8	86.3	127.6	229.3	65.4	38.7	344.0
87	25.5	7.97	290	77.6	-3.3	4.8	123.6	94.0	72.9	175.4	217.0	119.6	199.8	248.0
88	23.9	7.77	469	62.2	-3.0	-5.0	112.4	81.7	61.8	149.0	172.0	92.1	128.0	150.9
89	24.6	8.20	582	62.0	-3.3	-5.1	112.2	81.5	61.6	142.2	159.4	93.8	122.2	126.5
90	18.0	8.13	186	72.7	-3.7	1.8	120.2	90.2	69.5	137.5	193.3	98.1	169.1	213.8
91	24.0	7.30	48	81.7	-3.4	7.2	126.2	96.9	75.6	120.4	240.8	77.7	150.2	403.8
92	21.9	6.99	50	82.6	-3.1	7.6	126.8	97.5	76.1	120.2	240.8	72.0	154.9	404.0
93	23.2	7.47	239	95.2	-3.1	14.5	134.4	106.1	83.8	132.0	240.9	82.1	107.5	383.8
94	18.6	8.34	1436	62.5	-3.2	-4.8	112.6	81.9	62.0	257.0	181.7	178.4		119.7
95	24.1	8.20	192	43.2	-3.8	-19.7	95.3	63.0	44.9	144.6	176.1	105.3	156.8	163.6
96	22.6	7.01	27	72.9	-3.2	2.0	120.3	90.4	69.7	113.9	255.3	70.0	125.6	488.7
97	22.6	6.64	87	101.8	-2.4	17.8	138.2	110.3	87.6	139.9	257.6	75.0	139.5	443.3
99	25.7	7.13	469	63.5	-2.3	-4.1	113.4	82.8	62.8	39.1	121.7	-0.9		117.8
100	26.3	6.95	263	100.5	-1.8	17.2	137.5	109.5	86.9	147.5	228.5	67.8	162.2	313.5
101	20.0	7.65	176	77.0	-2.7	4.4	123.1	93.5	72.5	124.2	274.3	68.7	123.9	568.8

Table 5.14 (contd) Various SiO_2 and alkali cation geothermometers calculated for all Rift Valley water samples.

102													
103													
104	19.6		655	121.9		27.2	148.5	122.0	98.1	211.2	161.9		158.8	99.0
105														
106	52.0		417							218.1	292.1	0.0	275.8	
107	32.4		2318							207.6	157.2			91.6
108	23.0		1282	85.6		9.4	128.7	99.7	78.1	182.4	182.2		133.0	153.9
109	72.0		1350	145.5		37.0	159.2	134.2	109.0	150.3	114.1			36.9
110	152.0	6.25	1590	117.9	-0.3	25.5	141.6	119.8	96.1	489.8	292.1	204.4		278.6
111	159.0	6.05	676	534.7	0.3	134.9	231.2	253.7	214.3	358.6	254.6	134.0		236.9
112	157.0	6.20	1091	453.5	0.6	119.2	219.6	234.9	197.9	403.5	235.9	143.8		180.1
113	148.0	6.20	1258	530.5	-0.3	134.1	230.7	252.8	213.5	479.8	273.5	201.0		238.1
114	153.0	6.20	764	528.3	0.3	133.7	230.3	252.3	213.0	386.2	253.1	145.2		222.6
115	152.0	6.20	1152	560.4	0.3	139.6	234.6	259.4	219.2	487.6	268.4	185.4		224.7
116	156.0	6.20	17	4.9	0.0	-82.2	28.9	-17.0	-28.5					
118	27.9	7.00	306	81.3	-1.7	6.9	126.0	96.6	75.3	123.7	213.8	51.2	153.2	292.5
119														
120														
121	37.1	6.95	1632	126.2	-0.8	29.1	150.6	124.4	100.2	167.7	200.4	64.2	189.8	208.3
122	30.0	7.00	950	105.7	-1.2	19.7	140.3	112.7	89.7	136.0	203.6	50.5	156.4	245.4
123														
124	32.4	6.40	1702	130.5	-0.3	31.0	152.6	126.7	102.3	169.8	213.9	56.8	164.8	243.7
125	27.8	7.95	1541	66.3	-2.0	-2.2	115.6	85.2	64.9	181.8	185.6	94.1	23.8	162.1
127														
128														
129	25.0	7.00	898	92.0	-1.2	12.8	132.6	104.0	82.0	156.7	233.0	64.6	57.8	318.2

The foregoing evidence (particularly the $^3He/^4He$ and inert gas radioisotope data) points to the fact that there is no sign shown by groundwaters of mixing with a deep, long residence component, except at Bala. Only groundwaters closely associated with volcanic centres (e.g. at 124) show large He enhancement, and even this seems to be caused by volcanic gas inflow rather than long residence of water.

5.7 Geothermometry

5.7.1 Water chemistry

These geothermometers involve consideration of the effect of temperature either on solubility of a species (normally a form of silica) or on the amount of exchange of various cations (the alkali and alkaline earth metals). In older rocks and at temperatures above 150°C quartz is likely to be the controlling mineral phase for the silica geothermometer, but in rocks of Rift age below 150°C control is likely to be by cristobalite or chalcedony. The original basic alkali geothermometer of Na/K (White 1965), which assumes cation exchange with alkali feldspar, has been supplemented by versions including Ca and Mg (Truesdell 1975, Fournier and Potter 1979) and a correction for low temperature waters (Paces 1975). Table 5.14 shows the results of nine geothermometer calculations based on these various premises for all the Rift Valley Geothermal Project samples for which appropriate chemical data exist. These are now discussed with reference to the various sectors of the Rift studied during the project - Magadi, Suswa-Nakuru, north of Menengai, and north eastern margins of Lake Victoria.

The Magadi hot springs have surface temperatures of up to 85°C and TDS values rising to over 40,000 mgl^{-1} (Section 7). As a consequence of the highly alkaline chemistry of the springs the simple Na/K geothermometer gives unrealistically low temperatures, while low levels of Ca and Mg make use of the corrected versions inappropriate. (Indeed most of the more obviously thermal waters in the Rift are low in Ca and Mg as a consequence of various mineral controls.) Of the SiO_2-based geothermometers, amorphous silica can be ruled out, as it can be in the whole of the Rift. Cristobalite gives results often little different from the sampling temperatures, but both chalcedony and quartz give reasonably steady temperatures well in excess of sampled temperatures which suggests that these warm springs have a single source at a temperature between 100°C and 130°C variously affected by cooling and/or mixing processes (Section 7). Two boreholes between Magadi and Suswa - Oltepesi and Mosiro (22 and 129) - have medium TDS waters of ambient temperature which on chemical and isotopic grounds show little evidence of a thermal origin. The lowest temperatures suggested by geothermometers for the two sites are 76°C (cristobalite) and 58°C (Mg corrected alkali) respectively, but it seems unlikely that these well waters have ever reached such temperatures. The same is probably true for most of the groundwaters in the Suswa-Nakuru sector of the Rift (with the obvious exception of the Olkaria-Hells Gate area, which is considered separately) where for most of the waters the alkali geothermometers are excessive and even the silica-based ones are rather high. It is unlikely, for example, that borehole waters of ambient temperature (i.e. around 20°C) in the vicinity of Lake Naivasha have been raised to over 65°C then cooled again during their passage from recharge to discharge. Such waters are characterised by low TDS values, virtually precluding mixing with thermal components. The chemical geothermometers are therefore also unconvincing in this sector of the Rift, with the exception of the wells north of Eburru and the warm spring on the edge of Lake Elmenteita (121-125 and 41-42) which are considered on other grounds to have a thermal component.

The sampled waters of the Bogoria-Silale area are generally hot (up to boiling) and the quartz and CO_2-corrected alkali geothermometers suggest a source for Kapedo and Lorusio waters at a temperature of 120-160°C, probably at the lower end of this range. The boiling spring of Ol Kokwe Island in Lake Baringo (71) yields a higher-temperature set of results of which quartz and CO_2-corrected alkali geothermometers agree well (about 175°C) though cristobalite at 152°C is also plausible.

The Bala hot springs of the Homa Bay area of northeast Lake Victoria range in temperature from 35°C to 75°C. Only the quartz geothermometer gives a credible temperature range, 112°C to 118°C. The appropriate Na/K/Ca geothermometer gives a rather high temperature.

Various factors affect the performance of geothermometers. Steam separation can affect silica concentrations, owing to adiabatic rather than conductive cooling, but this is only likely to apply to large, vigorously boiling springs, which are uncommon in the Rift. More importantly, amounts of silica in cooler Rift groundwaters may be raised to levels in excess of cristobalite or chalcedony equilibrium concentrations by release of silica from alteration of silicate minerals, eg by influx of CO_2 (Fournier, 1981). The ubiquity of of CO_2 in the Rift (Bailey, 1980) is consistent with this interpretation. As mentioned earlier the alkali geothermometers can be affected by high Mg contents, but this element is almost always present at very low levels in Rift Valley groundwaters.

The overall impression given by the geothermometer results is that those based on cations must be used cautiously in the Rift Valley. Of the silica-based geothermometers, quartz and chalcedony appear to be useful for hot springs, but for cooler waters, although chalcedony is the least oversaturated SiO_2 species (Table 5.15) and therefore theoretically most likely to tend towards the actual maximum temperature achieved at depth, it still produces temperature estimates which appear to be excessive. In this respect cristobalite is more reasonable, although it also often appears to overestimate temperatures at depth.

5.7.2 Gas geothermometers

These depend on temperature-controlled gas-mineral equilibria being achieved in the reservoir(s) which feed the fumarole, well or spring. Various versions exist, some using single gases and some gas ratios (Arnorsson and Gunnlaugsson, 1985). Carbon dioxide, hydrogen and hydrogen sulphide are the most suitable gases to use for geothermometry because the reactions controlling them seem to approach equilibrium over a large temperature range, but H_2 and H_2S are often only present (if at all) below detection limit in Rift Valley fumarole gases. Methane, although usually second only to CO_2 as a 'geothermal' gas, is more loosely related to reservoir temperatures owing to departures from the controlling reactions (Arnorsson and Gunnlaugsson 1985), the main one of which may be the Fischer-Tropsch reaction between CO_2 and molecular H_2.

Armannsson (1987b) dealt with the application of gas geothermometers to the Suswa, Longonot and Domes areas. This study has used the CO_2/H_2 geothermometer to estimate temperatures at depth, but this has been possible at only two sites (Table 5.16). Methane/carbon dioxide ratios from these and other sites have been applied to the theoretical CH_4/CO_2 - temperature curve of Ellis and Giggenbach presented in Glover (1972). The results are also given in Table 5.16.

Table 5.15 Saturation indices for selected species in groundwaters of the Suswa-Nakuru sector of the Rift Valley.

SITE	CHALCEDONY	CRISTOBALITE	QUARTZ	CALCITE	MAGNESITE	NAHCOLITE	MAGADIITE
24	+0.027	+0.149	+0.616	-0.383	-1.056	-4.516	-
25	+0.516	+0.558	+0.960	-1.001	-1.622	-4.366	-1.808
26	+0.032	+0.057	+0.446	-0.682	-0.965	-4.639	-4.207
27	+0.666	+0.747	+1.180	-1.883	-2.400	-4.955	-3.025
28	+0.526	+0.582	+0.616	-0.165	-1.056	-4.889	-2.250
37	+0.660	+0.713	+1.123	-1.659	-2.224	-4.750	-2.212
39	+0.684	+0.739	+1.151	-1.611	-2.456	-5.264	-1.728
41	+0.393	+0.415	+0.801	+0.026	-0.643	-3.070	0.026
80	+0.687	+0.760	+1.187	-0.358	-1.070	-4.420	-1.925
81	+0.558	+0.627	+1.051	+0.328	-0.226	-3.591	-2.360
82	+0.702	+0.775	+1.203	+0.396	-1.403	-4.368	-1.857
83	+0.540	+0.600	+1.017	+0.291	-0.047	-3.733	-1.992
84	+0.624	+0.697	+1.123	-0.011	+0.934	-3.468	-1.935
85	+0.637	+0.710	+1.138	-0.052	-0.984	-4.348	-1.790
86	+0.728	+0.788	+1.205	+0.077	-0.194	-3.949	-1.076
87	+0.624	+0.689	+1.104	+0.150	-1.075	-3.773	-1.159
88	+0.548	+0.614	+1.035	+0.091	-0.821	-3.515	-2.224
89	+0.533	+0.597	+1.017	+0.729	-0.213	-3.321	-1.861
90	+0.683	+0.761	+1.193	-0.030	-1.260	-4.087	-1.499
91	+0.667	+0.732	+1.153	-1.616	-2.356	-5.382	-2.129
92	+0.696	+0.766	+1.191	-1.867	-2.662	-5.286	-2.385
93	+0.742	+0.809	+1.231	-0.262	-0.860	-4.348	-1.009
94	+0.607	+0.684	+1.115	+0.301	-0.856	-2.675	-1.386
95	+0.382	+0.447	+0.868	-0.410	-1.455	-4.283	-3.250
96	+0.634	+0.703	+1.126	-2.478	-2.963	-5.926	-2.939
97	+0.780	+0.848	+1.271	-1.899	-2.511	-4.965	-1.843
99	+0.539	+0.601	+1.018	+0.158	-0.244	-4.247	-3.389
100	+0.926	+1.023	+1.470	-1.746	-2.676	-4.526	-1.551
101	+0.810	+0.907	+1.354	-1.727	-2.406	-5.135	-2.308
104	+0.893	+0.968	+1.397	-2.276	-3.029	-3.742	-1.331
108	+0.700	+0.767	+1.190	-0.720	-1.524	-3.266	-1.842
109	+0.444	+0.419	+0.766	-1.396	-2.906	-4.167	-0.919
110	+0.996	+1.093	+1.540	-3.203	-4.529	-4.067	-0.233
111	+1.652	+1.750	+2.197	-3.035	-4.161	-4.091	+3.913
112	+1.581	+1.678	+2.125	-2.831	-3.736	-3.442	+3.369
113	+1.649	+1.747	+2.194	-3.500	-4.526	-4.160	+4.144
114	+1.649	+1.745	+2.191	-2.917	-3.948	-3.797	+3.895
115	+1.673	+1.770	+2.217	-3.320	-4.044	-3.750	+4.166
118	+0.621	+0.678	+1.092	-1.019	-1.974	-4.587	-2.231
121	+0.714	+0.752	+1.150	+0.163	-1.205	-3.185	-0.467
122	+0.948	+1.045	+1.492	-0.357	-1.594	-3.441	-1.117
124	+0.779	+0.826	+1.233	-0.298	-1.323	-3.153	-0.787
125	+0.530	+0.587	+1.001	+0.488	+0.540	-3.173	-1.662
129	+0.888	+0.985	+1.432	-0.445	-0.905	-3.518	-1.364

NOTE: Saturation Index = $\log \left(\frac{\text{Ion Activity Product}}{\text{Solubility Product}} \right)$

Values within the range ± 0.10 are saturated, otherwise + is supersaturated and - is undersaturated.

Table 5.16 Gas geothermometer temperatures for fumaroles in the Suswa, Longonot, Olkaria-Domes and Eburru sector of the Rift Valley.

SITE NO	LOCALITY	t CO_2/ H_2	t CO_2/CH_4	t CO_2 [1]
29/F-27	Mt. Margaret	-	330	423
31/H-1	Akira Ranch	-	314	246
44-47	Lorusio Springs [2]	246	338	-
53-54	Bala Springs [2]	-	314	-
110	Olkaria OW2	-	308	-
111	Olkaria OW26	-	322	-
119	Eburru EF-2	256	296	-
123	W. Olkaria	-	400	-
124	Soysambu DEL [2]	-	319	-
126	Suswa, rim	-	384	324
127	Domes	-	313	
				316
127/F-15	Domes	-	320	
128	Longonot, crater	256	311	
				409
128/F-23	Longonot, crater	255	315	
F-7	Suswa, caldera floor	-	307	303
F-12	Suswa, ring graben	-	324	298
F-28	Suswa, central island	-	316	370
K-1	Meru, Chogoria	-	315	-
K-2	Meru, Chogoria	-	383	-

[1] Figures from Armannsson (1987b) for directly-calculated CO_2 geothermeter.

[2] Gas samples collected from water

Samples with F, H and K prefixes collected by Dr H Armannsson of the UNDP.

While the CO_2/H_2 geothermometer gives apparently plausible results for Longonot and Eburru, the CH_4/CO_2 temperatures seem too high. Arnorsson and Gunnlaugsson (1985) warn that these cannot necessarily be interpreted as equilibrium temperatures preserved from greater depths.

5.7.3 Isotope geothermometers

Various isotope fractionations can in principle yield information on temperatures at depth. The fractionation of water can itself reveal information on boiling temperatures if certain assumptions are made; this subject has been dealt with in passing in Section 5.3. Differences between $\delta^{18}O$ values in steam condensate and accompanying CO_2 from fumaroles could also be used since isotopic exchange ceases in the vapour phase, but rapid re-equilibration at condensation temperatures can only be prevented with sophisticated sampling techniques such as cryotrapping. Another possible geothermometer is the fractionation of $\delta^{13}C$ between DIC and CO_2 gas, but since this requires a sample of liquid from which to obtain the DIC the exercise is usually academic. However, it may be noted that at the Soysambu DEL well (site 124) the $\delta^{18}O$ CO_2-H_2O and $\delta^{13}C$ DIC-CO_2 equilibria are in exact agreement with the measured temperature (Table 5.8).

Other geothermometers which have been used in geothermal systems elsewhere are the H_2-H_2O (Arnason, 1977) and the $\delta^{13}C$ CO_2-CH_4 fractionation (Hulston, 1977). Insufficient sample volumes were collected to attempt isotopic measurement of H_2 or CH_4 except at Eburru, where a $\delta^{13}C_{CH4}$ was measured on a sample from site 119. This gave the very enriched result of -6.7‰ which indicates a very high temperature and may be incorrect, though it is worth noting that samples collected previously from Eburru fumaroles gave unexpectedly high $\delta^{13}C_{CH4}$ values averaging -14.7‰ corresponding with measured $\delta^{13}C_{CO2}$ values to temperatures of around 500°C (Glover, 1972). However the $\delta^{13}C_{CO2-CH4}$ geothermometer may not be universally applicable, depending as it does on the attainment of equilibrium for the Fischer-Tropsch reaction mentioned above - for example, at Olkaria this geothermometer indicates temperatures well in excess of 300°C (Glover, 1972), while subsequent well drilling has yielded fluid of significantly lower temperature. In view of the strong indications from stable isotopes that water from Lake Naivasha reaches Olkaria and perhaps some of the other high temperature areas in the Suswa-Eburru zone, the presence of biogenic methane produced from organically-rich lake water cannot be excluded. Such methane would upset any isotopic geothermometer on the Fischer-Tropsch equilibrium.

5.7.4 Geothermometers - Summary

The application of chemical geothermometers to ambient and warm groundwaters in the Rift Valley is often inappropriate. Most ambient groundwaters are local and will not have been raised to much higher temperatures or mixed with thermal waters during their travel, but many give excessive alkali and Si geothermometer temperatures, for reasons explained above. In hot springs and geothermal wells, however, both alkali and quartz temperatures are plausible unless, such as Magadi, local conditions are such that the Na/K/Ca geothermometer is rendered useless.

There are however comparatively few opportunities for sampling hot water in the Rift - most areas of thermal upflow appear as fumarolic discharges. The gas geothermometers are potentially useful here, though the ratio types, CO_2/H_2 and CO_2/H_2S, which are perhaps easiest to measure accurately, cannot often be applied because of the scarcity of H_2S and H_2 in Rift fumarole

gases. CH_4/CO_2 ratios, though available for all gases, are a rather unreliable geothermometer both on account of the controlling reactions and the possibility of a biogenic component. The straightforward CO_2 geothermometer may be the most universally applicable one in the Rift, though Armansson (1987a) points out that cold CO_2 wells exist inside and outside the Rift where the CO_2 geothermometer cannot sensibly be applied. This is despite the indications from carbon isotope measurements that all the CO_2 has a similar origin.

Isotope fractionations are by and large not particularly good geothermometers. Oxygen and hydrogen isotope fractionations between liquid and vapour phases only indicate the temperature of separation, which in fumaroles can be much cooler than reservoir temperature. The CH_4-CO_2 isotope geothermometer suffers from the same problems as the CH_4/CO_2 gas geothermometer. Other potential isotope geothermometers require difficult collection techniques (eg $\delta^{18}O$ liquid - CO_2gas) or collecting large amounts of gas (eg δ^2H liquid - H_2 gas) and may only serve to indicate separation temperatures.

6 OLKARIA AND HELL'S GATE

6.1 Hydrogeology of the Olkaria Geothermal Field

Geothermal exploration at Olkaria started in the 1950's, and the first exploration well was drilled in 1956, followed by a second well in 1958. However these wells failed to produce steam and exploration drilling was abandoned until the 1970's when several successful wells were drilled (Noble and Ojiambo, 1975).

During the last decade production drilling has been carried out at Olkaria, and a 45 MW_e power station has been constructed in the eastern part of the field. By early 1987 34 wells had been drilled at Olkaria, of which 25 are in the East Olkaria production field which covers an area of approximately 2 km^2. Well depths generally range from 1000 m to 1600 m with the deepest well reaching 2484 m (Bodvarsson and others, 1987).

The stratigraphic sequence in the area comprises subhorizontal intercalated rhyolite, trachyte and basalt lavas with thin pyroclastic beds (Browne, 1981). A thick trachyte extends from 200 m to 400 m below which basalts and rhyolites predominate to 900 m. At greater depths trachytes form the main rock type (Bodvarsson and others, 1987).

A basaltic caprock between 500 m and 700 m is thought to confine the geothermal reservoir at Olkaria. A steam zone, between 50 m and 100 m thick at a pressure of 3.5 MPa and with a temperature of 240°C underlies the caprock. Below the steam zone is a liquid-dominated reservoir which follows a boiling point for depth relationship with a temperature of 300°C at a depth of 1500 m (Bodvarsson and others, 1987). Above the caprock are shallow aquifers containing cool saline waters.

Zones of high permeability (feed zones) exist both in the steam zone and in the underlying liquid-dominated reservoir. These are few in number with normally one major feed in the feed zone and one or two in the liquid zone. There is no good correlation between rock type and permeability although it has been suggested that the pyroclastics may be more permeable (Browne, 1981). Permeability values are discussed in Section 4.4.3.

The East Olkaria field shows a substantial north-south pressure gradient of 1.1 MPa/km from which it has been inferred that an upflow zone exists to the north of the present field (Bodvarsson and others, 1987). Well temperature measurements (Haukwa, 1986) and the distribution of epidote (Browne, 1981) also indicate that the hottest, upwelling part of the field is to the north. Southerly flow beneath the caprock may then have created the steam zone by phase separation (Grant and Whittome, 1981). In a recent interpretation of reservoir hydrology (Barnett and others, 1987) it has been suggested that a major fault running east-west across the field - the Olkaria Fault - acts as a conduit for hot upwelling fluid, and that at shallow levels the upflow is perturbed by cooler fluids associated with a major north-south structure, the Ololbutot Fault.

In recent years exploration drilling has discovered extensions of the field to the west and north. Wells in the west Olkaria field have in general lower temperatures than those in the east, but they have encountered mainly liquid (and therefore their mass output is potentially higher). Permeability values in this area are similar to those in the east (Haukwa, 1984).

6.2 Geochemistry

The Olkaria geothermal field has already been mentioned as the only locality in the Rift where deep thermal fluid can be sampled, and as such has provided useful information, particularly isotopic, about flow southwards from Lake Naivasha. In addition to this larger scale picture, the relatively high density of sampling points in the eastern wellfield and the Hell's Gate (Ol Njorowa) Gorge permits closer analysis of the relationship between the wellfield and possible outflow in the gorge.

Figures 6.1a to 6.1l show plans of sampling sites in the wellfield (oblongs) and gorge (circles) with chemical and isotopic values indicated. It is apparent that there are changes in chemical and isotopic species, and also that there are similarities and dissimilarities in various species between the wellfield and gorge sampling sites. While the geochemistry of the Olkaria geothermal field has been investigated in considerable detail by other workers (Arnorsson et al, in prep.), a brief description of the changes across the wellfield is now given . Total dissolved solids (TDS) rise north to south from 676 to 1590 mg/l, an increase of some 2.4 times. Individual ions show fairly even increases of this order, except for SO_4 which does increase but is low in the southernmost well (OW2), HCO_3 which rises then declines again, and Si which is constant except for a lower level in OW2. This general increase in TDS content across the eastern wellfield from north to south fits the regional model of southerly flow from Lake Naivasha deduced from isotopic evidence: water at the southern end of the wellfield has been in residence longer than water in the north and has thus had more time for reaction with the reservoir rock at high temperature. Clearly the water has achieved supersaturation in some species before others; silica values hardly change across the wellfield. Isotopic changes across the wellfield are not regular (Figures 6.1i and 6.1j). The southernmost well (OW2) is comparatively depleted, and if this represents a local dilution effect it may also explain the drop in Si and SO_4 already noted above. Otherwise, the variations between wells may be due to steam loss (a loss curve from OW26 is shown in Figure 5.9), though is more likely to be due to a combination of variable water-rock $\delta^{18}O$ shifting and local dilution. If the total fluid compositions are considered to derive from mixing of Rift-wall groundwater and Naivasha water, a 55 to 75% lakewater contribution is suggested.

The relationship of the three northern Hell's Gate (Ol Njorowa) water sampling points to the geothermal field seems fairly straightforward. The only sample from the western side of the gorge (107) has a very high TDS (>2000 mg/l) and most probably represents natural outflow or artificial effluent from the field. Although the temperature of this manifestation is only 32°C, the enrichment in dissolved solids is probably due to steam loss/evaporation. Sites 108 and 109, on the eastern side of the gorge opposite the wellfield, have a chemistry much closer to wellfield values which suggests that they are sampling relatively unmodified outflow. The higher TDS level in 109 shows that evaporation is likely to have occurred which, as for site 107, is likely to be related to steam heating because SO_4/Cl ratios are higher than in the deep fluids. Simple evaporation would tend to cause isotopic enrichment, and 109 with a higher TDS and temperature is accordingly slightly heavier than 108.

South of these sites, on the eastern side of the gorge, four sampling sites possess stable isotopic values similar to those from the wellfield. In terms of chemistry, however, these sites are very much lower in TDS which implies that they are not directly derived from deep fluid. Instead they are probably the result of condensation of steam which was separated from an

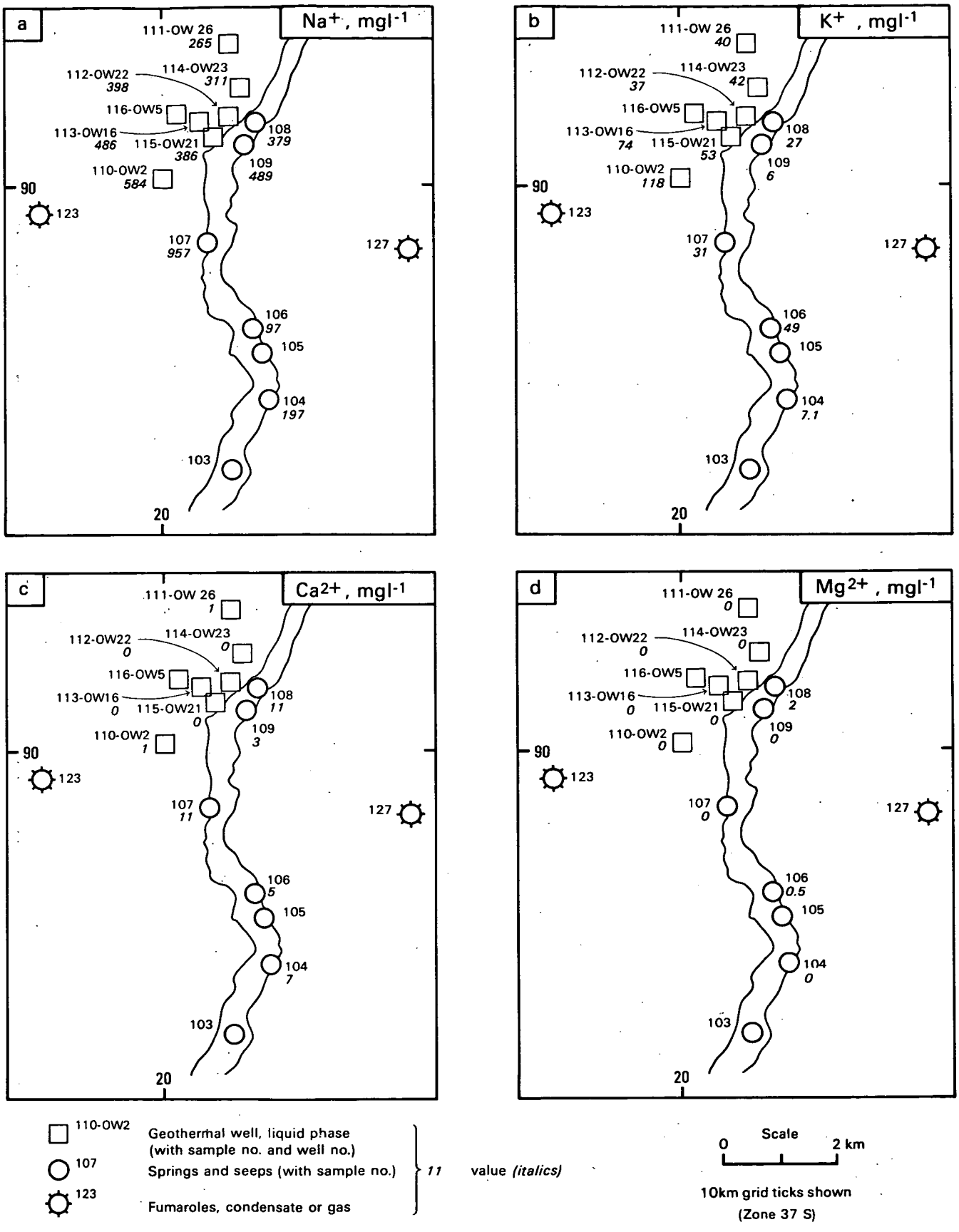

Figure 6.1a-d Maps of chemical and isotopic data for the Olkaria-Ol Njorowa (Hell's Gate) geothermal area.

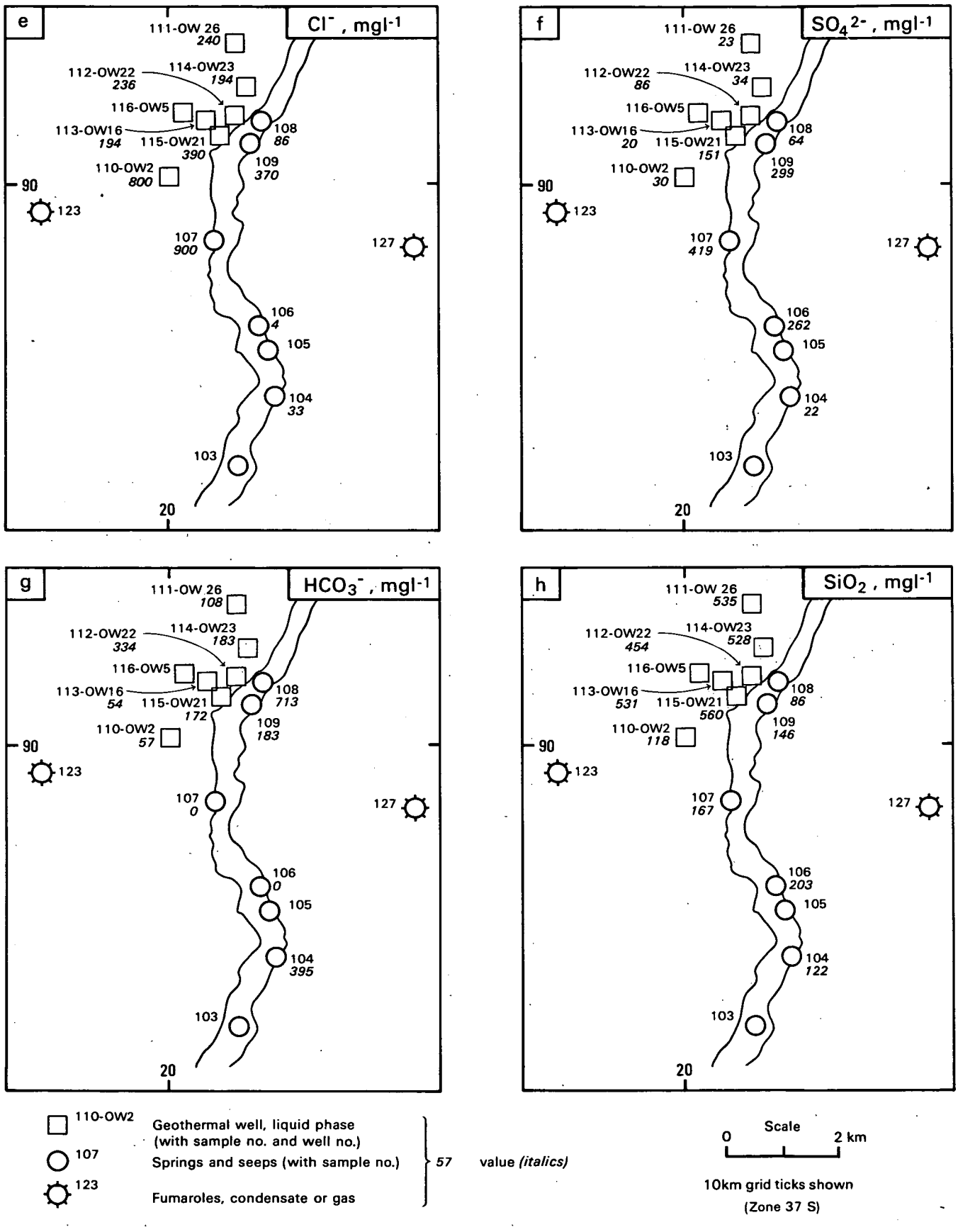

Figure 6.1e-h Maps of chemical and isotopic data for the Olkaria-Ol Njorowa (Hell's Gate) geothermal area.

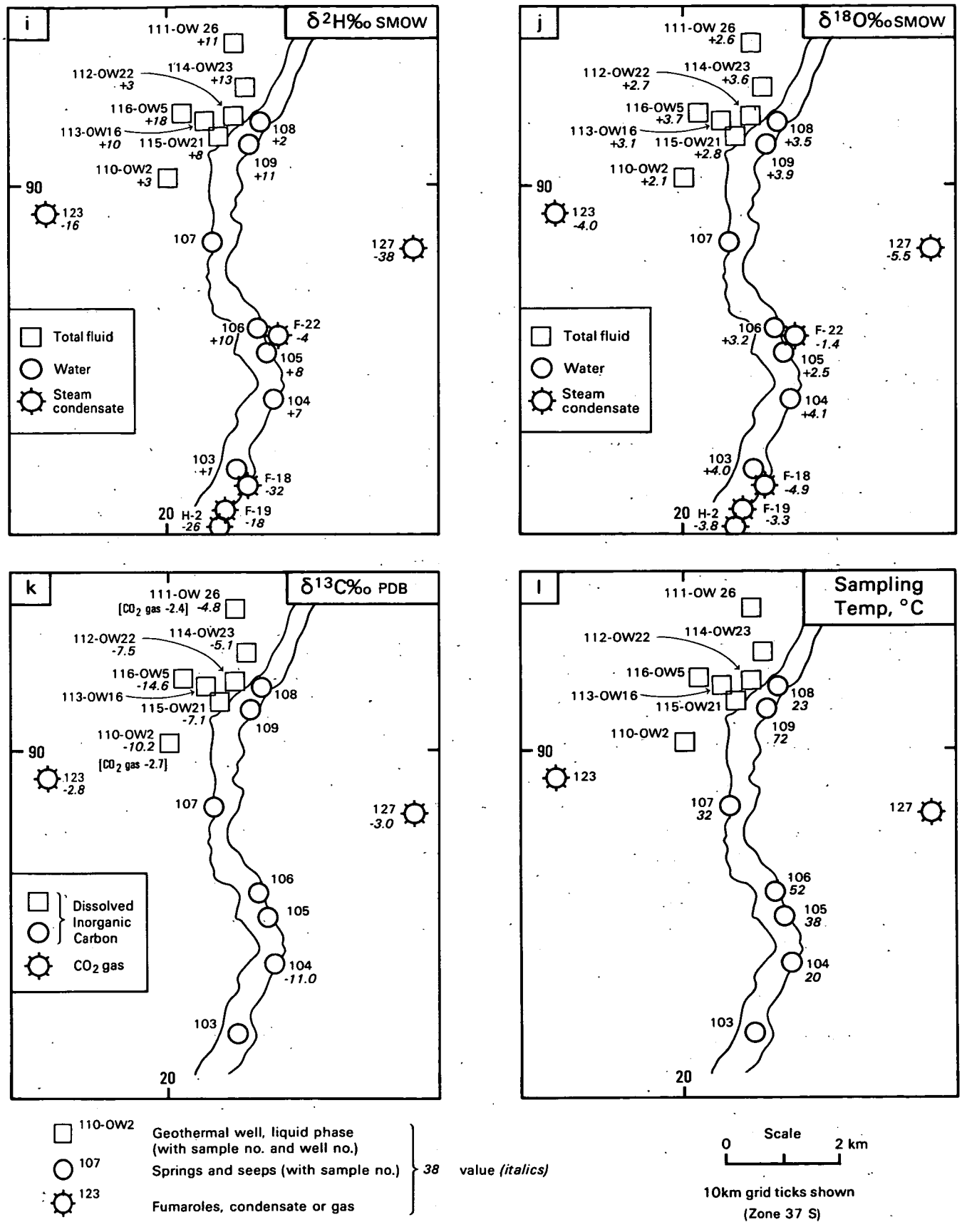

Figure 6.1i-1 Maps of chemical and isotopic data for the Olkaria-Ol Njorowa (Hell's Gate) geothermal area.

Olkaria-type deep fluid which is undergoing progressively greater dilution with Rift-wall water as it flows to the south. In some cases the sampled springs or seeps are clearly associated with nearby fumaroles while in others the connection with a steam source is less obvious, but similar mechanisms seem to apply in each case. The end result is that although sites 103-106 have similar isotopic values to the wellfield and sites 108 and 109, they are actually produced from lighter waters. Figure 6.2 shows the primary steam line for a 20% lakewater component. This line passes near F18, F19 and H2, suggesting that their steam shares a common origin. Site 103 appears to result from surface (or near-surface) condensation of F18, and an evaporative slope connects the fumarole with the seep. Similarly sites 105 and 106 are associated with F22 along a trend of similar gradient, while the fumarole itself lies near the 30% lakewater primary steam line. Site 104, which is situated about halfway between F18 and F22, has no obvious steam source, but an evaporative line sub-parallel to the other two would suggest that the source is around 25% lakewater, in accordance with the progressive southward dilution.

Fumaroles 01 to 03 were sampled in the wellfield itself. These samples lie outside the range of likely primary steam composition (Figure 5.9) and are probably the consequence of steam heating of cooler, more diluted lakewater overlying the Olkaria reservoir with values of about 0‰ δ^2H, 0‰ $\delta^{18}O$. A fumarole in the western Olkaria field could possibly be related to this process but may alternatively be a product of primary steam separation from a more dilute reservoir. In view of the major north-south fault (Ololbutot) dividing the eastern and western wellfields the latter is a tempting conclusion, but more western wellfield fumarole and/or wellfield data are required to confirm or refute this interpretation.

Carbon isotope ratios show a steady depletion in $\delta^{13}C$ DIC southwards across the geothermal field (Figure 6.1k). On the other hand, CO_2 gas from OW2, OW26, F15 and the western Olkaria fumarole already referred to are remarkably similar ($\delta^{13}C$ -2.4 to -3.0‰ PDB). Although HCO_3^- and CO_2 may almost be in isotopic equilibrium for OW26, indicating a temperature of about 200°C, they are completely out of equilibrium for OW2. This is unlikely to be a result of sampling technique; the fact that $\delta^{13}C$ DIC depletion is steady, $\delta^{13}C_{CO_2}$ values remain constant and bicarbonate concentration does not correlate with $\delta^{13}C$ depletion suggests that the explanation lies elsewhere. Changes in the $\delta^{13}C$ of well CO_2 in other geothermal fields have been attributed to the precipitation of calcite caused by near-well boiling conditions. As discussed below, there is no evidence for this occurring in the Olkaria wells on the basis of the water chemistry presented here, and in any case $\delta^{13}C$ CO_2 does not appear to change. In addition there is no reason why this should affect the $\delta^{13}C$ CO_2-DIC equilibrium, which would be expected to re-establish itself during transit to the surface. In the absence of further data the question remains open

Gas samples were collected from OW2 and OW26 and results are given in Table 5.10. The geothermometric aspects of these gas samples are considered in Section 5.7.2 of this report, where it is suggested that the presence of a large percentage of lakewater in the Olkaria reservoir could be responsible for a proportion of the methane measured in the gases. Such biogenic methane would render unreliable chemical and isotopic geothermometers based on inorganic thermal CH_4. The ethane values from OW2 and OW26 appear to indicate a lakewater rather than a thermogenic origin: OW26 has the highest C_2H_6/CH_4 ratio of any gas sample collected while OW2, situated downflow, is lower. By contrast a very strong upflow like Longonot F23 (indicated by the presence of He and H_2) has a low C_2H_6/CH_4 ratio. On this rather tenuous

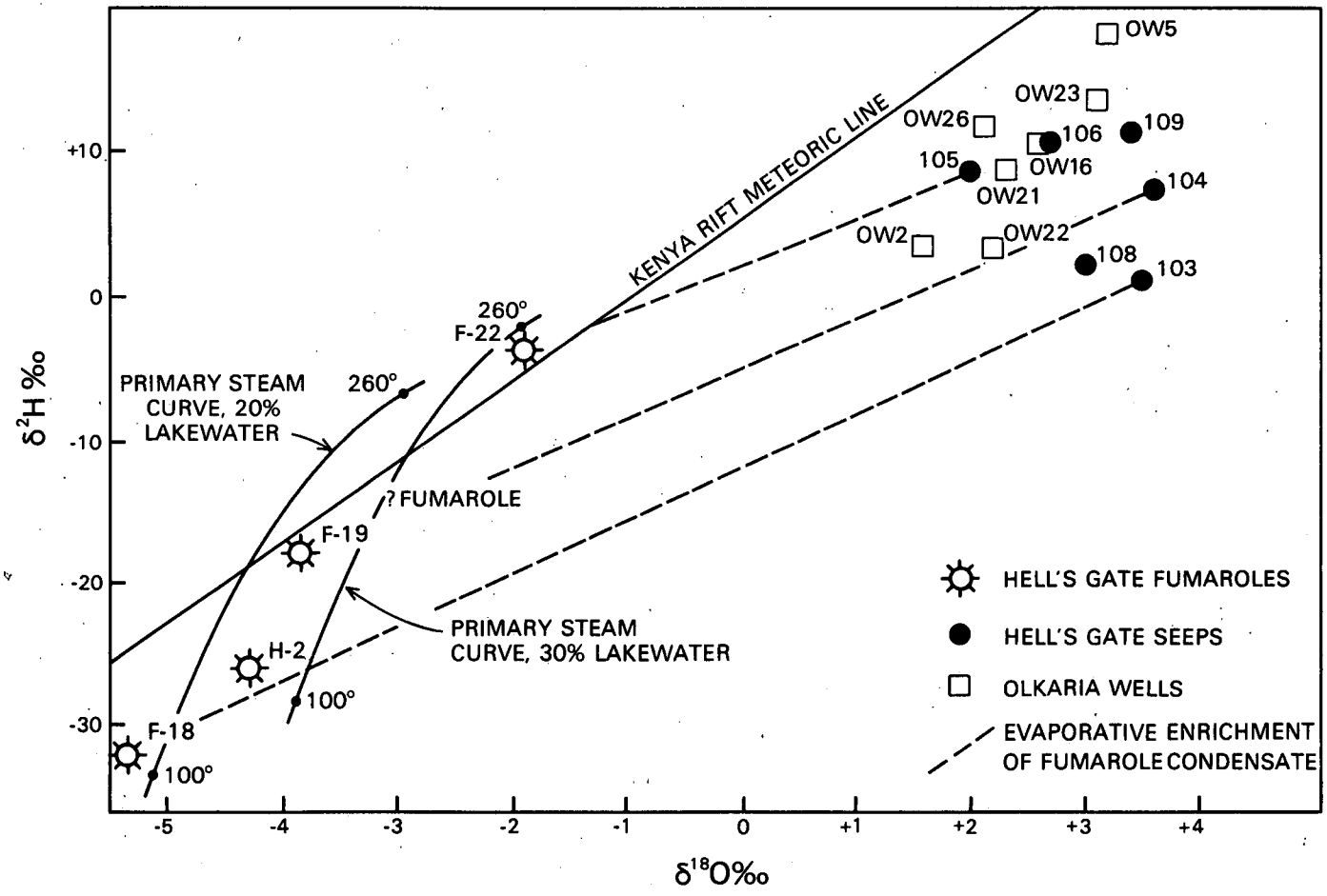

Figure 6.2 Delta-diagram of stable isotope data from the Olkaria-Ol Njorowa (Hell's Gate) geothermal area.

evidence, the West Olkaria fumarole sampled may have a larger lakewater contribution than its H and O isotopic values suggest.

The lack of readily detectable He or H_2 at Olkaria suggests that the wells are further from an upflow than for example the Longonot crater fumarole F23 or the Eburru fumarole EF2.

Chemical geothermometers give good results for the Olkaria wellfield. There is reasonable agreement for most wells between the quartz and Na/K results. Samples from five wells give an average temperature of 255°C for quartz, and 240°C for Na/K (Table 5.14). The results can be compared with the average main feed temperature of eight (unidentified) Olkaria wells of 242°C (Armannsson, 1987b). In the same report, CO_2 geothermometry results were reported averaging 245°C, and it was assumed that calcite was a primary control of CO_2 concentrations. The WATEQF-calculated saturation indices (Table 5.15), though not as ideal for high temperature geothermal systems as some specific codes, suggest that it is indeed the case. Calcite, although undersaturated, is the major carbonate phase, though not so very much in excess of magnesite and nahcolite. This undersaturation of calcite may be a consequence of cooling by conduction, or perhaps limited dilution, after upflow. The wells do of course show supersaturation with respect to quartz and, it is interesting to note, magadiite - a sodium silicate mineral, $NaSi_7O_{13}(OH)_3.3H_2O$, first identified by Eugster (1970) in the Lake Magadi area.

Tritium results from OW2 and OW26 are identical within measurement error, averaging 0.23 TR (Table 5.9). This level implies either that inflow has been in transit for at least 40 years, or that it is older than this but has a small amount of thermonuclear tritium (i.e. post 1954) as a result of leakage from the surface. Alternatively the ^3H content might result from the decay of ^6Li, though this process is probably of most significance in granitic rocks (Andrews and Kay, 1982).

Helium isotope ratios of corrected R/Ra values 5.69 and 5.83 (Table 5.11) were noted for OW2 and OW26. The values are close to those of Longonot F23 and Eburru EF2 and are probably derived from the same local crustal reservoir. The fact that they are slightly lower than the volcanic upflows is presumably due to the fact that they are not directly situated over the local Olkaria upflow. A very similar R/Ra value of 5.62 was noted for the West Olkaria fumarole sampled. While this does not necessarily imply that the western wellfield is intimately linked to the eastern, it does suggest a similar proximity to an upflow. The Domes fumarole F15 gave a lower R/Ra value of 2.92 - this may suggest increasing distance from an upflow, but gas analyses indicate that air entrainment could have affected the ratio.

Olkaria Area - Conclusions.

Geochemical indications are that flow across the eastern wellfield is taking place from north to south. While it should be borne in mind that the chemistry of the water fraction will not be identical to that of total fluid at depth in the reservoir (due to steam and gas separation), the data serve to indicate a general rise in solutes across the wellfield presumably due to increasing amounts of water-rock interaction and perhaps steam loss. The TDS of the fluid is however low by the standards of many other geothermal fields, which may suggest a relatively short flow path and/or residence time, though the latter is constrained as to its lower limit by the tritium data. Chemical geothermometers give reliable results where they can be compared with well-bottom temperatures.

Water stable isotopes indicate a decreasing lakewater contribution to the deep fluid in a southerly direction. They also show that only a limited $\delta^{18}O$ shift is presently occurring: this implies a system of some antiquity where rock is approaching isotopic equilibrium with original water values after a large amount of throughflow. The alternative explanation, a younger but very 'wet' geothermal system seems less likely from the preliminary interpretation of the local water balance presented in this report. Core material obtained from some Olkaria wells will be subjected to stable isotope analysis to see what light can be shed on the field's history.

Gas data suggest that eastern Olkaria is not situated directly over an upflow since He and H_2 are only present at lower concentrations. Although the R/Ra values are relatively high these are not infallible indicators of proximity to upflow - for example the DEL well (site 124) on the Eburru outflow has a very similar R/Ra to EF2, even though it is situated some 10 km away.

The relationship between $\delta^{13}CCO_2$ and $\delta^{13}CDIC$ is problematic, but the hydrocarbon gas ratios appear to confirm that substantial amounts of lakewater are present at Olkaria.

7 LAKE MAGADI THERMAL SPRINGS

7.1 Introduction

As a result of extreme evaporation of the alkaline lake brine (Na+, HCO_3^{2-} + CO_3^{2-} type; salinity 290 000 mg/l), Lake Magadi contains a deposit of crystalline trona up to 40 m thick (Jones and others, 1977). This is composed of crystalline carbonates of sodium (principally sodium sesquicarbonate [$Na_2CO_3.NaHCO_3.2H_2O$]) which is dredged by the Magadi Soda Company and treated before being calcined in large kilns to produce soda ash.

The lake is fed by groups of alkaline springs with temperatures varying between 34°C and 86°C which occur at several points around the periphery of the lake (Figure 7.1, adapted from Baker, 1958). In general the hottest springs are the most dilute and occur in the north, and the cooler more saline springs are found to the south of the lake. The values of discharge of the springs are very variable. Some are only seepages rising in the mud and shingle of the lake shore (for example those at Bird Rock). Others such as the main hot springs feeding Little Magadi are much larger, with flows of several litres/second.

According to Baker (1958) most springs issue from scree at the base of the fault escarpments bounding the lake and nearly all the spring waters then find their way into the stagnant lagoons that border the main trona bed at lake level. During and immediately after the rainy seasons the lagoons are connected with the shallow brine body covering the lake surface (Jones and others, 1977). This brine body vanishes during the dry seasons exposing a porous but firm trona deposit. As a result of the economic and scientific importance of Lake Magadi a number of studies have been carried out, usually aimed at determining the origin of the solutes forming the trona. These attempts have naturally included studies of the springs bordering the lake and it is therefore pertinent to review them where they bear on the origin and nature of the hot springs.

7.2 Origin of the Hot Springs - Previous Work

Early ideas concerning the origin of the springs are discussed by Baker (1958). He considers three hypotheses, namely Parkinson's, Stevens' and the re-circulation hypothesis.

Parkinson's hypothesis (1914) was that the spring water is of juvenile origin. The water, he suggested, contains magmatic CO_2 and reacts with the sodium silicates in the lavas through which it passes, forming sodium carbonate and silica. This hypothesis may be dismissed on the basis of the isotope evidence which proves the water to be meteoric in origin - although the chemical reaction suggested is valid.

Gregory in 1921 (cited in Baker, 1958) raised the possibility that the lake was an evaporating pan in which trona, leached from adjacent lavas by percolating waters was deposited, but he rejected the idea in favour of Parkinson's hypothesis.

Stevens (1932) concluded that the greater part of the lake salts at Magadi must be derived from spring solutes and he suggested that the constancy of the carbonate/chloride ratio in the springs implied a common source for them all, which he considered to be a large body of 'mother liquor' at depth. Later, in 1951, Guest and Stevens, having estimated the flows of the springs (by considering the rate of lake evaporation) concluded that the rate of

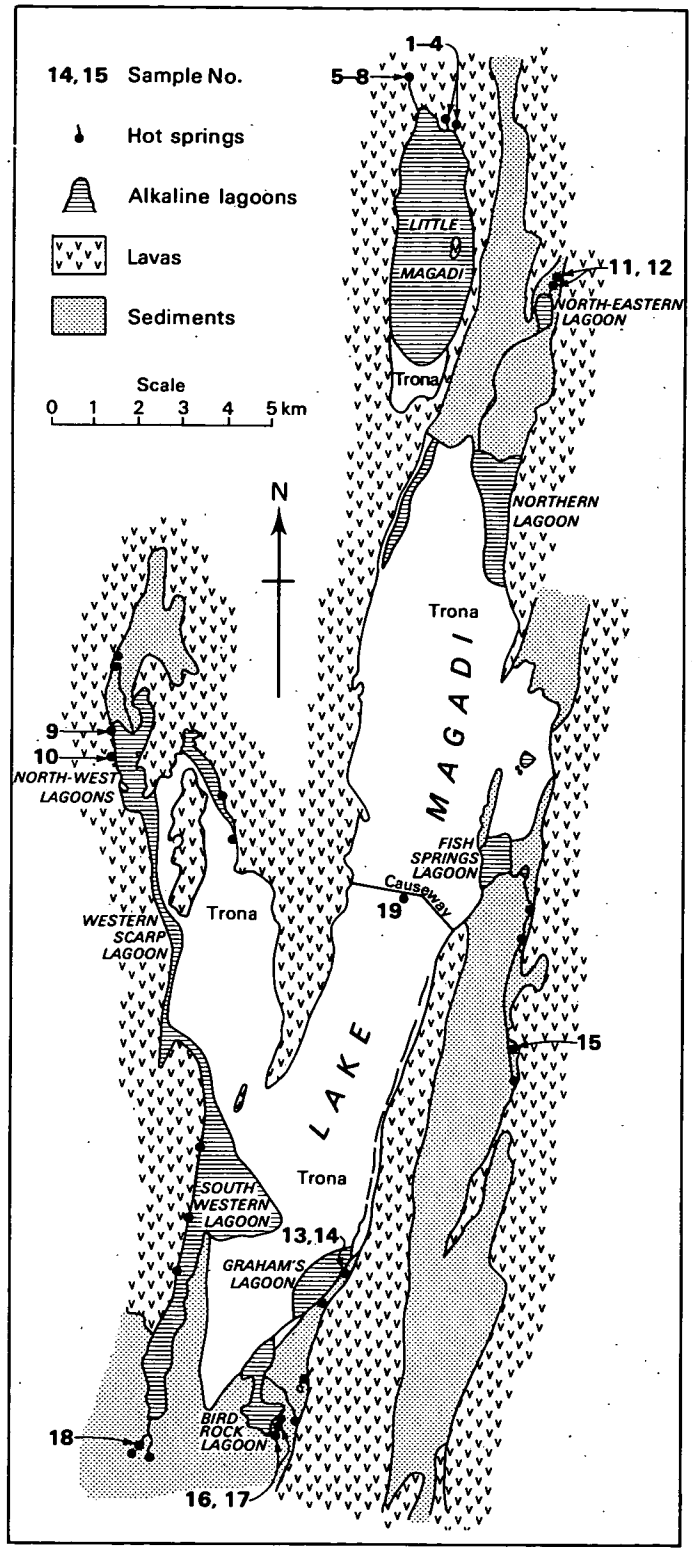

Figure 7.1 Location map of the Magadi hot springs.

solute addition to the lake was too great to account for its age (Guest and Stevens, 1951). They therefore reasoned that a proportion of the lake liquor must recirculate, with heavy liquor descending and becoming mixed with ascending hot spring water.

Bakers own hypothesis (1958) was that groundwater in the Rift Valley leaches salt from igneous silicates over a large area. These salts become concentrated by repeated evaporation of lake water, and re-leaching in the numerous pans between fault escarpments in the southern Rift Valley. Such waters would ultimately accumulate as alkaline groundwater in the Magadi basin at the lowest point in the Rift Valley, and would provide trona by evaporation of the spring waters.

More recently Eugster and others have proposed a detailed model for brine evolution at Magadi involving evaporative concentration as the main process for solute acquisition (Eugster, 1970; Jones, Eugster and Rettig, 1977; Eugster, 1980).

The basis for the model is that, according to Eugster, the Na/Cl ratios of stream waters on the sides of the Rift are similar to those of groundwaters, and for the springs bordering the lake. Eugster therefore proposes that the increase in solute concentration observed between the peripheral streams and the lake brines is principally a result of surface evaporation, and can be followed by using NaCl as a tracer (assuming that NaCl remains in solution until very late in the concentration process). Eugster argues that constituents such as Ca, Mg, HCO_3 and CO_2, SiO_2 and K which are not concentrated to the same degree as NaCl are lost during brine evolution, chiefly by precipitation (or in the case of CO_2, by degassing).

The main mechanism for evaporative concentration proposed by Eugster is the dissolution of efflorescent crusts. These crusts are formed either by the evaporation of runoff, or by capillary evaporation of shallow groundwater. Once formed, only the more soluble constituents of the crusts are dissolved by subsequent contact with dilute rainwater. Thus for example, NaCl and Na_2CO_3 dissolve, while calcite, magnesium calcite, dolomite silica and silicates remain.

Eugster's postulated circulation system "involves inflow from dilute rim streams descending into the Rift Valley and ephemeral runoff within the valley floor feeding local dilute groundwater bodies. It also stipulates the presence of a hot saline groundwater body at some depth within the trachyte lavas [under Lake Magadi]. This body is inferred from the constancy of the spring temperatures over 40 years" (Eugster, 1980).

In order therefore to arrive at the various spring concentrations, composition and temperatures Eugster postulates three sources which are mixed in different proportions for each spring: shallow groundwater (cold, dilute), deep groundwater (hot, saline) and recirculated surface brine (cold, more saline, high pH). The solutes in all three sources originate ultimately by evaporative concentration.

Recently Hillaire-Marcel and Casanova (1987) have used Eugster's model and with the addition of isotopic data have attempted to identify the different types of water in the model. The authors obtained δ^2H and $\delta^{18}O$ values for the lake, for several of the surrounding springs, and for local precipitation.

Hillaire-Marcel and Casanova found a linear relationship between the δ^2H and

$\delta^{18}O$ values for the springs and the interstitial lake brine which indicated evaporation. By regressing this line to the World Meteoric Line they obtained an intersection value which they considered to represent the value of deep thermal water. This value is significantly depleted isotopically with respect to the average value for present day recharge and, the authors suggest, represents recharge during the last humid episode in Kenya. This period was determined by Hillaire-Marcel and Casanova as 12000-10000 years BP from stromatolite dating, when the lake level was significantly higher than at present.

A study by Crane (1981) has concentrated more on the geothermal aspects of the springs. She compiled thermal, seismic and rainfall data collected over periods of up to 60 years and attempted to correlate spring temperature variation with volcanic, tectonic and meteoric activity.

Crane found that the southern cooler springs have a rapid temperature response to rainfall fluctuations over several decades. She concluded that these springs therefore have a shallow source and, following Eugster's model, that they therefore recirculate lake brines rapidly.

No such relation between temperature and rainfall was evident for the northern springs leading Crane to conclude that these arise from a deep-seated saline water body. She did however attribute temperature variations in the northern springs partially to volcanic activity in Tanzania and suggested that this inferred a greater hydraulic connection with the Rift to the south than with the north. Other temperature variations were postulated by Crane to have been caused by local seismic activity affecting circulation patterns.

The total heat output of the Magadi region was estimated by Crane to be around 900 MW, based on aerial infra-red measurements.

Additional hydrochemical work in the Magadi area was carried out by Glover (1972) who favoured an origin for the springs as locally steam-heated groundwater, and a limited number of stable isotopic analyses (mainly $\delta^{18}O$) have been reported by Panichi and Tongiorgi (1974) and Bwire-Ojiambo (1984).

7.3 Sampling.

Samples for chemical and isotopic analysis were taken from all the main groups of springs and from several of the minor groups, as shown in Figure 7.1. Samples 1-4 and 5-8 were taken from two groups of hot springs to the north-east and north respectively of Little Magadi. These groups contain the hottest springs found around Lake Magadi, with temperatures of up to 85.3°C. Flow rates of individual springs range up to an estimated 6 l/s. The springs are mainly associated with fault scarps, and some occur within the lagoon.

Samples 9 and 10 were taken from a series of springs and seeps spread over a distance of over a kilometre to the west of the North-West Lagoons. The temperature of the sampled springs, 45°C, was significantly lower than that of the Little Magadi springs and flow rates were also lower, ranging up to 2 l/s for individual springs.

Samples 11 and 12 were obtained from a group of three springs and seep zones on the east side of a small graben to the north of the North-East Lagoon. Spring temperatures were intermediate to the previous groups at 65-67°C and spring discharges totalled 5 l/s.

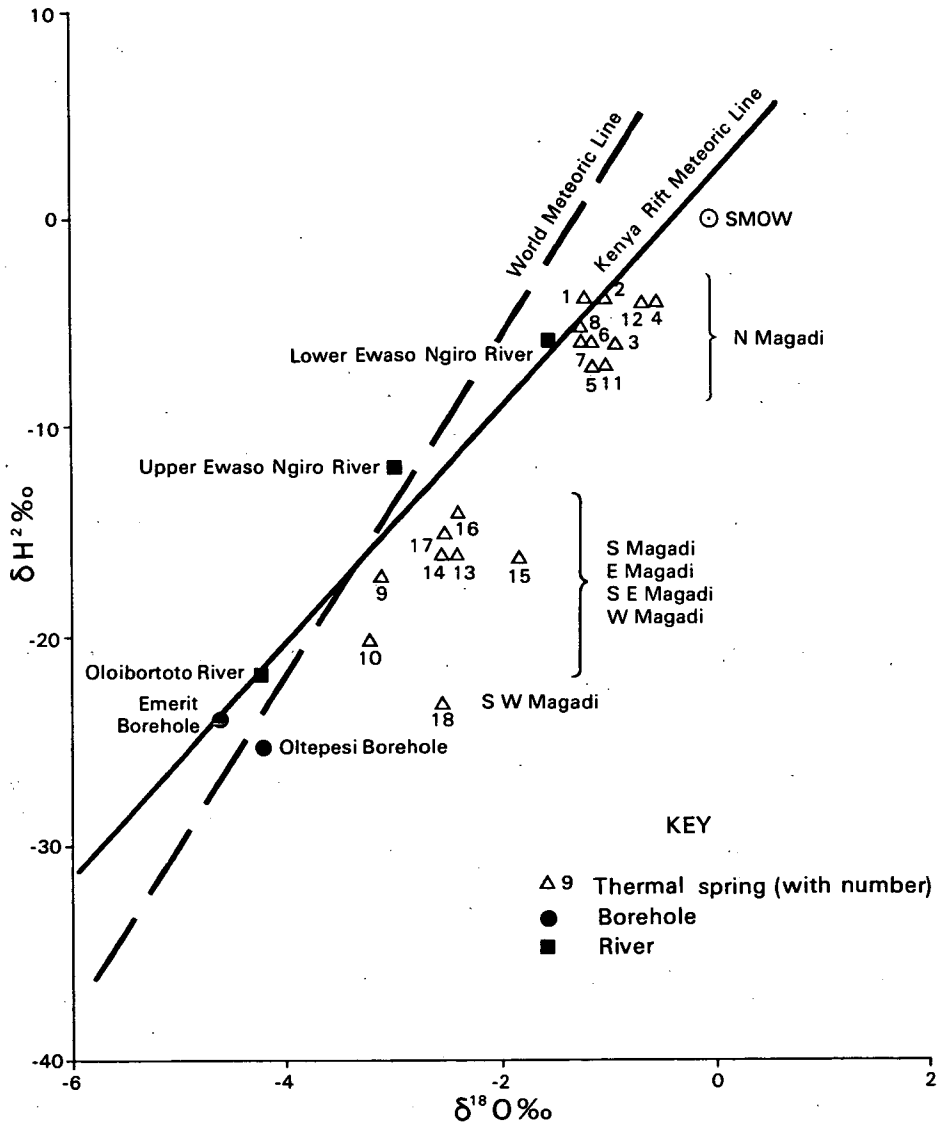

Figure 7.2 Stable isotope characteristics of waters in the Magadi area.

A small spring group on the edge of Graham's Lagoon producing water at 38-39.5°C was sampled (samples 13 and 14), as was a group of springs further north with low discharge rates and the lowest temperatures recorded - 34°C (sample 15).

At the southern end of Lake Magadi by the Bird Rock Lagoon, a group of seeps and small springs (flow rates less than 1 l/s) with temperatures of 40.5-40.8°C were sampled (samples 16 and 17). To the west sample 18 was taken from a powerful set of springs with an estimated total discharge of 100 l/s and a temperature of 45.3°C.

Finally a sample of lake liquor was taken from a point near the causeway (sample 19).

In addition to springs and lakewater samples were taken from the Ewaso Ngiro and Oloibortoto rivers to the west (samples 20,21,32) and from boreholes at Oltepesi and Emerit, about 40 km to the NE of Magadi.

7.4 Isotopic Characteristics.

Isotopic determinations ($\delta^{18}O$, $\delta^{2}H$) are listed in Table and illustrated in Figure 7.2, which includes for reference the standard World Meteoric Line of Craig (1963) and the Kenya Rift Meteoric Line determined previously (Section 5.3).

Ambient water samples.

Three samples from rivers near to Magadi are shown in Figure 7.2. Two of the samples were taken from the Ewaso Ngiro River which is the only perennial river in the area; one sample was from the upper reaches of the river, near Narok, and the other was taken where the river reaches the Ewaso Ngiro plain at the base of the Nguruman Escarpment. The slope of 4.3 between the two samples' isotopic compositions (Figure 7.2) suggests that evaporation has occurred between the upper and lower reaches of the river, and this is supported by the higher concentration of solutes found in the lower sample.

Thermal springs.

The isotopic characteristics of the thermal springs (Figure 7.2) fall mainly into two groups. The northern, hotter springs from the north shores of Little Magadi and the North-Eastern Lagoon form a tight cluster about the local meteoric line, with an average value of -5‰ $\delta^{2}H$ and -1‰ $\delta^{18}O$ (samples 1-8, 11-12). The cooler spring groups of the North-West Lagoon (samples 9-10) and the spring groups to the east and south east of the lake (samples 13-17) form a looser, more isotopically more depleted cluster near the meteoric line with an average vale of around -17‰ $\delta^{2}H$, -2.5‰ $\delta^{18}O$. Sample 18, taken from a powerful warm spring at the southern end of the lake may not form part of this second cluster, being slightly more depleted in deuterium and enriched in ^{18}O.

Many thermal waters throughout the world exhibit a significant increase in $\delta^{18}O$ as a result of interaction with silicates or carbonates at depth, an effect known as the 'oxygen shift'. However the Magadi spring samples show very little evidence of any shift and in fact the hottest springs fall closest to the meteoric line whereas these would be expected to be the most shifted. Hillaire-Marcel and Casanova (1987) suggest that the oxygen shift has indeed occurred, but that isotopically depleted CO_2, associated with the carbonatitic volcanism of the Oldoingo Lengai volcano to the south of Magadi,

has mixed with the springwaters and has resulted in depletion by isotopic exchange. However, while it is true that the waters around Magadi are CO_2-rich, the above hypothesis is unnecessary and unproven. Apart from the unlikelihood of waters being shifted away from the meteoric line and then fortuitously back onto it (in the case of the hottest springs) the quantities of CO_2 required to exchange with the springwaters would be enormous. A similar explanation is that little or no shift has occurred, probably because flow paths and groundwater residence times of the springwaters are too short for exchange to occur.

Another possible mechanism which may have affected the isotopic compositions of the springwaters is evaporation, such as the trend suggested by Hillaire-Marcel and Casanova (1987) and discussed in Section 7.2. In general terms it is possible that all values which lie to the right of the Kenya Rift Meteoric Line on Figure 7.2, may indeed lie on an evaporative trend even though they are close to the meteoric line. This is because the Kenya Meteoric Line is itself a reflection of evaporative effects, which is why it departs from the World Meteoric Line.

However the data do not support Hillaire-Marcell and Casanova's contention that all the springs lie on an evaporative trend because the most enriched samples (which would be expected to be the most evaporated) lie closest to the local meteoric line. Also the cooler springs, which according to Hillaire-Marcel and Casanova have mixed with recirculated (and therefore highly evaporated) lake brines should therefore be further along the evaporation trend than the hot brines, which they are not.

Eugster's hypothesis concerning spring evolution depends on evaporation for solute concentration but this is not supported by a plot of Cl^- v. $\delta^{18}O$ (Figure 7.3) which shows that an increase of salinity of three orders of magnitude is not accompanied by any isotopic enrichment. However his hypothesis is not rejected by such data if the re-dissolution of evaporites by meteoric waters is postulated as the dominant mechanism for brine concentration.

In summary, the hottest springs appear to represent unaltered meteoric water, and their tight clustering indicates that they have not mixed substantially with waters of different composition. This in turn suggests that their original source had a similar isotopic composition to the springs. Such a source is apparent in the Lower Ewaso Ngiro River, which has an isotopic composition which is very similar to those of the hot springs (in fact it is very slightly depleted with respect to the spring isotopes, but this difference could be accounted for by a small amount of evaporation). The river flows along the base of the Nguruman Escarpment approximately 20 km to the west of Lake Magadi and is perennial. The postulated recharge mechanism would therefore be via the river alluvium on the Ewaso Ngiro plain.

Lake water.

The enrichment of $\delta^{18}O$ of the lake brines at Magadi is not accompanied by enrichment in δ^2H to give the usual evaporative gradient. This is because of the extreme salinity of the brines (approximately 300,000 mg/l) which causes a reversal of the isotopic gradient to occur, leading to a reduction in δ^2H (Gat, 1980).

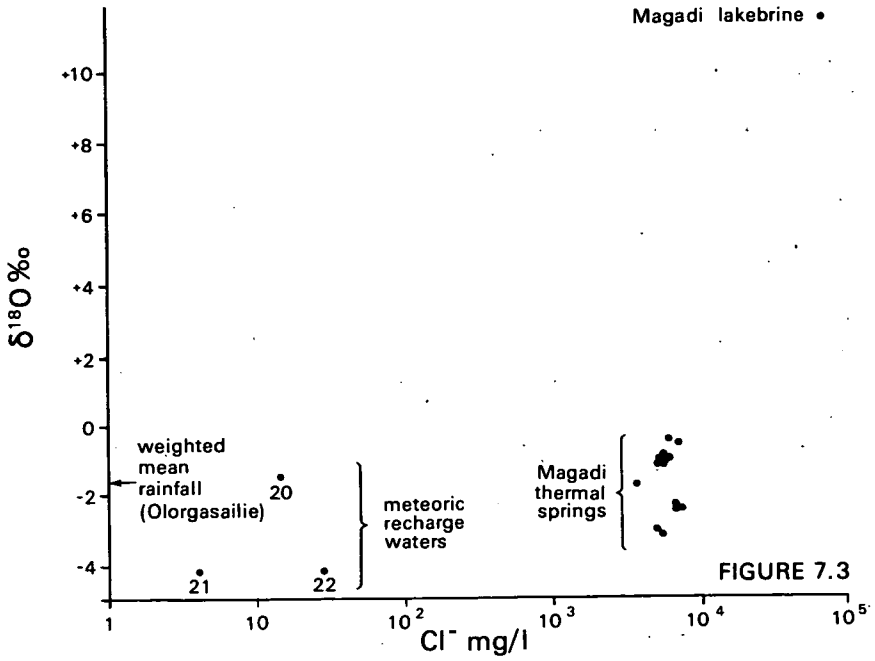

FIGURE 7.3

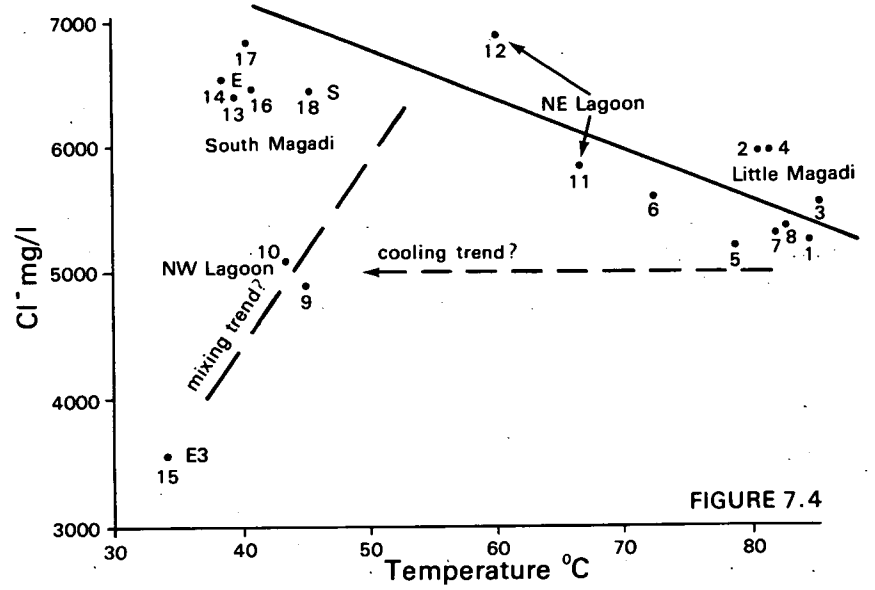

FIGURE 7.4

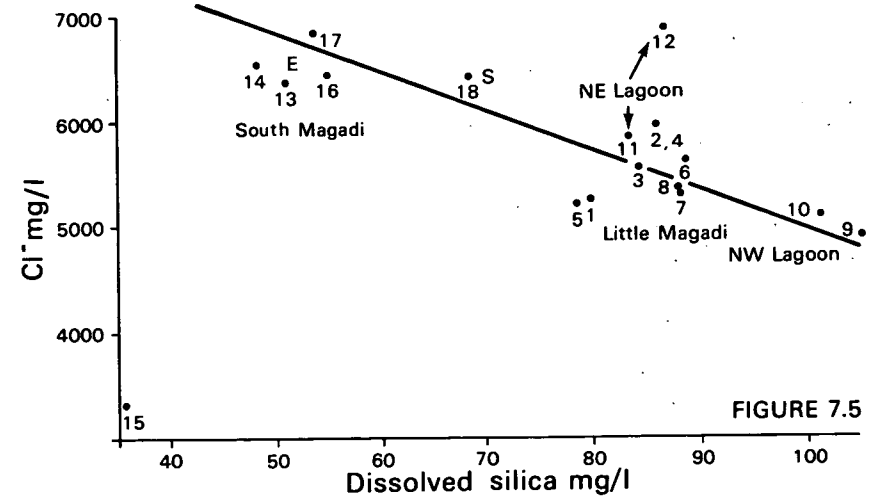

FIGURE 7.5

Figure 7.3 Variation of chloride with $\delta^{18}O$ for Magadi water samples.

Figure 7.4 Variation of chloride with temperature for Magadi spring samples.

Figure 7.5 Variation of chloride with silica for Magadi spring samples.

7.5 Hydrochemistry.

The springs around Lake Magadi are alkaline Na-HCO_3 brines with chloride a subordinate anion and a salinity range of 30,000 mg/l to 40,000 mg/l. Their hydrochemistry has been described in some detail by Jones and others (1977).

With three exceptions the present data show a direct inverse relationship between dissolved chloride Cl^-, and discharge temperature (Figure 7.4). Sample 15 is interpreted as a local spring at ambient temperature unrelated to the thermal system. This linear relationship between Cl^- and temperature implies that the Magadi springs discharge a mixture of two components. A thermal relatively less saline component appears to mix in varying proportions with a cooler saline component prior to discharge. Samples 9 and 10 which do not appear to conform with this view may be on a cooling trend or a mixing trend.

The dependence of silica solubility on temperature controls the levels of SiO_2 in solution above about 100°C and dissolved SiO_2 is commonly preserved in solution on subsequent cooling or mixing. A plot of dissolved chloride versus silica (Figure 7.5) supports the inverse mixing relationship and suggests that the NW lagoon springs have cooled on ascent (i.e. they have the highest silica concentrations).

Additional support for the mixing hypothesis comes from a linear relationship between temperature and lithium, sodium and potassium. Overall chemical evidence suggests that a low temperature component with relatively low concentrations of lithium and potassium and higher concentrations of chloride and sodium (and to some extent sulphate) mixes with a thermal component with the inverse properties.

7.6 Discussion

Lake Magadi lies at the lowest point of the southern Kenya Rift Valley and is therefore the point to which all groundwaters in the Rift from Lake Naivasha southwards are directed. This in turn means that the region is a discharge area and a terminus for solutes leached from the rocks composing the Rift by circulating groundwaters, and the presence of evaporites and saline springs in the area is therefore to be expected, as discussed by Baker (1958).

Various attempts have been made to explain more precisely the mechanism for solute concentration and trona formation, and by far the most detailed and most widely accepted in the literature is that of Eugster and others, based on evaporative concentration.

Eugster's hypothesis hinges on the assumption that Na/Cl ratios remain constant from marginal streams to lake brines. This assumption is well supported by data for the sequence from springs to trona formation; but there are few data for the sequence from marginal streams through groundwaters to springs. Eugster proposes surface and capillary evaporation and dissolution of efflorescent crusts as mechanisms of evaporative concentration (Eugster, 1980). The results of the present study indicate that if Eugster's hypothesis is to be accepted only the dissolution of efflorescent crusts by meteoric waters is a possible mechanism for solute concentration.

Of greater importance to the present study, however are Eugster's proposals, supported by Hillaire-Marcel and Casanova (1987) and Crane (1981), regarding the sources of the waters supplying the Magadi thermal springs. Eugster proposes two cool components (Section 7.2) mixing with the thermal component

and Crane cites evidence that the cool meteoric component is a relatively shallow system. Data from the present study, however, indicate essentially a two-component mixing series, with one cool saline end-member and a hot less saline end-member. Also, whereas one of Eugster's cool components is recirculated lake brine the present study indicates that the cool end-member shows little of the evaporation that characterises the true lake brines. On the other hand the interstitial lake brines are so saline (with chloride contents ranging between 37000 mg/l and 96000 mg/l [Eugster, 1980]) that the ratio of groundwater to lakewater would be high to obtain the salinity of the warm springs (c. 7500 mg/l). Eugster's model and the two component mixing model are not necessarily incompatible therefore if a body of ambient groundwater, with a salinity of around 7500 mg/l chloride, is postulated to exist in the sediments underlying the lake formed by a mixture of meteoric water and either recirculated lakewater or perhaps dissolved evaporites.

Some evidence for the existence of a saline groundwater body is that a borehole drilled to 297 m encountered brines with a salinity of 20000 mg/l chloride in the lavas beneath the lake (Eugster, 1980). This borehole was stated as being artesian (i.e. indicating upward flow within the lavas towards some discharge area) but no temperature data were given.

The third and geothermally significant component of Eugster's spring model is the proposed hot saline groundwater body with a composition similar to the hottest springs at Little Magadi (i.e. with a chloride content of around 5000 mg/l and a TDS of around 30000 mg/l). Eugster's evidence for such a body is the constancy of spring temperatures and chemistry over several decades. Paradoxically Crane (1981) presents data of variations in spring temperature over several decades but concludes that as the hot spring temperatures do not vary with changes in rainfall then they must originate in a deep reservoir.

Data from the present study support Eugster's hot spring source. The chemical data suggest a single end-member source for the hot springs and the clustering of the isotopic data indicate that the hottest springs have not mixed significantly with other waters and therefore represent the hot end-member of the mixing series. If this is so then Silica geothermometry may be used to estimate the temperature of the springs at depth (other cation geothermometers cannot be used because of the origin of the solutes). Table 5.14 shows that these temperatures are low, never reaching 150°C. (The highest temperatures estimated by silica geothermometry are in fact those for the two NW Lagoon samples, which do not fall in the same isotope cluster on Figure 7.2 as the other hot springs, for reasons which are unknown).

An alternative interpretation of the data is raised by Mahon's (1972) suggestion that much of the Rift is underlain by a hot body of water containing a few hundred parts per million of chloride. This view was based on similarities in the chemistry of fluids at Olkaria and hot springs further north near lakes Elmenteita, Bogoria and Baringo. If it were assumed that a hot end-member of the Magadi mixing series existed with a chloride content of 450 mg/l (similar to that found at Olkaria) then this body of water would, from Figure 7.4, have a temperature slightly in excess of 200°C. There is however no direct evidence for any such water in the Magadi area and the hypothesis is regarded as unlikely.

The best indications of the likely source of the Magadi thermal water are provided by the stable isotope data. These show (Figure 7.2) that the water is meteoric but more enriched than the sampled groundwaters (although these were obtained from a significant distance to the north-west). From the

available data, the most likely source is the Ewaso Ngiro River which runs along the base of the Nguruman Escarpment some 25 km to the west of Lake Magadi. In this area the Ewaso Ngiro River has undergone some evaporation and is somewhat enriched isotopically, compared with its headwaters. Figure 7.2 shows that its isotopic composition is in fact very close to that of the northern Magadi hot springs and the very small difference in composition could readily be attributed to further evaporation and some mixing with local groundwaters. (Mixing could also explain the displacement of the NW Lagoon springs from the main hot spring cluster).

It has sometimes been suggested that the Magadi hot springs could have their origin in the groundwater recharge from Lake Naivasha, but this may be refuted on two accounts. Firstly the hot spring stable isotope data show no connection with the highly enriched samples obtained from Lake Naivasha. Secondly isotopic evidence from groundwaters around Lake Naivasha indicates that the lakewater becomes significantly diluted by mixing with local groundwaters within a short distance of the lake, and dilution would increase as the lakewater flowed south. Therefore, while some lakewater may eventually reach the Magadi springs, it would be so diluted as to be unrecognisable.

A more pertinent question therefore is whether the Magadi hot springs have their origin in the mix of waters flowing from the north, or from essentially local sources such as the Ewaso Ngiro and the Nguruman Escarpment, and in the absence of other data the isotopic evidence favours a local origin. The lack of an oxygen isotope shift in the hot springs also suggests a local origin by implying a short contact time between water and rock, and therefore a short flow path. The postulated recharge mechanism would therefore be via the river alluvium of the Ewaso Ngiro plain to the west of Lake Magadi.

The short distance between recharge and discharge areas suggests a convective cell driven by a local heat source probably to the west of Magadi, of unknown origin.

In conclusion, the Magadi hot springs appear to derive from a hot, saline groundwater body with a temperature of between 100-150°C. Recharge is considered to be provided by the lower Ewaso Ngiro River and local groundwaters derived from the sides of the Rift, with cold waters percolating through the river alluvium and underlying volcanics and rising, after being heated, via active grid faults around Lake Magadi. The heat source for the springs is probably local and lies to the west of Lake Magadi. Although the heat output of the springs is significant (estimated as greater than 250 MW from their discharge, and 900 MW from infra-red analysis) the low indicated reservoir temperature would rule out the use of the resource for electrical power generation unless binary systems were to be considered.

Finally it is suggested that further geothermal research in the Magadi area should include shallow borehole drilling to the north of Magadi in order to identify the characteristics of fluid flowing from the north, and geophysical work/borehole drilling to the west of Little Magadi to attempt to identify the postulated thermal upflow in this area.

8 CONCLUSIONS

On a regional scale the Rift Valley between Lakes Nakuru and Magadi broadly exhibits the hydrogeological features expected of a Valley-interfluve system with lateral groundwater flows from the Rift escarpments to discharge areas on the Rift floor, and axial groundwater flows away from the Rift floor culmination at Lake Naivasha. This model is modified by the presence of the major Rift faults, which act as barriers to lateral flow, leading to longer, deeper, flow paths, and by the grid faulting in the Rift floor which tend to align flow paths within the Rift along its axis.

The permeabilities of the volcanic rocks underlying the Rift Valley are generally low, although there is considerable local variation. Aquifers are normally found in fractured or reworked volcanics, or along the weathered contacts between different lithological units. The highest values of permeability are found in the reworked volcanics composing the sediments of the Naivasha area, where the specific capacities of wells often exceed 3 l/s/m and where estimated hydraulic conductivities of greater than 10 m/d are common. In the Rift floor to the north, where the sediment size decreases, borehole specific capacities fall, to around 0.3 l/s/m in the Elmenteita-Nakuru area (leading to an estimated average hydraulic conductivity of 2 m/d). On the Rift escarpments the permeabilities of the different rock types are uniformly low. Mean borehole specific capacities and estimated hydraulic conductivities range from 0.03 l/s/m and 0.1 m/d for the South Kinangop Pyroclastics to 0.2 l/s/m and 1.1 m/d for the Rift Escarpment Trachyte to the east of Suswa and the Mau Forest pyroclastics.

These figures are only applicable to the drilled depths of the boreholes, normally less than 250 m. Below this depth permeabilities will fall, mainly as a result of the closure of fissures by overburden stresses. The only available data for permeability at depth are from the Olkaria Geothermal Field where values of around 5 mD have been found, equivalent to a cold water hydraulic conductivity of about 3×10^{-3} m/d. Simple modelling in the present study has suggested an upper limit of 0.1 m/d for rocks at depth in the Naivasha area.

Preliminary estimates of subsurface flows from the Naivasha catchment suggest that the amount contributed by Lake Naivasha is around 50×10^{6} m^3/y (which is 20% of the total recharge estimated by a previous water balance study). Flow to the south via relatively shallow aquifers (i.e. at depths of less than about 500 m) may be the most significant route for water flow from the catchment, accounting for perhaps 50% to 90% of the total.

Chemical data obtained during the present study have enabled the model of the ambient flow systems to be refined. Stable isotope determinations on samples of rainfall taken over a wide area have enabled an isotopic meteoric line for the Rift to be constructed which is similar to the trend for ambient and slightly thermal groundwaters. In addition an approximate correlation of isotopic composition with height has been found. This correlation suggests that much of the groundwater in the Naivasha-Nakuru area is relatively local in origin, particularly at lower altitudes according to the inert gas data. Such an interpretation is supported by modern radiocarbon ages and the lack of enhancement in radiogenic inert gases. The implication is that deep components of flow are not important in the shallow hydrology of the Rift floor, and therefore supports the contention that permeabilities at depth are low.

The most important result of the chemical analyses with regard to ambient

(and geothermal) water flows in the Study Area of the Rift is the tracing of water from Lake Naivasha using stable isotope data. River water entering the Lake has a very depleted composition indicative of its origin at high altitudes (principally in the Nyandarua Mountains). Meteoric water entering the lake directly has a less depleted composition similar to that of local groundwaters. However the lake itself is highly enriched by virtue of the intense evaporation to which it is subjected. Enriched lakewater flowing both to the north and to the south can therefore be detected in groundwater and geothermal fluid samples by stable isotope analysis. By this method it has been shown that Lake Naivasha water flows northwards via Gilgil - but not apparently under Eburru - at least as far as Lake Elmenteita, where it is estimated to form 30% of the discharge of warm springs bordering the lake. To the south a component of Naivasha lakewater has been detected as far as Suswa, but there is no evidence that it reaches Lake Magadi in an identifiable form.

The interpretation of geochemical analyses of geothermal fluids from Eburru, Olkaria, Longonot and Suswa has led to the important conclusion that all the fluids can be explained in terms of a mixing series between Rift-wall meteoric water and water from Lake Naivasha and that there is no evidence of a unique deep thermal water. At Eburru, analysis of fumarole condensates and gases indicates that the steam is basically primary and is derived from local Rift-wall groundwater; well and spring-waters to the north of Eburru show evidence of outflow of geothermal fluids in this direction. At Olkaria the wellfield shows evidence of a 55-75% lakewater component mixing with Rift-wall groundwater; fumaroles in the Domes area further east indicate a smaller but significant (>30%) lakewater contribution, and fumaroles in Longonot crater, east of the Domes, show only traces of lakewater. Between Longonot and Mt. Margaret, fumaroles show no evidence of lakewater influence. The Suswa area shows evidence of lakewater, but only in fumaroles in the ring graben and central island (where however a substantial contribution - 30% - of lakewater has been detected).

Further south, at Magadi, the hot springs are considered to derive from a hot saline groundwater body, whose origin lies in a mixture between recharging waters from the lower Ewaso Ngiro River and local groundwaters. No evidence of the presence of Naivasha lakewater has been found.

To the north, basic geochemical sampling of the Lake Bogoria and Lake Baringo thermal systems tends to confirm that lakewater mixing is involved, although at Baringo this appears to take place in an unexpected manner. The Kapedo and Lorusio springs north of Lake Baringo are not obviously affected by subsurface outflow from the lake

There is no evidence in any of the geothermal fluids sampled of a $\delta^{18}O$ shift of the magnitude commonly seen in other geothermal systems. This could be due to rapid transit times, or to equilibration of rock and water $\delta^{18}O$ values, but too little is yet known of rock $^{18}O/^{16}O$ values to understand which process is involved.

Gases in the geothermal fluids are dominated by crustally-derived CO_2 usually followed by CH_4 - although at a much lower level. (There is also evidence of a pervasive CO_2 flux over much of the Rift which is unrelated to specific geothermal fields). The presence of He and H_2 - regarded as indicators of upflow conditions - has been confirmed at Eburru and at Longonot. High $^3He/^4He$ ratios, taken to represent evidence of the transport of mantle helium, are found at Eburru, Longonot and Olkaria. The ratio of C_2H_6/CH_4 may be an index of lakewater contribution to groundwaters and geothermal fluids

and is found to vary with distance from Lake Naivasha, thus supporting the mixing model.

The use of chemical geothermometers in the Rift has met with variable success. In the Olkaria geothermal field quartz, alkali and gas geothermometers give plausible temperatures. However in the other thermal areas there are few opportunities to sample hot water, and the gas geothermometers are often problematic; the ratio types commonly cannot be used because of the scarcity of H_2 and H_2S in fumarolic gases. At Magadi the highly alkaline nature of the springs precludes the use of the alkali geothermometers, although those based on quartz seem to be reliable. Ambient or slightly thermal waters elsewhere in the study area often give excessive indications of temperature which are unsupported by other evidence.

Two thermal areas, Olkaria and Magadi were examined in some detail during the study. At Olkaria the results support the conclusion of other workers that the present wellfield is situated somewhat to the south of a thermal upflow. Also there are indications that short flow paths may be involved, and that the system may be quite old. At Magadi it is concluded that the thermal springs are formed by a two-component mixing series, probably with a local heat source, and that the hot end member is at a temperature of 100-130°C.

With regard to the warm springs found at various points along the Rift margins, there is no indication that these are anything other than local phenomena associated with Rift faults and result from deep groundwater circulation under ambient geothermal gradients. The geothermal potential of these springs is therefore low.

In summary, the main conclusions of this study are that the geothermal areas at Eburru, Olkaria-Domes, Longonot, Suswa and Magadi are individual geothermal fields where local heat sources set up convective cells which circulate fluids which originate as mixtures of ambient groundwaters and Naivasha Lakewater (or in the case of Magadi, probably a mixture of groundwater and recharging river water). There is no evidence of a deep thermal fluid pervasive over large areas of the Rift - chemical similarities between geothermal fluids from different areas are caused by similar groundwaters reacting with similar rock types. Thermal areas north of Nakuru (Bogoria, Baringo, Kapedo and Lorusio) though sampled in much less detail during this study, are considered to have a fundamentally similar mode of origin.

It is also tentatively concluded from the limited available data that recharge into the Naivasha catchment should be ample to sustain production from geothermal fields bordering the catchment - however a thorough water balance study would be needed to be certain of this. Further south, groundwater conditions around Suswa are virtually unknown, and therefore the availability of recharge is speculative. There are indications however of at least some hydraulic connection with the Naivasha catchment.

It is recommended therefore that future exploration should concentrate on areas where high temperatures and thermal upflow conditions are expected, and present data suggest that these are to be found principally at Eburru, Olkaria, Longonot and probably Suswa. Magadi appears to have limited potential in view of the low temperatures indicated - although the heat output from the area is high. Areas of outflow from the fields, that is to the north of Eburru and to the south of Olkaria, Longonot and Suswa are not expected to possess significant geothermal potential, nor are areas between the fields.

REFERENCES

General References

Andrews, J.N. and Kay, R.L.F. 1982. Natural production of tritium in permeable rocks. Nature, 298, 361-363.

Armannsson, H. 1987a. Geochemistry of steam in the Suswa and Longonot geothermal areas. Technical Report. Project KEN/82/002. United Nations Department of Technical Co-operation for Development.

Armannsson, H. 1987b. Studies on the geochemistry of steam in the Suswa and Longonot areas and water in the Lake Magadi, Kedong Valley and Lake Turkana areas, Rift Valley, Kenya. Final Technical Report. Project KEN/82/002. United Nations Department of Technical Co-operation for Development.

Arnason, B. 1977. The hydrogen and water isotope thermometer applied to geothermal areas in Iceland. Geothermics, 5, 125-151.

Arnorsson, S. and Gunnlaugsson, E. 1985. New gas geothermometers for geothermal exploration - calibration and application. Geochimica et Cosmochimica Acta, 49, 1307-1325.

Bailey, D.K. 1980. Volcanism, Earth degassing and replenished lithosphere mantle. Philosophical Transactions Royal Society London, A297, 309-322.

Baker, B.H. 1958. Geology of the Magadi Area. Report Geological Survey of Kenya 42.

Baker, B.H., Mohr, P.A. and Williams, L.A.J. 1972. Geology of the Eastern Rift System of Africa. Geological Society of America Special Paper 136. 67 pp.

Baker, B.H., Williams, L.A.J., Miller, J.A. and Fitch, F.J. 1971. Sequence and geochronology of the Kenya Rift volcanics. Tectonophysics, 11, 191-215.

Bennion, D.W. and Griffiths, J.C. 1966. A stochastic model for predicting variations in reservoir rock properties. Transactions American Institute of Mining Engineers, 237, 9-16.

Bodvarsson, S., Pruess, K., Stefansson, V., Bjornsson, S. and Ojiambo, S.B. 1987. East Olkaria Geothermal Field, Kenya. 1: History Match With Production and Pressure Data Decline. Journal of Geophysical Research, 92, No. B1, 521-539.

Browne, P.R.L. 1984. Subsurface stratigraphy and hydrothermal alteration of the eastern section of the Olkaria Geothermal Field,Kenya. Proceedings 6th New Zealand Geothermal Workshop, Auckland, N.Z., 33-41.

Bwire-Ojiambo, S. 1984. Isotope hydrogeochemistry of Lakes Elmenteita and Naivasha catchment areas. Unpublished paper to Olkaria review meeting, Nairobi December 1984, 8 pp.

Craig, H. 1963. In "Nuclear Geology on Geothermal Areas", (E.Tongiorgi, ed.), 17-53. Consiglio Nazionale della Richerche, Lab. di Geol. Nucl. Pisa.

Craig, H. Lupton, J.E. and Horowitz R.M. 1977. Isotopic geochemistry and hydrogeology of geothermal waters in the Ethiopian Rift Valley. Scripps Institute of Oceanography. Reference Number 77-14, University of California, San Diego.

Crane, K. 1981. Thermal variations in the Gregory Rift of southern Kenya. Tectonophysics, 74, 239-262.

Dansgaard, W. 1964. Stable isotopes in precipitation. Tellus 16, 436.

Darling, W.G. and Armannsson, H. 1989. Stable isotopic aspects of fluid flow in the Krafla, Namafjall and Theistareykir geothermal systems of north-east Iceland. Chemical Geology 76, No. 3/4.

Darling, W.G., Bath, A.H. and Brunsdon, A.P. 1982. Revised procedures for the measurement of $^{2}H/^{1}H$ and $^{18}O/^{16}O$ in water samples. BGS Hydrogeology Group Stable Isotope Technical Report No. 16.

Darling, W.G. and Lardner, A.J. 1985. The effect of altitude on the stable isotope composition of rainfall in the Balquhidder research catchments. BGS Hydrogeology Research Group Stable Isotope Technical Report No. 27.

Eugster, H.P. 1970. Chemistry and origin of the brines of Lake Magadi, Kenya. Mineralogical Society of America Special Paper 3, 215-235.

Eugster, H.P. 1980. Lake Magadi, Kenya, and its précursors. In "Developments in Sedimentology", 28, Hypersaline brines and evaporitic environments. Editor, A. Nissenbaum. Elsevier.

Fournier, R.O and Potter R.W. 1979. Magnesium correction to the Na-K-Ca chemical geothermometer. Geochimica et Cosmochimica Acta, 43,1543-1550.

Freeze, R.A. and Cherry J.A. 1979. Groundwater. Prentice-Hall. 604 pp.

Geotermica Italiana Srl. 1987. Geothermal Reconnaissance Survey in the Menengai-Bogoria Area of the Kenya Rift Valley. Final Draft Report Part IV - Hydrogeology. TCD CON 7/85 KEN 82/002.

Glover, R.B. 1972. Chemical characteristics of water and steam discharges in the Rift Valley of Kenya. Unpublished Report to the UNDP, 56 pp.

Grant, M.A. and Whittome, A.J. 1981. Hydrology of Olkaria Geothermal Field. Proceedings 3rd New Zealand Geothermal Workshop, Auckland N.Z., 125-129.

Haukwa, C.B. 1984. Recent measurements within Olkaria East and West Fields. Paper for Kenya Power Company Scientific and Technical Review Meeting, 13 pp.

Haukwa, C.B. 1986. Interpretation of well measurements for exploration

areas and reservoir changes in Olkaria East Field. Paper for Kenya Power Company Scientific and Technical Review Meeting, 11 pp.

Hillaire-Marcel, C. and Casanova, J. 1987. Isotopic hydrology and paleohydrology of the Magadi (Kenya) - Natron (Tanzania) basin during the late Quaternary. Palaeogeography, Palaeoclimatology, Palaeoecology, 58, 155-181.

Hulston, J.R. 1977. Isotope work applied to geothermal systems at the Institute of Nuclear Sciences, New Zealand. Geothermics, 5, 89-96.

Jones, B.F., Eugster H.P. and Rettig, S.L. 1977. Hydrochemistry of the Lake Magadi basin, Kenya. Geochimica et Cosmochimica Acta. 44, 53-72.

Logan, J. 1964. Estimating transmissibility from routine production tests of water wells. Groundwater, 2, No. 1,35-37.

Mahon, W.A.J. 1972. The general geochemistry of the Rift Valley of Kenya, Lake Baringo to Lake Magadi, and the geochemistry of Olkaria, Eburru and Lake Hannington geothermal prospects. Technical Review Meeting Report. United Nations Geothermal Resources Exploration Project.

Mazor, E. 1977. Geothermal tracing with atmospheric and radiogenic noble gases. Geothermics, 5, 21-36.

McCall, G.J.H. 1957. Geology and groundwater conditions in the Nakuru area. Ministry of Works (Hydraulic Branch) Technical Report No. 3.

McCall, G.J.H. 1967. Geology of the Nakuru-Thompson's Falls-Lake Hannington area. Report Geological Survey of Kenya 78.

McCann, D.L. 1972. A preliminary hydrogeologic evaluation of the long-term yield of catchments related to the geothermal prospect areas in the Rift Valley of Kenya. Unpublished U.N Report. 23 pp.

McCann, D.L. 1974. Hydogeologic investigation of the Rift Valley catchments. Unpublished U.N Report. 47 pp.

Nier, A.O. 1950. A redetermination of the relative abundances of the isotopes of carbon, nitrogen, oxygen, argon and potassium. Physics review, 77, 789.

Noble, J.W. and Ojiambo, S.B. 1975. Geothermal exploration in Kenya. Second U.N. Symposium, Development and use of Geothermal Research, San Francisco, California, U.S.A., 189-204.

Ogoso-Odongo, M.E. 1986. Geology of the Olkaria geothermal field. Geothermics, 15, No. 5/6, 741-748.

Paces, T. 1975. A systematic deviation from the Na-K-Ca geothermometer below 75 C and above 10^{-4} atm P_{CO_2} . Geochimica et Cosmochimica Acta, 39, 541-544.

Panichi, C. and Tongiorgi, E. 1974. Isotopic study of the hot water and steam samples of the Rift Valley, Kenya. Unpublished report to the U.N.D.P, 56 pp.

Parkinson, J. 1914. The East African Trough in the neighbourhood of the soda lakes. Geographical Journal, 44, 33-49

Sikes, H.L. 1935. Notes on the Hydrology of Lake Naivasha. Journal of The East Africa and Uganda Natural History Society, 13, 74-89.

Stevens, J.A. 1932. Lake Magadi and its alkaline springs.. Unpublished report to the Magadi Soda Co. Ltd., Kenya.

Thiem, G. 1906. Hydrologische Methoden. Gebhardt,Leipzig. 56 pp.

Thompson, A.O. 1964. Geology of the Kijabe Area. Report Geological Survey of Kenya 67.

Thompson, A.O. and Dodson, R.G. 1963. Geology of the Naivasha area. Report Geological Survey of Kenya 55.

Tobin, D.G., Ward P.L. and Drake C.L. 1969. Microearthquakes in the Rift Valley of Kenya. Geological Society of America Bulletin, 80, 2043-2046.

Truesdell, A.H. 1975. Geochemical techniques in exploration. In Proceedings of the Second United Nations Symposium on the development and use of Geothermal Resources, 1, 53-86.

Warren, J.E. and Price, H.S. 1961. Flow in heterogeneous porous media. Journal Society of Petroleum Engineers, 1, 153-169.

BGS Internal Reports in Chronological Order

Burgess, W.G. 1985. Report on a visit 22 October to 30 November 1985. Report WD/OS/85/31

Burgess, W.G. 1986. Report on a visit 17 March to 26 April 1986. Report WD/OS/86/4.

Burgess, W.G. 1986. Hydrogeology and geothermics of the Magadi-Longonot Sector. Report WD/OS/86/5.

Burgess, W.G. 1986. Notes on the groundwater conditions in the Longonot-Nakuru Sector of the Rift Valley. Report WD/OS/86/6.

Allen, D.J. 1986. Report on a visit 11-17 October 1986.

Allen, D.J. and Darling W.G. 1987. Interpretation of fluid sample analyses from Magadi-Silale area. Report WD/OS/87/3

Allen, D.J. 1987. Report on a visit 10 March to 3 April 1987. Report WD/OS/87/8.

Allen, D.J. 1987. Report on a visit 18 May to 30 May 1987. Report WD/OS/87/14.

Allen, D.J. and Darling W.G. 1987. Hydrogeology progress Report, March-August 1987. Report WD/OS/87/16.

Darling, W.G. 1987. Report on a visit 28 April to 28 May 1987. Report WD/OS/87/12.

APPENDICES

APPENDIX 1 - GENERAL BOREHOLE DATA

BOREHOLE NUMBER	EASTING	NORTHING	MAP NO.	BORE-HOLE ALT. (m)	REST WATER ALT. (m)	BOREHOLE COMPLETION DATE
0001C	2263	99149	143/3	2450	2317	16/05/85
C0054	2094	99264	133/2	1910	1895	27/10/39
C0057	2187	99111	133/4	2088	<1994	27/10/39
C0059	1799	99411	133/1	1880	1776	03/12/39
C0079	1798	99413	133/1	1880	1784	25/04/33
C0092	2191	99108	133/4	2118	<1960	31/12/39
C0107	1563	99607	118/4	2261	<2186	-/12/30
C0108	1392	99694	118/4	2480	2460	-/12/30
C0115	2038	98844	147/2	1600	<1350	17/07/41
C0131	1391	99697	118/4	2480	2467	04/10/40
C0132	1394	99693	118/4	2480	2464	14/10/40
C0152	1793	99685	119/3	1861	1813	19/11/41
C0164	1555	99598	118/4	2332	2313	23/12/41
C0165	1818	98719	147/1	2030	<1875	10/04/47
C0202	1567	99595	118/4	2320	2282	26/11/42
C0204	1795	99684	119/3	1860	1834	30/10/42
C0205	1582	99625	118/4	2195	2091	14/12/42
C0208	1548	99651	118/4	2292	<2092	24/01/43
C0210	2092	99094	133/4	1910	1895	15/02/43
C0211	1587	99615	118/4	2220	2130	18/02/43
C0214	1657	99674	118/4	1880	1825	28/02/43
C0220	1589	99563	118/4	2300	2267	24/04/43
C0223	1574	99554	118/4	2406	2353	26/05/43
C0227	1567	99567	118/4	2367	2304	17/06/43
C0231	2143	99198	133/2	1896	1887	06/07/43
C0258	1536	99662	118/4	2228	2173	21/03/43
C0261	1767	99337	133/1	2120	2049	31/07/43
C0264	2272	99034	134/3	2580	2437	24/08/43
C0266	1836	99418	133/1	1880	1776	10/09/43
C0288	1440	99684	118/4	2220	2138	19/02/44
C0295	2157	99260	133/2	2000	1962	17/07/43
C0306	1724	99625	119/3	1780	1761	28/06/44
C0307	1723	99637	119/3	1780	1770	04/08/44
C0321	1802	99678	119/3	1880	1813	17/05/47
C0325	2084	99724	119/4	2360	2337	03/12/43
C0376	1456	99673	118/4	2411	2374	05/09/45
C0379	1443	99714	118/4	2257	<2257	21/09/45
C0381	2434	97868	161/3	1650	1627	03/10/45
C0407	2327	98695	148/1	2140	2002	01/05/46
C0408	1790	99685	119/3	1885	1788	24/04/47
C0416	2355	98723	148/1	2140	2073	03/06/46
C0417	1971	99679	119/4	2480	2341	08/06/46
C0419	1680	99619	119/3	1970	1840	24/05/46
C0423	1472	99687	118/4	2280	2216	03/11/45
C0429	1889	99431	133/1	1840	1768	22/06/46
C0431	1828	99389	133/1	1940	1781	27/04/40
C0440	2353	98613	148/3	2020	1974	11/07/46
C0451	2390	97883	161/3	1520	1476	28/08/46
C0456	1944	99552	119/4	1860	1813	05/08/46
C0457	2110	99354	133/2	2000	1973	31/08/46
C0458	2124	99331	133/2	1928	1891	22/08/46
C0463	1464	99557	118/4	2760	2747	06/09/46
C0465	2087	99374	133/2	1960	1919	19/09/46

BOREHOLE NUMBER	EASTING	NORTHING	MAP NO.	BORE-HOLE ALT. (m)	REST WATER ALT. (m)	BOREHOLE COMPLETION DATE
C0466	1911	99165	133/3	1940	1891	26/09/46
C0467	2156	99142	133/4	1960	1877	11/10/46
C0468	2090	99257	133/2	1910	1893	10/10/46
C0485	1636	99646	118/4	2087	2023	11/11/46
C0510	1847	98788	147/1	2040	<1875	28/02/47
C0511	1847	98732	147/1	1770	<1599	07/02/47
C0531	2146	99196	133/2	1920	1904	29/05/47
C0533	1846	99364	133/1	1990	1784	30/05/47
C0553	2375	99219	134/1	2560	2472	10/7/30-
C0562	2109	99116	133/4	1900	1877	25/06/47
C0563	1959	99106	133/4	1900	1893	23/07/47
C0567	2139	99098	133/4	1955	1899	18/06/47
C0570	2022	99552	119/4	2340	2310	03/08/47
C0572	2228	99138	134/3	2220	2010	29/08/47
C0579	2013	99103	133/4	1900	1878	13/09/47
C0580	2142	99146	133/4	1925	1879	06/09/47
C0581	2002	99098	133/4	1900	1877	12/07/47
C0582	2119	99125	133/4	1895	1881	07/07/47
C0605	2381	97887	161/3	1500	1378	20/09/47
C0624	1538	99654	118/4	2236	2175	22/01/48
C0628	2107	99148	133/4	1900	1854	08/10/47
C0631	1975	99208	133/2	1910	1883	17/11/47
C0633	2317	99074	134/3	2670	2506	17/06/85
C0634	2349	99126	134/3	2600	2561	15/01/48
C0648	1549	99671	118/4	2217	<1988	09/03/48
C0651	2345	99316	134/1	2580	<2419	10/3/48
C0655	1516	99674	118/4	2174	2098	04/03/48
C0665	1456	99704	118/4	2280	2143	08/04/48
C0667	2111	99145	133/4	1904	1881	15/10/47
C0670	1803	99676	119/3	1850	1798	21/05/48
C0677	2389	99233	134/1	2610	<2427	28/05/48
C0678	2390	99228	134/1	2590	2557	02/06/48
C0691	2268	99193	134/1	2520	<2410	12/06/48
C0692	2269	99189	134/1	2520	2362	26/06/48
C0699	2371	99198	134/1	2520	2444	02/07/48
C0703	2328	99092	134/3	2650	2565	10/07/48
C0704	1964	99285	133/2	2460		21/04/48
C0705	1965	99296	133/2	2440	<2394	26/04/48
C0706	1966	99294	133/2	2460	<2400	29/04/48
C0707	1966	99290	133/2	2480		07/05/48
C0719	1803	99676	119/3	1880	1814	18/09/49
C0729	2125	99039	133/4	2050	1890	30/09/48
C0732	1816	99668	119/3	1870	1809	12/10/48
C0733	2019	99405	133/2	2042	1849	26/06/48
C0741	1643	99470	118/4	2320	2278	21/10/48
C0745	1574	99606	118/4	2240	2145	05/11/48
C0780	2268	99185	134/1	2540	2358	18/08/48
C0783	1721	99406	133/1	2180	2089	27/11/48
C0804	2079	99702	119/4	2360	2318	23/12/48
C0805	1698	99688	119/3	1870	1757	00/12/48
C0811	2474	98029	161/3	1760	1742	30/01/49
C0813	1851	99621	119/3	1900	1779	08/03/49
C0814	2200	99243	133/2	2179	2136	23/02/48
C0822	1844	99621	119/3	1900	<1762	00/11/48
C0824	2416	97788	172/1	1640	1503	07/03/49
C0836	1823	99650	119/3	1890	1821	12/04/49

BOREHOLE NUMBER	EASTING	NORTHING	MAP NO.	BORE-HOLE ALT. (m)	REST WATER ALT. (m)	BOREHOLE COMPLETION DATE
C0839	2435	98563	148/3	1880	1855	29/12/48
C0845	1759	99415	133/1	1920	1794	09/04/49
C0855	1665	99703	119/3	1954	1771	00/14/49
C0858	1831	99598	119/3	1882	1766	07/05/49
C0869	1841	99615	119/3	1900	1769	01/06/49
C0870	2014	99720	119/4	2620	2542	02/03/49
C0872	2076	99718	119/4	2400	2352	02/04/49
C0875	2408	97759	172/1	1540	1467	31/05/49
C0882	1696	99702	119/3	1929	1769	11/05/49
C0910	2097	99081	133/4	1940	1927	28/05/49
C0916	1598	99595	118/4	2140	2022	23/06/49
C0921	1508	99595	118/4	2500	2402	06/04/49
C0939	2204	99171	133/2	2127	2001	19/09/49
C0946	2236	99216	134/1	2330	2092	06/07/49
C0947	2124	99121	133/4	1905	1881	17/05/49
C0953	1629	99518	118/4	2300	2206	06/08/49
C0965	1986	99386	133/2	1950	<1767	12/10/49
C0984	1478	99696	118/4	2240	2200	04/10/49
C0994	2355	99136	134/3	2580	2537	23/11/49
C1000	2331	99147	134/3	2600	2475	
C1001	1705	99589	119/3	1958	<1714	16/12/49
C1007	2364	99139	134/3	2560	2537	08/12/49
C1013	2258	99201	134/1	2520	2355	15/12/49
C1013	2258	99201	134/1	2520	2355	15/12/49
C1019	2015	99630	119/4	2440	2277	03/12/49
C1021	1453	99663	118/4	2403	2382	31/12/49
C1027	1754	99468	119/3	1810	1731	04/01/50
C1029	2278	99263	134/1	2480	<2343	18/11/49
C1033	1444	99668	118/4	2414	2379	04/02/50
C1043	2059	99557	119/4	2260	2125	17/03/50
C1051	2294	99190	134/1	2560	2400	15/03/50
C1062	1975	99194	133/2	1900	1989	16/03/50
C1063	1984	99203	133/2	1900	1890	23/03/50
C1080	1805	99657	119/3	1870	1763	17/05/50
C1082	1812	99667	119/3	1870	1810	17/05/50
C1082	2017	99627	119/4	2530	2470	17/05/50
C1089	1560	99705	118/4	2149	<1905	17/05/50
C1112	2365	99283	134/1	2780	<2628	29/09/49
C1125	1626	99636	118/4	2100	2015	24/06/50
C1126	2365	98545	148/3	2020	1816	28/07/50
C1148	1625	99425	132/2	2520	2510	15/06/51
C1161	2242	99024	134/3	2160	1965	03/03/50
C1250	1853	99629	119/3	1910	1761	07/12/50
C1259	2420	98413	148/3	1820	1811	02/12/50
C1265	2226	99108	134/3	2240	<1995	19/12/50
C1277	2388	99188	134/1	2520	2451	02/10/50
C1279	2142	99072	133/4	2000	1878	26/10/50
C1281	2094	99104	133/4	1900	1876	08/11/50
C1287	1883	99488	119/3	1815	1764	01/12/50
C1294	2413	98410	148/3	1840	1831	19/01/51
C1325	1481	99691	118/4	2270	2180	10/03/51
C1356	2112	99121	133/4	1895	1883	21/03/51
C1358	1996	99631	119/4	2460	2313	24/03/51
C1361	2059	99553	119/4	2280	2094	13/11/54
C1362	1644	99666	118/4	2040	1865	14/04/51
C1374	1814	99667	119/3	1875	1814	26/05/51

BOREHOLE NUMBER	EASTING	NORTHING	MAP NO.	BORE-HOLE ALT. (m)	REST WATER ALT. (m)	BOREHOLE COMPLETION DATE
C1379	2064	99646	119/4	2380	2344	01/05/55
C1383	1828	99489	119/3	1845	1790	10/05/51
C1390	2329	97909	161/3	1420	<1249	06/03/51
C1391	2369	97893	161/3	1480	1369	31/03/51
C1394	1797	99416	133/1	1880	1790	21/05/51
C1402	2072	98910	133/4	1710		21/04/51
C1404	1902	99153	133/3	1940	1882	04/03/50
C1425	2235	99019	134/3	2120	1859	13/06/51
C1434	1855	99704	119/3	1960	1923	14/02/51
C1436	1860	99713	119/3	1980	1935	28/02/51
C1464	1972	99180	133/2	1888	1880	10/03/50
C1475	2278	99078	134/3	2600	2539	07/07/51
C1482	2139	99166	133/4	1894	1880	23/06/51
C1483	2157	99257	133/2	1974	1943	25/06/51
C1486	2159	99129	133/4	1974	1963	13/07/51
C1487	2156	99126	133/4	1974	1883	18/07/51
C1488	2180	99223	133/2	2088	2012	23/07/51
C1491	1626	99634	118/4	2120	2035	28/07/51
C1499	2349	97803	161/3	1400	<1271	27/07/51
C1503	2239	99019	134/3	2140	1879	22/08/51
C1504	1404	99714	118/4	2380	2289	12/08/51
C1523	2253	97658	172/1	1340	<1208	07/09/51
C1524	2009	98951	133/4	1737		12/06/51
C1525	2000	98903	133/4	1631	<1414	21/07/51
C1535	1701	99708	119/3	1950	1773	28/09/51
C1545	1621	99411	132/2	2520	2514	03/10/51
C1558	1802	99680	119/3	1900	1775	26/10/51
C1559	2181	98278	160/2	990	906	27/10/51
C1584	1801	99513	119/3	1804	1786	14/11/51
C1585	1581	99582	118/4	2280	2271	25/01/51
C1602	2302	99053	134/3	2680	2530	31/10/51
C1614	2225	99293	134/1	2480	2362	14/12/51
C1625	1446	99686	118/4	2380	2341	12/12/51
C1641	1447	99722	118/4	2220	2144	29/11/51
C1652	2134	99154	133/4	1900		14/01/52
C1662	2081	98118	160/2	860		12/01/52
C1666	1820	99664	119/3	1880	1817	23/01/52
C1713	2432	98255	161/1	1840	1785	04/03/52
C1726	2234	99004	134/3	2080	1821	31/03/52
C1749	1577	99587	118/4	2280	2195	10/04/52
C1794	2294	99072	134/3	2740	2560	21/06/52
C1795	2296	99254	134/1	2510	2378	14/07/52
C1795	2296	99254	134/1	2510	2378	14/7/52
C1798	1812	99405	133/1	1900	1768	08/07/52
C1830	2282	99262	134/1	2500	2372	17/08/52
C1843	2105	98983	133/4	2070	<1814	
C1850	2329	99226	134/1	2550	2410	09/09/52
C1851	2237	99119	134/3	2340	2083	23/01/52
C1877	1869	99371	133/1	1940	1782	22/11/52
C1892	2214	99107	133/4	2200	1966	26/12/52
C1898	2164	99252	133/2	2020	1959	20/01/53
C1911	1667	99295	133/1	2900	<2728	29/01/53
C1912	1668	99293	133/1	2860	<2709	16/02/53
C1913	1663	99292	133/1	2900	2861	16/02/53
C1914	1656	99280	132/2	2890	2867	28/02/53
C1924	2095	99577	119/4	2260	2137	21/03/53

BOREHOLE NUMBER	EASTING	NORTHING	MAP NO.	BORE-HOLE ALT. (m)	REST WATER ALT. (m)	BOREHOLE COMPLETION DATE
C1926	2094	99054	133/4	1980	1890	20/02/53
C1927	2069	99078	133/4	1895	1877	26/03/53
C1929	2337	99139	134/3	2600	2500	09/03/53
C1935	1596	99627	118/4	2160	2045	15/01/53
C1941	1802	99402	133/1	1920	1781	28/03/53
C1947	2146	99194	133/2	1920	1905	17/04/53
C1951	2123	99566	119/4	2220	2111	02/04/53
C1952	2126	99572	119/4	2290	2178	07/05/53
C1970	1869	98992	133/3	2580	2451	02/05/53
C1990	1889	99428	133/1	1840	1778	21/01/53
C1997	2277	99166	134/3	2560	2360	30/06/53
C2005	2293	99143	134/3	2600	2372	
C2007	1851	99516	119/3	1884	1785	04/09/53
C2033	2025	99706	119/4	2600	2525	24/09/53
C2039	2035	99720	119/4	2640	<2460	06/10/53
C2042	1878	99092	133/3	2080	<1889	25/07/53
C2058	2141	99157	133/4	1910	1995	04/11/53
C2059	1799	99447	119/3	1830	1810	25/04/53
C2061	2163	99658	119/4	2300	2279	01/11/53
C2062	2283	99185	134/3	2620	2392	27/10/53
C2063	2306	99099	134/3	2670	2571	
C2069	1989	99087	133/4	1920	1874	24/09/53
C2071	2028	99092	133/4	1900	1888	05/10/53
C2076	2030	99467	119/4	2020	1901	27/07/50
C2077	2044	99461	119/4	2000	1906	27/08/50
C2097	2041	99665	119/4	2500	2381	28/11/53
C2108	2281	99212	134/1	2530	2364	15/12/53
C2109	2024	99717	119/4	2600	2558	16/12/53
C2110	2210	99559	119/4	2440	2341	22/12/53
C2117	2139	99161	133/4	1900	1888	11/11/53
C2118	1949	99595	119/4	2220	2071	23/12/53
C2128	1830	99680	119/3	1902	1870	06/11/53
C2129	1844	99677	119/3	1919	1870	09/12/53
C2138	2318	98981	134/3	2200	2165	25/11/53
C2149	2316	99244	134/1	2540	2396	16/02/54
C2160	2215	99567	119/4	2480	2349	13/03/54
C2170	2361	99247	134/1	2610	2424	18/03/54
C2170	1920	99003	133/3	2160	<1935	19/07/57
C2172	2315	98979	134/3	2180	2138	22/02/54
C2176	2371	99150	134/3	2540	2524	14/01/54
C2197	2346	99191	134/1	2540	2427	19/05/54
C2234	1943	99552	119/4	1860	1783	12/06/54
C2241	1901	99199	133/1	1980	1871	17/07/54
C2246	2107	99246	133/2	1890	1876	24/07/54
C2263	2290	99050	134/3	2710	<2436	
C2264	2297	99058	134/3	2740	2591	28/07/54
C2269	1813	99668	119/3	1874	1814	14/10/54
C2276	1596	99556	118/4	2315	2282	09/09/54
C2288	1807	99345	133/1	2060	<1787	01/10/54
C2289	1764	99350	133/1	2020	1933	20/10/54
C2292	2078	99705	119/4	2360	2298	25/11/54
C2294	2394	98521	148/3	1880	1864	05/01/55
C2296	2141	99649	119/4	2320	2290	10/12/54
C2300	1901	99099	133/3	2000	1899	18/11/54
C2304	1973	99176	133/2	1900	1894	08/12/54
C2322	1978	99705	119/4	2540	2428	30/01/55

BOREHOLE NUMBER	EASTING	NORTHING	MAP NO.	BORE-HOLE ALT. (m)	REST WATER ALT. (m)	BOREHOLE COMPLETION DATE
C2332	1978	99678	119/4	2480	2425	18/02/55
C2338	2430	98588	148/3	2000	1805	19/01/51
C2347	2183	99186	133/2	2060	1941	12/02/55
C2358	2324	98668	148/1	2160	1895	25/03/55
C2388	2024	99462	119/4	2030	1788	04/06/55
C2402	1805	99675	119/3	1866	1799	18/06/53
C2420	2339	99090	134/3	2640	2572	30/09/55
C2421	2347	99084	134/3	2620	2432	05/10/55
C2430	2119	99184	133/2	1900	1894	01/10/55
C2432	1649	99608	118/4	2060	1944	21/09/55
C2447	2347	98678	148/1	2080	1878	28/11/55
C2448	1652	99510	118/4	2180	2023	22/11/55
C2466	2365	98865	148/1	2360	2305	22/12/55
C2468	2371	97801	161/3	1460	1328	12/12/55
C2480	1808	99479	119/3	1810	1770	01/02/56
C2482	1665	99310	133/1	2820	<2715	24/02/56
C2493	1879	99658	119/3	1930	1836	01/03/56
C2496	1621	99270	132/2	2820	2676	06/03/56
C2497	1553	99284	132/2	2750	2645	22/03/56
C2499	1929	99589	119/3	1928	1822	14/04/56
C2504	1861	99682	119/3	1940	1870	02/05/56
C2521	1918	99213	133/1	1940	1866	08/04/56
C2522	1940	99198	133/2	1940	1894	28/04/56
C2523	2002	99206	133/2	1900	1870	28/05/56
C2534	2096	99100	133/4	1910	1893	13/06/56
C2535	2035	99229	133/2	1897	1890	22/06/56
C2536	2025	99216	133/2	1890	1886	25/06/56
C2537	2046	99208	133/2	1900	1897	27/06/56
C2538	2008	99213	133/2	1891	1881	29/06/56
C2539	2022	99207	133/2	1900	1895	01/07/56
C2541	1912	99363	133/1	1960	<1911	06/01/56
C2542	1915	99338	133/1	2160	<2100	27/01/56
C2543	1915	99325	133/1	2180	2030	02/04/56
C2564	1483	99723	118/4	2120	2011	27/08/56
C2600	1915	99355	133/1	2020	1834	15/10/56
C2620	2465	98553	148/3	1820	1753	12/10/56
C2636	2101	99109	133/4	1895	1890	06/02/57
C2646	2468	97862	161/3	1680	1629	06/03/57
C2647	2387	97632	172/1	1600	1582	24/03/57
C2657	1948	99125	133/4	1920	1897	17/04/57
C2659	1974	99121	133/4	1900	1893	06/03/57
C2660	1969	99120	133/4	1900	1880	23/05/57
C2662	2280	99070	134/3	2620	2419	11/03/57
C2663	2309	99094	134/3	2665	2345	20/03/57
C2664	1877	98998	133/3	2300	<2105	21/03/57
C2667	2262	99153	134/3	2420	2265	06/02/57
C2670	1656	99668	118/4	2000	1833	15/04/57
C2680	1397	99705	118/4	2440	2392	01/12/56
C2697	2164	99646	119/4	2300	2270	14/03/57
C2701	1967	99089	133/4	1890	1883	26/07/57
C2703	2050	99215	133/2	1900	1897	04/05/57
C2704	1798	99444	133/1	1840	1780	01/07/57
C2705	1987	99208	133/2	1899	1882	24/07/57
C2706	2006	99222	133/2	1920	1881	12/08/57
C2709	1872	99083	133/3	2140	1944	24/06/57
C2717	2311	98609	148/3	1940	1701	08/10/57

BOREHOLE NUMBER	EASTING	NORTHING	MAP NO.	BORE-HOLE ALT. (m)	REST WATER ALT. (m)	BOREHOLE COMPLETION DATE
C2720	2288	99102	134/3	2660	2384	04/10/57
C2745	1575	99606	118/4	2240	2148	18/12/57
C2753	2074	99497	119/4	2220	2097	06/03/58
C2758	2315	98675	148/1	2054	1952	12/02/58
C2773	2071	99490	119/4	2170	2098	26/03/58
C2813	1974	99204	133/2	1887	1846	14/04/58
C2823	2199	99025	133/4	2130	1870	15/09/58
C2851	1793	99348	133/1	2040	1809	22/01/59
C2863	2068	99082	133/4	1900		
C2866	2271	98458	148/3	1570	1481	05/03/59
C2870	1950	99293	133/2	2637		05/02/59
C2871	1934	99305	133/1	2620	2583	16/02/59
C2883	2130	99294	133/2	1939	1886	03/01/60
C2885	1968	99043	133/4	2020		
C2886	1985	99053	133/4	1980		
C2887	1947	99295	133/2	2640		12/02/59
C2894	1606	99576	118/4	2230	2218	21/03/59
C2899	1966	99335	133/2	2133		25/04/59
C2900	1960	99316	133/2	2124		30/04/59
C2901	1959	99314	133/2	2124		06/05/59
C2902	2364	98641	148/1	2020	1961	27/05/59
C2910	2322	98778	148/1	2185	2008	11/07/59
C2966	2101	99606	119/4	2260	2206	
C2970	1832	99680	119/3	1910	1884	19/02/59
C2997	2099	98999	133/4	2160	1880	22/01/60
C3003	2272	98596	148/3	1770	1530	09/03/60
C3005	1446	99605	118/4	2403	2365	18/03/60
C3024	1805	99238	133/1	2400	2308	04/05/60
C3032	1801	99248	133/1	2400	2358	16/04/60
C3047	1796	99664	119/3	1822	1763	08/06/60
C3064	1998	99203	133/2	1900	1885	09/08/60
C3066	2061	99721	119/4	2460	2390	00/02/60
C3067	2098	99631	119/4	2300	2240	
C3087	2363	98624	148/1	1990	1949	13/07/60
C3136	1945	99643	119/4	2320	2275	19/08/61
C3164	1825	99248	133/1	2400	2381	07/03/62
C316D	1810	99690	119/3	1875	1798	17/04/50
C3216	2115	99210	133/2	1900	1895	
C3217	2114	99204	133/2	1900	1895	
C3243	1578	99593	118/4	2260	2192	08/06/63
C3266	2355	98775	148/1	2280	2187	30/10/63
C3280	2365	98585	148/3	2000	1918	24/01/63
C3292	2134	99215	133/2	1893	1885	16/05/64
C3298	2104	99244	133/2	1900	1895	22/05/64
C3299	2103	99230	133/2	1887	1885	14/06/64
C3324	1691	99612	119/3	1940	1750	
C3327	1665	99339	133/1	2660	2593	05/02/65
C3351	1600	99288	133/1	2880	2727	
C3352	1665	99291	133/1	2900	2687	
C3353	1649	99273	132/2	2880	2843	03/07/65
C3358	2381	97822	161/3	1500	<1318	05/08/65
C3363	2390	97889	161/3	1500	1421	30/10/65
C3365	2114	99235	133/2	1900	1889	08/11/65
C3366	2120	99233	133/2	1899	1889	27/10/65
C3371	1634	99586	118/4	2145	2044	02/11/65
C3377	2363	98812	148/1	2340	2247	23/11/65

BOREHOLE NUMBER	EASTING	NORTHING	MAP NO.	BORE-HOLE ALT. (m)	REST WATER ALT. (m)	BOREHOLE COMPLETION DATE
C3397	1671	99315	133/1	2730	2622	23/08/66
C3417	2091	99261	133/2	1900	1892	04/12/66
C3418	2365	98653	148/1	2080	1938	03/02/67
C3422	2367	98882	148/1	2400	2343	17/10/64
C3431	1783	99301	133/1	2200	2084	20/02/67
C3436	2445	97865	161/3	1620	1577	06/05/67
C3451	2480	97692	172/1	1620	1605	30/06/67
C3467	1625	99622	118/4	2135	<1906	25/11/67
C3490	1608	99627	118/4	2280	2173	02/05/68
C3523	2427	98626	148/1	1900	1875	20/10/68
C3524	2427	98630	148/1	1920	1907	20/10/68
C3525	1811	98475	147/3	1380	1293	19/10/68
C3551	2112	99228	133/2	1900	1895	22/02/69
C3562	1762	98973	133/3	2760	<2669	
C3576	2408	98377	148/3	1880	1876	21/05/69
C3615	2396	98657	148/1	2060	1988	10/03/69
C3616	2022	99091	133/4	1920	1898	21/09/67
C3627	1624	99627	118/4	2132	2932	05/11/68
C3650	1646	99283	132/2	2830	2822	10/01/70
C3674	2034	99252	133/2	1885	1879	20/04/70
C3675	2122	99223	133/2	1890	1885	04/03/70
C3677	2120	99244	133/2	1900	1885	25/02/68
C3678	2114	99249	133/2	1901	1884	17/04/70
C3693	2450	98633	148/1	1880	1869	05/07/70
C3694	2410	98670	148/1	2140	2107	03/07/70
C3710	2395	98651	148/1	2080	2022	21/09/70
C3713	2346	98803	148/1	2380	<2308	12/11/70
C3721	2433	98635	148/1	1940	1901	22/12/70
C3739	2449	98617	148/1	1900	1852	01/10/69
C3740	2131	99142	133/4	1905	1888	15/01/71
C3763	2441	98638	148/1	1920	1894	21/03/71
C3764	2414	98648	148/1	1900	1866	23/05/71
C3765	2416	98626	148/1	1980	1944	05/02/71
C3767	1946	99093	133/4	1900	1874	26/05/71
C3771	2492	98693	148/1	1880	1841	14/07/71
C3779	2087	99710	119/4	2340	2330	30/08/71
C3784	2087	99706	119/4	2340	2334	07/10/71
C3799	2383	98626	148/1	2240	2199	03/12/71
C3870	2458	97868	161/3	1660	<1552	26/05/72
C3874	1795	99661	119/3	1800	1746	30/11/72
C3875	1797	99666	119/3	1800	1747	11/11/72
C3897	2458	98822	148/1	2170	2135	03/03/73
C3910	2466	98633	148/1	1847	1829	10/05/73
C3919	2495	98814	148/1	1980	1952	10/03/73
C3924	2051	99081	133/4	1900	1893	14/06/73
C3925	1434	99696	118/4	2400	2306	02/07/73
C3929	2062	99313	133/2	1900	1884	02/07/73
C3932	1819	99215	133/1	2200	2077	16/05/75
C3937	2397	98509	148/3	1900	1897	08/08/73
C3939	2368	97628	172/1	1540	1459	07/09/77
C3942	2371	97908	161/3	1500	1400	06/10/73
C3951	2459	97876	161/3	1640	1611	23/11/73
C3955	1453	99658	118/4	2440	2437	05/10/73
C3965	1881	99706	119/3	2060	1998	07/11/73
C3970	2410	97886	161/3	1600	1573	31/01/74
C3976	2402	98715	148/1	2140	2084	19/03/74

BOREHOLE NUMBER	EASTING	NORTHING	MAP NO.	BORE-HOLE ALT. (m)	REST WATER ALT. (m)	BOREHOLE COMPLETION DATE
C3995	2470	98733	148/1	1940	1927	11/04/74
C3999	2397	98606	148/3	2000	1952	25/04/74
C4003	2494	98724	148/1	2000	1997	19/06/74
C4037	2400	98710	148/1	1920	1874	15/07/74
C4057	2104	99114	133/4	1900	1897	10/09/74
C4061	1976	98991	133/4	2068	1948	04/03/74
C4062	1990	99012	133/4	1941	1377	07/08/74
C4077	1644	99565	118/4	2120	2036	31/10/74
C4092	2413	98467	148/3	1900	1892	14/03/80
C4116	1704	99468	119/3	2010	1866	05/03/75
C4121	1992	99680	119/4	2480	2387	08/03/75
C4131	1587	98675	146/2	1880	<1698	
C4143	1580	98674	146/2	1880	1708	
C4152	2326	98956	134/3	2180	2169	23/09/77
C4155	2145	99266	133/2	1940	1913	15/08/78
C4157	2135	99216	133/2	1894	1883	30/06/75
C4161	2133	99236	133/2	1900	1884	11/08/75
C4168	2120	99237	133/2	1900	1883	04/09/75
C4174	2304	98709	148/1	2080	2023	18/12/75
C4177	2140	99235	133/2	1910	1894	24/11/75
C4178	2131	99234	133/2	1902	1886	12/11/75
C4179	2425	98428	148/3	1840	1738	16/10/75
C4185	2488	97659	172/1	1680	<1560	30/01/76
C4186	2422	98416	148/3	1870	1865	21/11/75
C4200	2427	98466	148/3	1820	1746	24/06/76
C4201	2422	98486	148/3	1900	1884	18/03/76
C4206	1594	99631	118/4	2160	2052	17/05/76
C4208	2135	99205	133/2	1890	1884	14/07/76
C4209	2130	99202	133/2	1889	1885	20/02/76
C4214	1605	99629	118/4	2150	2047	27/03/76
C4252	1985	99707	119/4	2570	2450	01/07/76
C4279	2431	98831	148/1	2771	2194	24/11/76
C4292	2459	98696	148/1	1940	1914	26/08/77
C4301	2110	99263	133/2	1916	1883	04/03/77
C4302	2136	99215	133/2	1900	1890	09/06/77
C4306	2475	98596	148/3	1820	1767	17/03/77
C4331	1835	98845	147/1	2180	<1980	03/06/77
C4332	1709	98781	147/1	1850	1788	04/11/77
C4350	1573	99264	132/2	2790	2777	30/04/77
C4360	2443	98743	148/1	1960	1938	22/06/77
C4369	1816	99714	119/3	1910	1879	26/08/77
C4370	1804	99690	119/3	1880	1838	12/10/77
C4397	2045	99085	133/4	1900	1893	16/08/77
C4403	2380	99130	134/3	2540	2497	
C4413	1571	99558	118/4	2340	2272	14/10/77
C4416	2371	98554	148/3	2000	<1817	13/01/78
C4420	2039	99086	133/4	1900	1893	09/09/77
C4431	2371	98643	148/1	2032	1971	28/02/78
C4461	2398	98678	148/1	2040	2027	27/03/78
C4484	2299	97899	161/3	1380	1298	03/07/78
C4491	1888	99685	119/3	2030	2022	00/03/78
C4492	1886	99689	119/3	2020	1962	28/09/77
C4493	1875	99686	119/3	1960	1948	20/01/78
C4498	2471	98013	161/3	1720	1695	19/06/78
C4499	1949	99158	133/4	1940	<1727	28/04/77
C4500	1964	99144	133/4	1900	1885	28/08/77

BOREHOLE NUMBER	EASTING	NORTHING	MAP NO.	BORE-HOLE ALT. (m)	REST WATER ALT. (m)	BOREHOLE COMPLETION DATE
C4501	1961	99138	133/4	1910	1889	03/11/77
C4502	1669	99515	119/3	2096	2045	01/10/76
C4504	2036	99258	133/2	1890	1878	18/05/77
C4510	1816	99713	119/3	1893	1865	20/07/78
C4511	1816	99715	119/3	1910	1883	11/11/78
C4512	1815	99716	119/3	1910	1882	31/01/79
C4517	1572	99602	118/4	2280	2183	30/05/78
C4531	2080	98112	160/2	860	790	16/09/78
C4554	2414	98802	148/1	2280	2234	19/08/78
C4555	2102	99317	133/2	1830	1802	15/08/78
C4564	1765	99448	133/1	1840	1787	24/11/70
C4565	2185	98051	160/4	1020	<820	21/01/79
C4575	2356	98524	148/3	1950	1828	08/01/79
C4591	1957	99152	133/4	1900	1879	04/01/79
C4594	1918	99193	133/1	1940	1834	19/12/82
C4597	2374	98720	148/1	2220	2105	14/07/79
C4610	2132	99233	133/2	1890	1874	28/03/79
C4615	2385	98663	148/1	2100	2038	10/05/79
C4624	2454	98490	148/3	1800	1767	05/06/79
C4634	2325	98961	134/3	2220	2201	06/01/78
C4665	2460	98738	148/1	1940	1903	18/10/79
C4669	1586	99592	118/4	2240	2219	20/09/79
C4685	2395	98666	148/1	2080	1999	27/11/81
C4687	2452	98428	148/3	1820	1805	13/12/80
C4713	2493	98457	148/3	1750	1707	21/01/80
C4743	2404	98462	148/3	2000	1994	05/05/80
C4792	2366	98644	148/1	2060	1968	28/07/80
C4804	2412	98562	148/3	1880	1816	16/01/81
C4807	2363	98645	148/1	2060	1890	02/03/81
C4812	2362	98647	148/1	2060	1981	18/11/80
C4829	2277	97682	172/1	1380	<1195	05/11/80
C4850	2405	98675	148/1	2140	2135	11/02/81
C4855	2395	98703	148/1	2120	2112	18/11/80
C4863	2426	98425	148/3	1820	1805	10/01/81
C4881	2448	98498	148/3	1920	1866	17/02/80
C4893	2315	98764	148/1	2220	<1924	11/04/81
C4897	1863	99123	133/3	2220	2007	08/01/82
C4907	2422	98484	148/3	1880	1873	30/11/81
C4909	2329	98636	148/1	2060	1931	17/04/81
C4924	1815	99665	119/3	1870	1724	04/07/81
C4927	2442	98536	148/3	1880	1763	20/06/81
C4966	2429	98465	148/3	1840	1767	31/12/81
C4968	2428	98502	148/3	1860	1801	15/09/81
C4971	2246	98723	148/1	1550	<1250	08/11/81
C4974	2306	98710	148/1	2080	1861	09/09/81
C4981	2430	98440	148/3	1840	1805	12/10/81
C4986	2085	99092	133/4	1900	1895	16/06/81
C4989	2086	99093	133/4	1900	1899	04/07/81
C4997	2430	98438	148/3	1820	1749	04/01/82
C5002	2197	99293	133/2	2280	2174	09/09/81
C5029	1595	99596	118/4	2210	2122	01/01/82
C5111	1883	99650	119/3	1900	1800	23/12/81
C5117	2397	98502	148/3	1920	1911	23/02/83
C5143	1789	99694	119/3	1890	1855	28/09/82
C5161	2451	98436	148/3	1800	1775	17/06/82
C5175	2408	98752	148/1	2160	2122	19/08/82

BOREHOLE NUMBER	EASTING	NORTHING	MAP NO.	BORE-HOLE ALT. (m)	REST WATER ALT. (m)	BOREHOLE COMPLETION DATE
C5206	1596	99588	118/4	2215	2180	08/11/82
C5257	1548	99236	132/2	2720	2609	17/12/82
C5343	2377	98687	148/1	2120	2023	25/05/83
C5348	2384	98672	148/1	2100	1976	26/06/83
C5375	2397	98630	148/1	2060	1984	24/10/83
C5411	2400	98645	148/1	2140	2057	19/10/83
C5520	2273	99406	134/1	2438	2374	17/03/84
C5564	2407	98418	148/3	1920	1904	29/08/84
C5754	1919	99673	119/3	2240	2232	
C5798	2399	98442	148/3	2000	1962	06/09/84
C6056	1606	99252	132/2	2770	2756	29/01/85
C6095	1922	99682	119/3	2260	2250	25/03/85
C6186	2441	98601	148/3	1880	1872	16/08/85
C6211	2403	98471	148/3	1900	1858	27/07/84
C6213	2382	98697	148/1	2134	2004	25/09/84
C6271	1571	99589	118/4	2260	2225	
C6290	2008	99403	133/2	2030	1833	00/07/85
C6300	2264	99149	134/3	2490	2357	17/06/85
C630D	1983	99067	133/4	1970	1870	29/10/53
C6377	2397	98483	148/3	1966	1918	16/12/85
C6378	2369	98606	148/3	2000	1900	09/11/85
C6494	2391	98478	148/3	1990	1984	06/03/86
C6495	1692	99141	133/3	2854	<2755	
C6524	2409	98525	148/3	1880	1817	13/11/85
C6613	2376	98684	148/1	2109	2019	19/01/86
KJ1	2260	99081	134/3	2500	<2268	00/00/84
M0001	2036	99394	133/2	1960	1805	
P0002	2385	98514	148/3	1940	1924	10/11/27
P0012	2387	98503	148/3	1900	1876	20/03/28
P0016	2268	98487	148/4	1580	1486	09/08/28
P0023	2258	98512	148/3	1500	1430	06/10/28
P0027	2043	98563	147/4	1230		
P0036	2189	98565	147/4			
P0037	2189	98562	147/4			
P0053	2264	98939	134/3	1860	1647	28/08/29
P0065	2342	99122	134/3	2620	2559	10/10/29
P0071	2306	98606	148/3	1940	<1750	
P0089	2297	99181	134/1	2570	<2528	24/3/30
SA58	1791	99687	119/3	1856	1808	16/08/41

APPENDIX 2 - BOREHOLE COMPLETION DATA

BOREHOLE NUMBER	BOREHOLE DEPTH (m)	BOREHOLE DIAMETER (m)	PLAIN CASING DEPTH (m)	AQUIFER LITHOLOGY
0001C	206.9	0.20		
C0054	46.0	0.15		
C0057	93.9			
C0059	140.2	0.20	129.8	SAND
C0079	116.4	0.15	102.6	
C0092	158.5			
C0107	74.9	0.20		
C0108	39.6	0.15	24.9	
C0115	249.9	0.15	16.0	
C0131	45.7	0.15	26.7	
C0132	45.7	0.15	25.3	
C0152	66.9	0.15		ALLUVIAL SEDIMENTS
C0164	66.5	0.15	20.1	LAVA + PUMICE
C0165	155.0	0.15		
C0202	137.2	0.15	58.5	LAVA + CLAY + SAND
C0204	76.0	0.20	22.2	
C0205	140.0	0.15	56.1	AGGLOMERATE
C0208	199.6			
C0210	67.1	0.20		
C0211	135.3	0.15	57.0	TRACHYTE
C0214	121.9	0.15		
C0220	152.4	0.15	35.7	ASH + PHONOLITE
C0223	186.8	0.15	36.3	
C0227	167.6	0.15	65.8	ASH
C0231	45.7	0.15	34.0	
C0258	106.1	0.15	40.5	
C0261	150.0	0.20	56.4	
C0264	182.9	0.15		LAVA
C0266	150.0	0.20	14.4	
C0288	182.9	0.15	23.7	
C0295	86.0	0.15		
C0306	73.2	0.20	71.0	LAKE SEDIMENTS
C0307	70.1	0.20	69.8	LAKE SEDIMENTS
C0321	98.1	0.20	43.3	
C0325	132.6	0.15	78.6	CLAY + SAND
C0376	91.4	0.15	38.2	
C0379	75.0	0.15	26.5	
C0381	128.3	0.15	19.1	
C0407	200.0	0.15		
C0408	138.0	0.20	109.5	
C0416	146.0	0.20	71.0	
C0417	182.1	0.20	142.5	TUFF + CLAY
C0419	182.9	0.20	160.0	LAKE SEDIMENTS
C0423	213.4	0.15	57.3	
C0429	100.8	0.20	90.9	LAKE SEDIMENTS
C0431	216.0	0.20		LAVA
C0440	167.6	0.15	54.3	LAVA + CLAY
C0451	137.2	0.15		
C0456	190.0	0.15	169.0	LAKE SEDIMENT
C0457	76.2	0.20	56.0	LAKE SEDIMENTS
C0458	102.4	0.15	10.3	LAKE SEDIMENTS
C0463	106.7	0.15	94.0	TUFF + PHONOLITE
C0465	99.0	0.13		

BOREHOLE NUMBER	BOREHOLE DEPTH (m)	BOREHOLE DIAMETER (m)	PLAIN CASING DEPTH (m)	AQUIFER LITHOLOGY
C0466	77.4	0.20	75.9	PUMICE + LAVA
C0467	95.4	0.15		
C0468	46.3	0.20		FINE GRAVEL
C0485	120.1	0.15	40.8	
C0510	183.0			
C0511	171.0	0.15		
C0531	61.0	0.20	18.0	PYROCLASTICS
C0533	220.1	0.15	162.5	ASH
C0553	106.7	0.15	48.8	BASALT + LAKE SEDIMENTS
C0562	56.4	0.15		
C0563	31.0	0.15	12.0	LAKE SEDIMENTS & LAVAS
C0567	102.1	0.15	73.8	LAVA PEBBLES
C0570	142.5	0.15	82.5	LAVA
C0572	229.0	0.15		
C0579	42.7	0.15	14.9	ASH
C0580	67.1	0.15	13.9	TUFF
C0581	30.5	0.15	14.0	LAKE SEDIMENTS
C0582	56.1	0.15	13.7	LAKE SEDIMENTS
C0605	149.0	0.17	77.0	GNEISS
C0624	91.4	0.15	88.4	TUFF + LAKE SEDIMENTS
C0628	45.7	0.15	35.1	LAVA & ASH
C0631	46.0	0.15	23.0	
C0633	183.0	0.15	42.7	TUFF
C0634	104.0	0.15		TUFF
C0648	229.0	0.15		
C0651	161.5			
C0655	149.4	0.20	38.1	
C0665	204.0			
C0667	36.6	0.20	29.9	ASH & SEDIMENT
C0670	112.7	0.15	25.1	SEDIMENTS + LAVAS
C0677	182.9	0.15		
C0678	61.0	0.15	1.8	
C0691	109.7	0.15		
C0692	192.0	0.15	9.5	LAKE SEDIMENTS + TUFF
C0699	91.4	0.20		SAND + TUFF
C0703	310.0	0.15	7.0	TUFF
C0704	152.0	0.15	12.0	
C0705	46.0	0.15		
C0706	40.0	0.15		
C0707	103.0	0.15	22.6	
C0719	153.0	0.15	30.3	
C0729	182.9	0.15	69.2	FRACTURED LAVA
C0732	152.4	0.15	68.9	PYROCLASTICS
C0733	240.8	0.15	40.2	
C0741	133.5	0.15	30.9	TUFF + LAKE SEDIMENTS
C0745	182.8	0.15	50.7	
C0780	210.3			TUFF + PALEOSOIL
C0783	120.0	0.20	20.3	LAKE SEDIMENTS
C0804	100.8	0.15		PYROCLASTICS
C0805	166.4	0.15	29.6	FRACTURED LAVA
C0811		0.10	12.4	
C0813	152.7	0.15	4.3	SEDIMENTS
C0814	102.4	0.15		LAKE SEDIMENTS + ASH
C0822	138.0			
C0824	183.0	0.15		GNEISS
C0836	172.8	0.20	104.7	LAKE SEDIMENTS

BOREHOLE NUMBER	BOREHOLE DEPTH (m)	BOREHOLE DIAMETER (m)	PLAIN CASING DEPTH (m)	AQUIFER LITHOLOGY
C0839	45.7	0.20	25.9	ASH + LAVA
C0845	217.0	0.20	70.8	LAKE SEDIMENTS + LAVA
C0855	189.9	0.15	23.2	PYROCLASTICS
C0858	150.5	0.15	20.1	PALEOSOIL
C0869	137.0	0.20	43.4	LAKE SEDIMENTS
C0870	102.9	0.10		TUFF + CLAY
C0872	109.2	0.15		
C0875	152.0	0.15		GNEISS
C0882	182.0	0.15	13.2	
C0910	32.9	0.15	7.3	LAKE SEDIMENTS & PUMICE
C0916	213.4	0.15	75.0	TUFF
C0921	228.6	0.15	87.0	BASALT + TUFF + TRACHYTE
C0939	150.0	0.15	76.2	
C0946	245.4	0.15	40.2	LAVA + SAND + GRAVEL
C0947	49.4	0.15	5.5	SEDIMENT
C0953	143.2	0.15	101.7	TUFF + LAVA + SEDIMENTS
C0965	183.5	0.15		
C0984	106.9	0.15	19.8	
C0994	98.0	0.15		CLAYEY TUFF
C1000	148.0	0.15		LAVA
C1001	243.8	0.15		
C1007	61.0	0.20		DECOMPOSED LAVA
C1013	201.8	0.15	189.0	TUFF + GRAVEL + SAND + CLAY
C1013	201.8	0.15	189.0	TUFF + GRAVEL + SAND + CLAY
C1019	217.2	0.20	49.5	CLAYS + TRACHYTE
C1021	118.9	0.20	90.0	WEATHERED TRACHYTE
C1027	106.7	0.15	65.8	TUFF
C1029	137.2			
C1033	183.0	0.20	90.0	
C1043	210.0	0.15	0.0	
C1051	194.2	0.15	177.0	TUFF + CLAY + GRAVEL
C1062	32.0	0.15	21.6	
C1063	40.8	0.15	23.5	
C1080	160.0	0.15	96.6	FRACTURED LAVA + SEDIMENTS
C1082	110.5	0.15	161.0	FRACTURED LAVAS
C1082	108.9	0.15	73.5	TUFF + TRACHYTE
C1089	244.0	0.15		
C1112	152.4			
C1125	125.0	0.15	19.2	
C1126	215.5	0.15	27.7	OLD LAND SURFACE
C1148	72.5	0.15	23.2	
C1161	216.0	0.15		
C1250	168.0	0.15	80.0	FRACTURED LAVA
C1259	142.0	0.25	20.0	
C1265	245.0	0.15		
C1277	114.3	0.20	13.3	SAND + TRACHYTE
C1279	182.9	0.20	6.4	LAVA
C1281	31.0	0.15	11.5	PUMICE & ASH
C1287	102.7	0.20	100.3	PEBBLES + ASH
C1294	182.9	0.25		
C1325	192.0	0.20	108.0	SANDS
C1356	30.8	0.20	21.0	LAVA PEBBLES
C1358	204.0	0.20	32.1	RHYOLITE
C1361	249.9	0.15	5.4	TUFF +TRACHYTE
C1362	199.4	0.15		WEATHERED TRACHYTE
C1374	105.0	0.15	4.8	FRACTURED LAVAS

BOREHOLE NUMBER	BOREHOLE DEPTH (m)	BOREHOLE DIAMETER (m)	PLAIN CASING DEPTH (m)	AQUIFER LITHOLOGY
C1379	126.0	0.15	36.0	TUFF
C1383	97.5	0.15	9.1	TRACHYTE
C1390	171.0	0.20		
C1391	152.0	0.20		
C1394	181.8	0.25	32.7	PUMICE + LAVA
C1402	232.0	0.25	22.7	
C1404	103.5	0.20	75.3	SAND
C1425	283.0	0.15		
C1434	137.2	0.15	85.8	
C1436	142.0	0.15		
C1464	31.1	0.15	11.0	
C1475	107.0	0.15	91.0	
C1482	36.3	0.15	5.0	LAKE SEDIMENTS
C1483	45.7	0.15	6.1	
C1486	152.4	0.25	77.0	TRACHYTE
C1487	155.4	0.25	83.6	LAVA
C1488	91.4	0.20	11.0	TUFF + LAKE SEDIMENTS
C1491	162.1	0.15	20.7	
C1499	129.5	0.15		
C1503	296.4	0.15		DECOMPOSED TRACHYTE
C1504	152.4	0.15	128.7	
C1523	132.0	0.15		
C1524	244.0	0.20		
C1525	217.0			
C1535	188.9	0.15	18.0	PALEOSOILS + LAVAS
C1545	46.0	0.15	29.6	
C1558	135.0	0.15	50.1	SEDIMENTS
C1559	119.2	0.20	13.4	LAVA
C1584	86.3	0.15	43.6	
C1585	155.0	0.15	6.6	WEATHERED LAVA
C1602	172.0	0.15		
C1614	189.0	0.15	39.3	TUFF + WEATHERED TRACHYTE
C1625	91.4	0.15	31.5	TUFF
C1641	182.9	0.15	5.5	
C1652	61.0	0.15	18.3	
C1662	182.9	0.15	142.0	
C1666	187.4	0.15	109.5	LAKE SEDIMENTS+FRACTURED LAVA
C1713	259.7	0.20		LAVA
C1726	283.6	0.20	30.5	BASALT + BASALT SAND
C1749	175.3	0.15	6.0	WEATHERED LAVA
C1794	236.3	0.15		LAVA
C1795	162.8	0.15	6.1	LAVA + PUMICE
C1795	162.8	0.15	6.1	LAVA + PUMICE
C1798	186.6	0.20	151.5	FRACTURED LAVA
C1830	170.4	0.15	4.3	TUFF + SAND
C1843	256.0	0.15	13.3	
C1850	192.0	0.15	5.8	LAVA
C1851	306.3	0.15		
C1877	191.1	0.25	169.5	LAVA + TUFF
C1892	256.3	0.15	30.8	
C1898	102.4	0.20	3.3	
C1911	172.2	0.15		
C1912	151.2	0.20		
C1913	147.0		6.9	CLAY + SAND
C1914	76.2	0.15	51.8	TUFF
C1924	157.5	0.15	5.6	TUFF SAND + GRIT

BOREHOLE NUMBER	BOREHOLE DEPTH (m)	BOREHOLE DIAMETER (m)	PLAIN CASING DEPTH (m)	AQUIFER LITHOLOGY
C1926	125.0	0.20	26.5	SEDIMENT
C1927	41.8	0.20	5.8	ASH
C1929	136.0	0.20		GRAVEL
C1935	197.0	0.15	60.0	
C1941	170.1		150.3	TRACHYTE
C1947	67.0	0.25	16.8	
C1951	147.6	0.15	1.5	TUFF
C1952	138.0	0.15	4.8	TUFF + TRACHYTE
C1970	225.0	0.20		SAND + CLAY + BASALT
C1990	102.0	0.25	45.3	LAKE SEDIMENTS
C1997	223.5	0.15		HETEROGENEOUS SAND IN BUFF MTX
C2005	255.0	0.15		
C2007	107.6	0.20	100.3	BASALT
C2033	126.6	0.15	6.9	ASH + TUFF
C2039	180.0	0.20		
C2042	191.4	0.20		
C2058	46.6	0.20	0.0	
C2059	118.3	0.15		
C2061	123.9	0.15	6.2	PUMICE + SAND
C2062	260.8	0.15		CLAYEY SANDY SEDIMENTS
C2063	129.0	0.15	12.2	SCORIA
C2069	79.0	0.15	76.2	
C2071	18.9	0.20	11.6	
C2076	221.4			
C2077	204.0			LAVA
C2097	180.9	0.15	21.0	TUFF
C2108	187.8	0.15	14.9	LAVA + LAKE SEDIMENTS
C2109	90.0	0.15	66.3	TUFF + PUMICE
C2110	129.3	0.15	10.5	
C2117	26.2	0.20	6.4	ASH
C2118	208.8	0.15	190.8	SAND + GRAVEL
C2128	135.0	0.20	51.6	WELDED PYROCLASTICS
C2129	183.0	0.20	90.9	PYROCLSTICS + LAVAS
C2138	124.1	0.20	48.7	PEBBLES + GRAVEL
C2149	198.1	0.15	16.2	TUFF + GRAVEL
C2160	185.1	0.15	37.2	BASALT
C2170	228.6	0.15	12.3	TUFF + PUMICE + CLAY
C2170	225.0	0.20		
C2172	142.0	0.20		SAND
C2176	76.0	0.15	23.9	COARSE GRAVEL
C2197	182.9	0.15	14.3	SAND
C2234	162.9		111.0	CLAY + TUFF
C2241	145.5	0.20	75.3	LAVA + ASH
C2246	38.1	0.20	32.0	SEDIMENTS
C2263	274.0			
C2264	273.0	0.15	146.3	
C2269	150.0	0.15	58.2	
C2276	137.2	0.20	126.4	TUFFS
C2288	273.0	0.15		
C2289	139.2	0.15	24.6	PHONOLITE
C2292	127.2	0.15	3.0	LAKE SEDIMENT + CLAY
C2294	155.5	0.20	51.2	BASALT
C2296	96.0	0.15	3.3	TUFF + PUMICE
C2300	223.5	0.15	98.4	ASH
C2304	42.0	0.25	12.3	
C2322	138.0	0.15	29.4	IGNIMBRITE + GRAVEL

BOREHOLE NUMBER	BOREHOLE DEPTH (m)	BOREHOLE DIAMETER (m)	PLAIN CASING DEPTH (m)	AQUIFER LITHOLOGY
C2332	119.1	0.15	24.6	TUFF + PHONOLITE
C2338	238.0	0.15	38.7	TUFFS + SANDS
C2347	41.0	0.20	40.8	
C2358	311.0	0.15	4.6	SANDS
C2388	264.0	0.23	6.9	SAND + SILT
C2402	99.1	0.20	8.1	FRACTURED LAVA
C2420	124.0	0.20	19.5	
C2421	193.0	0.15	39.6	TUFF
C2430	31.0	0.25	17.4	
C2432	173.0	0.20	59.1	
C2447	213.0	0.20	49.0	TUFF
C2448	288.0	0.20	17.7	
C2466	98.0	0.20	88.4	LAVA SAND
C2468	179.0	0.15		GNEISS
C2480	71.6	0.15	18.3	FELDSPATHIC SAND
C2482	105.0	0.20		
C2493	146.9	0.20	8.4	LAVA SAND
C2496	167.6	0.15	86.9	TUFF
C2497	158.5	0.15	21.6	
C2499	213.4	0.15	122.8	TUFF
C2504	167.6	0.15	34.2	PYROCLASTICS
C2521	102.6	0.20	55.2	FRACTURED LAVA
C2522	51.5	0.20	39.3	
C2523	56.7	0.13	13.5	FRACTURED LAVA
C2534	22.3	0.15	13.0	TUFF & PUMICE
C2535	12.8	0.20	6.7	LAVA
C2536	9.7	0.20	3.0	VESICULAR LAVA
C2537	15.8	0.20	3.0	VESICULAR LAVA
C2538	13.7	0.31	6.1	PUMICE
C2539	12.5	0.20	1.5	TUFF
C2541	49.5	0.31		
C2542	60.0	0.15		
C2543	150.0	0.15		
C2564	218.0	0.23	13.0	FRACTURED LAVA
C2600	213.0	0.20	15.6	TUFF + LAVA SAND
C2620	152.4	0.15	6.1	TRACHYTE + PHONOLITE
C2636	30.5	0.10	11.6	SEDIMENTS
C2646	91.4	0.15		GNEISS
C2647	104.0	0.15		
C2657	32.6	0.15	33.1	ASH
C2659	24.4	0.25	11.9	SEDIMENTS & PUMICE
C2660	28.3	0.20	25.2	
C2662	256.2	0.15		
C2663	137.0	0.15	38.7	SAND
C2664	195.0	0.20		
C2667	205.9	0.15		
C2670	192.7	0.15	6.3	
C2680	85.3	0.15		
C2697	165.0	0.15	34.5	ALLUVIUM + ASH MATRIX
C2701	25.9	0.25	18.0	VOLCANIC SAND
C2703	30.8	0.20	14.7	
C2704	76.2	0.20	76.5	ASH
C2705	31.0	0.20	30.2	LAVA
C2706	62.5	0.20		ASH
C2709	225.0	0.20	202.5	FRACTURED LAVA
C2717	324.0	0.25	10.4	OLD LAND SURFACE

BOREHOLE NUMBER	BOREHOLE DEPTH (m)	BOREHOLE DIAMETER (m)	PLAIN CASING DEPTH (m)	AQUIFER LITHOLOGY
C2720	301.0	0.15		
C2745	178.3	0.20	11.7	LAKE SEDIMENTS
C2753	210.0	0.15	0.0	ALLUVIUM + ASH MATRIX
C2758	177.1	0.15	63.2	FRACTURED TRACHYTE + TUFF
C2773	159.0	0.20		TUFF
C2813	63.1	0.36	14.4	LAVA
C2823	305.5	0.15	83.0	
C2851	259.0	0.15	6.0	LAVA + LAKE SEDIMENTS
C2863	152.0			
C2866	147.5	0.25	98.4	LAVA
C2870	105.5	0.15	3.0	LAVA
C2871	36.6	0.15	3.0	
C2883	106.7	0.20	85.9	TUFFS
C2885	377.0			
C2886	933.3			
C2887	97.5		3.0	
C2894	180.4	0.20	18.0	TUFF + GRAVEL
C2899	39.6	0.15		LAVA
C2900	77.1	0.15	3.0	LAVA
C2901	77.1	0.15	3.0	
C2902	110.0	0.25	33.0	VOLCANIC SAND
C2910	305.0	0.15		TRACHYTE SAND
C2966	123.0			
C2970	53.0	0.25	68.5	PALEOSOILS + PYROCLASTICS
C2997	320.0	0.15	52.1	ASH & PUMICE
C3003	295.6	0.15		TRACHYTE
C3005	124.0	0.25	63.0	
C3024	105.0	0.15	3.6	TUFF + SAND
C3032	225.0	0.15		TUFF
C3047	73.2	0.30	52.1	
C3064	118.0	0.20		
C3066	93.0	0.15	12.0	
C3067	96.0	0.12		
C3087	76.0	0.15	6.0	TUFF
C3136	180.0	0.15	30.0	
C3164	73.5	0.20	6.3	SANDY CLAY
C316D	134.4	0.15	9.9	
C3216	42.7	0.30	9.9	LAKE SEDIMENTS
C3217	42.7	0.30	9.9	LAKE SEDIMENTS
C3243	188.9	0.15	43.9	WEATHERED PHONOLITE
C3266	111.0	0.15	24.0	SAND
C3280	137.2	0.10	6.1	LAVA + CLAY
C3292	76.0	0.20	50.2	
C3298	39.6	0.30	27.1	SAND + GRAVEL
C3299	39.4	0.30	52.0	PYROCLASTICS
C3324	201.2	0.20	182.9	
C3327	141.0	0.20	126.0	LAKE SEDIMENTS
C3351	186.0	0.20		
C3352	264.0			
C3353	142.7	0.15	115.2	TUFFS + LAKE SEDIMENTS
C3358	182.0			
C3363	165.0	0.15		WEATHERED GNEISS
C3365	82.0	0.20	72.0	LAKE SEDIMENTS
C3366	76.8	0.20	61.8	LAKE SEDIMENTS
C3371	185.9	0.15	50.0	LAVA + SEDIMENTS
C3377	165.0	0.15	44.0	

BOREHOLE NUMBER	BOREHOLE DEPTH (m)	BOREHOLE DIAMETER (m)	PLAIN CASING DEPTH (m)	AQUIFER LITHOLOGY
C3397	117.3	0.20	6.6	
C3417	91.7	0.20	6.7	SEDIMENTS + LAVA
C3418	240.0	0.20	61.2	
C3422	117.0	0.15	12.0	SAND + GRAVEL
C3431	174.6	0.25	18.0	
C3436	76.0	0.15		
C3451	122.0	0.15		
C3467	228.7	0.15		
C3490	193.9	0.15	34.4	TUFF + SAND
C3523	61.6	0.15	12.0	GRAVEL
C3524	106.7	0.15	15.8	GRAVEL
C3525	143.3	0.15	110.6	
C3551	76.8	0.20	4.5	SAND + GRAVEL
C3562	91.4	0.20		
C3576	137.2	0.15		LAVA
C3615	85.0	0.15	12.0	TUFF
C3616	57.0	0.20	19.8	LAVA
C3627	138.1	0.15	50.7	
C3650	121.9	0.15	24.7	TUFFS
C3674	30.4	0.15	6.0	TRACHYTE
C3675	61.0	0.20	45.3	SAND + GRAVEL
C3677	91.4	0.20	3.0	SEDIMENTS
C3678	72.5	0.20	61.2	SAND + GRAVEL
C3693	122.0	0.15	24.0	TUFF
C3694	122.0	0.15	37.0	
C3710	87.0	0.20	31.0	
C3713	80.8	0.15	18.0	
C3721	140.0	0.15	26.0	TRACHYTE
C3739	73.0	0.15	18.0	OLD LAND SURFACE
C3740	35.7	0.20	12.1	VOLCANIC SAND
C3763	85.0	0.15	12.0	OLD LAND SURFACE
C3764	107.0		6.0	OLD LAND SURFACE
C3765	67.0	0.15	6.0	
C3767	72.2	0.15	60.6	SCORIA
C3771	91.0	0.20	18.0	TUFFS + GRAVEL
C3779	150.6	0.15	111.9	TUFF
C3784	150.0			TUFF
C3799	83.0	0.15		GRAVEL + WEATHERED LAVA
C3870	107.9	0.15		
C3874	71.0	0.30	54.0	FRACTURED LAVAS
C3875	73.0	0.30	53.8	
C3897	105.5	0.20	42.7	OLD LAND SURFACE
C3910	98.0	0.20	9.0	
C3919	152.4	0.30	126.1	
C3924	37.8	0.30	56.0	
C3925	122.0		24.0	TUFF
C3929	61.0			TUFF
C3932	165.0	0.20	60.0	TUFF
C3937	260.6	0.15	66.5	
C3939	152.0			
C3942	152.4	0.15	87.8	GNEISS
C3951	122.0	0.15	6.1	GNEISS
C3955	143.0	0.15	40.0	TRACHYTE + SANDSTONE
C3965	158.5		12.5	PYROCLASTICS + FRACTURED LAVAS
C3970	137.5	0.15	12.2	GNEISS
C3976	126.5	0.15	37.6	

BOREHOLE NUMBER	BOREHOLE DEPTH (m)	BOREHOLE DIAMETER (m)	PLAIN CASING DEPTH (m)	AQUIFER LITHOLOGY
C3995	122.0	0.15	13.8	LAVA
C3999	138.5	0.20	44.8	TUFF + LAVA + SEDIMENTS
C4003	183.0	0.30	33.0	
C4037	198.5	0.20	13.5	
C4057	61.0	0.15	2.4	TUFF
C4061	1002.0	0.20	13.2	LAVA & TUFF
C4062	1350.0	0.20	13.0	LAVA & TUFF
C4077	226.0	0.15		
C4092	143.0	0.25		
C4116	251.0	0.15	36.5	TUFF + CLAY
C4121	178.0	0.15	12.0	
C4131	181.5			
C4143	197.0			
C4152	144.6	0.15		TUFF
C4155	128.0	0.15	12.0	
C4157	78.0	0.25		TUFF
C4161	52.0		46.0	SAND + GRAVEL
C4168	52.0	0.20	39.4	SAND + GRAVEL
C4174	68.0	0.15	12.0	SAND + GRAVEL
C4177	52.0	0.20	44.6	SAND + GRAVEL
C4178	52.0	0.25	46.5	SAND + GRAVEL
C4179	116.0	0.20	107.0	
C4185	120.0	0.15		
C4186	152.0	0.20		WEATHERED BASALT + TUFF
C4200	226.0	0.20	43.8	GRAVEL
C4201	155.0	0.20	19.3	GRAVEL
C4206	250.0	0.15	65.0	
C4208	61.0	0.25	8.0	PUMICE + SAND
C4209	62.0	0.25	12.0	
C4214	248.0	0.15	0.0	
C4252	181.0	0.15	43.0	
C4279	141.0	0.15	19.0	
C4292	200.0	0.20	21.4	GRAVEL
C4301	109.7	0.30	29.7	SAND
C4302	76.0		50.0	LAKE SEDIMENTS
C4306	232.0	0.32	30.3	LAVA + CLAY + SANDSTONE
C4331	200.0	0.25		
C4332	112.0	0.30	66.0	
C4350	170.0	0.15	12.0	
C4360	135.0	0.20	26.0	
C4369	166.0	0.20	111.8	
C4370	180.0	0.20	12.0	PALEOSOILS + PYROCLASTICS
C4397	33.5	0.25	16.8	
C4403		0.15	11.0	
C4413	137.0	0.15	18.3	SANDSTONE
C4416	183.0	0.25	25.0	
C4420	25.0	0.40	16.8	
C4431	240.0	0.30	78.6	BASALT + TRACHYTES
C4461	221.0	0.20		
C4484	200.0	0.15		
C4491	69.0	0.25	13.0	PYROCLASTICS + FRACTURED LAVAS
C4492	150.0	0.20	12.2	PYROCLASTICS + SCORIA
C4493	75.0	0.20	13.7	LAKE SEDIMENTS + PYROCLASTICS
C4498	100.0	0.15		MEDIUM/FINE SANDS
C4499	213.0	0.15		
C4500	61.0	0.30	46.0	LAVA

BOREHOLE NUMBER	BOREHOLE DEPTH (m)	BOREHOLE DIAMETER (m)	PLAIN CASING DEPTH (m)	AQUIFER LITHOLOGY
C4501	58.0	0.30	46.0	LAVA
C4502	112.0	0.15	45.0	SANDSTONE
C4504	30.5	0.30	2.0	LAVA
C4510	150.0	0.25		
C4511	148.0	0.25	90.0	
C4512	150.0	0.25		
C4517	188.0	0.15	24.0	GRAVEL + CLAY
C4531	150.0	0.15		
C4554	86.0	0.15		
C4555	128.0	0.15	12.0	LAKE SEDIMENTS
C4564				FRACTURED TRACHYTE
C4565	200.0	0.30		
C4575	196.0	0.22	23.0	
C4591	45.7	0.53	12.0	TUFF
C4594	213.6			
C4597	260.0	0.20	41.8	TRACHYTE
C4610	53.0	0.25	13.3	GRAVEL + SAND
C4615	157.0	0.20		
C4624	230.2	0.20	12.0	
C4634	110.0	0.20		TRACHYTE
C4665	153.0	0.20	6.0	
C4669	214.0	0.20	39.0	WEATHERED TUFF
C4685	122.0	0.25	29.0	
C4687	102.0	0.20	4.5	TUFFS
C4713	150.0	0.20	6.0	TRACHYTE
C4743	104.0	0.20	21.0	
C4792	204.0	0.25	17.0	TUFF
C4804	140.0	0.20	8.0	TRACHYTE + PHONOLITE
C4807	206.0	0.20		
C4812	193.0	0.25	15.4	
C4829	185.0	0.22		
C4850	80.0	0.20	53.0	WEATHERED TRACHYTE
C4855	150.0	0.15		
C4863	94.0	0.20	50.0	TUFFS
C4881	137.0	0.20	89.0	
C4893	296.0	0.25	23.0	
C4897	297.0	0.25	91.0	SEDIMENTS
C4907	60.0	20.00	8.0	WEATHERED GNEISS
C4909	300.0	0.30	16.5	
C4924	177.0	0.20	141.5	FRACTURED LAVA +LAKE SEDIMENT
C4927	180.0	0.20	9.0	
C4966	230.0	0.25	217.0	AGGLOMERATE + LAVA
C4968	240.0	0.30	186.0	ASH
C4971	300.0	0.15	12.4	
C4974	320.0	0.15	134.0	TRACHYTE
C4981	100.0	0.25	42.0	WEATHERED PHONOLITE
C4986	54.0	0.30	6.0	
C4989	25.0	0.30	25.0	
C4997	201.0	0.30	189.0	FRACTURED BASALT
C5002	186.0	0.20	2.0	LAKE SEDIMENTS
C5029	210.0	0.15	84.0	AGGLOMERATE
C5111	188.8	0.15	13.0	
C5117	117.0	0.20	39.0	WEATHERED BASALT
C5143	165.0	0.20	12.0	LAVAS + PYROCLASTICS
C5161	150.0	0.20	48.0	WEATHERED ASH
C5175	51.0	0.20	36.6	ASH

BOREHOLE NUMBER	BOREHOLE DEPTH (m)	BOREHOLE DIAMETER (m)	PLAIN CASING DEPTH (m)	AQUIFER LITHOLOGY
C5206	220.2	0.15	36.0	WEATHERED AGGLOMERATE
C5257	200.0	0.15	180.0	PYROCLASTICS + SEDIMENTS
C5343	152.0	0.20	54.0	WEATHERED TRACHYTE
C5348	154.0	0.20	36.0	WEATHERED TUFF
C5375	96.0	0.20	42.7	WEATHERED TUFF
C5411	116.0	0.20	43.0	WEATHERED TUFF
C5520	100.0	0.15	6.0	PUMICE + GRAVEL
C5564	160.0	0.20	4.0	BASALTS
C5754		0.18		
C5798	134.0	0.25	112.0	TRACHYTE
C6056	150.0	0.15	18.0	WEATHERED TUFF
C6095	120.0	0.18		
C6186	31.0	0.12	20.0	SILTSTONE
C6211	100.0	0.15	6.0	
C6213	185.0	0.15	35.0	
C6271	74.8			
C6290	208.0	0.20	107.0	
C6300	200.0	0.20	130.5	
C630D	126.0	0.20	101.8	
C6377	200.0	0.20	62.0	
C6378	131.0	0.20	11.5	TRACHYTE
C6494	160.0	0.20	30.0	
C6495	99.4			
C6524	134.0	0.25	89.0	
C6613	204.0	0.15	41.5	
KJ1	232.0	0.20	2.0	
M0001	183.0			
P0002	82.6		40.4	BRECCIA
P0012	96.9		14.3	
P0016	147.5		27.4	LAVA
P0023	82.9		42.5	
P0027	36.7			
P0036	34.1			
P0037	21.2			
P0053	229.0		34.7	
P0065	100.6	0.16	5.4	
P0071	189.8			
P0089	42.1			
SA58	98.5	0.15	26.6	FRACTURED LAVA

APPENDIX 3 - BOREHOLE WATER STRIKES AND LEVELS

BOREHOLE NUMBER	MINOR WATER STRIKE DEPTHS (m)	MINOR REST WATER LEVELS (m)	MAIN WATER STRIKE DEPTH (m)	MAIN REST WATER LEVEL (m)
0001C				133.4
C0054			30.0	15.0
C0057				
C0059			124.1	103.6
C0079			102.9	96.3
C0092				
C0107				
C0108			22.8	19.8
C0115				
C0131	24.3 36.0		41.0	13.1
C0132			42.1	15.8
C0152			48.4	48.4
C0164			60.9	18.8
C0165				
C0202	61.0		133.0	38.0
C0204			61.0	26.0
C0205			116.0	104.0
C0208				
C0210	15.8	15.2	36.6	15.2
C0211			93.0	89.9
C0214			64.0	54.9
C0220			62.5	33.5
C0223	106.7		173.7	53.3
C0227	118.9		143.3	63.1
C0231			8.8	8.8
C0258			91.4	55.5
C0261			81.0	70.8
C0264			149.3	143.3
C0266			139.5	104.0
C0288			106.7	82.0
C0295				37.5
C0306	18.2		72.5	18.9
C0307			13.7	10.1
C0321	69		95.0	67.0
C0325	54.8		115.8	23.2
C0376			70.0	37.9
C0379			40.0	0.0
C0381			31.1	22.6
C0407			146.3	138.1
C0408			72.3	96.9
C0416			80.8	67.1
C0417	171.0 179.0		182.0	138.7
C0419	159.4	159.9	182.9	159.9
C0423			195.0	64.0
C0429			77.4	70.5
C0431	201.0	159.0	198.0	159.0
C0440			76.2	45.7
C0451	110.0 120.0		134.0	44.0
C0456	34		48.9	47.4
C0457	61	27.0	76.0	27.0
C0458			44.8	36.6
C0463	11		61.0	13.0

BOREHOLE NUMBER	MINOR WATER STRIKE DEPTHS (m)	MINOR REST WATER LEVELS (m)	MAIN WATER STRIKE DEPTH (m)	MAIN REST WATER LEVEL (m)
C0465	87		96.6	41.4
C0466			52.5	49.2
C0467			87.0	82.9
C0468			18.3	17.0
C0485			84.0	64.0
C0510				
C0511				
C0531			16.0	16.0
C0533			205.7	205.7
C0553			88.4	88.4
C0562			42.7	22.9
C0563			21.3	7.3
C0567			81.4	56.1
C0570			115.8	30.0
C0572			227.0	210.0
C0579			27.4	22.3
C0580			51.8	45.7
C0581			27.4	23.2
C0582			21.3	13.7
C0605	113.0 130.0		136.0	122.0
C0624			61.0	61.0
C0628			33.5	33.5
C0631			33.2	27.4
C0633			180.0	164.0
C0634			91.0	39.0
C0648				
C0651				
C0655			130.0	76.0
C0665			139.0	137.0
C0667			22.9	22.9
C0670	64		101.0	52.0
C0677				
C0678	36.0 35.0		50.6	32.9
C0691				
C0692			167.6	158.5
C0699			76.2	76.2
C0703	80		85.3	85.3
C0704				
C0705				
C0706				
C0707				
C0719			69.0	66.0
C0729			164.0	160.0
C0732	67		137.0	61.0
C0733			223.0	193.2
C0741			124.9	42.0
C0745			133.5	94.8
C0780			183.2	181.7
C0783	115.5	91.4	98.1	91.4
C0804			78.0	42.0
C0805	112.8 136.2		160.6	112.8
C0811			23.8	17.9
C0813			146.3	121.3
C0814			79.2	42.7
C0822				

BOREHOLE NUMBER	MINOR WATER STRIKE DEPTHS (m)	MINOR REST WATER LEVELS (m)	MAIN WATER STRIKE DEPTH (m)	MAIN REST WATER LEVEL (m)
C0824			138.0	137.0
C0836			162.5	69.0
C0839			42.1	25.3
C0845			133.5	126.0
C0855			184.1	183.0
C0858			143.0	116.0
C0869			133.0	131.0
C0870			90.0	78.0
C0872			78.0	48.0
C0875			103.0	73.0
C0882			162.0	160.0
C0910			18.3	12.8
C0916	128.9		156.1	118.0
C0921			158.4	98.1
C0939			128.0	126.4
C0946			242.6	237.7
C0947			24.4	24.4
C0953			129.0	94.5
C0965				
C0984			57.3	39.6
C0994			45.7	42.7
C1000			125.9	125.0
C1001				
C1007			45.0	23.0
C1013			179.8	165.5
C1013			179.8	165.5
C1019	165.9		215.1	163.5
C1021			60.0	21.0
C1027			82.3	79.2
C1029				
C1033			61.3	34.3
C1043			135.0	135.0
C1051			167.6	160.0
C1062			12.2	11.3
C1063			18.9	10.5
C1080	109.7	107	147.8	107.0
C1082	65.5 85.3		107.0	60.0
C1082	64.5 85.3		105.0	60.0
C1089				
C1112				
C1125			108.0	85.3
C1126			207.3	204.2
C1148			71.6	9.8
C1161			201.0	195.0
C1250			160.0	149.0
C1259			17.7	9.1
C1265				
C1277			112.5	68.6
C1279			139.3	121.9
C1281			29.6	23.8
C1287			54.9	50.6
C1294			21.3	9.1
C1325	109.7	90	187.4	90.0
C1356	18.3	12.2	29.9	12.2
C1358			154.5	147.0

BOREHOLE NUMBER	MINOR WATER STRIKE DEPTHS (m)	MINOR REST WATER LEVELS (m)	MAIN WATER STRIKE DEPTH (m)	MAIN REST WATER LEVEL (m)
C1361			216.9	186.0
C1362	46		195.0	175.0
C1374	67.1	61	102.0	61.0
C1379	36.0 107.0		120.0	36.0
C1383	55.0 82.0	54.9 54.9	97.5	54.9
C1390				
C1391			137.0	111.0
C1394			96.0	90.0
C1402			228.0	
C1404			52.5	57.6
C1425			263.0	261.0
C1434			37.0	36.6
C1436			45.1	45.1
C1464			11.3	7.6
C1475			177.0	61.0
C1482			35.1	11.3
C1483			39.6	31.0
C1486			106.0	10.7
C1487			97.0	91.4
C1488			82.3	76.2
C1491			107.0	85.0
C1499				
C1503			265.0	261.0
C1504			147.0	91.0
C1523				
C1524				
C1525				
C1535			178.0	177.0
C1545			6.7	6.1
C1558			129.5	125.0
C1559			94.5	83.8
C1584			79.2	17.7
C1585			93.0	8.7
C1602			165.0	150.0
C1614			134.1	118.3
C1625	39.6	39	39.6	39.0
C1641			135.6	76.2
C1652				
C1662				
C1666			175.3	62.7
C1713			97.2	54.9
C1726			262.2	259.2
C1749	68		134.0	85.3
C1794	128	131	173.4	179.8
C1795			135.6	131.7
C1795			135.6	131.7
C1798			174.0	132.0
C1830	136.0	128.3	143.3	128.3
C1843				
C1850	164.6	150.0	190.5	139.6
C1851			259.9	256.6
C1877	161 186	156.4 164.6	194.2	157.6
C1892			236.2	233.8
C1898			62.6	60.7
C1911				

BOREHOLE NUMBER	MINOR WATER STRIKE DEPTHS (m)	MINOR REST WATER LEVELS (m)	MAIN WATER STRIKE DEPTH (m)	MAIN REST WATER LEVEL (m)
C1912				
C1913			75.0	39.0
C1914	54.9	22.9	71.6	22.9
C1924			141.0	123.0
C1926			103.6	90.5
C1927			35.1	18.3
C1929			124.6	100.3
C1935	122		195.0	115.2
C1941			168.0	139.5
C1947	22.0 41.0	15.0 15.0	51.0	15.0
C1951			117.0	109.5
C1952	119.4	109.7	137.7	111.9
C1970			135.0	129.5
C1990			81.0	61.8
C1997	206	196	208.0	199.8
C2005			249.0	241.5
C2007			105.5	98.5
C2033			84.0	75.0
C2039				
C2042				
C2058	39.6	21.0	44.2	15.2
C2059				20.4
C2061	25.9	22.6	115.8	21.3
C2062			259.3	228.0
C2063	107	99	112.7	99.0
C2069	47.0 55.0	45.7 45.7	76.2	45.7
C2071			16.8	11.6
C2076				118.8
C2077				94.2
C2097	135	118.8	174.0	118.8
C2108			168.8	166.4
C2109			84.0	42.0
C2110	105.9	99.4	125.4	99.3
C2117			22.0	12.2
C2118			202.5	148.8
C2128			36.5	32.3
C2129	91.4		191.4	48.8
C2138	50.2	41.5	42.6	34.7
C2149	153.0	140.2	195.0	144.2
C2160	132.6	131.4	148.5	131.4
C2170	189.0		207.3	186.5
C2170				
C2172			86.0	42.0
C2176	28.0		73.0	16.0
C2197	14.0 180.0		134.1	113.4
C2234	87.3 140.8	78.3 55.8	148.7	77.4
C2241			119.4	108.6
C2246			17.1	13.7
C2263				
C2264	103 207	149.4 149.4	219.5	149.4
C2269	67.0 107.0	61.0 60.0	132.6	60.0
C2276	69 108	61 42	132.0	33.0
C2288				
C2289	115 134		96.0	87.0
C2292	64		116.0	62.4

BOREHOLE NUMBER	MINOR WATER STRIKE DEPTHS (m)		MINOR REST WATER LEVELS (m)		MAIN WATER STRIKE DEPTH (m)	MAIN REST WATER LEVEL (m)
C2294	44.5	91.4	16.2	16.2	149.4	16.2
C2296					81.0	30.0
C2300					111.3	100.6
C2304					6.0	6.0
C2322					124.0	112.2
C2332					115.5	55.5
C2338	191.0		191.0		228.6	195.1
C2347					171.6	119.5
C2358					289.6	265.0
C2388	145.1		140.2		242.6	241.7
C2402	79.2		74.7		91.4	67.1
C2420	55	101	27	29	117.7	68.3
C2421	39	85	24	21	193.0	188.0
C2430	10.6		6.0		31.0	6.0
C2432	141				164.0	116.0
C2447	56.4	75.0	52.7	72.8	75.3	202.0
C2448	192	243	156.9	156.9	280.0	156.9
C2466	40.0		37.0		90.0	55.0
C2468					15.0	132.0
C2480					35.1	39.6
C2482						
C2493	105.0		95.1		138.7	93.9
C2496					155.0	144.5
C2497					112.8	104.9
C2499	120.0		113.4		173.7	106.0
C2504	85		70.4		158.0	70.4
C2521					98.1	74.1
C2522					50.9	46.0
C2523	32.3		30.8		52.7	30.5
C2534					15.2	17.1
C2535					7.3	6.7
C2536					5.2	4.3
C2537					7.9	3.0
C2538					15.6	9.8
C2539						4.6
C2541						
C2542						
C2543						
C2564	103	158	106	110	192.0	109.0
C2600					183.0	186.0
C2620					67.1	67.1
C2636					6.1	4.6
C2646	60.9		59.4		80.8	51.2
C2647	82.3				91.4	18.0
C2657					32.6	23.5
C2659					9.0	7.6
C2660					19.8	19.8
C2662					219.5	201.3
C2663					360.0	320.0
C2664						
C2667					189.1	154.8
C2670					181.4	166.7
C2680					79.2	48.2
C2697	75.0		30.0		156.0	30.0
C2701	8.5		7.0		25.4	7.0

BOREHOLE NUMBER	MINOR WATER STRIKE DEPTHS (m)	MINOR REST WATER LEVELS (m)	MAIN WATER STRIKE DEPTH (m)	MAIN REST WATER LEVEL (m)
C2703			3.4	3.4
C2704			64.3	60.3
C2705			18.9	16.8
C2706			39.0	38.7
C2709	198	196	213.0	195.7
C2717	159.7 245.0 256.0	152.4 187.0 205.4	323.0	239.3
C2720				276.0
C2745	109.7	92.4	170.7	92.4
C2753			123.0	123.0
C2758	114.3	108.2	128.0	102.1
C2773			72.0	72.0
C2813	45.7	41.5	63.1	41.5
C2823			275.3	260.4
C2851			237.0	231.0
C2863				
C2866	92.9	89.0	147.5	89.0
C2870			15.2	
C2871				
C2883	57.9	48.8	91.4	52.7
C2885				
C2886				
C2887	9.1			
C2894	19.5 35.5 89.3	10.1 9.8 10.7	188.5	11.6
C2899				
C2900				
C2901				
C2902	67.0	59.0	98.0	59.4
C2910	137.0	125.0	223.0	176.8
C2966	78		78.0	54.0
C2970	33	25.6	42.6	25.6
C2997			287.7	280.4
C3003			249.9	240.0
C3005				38.1
C3024			93.0	91.8
C3032			39.0	42.0
C3047	56.0 58.0	56.0 53.0	67.0	59.4
C3064			14.9	14.9
C3066	10.6	2.1	82.3	70.0
C3067			75.0	60.0
C3087			43.0	41.0
C3136	45.0 137.0	45.0 45.0	165.0	45.0
C3164	21.3	19.2	42.7	18.9
C316D	85		131.0	77.0
C3216			6.1	4.9
C3217			6.1	4.8
C3243			176.0	67.6
C3266			93.0	93.0
C3280			93.3	82.3
C3292	10.7	7.3	30.5	7.6
C3298			4.8	4.8
C3299			3.0	2.1
C3324			192.0	190.2
C3327			81.0	67.5
C3351			157.5	153.0
C3352	57.6	51.8	243.8	213.4

BOREHOLE NUMBER	MINOR WATER STRIKE DEPTHS (m)			MINOR REST WATER LEVELS (m)		MAIN WATER STRIKE DEPTH (m)	MAIN REST WATER LEVEL (m)
C3353	45.7			36.6		133.5	36.6
C3358	124.0						
C3363						87.0	79.0
C3365						15.0	10.9
C3366						13.7	9.9
C3371						152.0	100.6
C3377	87.0			97.0		131.0	93.0
C3397						108.0	108.0
C3417	10.4	27.4		8.2	8.2	46.0	8.2
C3418	85.3	146.3		85.3	138.1	240.0	141.7
C3422	27.0			22.0		113.0	57.0
C3431	75.0	128.0	134.0			170.7	115.8
C3436						42.7	42.7
C3451	19.0			13.0		73.0	14.9
C3467							
C3490	93	134		115.8		189.0	107.0
C3523	42.7			25.3		61.0	25.3
C3524	18.0			13.0		100.0	13.1
C3525						88.1	86.9
C3551						6.0	4.6
C3562							
C3576	12.2					17.1	4.5
C3615						79.0	72.0
C3616						24.4	21.6
C3627	54.9	105.8				54.9	99.6
C3650	12.2			6.7		118.9	8.2
C3674						6.0	5.8
C3675						9.1	4.8
C3677						18.3	15.2
C3678						21.3	16.7
C3693	80.0	111.0		13.0	11.0	116.0	11.0
C3694	43.0	76.0		32.0	34.0	116.0	33.0
C3710	77.7			58.0		83.2	58.0
C3713	40.0			32.0			
C3721	27.0			23.0		88.0	39.0
C3739	52.0			48.0		67.0	48.0
C3740						21.3	17.1
C3763	49.0			49.0		61.0	26.0
C3764	40.0			27.7		85.0	23.5
C3765	40.0			35.7		45.7	35.7
C3767	27.4	36.6		27.4	26.5	67.0	26.5
C3771	60.9			36.5		70.1	39.0
C3779	18.0	90.0		12.2	10.7	128.0	10.7
C3784	7.5	39.6		3.6	6.1	128.0	6.1
C3799	41.0			41.0		64.0	41.0
C3870							
C3874	58.5			54.3		66.5	54.2
C3875	55.5					58.0	53.3
C3897	30.0			25.2		90.0	35.0
C3910	10.0	66.0		17.0	18.0	93.0	18.0
C3919						39.2	27.1
C3924						10.7	7.5
C3925						120.0	94.0
C3929						16.8	15.9
C3932	129					152.0	122.7

BOREHOLE NUMBER	MINOR WATER STRIKE DEPTHS (m)			MINOR REST WATER LEVELS (m)			MAIN WATER STRIKE DEPTH (m)	MAIN REST WATER LEVEL (m)
C3937	45.0	80.0	128.0	4.0	2.4	4.3	255.0	3.0
C3939							82.0	81.5
C3942							106.7	100.0
C3951							36.6	28.7
C3955	2.6			2.6			118.0	2.6
C3965							64.0	62.5
C3970							25.6	17.1
C3976	70.0			60.7			118.0	56.4
C3995	25.0	50.0		78.0	13.4		110.0	13.4
C3999	77.0	85.0		49.0	47.0		115.0	48.5
C4003	3.0	45.0					91.0	3.0
C4037	62.0	89.0	128.0	31.0	31.0	36.0	182.0	45.7
C4057							6.0	3.0
C4061							618.0	120.0
C4062							786.0	564.0
C4077	84	91					152.0	84.0
C4092								7.7
C4116	167	210		166	160		234.0	144.0
C4121	151						170.0	93.0
C4131								
C4143								172.0
C4152	24	61		11	11		131.0	11.0
C4155	65.0	117.0	143.0	40.5	36.0	34.0	174.0	27.0
C4157							18.0	10.7
C4161	21.0	31.0		16.0	16.0		45.0	16.0
C4168							48.0	16.9
C4174	58.0			47.0			68.0	57.0
C4177	18.0	25.0		16.0	16.0		42.0	16.1
C4178							20.0	16.4
C4179							104.0	102.0
C4185								
C4186	70.0	123.0					141.0	4.9
C4200	19.0	82.0	108.0	14.0	14.0	19.0	224.0	74.0
C4201	26.0	38.0	64.0	12.0	12.0	16.0	104.0	16.0
C4206	130	157		102	98		240.0	108.5
C4208							6.0	5.6
C4209							5.0	4.3
C4214	12	110		51	104		146.0	103.0
C4252	108						153.0	122.0
C4279	23.0			24.0			140.0	77.0
C4292	144.8			24.0			176.7	26.2
C4301							54.8	32.7
C4302							17.6	10.0
C4306	180.0			68.0			200.0	53.4
C4331								
C4332							107.0	62.0
C4350	18.0			13.0			128.0	13.0
C4360	22.0						100.0	21.8
C4369							93.0	31.2
C4370	48			45			98.0	33.9
C4397	10.0			7.0			17.0	7.0
C4403	26			26			106.0	43.0
C4413	43						131.0	68.5
C4416								
C4420	8			7			17.0	7.0

BOREHOLE NUMBER	MINOR WATER STRIKE DEPTHS (m)	MINOR REST WATER LEVELS (m)	MAIN WATER STRIKE DEPTH (m)	MAIN REST WATER LEVEL (m)
C4431	95.0	61.0	170.0	61.0
C4461				12.8
C4484	90.0		124.0	82.3
C4491	44.8	9	54.0	8.0
C4492			44.8	58.5
C4493			67.0	12.2
C4498			45.0	25.0
C4499				
C4500	26	26	42.0	15.2
C4501	27	27	49.0	21.3
C4502	30		80.0	50.7
C4504			11.9	11.9
C4510	52		102.0	27.7
C4511	42	42.2	94.0	27.0
C4512			98.0	27.6
C4517			180.0	97.0
C4531	76.0	70.0	102.0	70.0
C4554			75.0	46.0
C4555	36	36	80.0	28.4
C4564	63	53	102.0	53.0
C4565				
C4575				122.0
C4591	23	21.4	35.4	21.4
C4594			178.0	105.7
C4597	142.0	260.0	230.0	114.6
C4610			26.0	16.0
C4615	71.0 81.0 92.0		104.0	62.2
C4624	40.0	33.0	210.0	33.0
C4634			85.0	18.6
C4665	22.0	17.8	100.0	36.8
C4669	14	9.5	118.0	20.6
C4685			95.0	81.0
C4687	18.0	12.0	76.0	15.0
C4713	50.0	44.0	138.0	43.0
C4743	12.0	5.2	25.0	6.2
C4792	96.0	89.0	114.0	91.8
C4804			122.0	63.8
C4807			90.3	170.0
C4812			98.0	79.5
C4829				
C4850			50.0	5.0
C4855			100.0	8.0
C4863	12.0	5.0	65.0	15.0
C4881	57.0	48.6	80.0	54.0
C4893				
C4897			267.0	213.0
C4907	9.0	7.2	14.0	7.4
C4909	270.0		285.0	135.5
C4924	132.0	146.0	152.0	146.0
C4927	45.0		162.0	116.8
C4966	24.0	18.0	216.0	73.0
C4968	58.0	32.0	186.0	59.0
C4971				
C4974				219.0
C4981	42.0	34.6	56.0	35.0

BOREHOLE NUMBER	MINOR WATER STRIKE DEPTHS (m)	MINOR REST WATER LEVELS (m)	MAIN WATER STRIKE DEPTH (m)	MAIN REST WATER LEVEL (m)
C4986			5.5	5.4
C4989			2.0	1.4
C4997	20	15	190.0	70.7
C5002			111.0	106.0
C5029	30	21.5	138.0	88.0
C5111			18.9	100.3
C5117			21.0	9.0
C5143	34.0	27.0	60.0	35.0
C5161			43.0	24.8
C5175	42	30	107.0	38.3
C5206	34	34.4	158.0	34.7
C5257	120.0		140.0	111.5
C5343	102		126.0	97.4
C5348	138.8	125.6	147.8	124.0
C5375			88.0	76.0
C5411	98.0	78.0	110.0	83.0
C5520			72.0	64.0
C5564			148.0	16.0
C5754				7.7
C5798			68.0	38.0
C6056			15.0	13.8
C6095				9.7
C6186			20.0	7.5
C6211	43.0	42.0	46.3	42.0
C6213	130.0	134.0	145.0	130.0
C6271				34.6
C6290			194.0	197.0
C6300			166.0	132.9
C630D			119.0	99.7
C6377			52.0	48.3
C6378	104.0	99.0	118.0	100.3
C6494			77.0	6.0
C6495				
C6524			88.0	62.7
C6613	130.0		150.0	90.0
KJ1				
M0001				155.0
P0002			34.0	16.5
P0012	29.3		69.5	24.4
P0016	96.9		147.5	94.5
P0023			74.6	70.0
P0027				
P0036				
P0037				
P0053			221.6	213.4
P0065	22 30		90.0	61.0
P0071				
P0089				
SA58			47.9	47.2

APPENDIX 4 - BOREHOLE PRODUCTIVITY

BOREHOLE NUMBER	YIELD (l/s)	---- PRODUCTION TEST ---- PUMP RATE (l/s)	PUMPED WATER LEVEL (m)	SPECIFIC CAPACITY (l/s/m)	NOTES
0001C					
C0054	3.4				
C0057	0.0	0.0		0.00	DRY
C0059	0.4				
C0079	1.9				
C0092	0.0	0.0		0.00	DRY
C0107	0.0	0.0		0.00	DRY
C0108	0.6				
C0115	0.0	0.0		0.00	DRY
C0131	0.2				
C0132	2.5				
C0152	5.2				
C0164	1.2				
C0165	0.0	0.0		0.00	DRY
C0202	0.2				
C0204	4.6				
C0205	0.2				
C0208	0.0	0.0		0.00	DRY
C0210	4.5				
C0211	0.5				
C0214	0.8				
C0220	0.1				
C0223	0.1				
C0227	0.6				
C0231	58.3				
C0258	2.9				
C0261	1.8				
C0264	0.1				
C0266	1.7				
C0288	2.1				
C0295	0.4				
C0306	3.8				
C0307	2.9				
C0321	3.8				
C0325	1.6				
C0376	3.3				
C0379	3.4				WELL OVERFLOWED
C0381	0.6				
C0407	0.3				
C0408	1.6				
C0416	4.3				
C0417	1.5				
C0419	1.3				
C0423	2.1				
C0429	2.1				
C0431	1.3				
C0440	2.7				
C0451	2.1				
C0456	0.5				
C0457	2.1				
C0458	0.5				

BOREHOLE NUMBER	YIELD (l/s)	---- PRODUCTION TEST ---- PUMP RATE (l/s)	PUMPED WATER LEVEL (m)	SPECIFIC CAPACITY (l/s/m)	NOTES
C0463	5.1				
C0465	1.5				
C0466	2.2				
C0467	2.5				
C0468	2.4				
C0485	3.8				
C0510	0.0	0.0		0.00	DRY
C0511	0.0	0.0		0.00	DRY
C0531	5.1				
C0533	1.3				
C0553	0.8				
C0562	2.5				
C0563	1.8				
C0567	1.7				
C0570	1.8				
C0572	0.9				
C0579	1.9				
C0580	1.9				
C0581	1.9				
C0582	2.3				
C0605	2.5				
C0624	2.3				
C0628	2.3				
C0631	2.3				
C0633					
C0634	1.9				
C0648	0.0	0.0		0.00	DRY
C0651	0.0	0.0		0.00	DRY
C0655	1.5				
C0665	0.1				
C0667	2.3				
C0670	4.0				
C0677	0.0	0.0		0.00	DRY
C0678	1.3				
C0691	0.0	0.0		0.00	DRY
C0692	0.8				
C0699	0.6				
C0703	3.8				
C0704	0.1				STEAM STRUCK
C0705	0.0	0.0		0.00	DRY
C0706	0.0	0.0		0.00	DRY
C0707					STEAM STRUCK
C0719	1.8				
C0729	1.1				
C0732	2.6				
C0733	1.0				
C0741	3.8				
C0745	0.5				
C0780	1.1				
C0783	2.5				
C0804	2.1				
C0805	2.3				HOT WATER
C0811	1.2				
C0813	2.6				

BOREHOLE NUMBER	YIELD (l/s)	---- PRODUCTION TEST ---- PUMP RATE (l/s)	PUMPED WATER LEVEL (m)	SPECIFIC CAPACITY (l/s/m)	NOTES
C0814	2.1				
C0822	0.0	0.0		0.00	DRY
C0824	0.1				
C0836	1.6				
C0839	2.5				
C0845	1.5				
C0855	1.3				WATER TEMP 59C
C0858	3.2				
C0869	1.1				
C0870	0.5	0.5	109.00	0.02	
C0872	1.0				
C0875	0.1				
C0882	1.5				
C0910	1.6				
C0916	1.0				
C0921	0.4				
C0939	1.5				
C0946	0.3				
C0947	1.3				
C0953	2.0				
C0965	0.0	0.0		0.00	DRY
C0984	2.3				
C0994	1.8				
C1000	1.1				
C1001	0.0	0.0		0.00	DRY
C1007	6.3				
C1013	0.7				
C1013	0.7				
C1019	1.0				WARM WATER.50C.
C1021	3.9				
C1027	2.3				
C1029	0.0	0.0		0.00	DRY
C1033	3.4				
C1043	0.2				
C1051	0.8				
C1062	3.4				
C1063	3.8				
C1080	2.3				
C1082	4.2				
C1082	4.2				
C1089	0.0	0.0		0.00	DRY
C1112	0.0	0.0		0.00	DRY
C1125	3.5				
C1126	0.3				
C1148	1.5				
C1161	0.8				
C1250	1.8				
C1259	5.1				
C1265	0.0	0.0		0.00	DRY
C1277	2.9				
C1279	1.9				
C1281	2.1				
C1287	2.9				
C1294	0.4				

BOREHOLE NUMBER	YIELD (l/s)	---- PRODUCTION TEST ---- PUMP RATE (l/s)	PUMPED WATER LEVEL (m)	SPECIFIC CAPACITY (l/s/m)	NOTES
C1325	1.3				
C1356	3.0				
C1358					
C1361	0.8	0.8	235.00	0.02	
C1362	1.3				
C1374	3.7				
C1379					
C1383	1.5				
C1390	0.0	0.0		0.0	DRY
C1391	2.9				
C1394	1.9				
C1402					STEAM STRUCK
C1404	3.8	3.6	96.00	0.09	
C1425	0.3				
C1434	1.7				
C1436	3.8				
C1464	3.5				
C1475	0.6				
C1482	0.6				
C1483	0.5				
C1486	0.5	0.5	91.40	0.01	
C1487	8.2				
C1488	15.1				
C1491	2.9				
C1499	0.0	0.0		0.00	DRY
C1503	0.6				WATER HOT
C1504	0.1				
C1523	0.0	0.0		0.00	DRY
C1524					STEAM STRUCK 158M
C1525	0.0	0.0		0.00	DRY
C1535	1.4				
C1545	1.6				
C1558	2.6				
C1559	3.6				
C1584	3.2				
C1585	2.9				
C1602	0.4				
C1614	0.2				
C1625	0.2				
C1641	1.7				
C1652	2.5				
C1662	0.1				NO WATER LEVEL DATA
C1666	4.4				
C1713	0.2				
C1726	1.1				RWL IS SUSPECT
C1749	1.5				
C1794	0.3	0.1	208.70	0.01	
C1795	2.2	2.2	146.30	0.15	
C1795	2.2	2.2	146.30	0.15	
C1798	2.5	2.2	138.10	0.36	
C1830	0.8	0.8	132.60	0.19	
C1843	0.0	0.0		0.00	DRY
C1850	1.5	1.5	182.90	0.04	
C1851	0.1				

BOREHOLE NUMBER	YIELD (l/s)	PUMP RATE (l/s)	PUMPED WATER LEVEL (m)	SPECIFIC CAPACITY (l/s/m)	NOTES
		---- PRODUCTION TEST ----			
C1877	1.9	1.9	157.60	>9.50	
C1892	1.1	0.9	237.70	0.23	
C1898	1.0				
C1911	0.0	0.0		0.00	DRY
C1912	0.0	0.0		0.00	DRY
C1913	0.2	0.2	100.00	<0.01	
C1914	2.0				
C1924	0.6	0.6	143.00	0.03	
C1926	1.9	1.4	111.20	0.07	
C1927	1.3				
C1929	0.8	0.8	118.60	0.04	
C1935	1.9	1.7	126.50	0.15	
C1941	1.5	1.5	160.00	0.07	
C1947	12.6	12.6	22.30	1.73	
C1951	0.5	0.5	138.00	0.02	
C1952	1.9	1.9	131.00	0.10	
C1970	0.3	0.3	150.30	0.01	
C1990	2.1				
C1997	0.9	0.9	216.60	0.05	
C2005	0.2	0.2	250.60	0.02	
C2007	2.3				
C2033	1.9	1.9	82.00	0.27	
C2039	0.0	0.0		0.00	DRY
C2042	0.0	0.0		0.00	DRY
C2058	1.8	1.5	30.80	0.10	
C2059	0.9				
C2061	3.3	2.3	27.70	0.36	
C2062	0.6	0.6	245.70	0.03	
C2063	1.5	1.5	150.00	0.03	
C2069	1.1	0.4	63.40	0.02	
C2071	1.1	1.1	11.60	>5.50	
C2076	1.9	1.9	147.00	0.07	150F @ 182.9M
C2077	1.8				
C2097	0.5	0.5	152.00	0.02	
C2108	1.6	1.6	179.80	0.12	
C2109	3.3	3.3	44.00	1.65	
C2110	3.8				
C2117	2.3				
C2118	0.8	0.8	176.00	0.03	
C2128	4.6				
C2129	1.6				
C2138	0.1	0.1	42.60	<0.01	WATER TEMP. 47.2C
C2149	0.3				
C2160	1.2	1.2	147.00	0.08	
C2170	0.9	0.9	210.30	0.04	
C2170	0.0	0.0		0.00	DRY
C2172	1.7	1.7	45.70	0.46	WATER TEMP. 43C
C2176	2.7	2.7	54.40	0.07	
C2197	1.5	1.5	174.90	0.02	
C2234	2.4	2.4	111.00	0.07	
C2241	2.5				
C2246	1.4	1.4	28.00	0.10	
C2263	0.0	0.0		0.00	DRY
C2264	1.4	1.1	176.80	0.04	

BOREHOLE NUMBER	YIELD (l/s)	---- PRODUCTION TEST ---- PUMP RATE (l/s)	PUMPED WATER LEVEL (m)	SPECIFIC CAPACITY (l/s/m)	NOTES
C2269	2.8	2.8	110.60	0.06	
C2276	2.5	2.0	73.20	0.05	
C2288	0.0	0.0		0.00	DRY
C2289	2.0	2.0	99.20	0.16	
C2292	1.3				
C2294	3.9	3.9	102.10	0.05	
C2296	3.1	3.1	92.00	0.05	
C2300	2.7				
C2304	13.9	13.9	6.60	23.20	
C2322	2.0				
C2332	2.0	2.0	91.00	0.06	
C2338	1.9	1.9	201.20	0.31	
C2347	1.1	1.1	129.50	0.11	
C2358	0.4				
C2388	1.5	1.5	243.00	1.15	
C2402	3.8	3.8	67.10	>19.00	
C2420	5.4				
C2421	5.4				WATER LOSS 193M. CO_2
C2430	6.3	6.3	6.00	>31.50	
C2432	1.5				
C2447	1.9				
C2448	2.0	2.0	185.00	0.07	
C2466	3.2	3.2	64.10	0.35	
C2468	0.1				
C2480	1.9				
C2482	0.0	0.0		0.00	DRY
C2493	0.3	2.5	100.00	0.41	
C2496	1.3	1.3	152.40	0.17	
C2497	1.9	1.9	104.90	9.50	
C2499	1.4				
C2504	1.2	1.2	128.00	0.02	
C2521					
C2522	3.5	3.5	46.00	>16.50	
C2523	2.5				
C2534	3.7	3.7	17.10	>18.50	
C2535	3.8				
C2536	3.2	3.2	4.30	>16.00	
C2537	3.8	3.8	3.00	>19.00	
C2538	3.8	3.8	9.80	>19.00	
C2539	2.5	2.5	7.50	0.86	
C2541	0.0	0.0		0.00	DRY
C2542	0.0	0.0		0.00	DRY
C2543	0.0	0.0		0.00	DRY
C2564	2.3	2.0	137.00	0.07	
C2600	1.8	1.8	186.00	>9.00	
C2620	3.3	3.3	146.30	0.04	
C2636	8.1	6.7	6.10	4.50	
C2646	0.4	0.4	86.60	0.01	
C2647	1.2				
C2657	3.8	3.8	25.30	2.10	
C2659	7.8	7.8	10.70	2.52	
C2660	8.1	8.1	19.80	40.50	
C2662	1.5	0.4	210.40	0.04	
C2663	3.2	3.2	341.30	0.15	

BOREHOLE NUMBER	YIELD (l/s)	---- PRODUCTION TEST ---- PUMP RATE (l/s)	PUMPED WATER LEVEL (m)	SPECIFIC CAPACITY (l/s/m)	NOTES
C2664	0.0	0.0		0.00	DRY
C2667	1.5				
C2670	0.8				
C2680	<0.1				
C2697	3.1				
C2701	3.8	8.8	11.60	1.91	
C2703	7.5	7.5	3.40	>37.50	
C2704	2.5				
C2705	2.8	2.8	16.80	>14.00	
C2706	7.6	7.6	39.00	25.30	
C2709	1.6	1.4	202.70	0.20	
C2717	1.0	1.0	281.00	0.02	
C2720	0.6				
C2745	2.7	2.7	121.90	0.09	
C2753	0.1				
C2758	3.8				
C2773	0.1	0.06	0.10	<0.01	
C2813	3.8	3.8	41.50	>19.00	
C2823					
C2851	0.9	0.9	243.20	0.07	
C2863					
C2866	1.3	1.3	108.20	0.07	
C2870					STEAM STRUCK
C2871	0.0	0.0		0.00	DRY
C2883	2.0	2.0	100.50	0.04	
C2885					X1 STEAM BOREHOLE
C2886					X2 STEAM BOREHOLE
C2887					
C2894	1.2				
C2899					STEAM STRUCK
C2900					STEAM STRUCK
C2901					STEAM STRUCK
C2902	1.5	1.5	97.50	0.04	
C2910	1.2	1.3	219.50	0.03	
C2966	0.6				
C2970	1.1	1.1	46.30	0.05	
C2997	2.2	2.2	282.90	0.88	
C3003	0.2				
C3005	5.0	5.0	47.50	0.53	
C3024	0.8	0.8	99.10	0.11	
C3032	0.3				
C3047	19.0	19.0	59.40	>95.00	
C3064					
C3066	1.3				
C3067	1.3				
C3087	1.3				
C3136	3.1	1.3	127.00	0.02	
C3164	1.5	1.5	21.60	0.56	
C316D	3.2				
C3216	1.2				
C3217	3.0				
C3243	3.0	3.0	67.60	>15.00	
C3266	3.2				
C3280	0.1	0.1	133.40	<0.01	

BOREHOLE NUMBER	YIELD (l/s)	---- PRODUCTION TEST ---- PUMP RATE (l/s)	PUMPED WATER LEVEL (m)	SPECIFIC CAPACITY (l/s/m)	NOTES
C3292	4.1	4.4	7.90	14.67	
C3298	5.1	4.6	4.90	46.00	
C3299	5.1	5.1	3.60	3.40	
C3324	0.8	0.8	190.20	>4.00	WARM WATER
C3327	1.9	1.5	69.00	1.00	
C3351	0.8				
C3352	0.1				WATER LOSS AT 213.4M
C3353	1.8	1.7	47.20	1.32	
C3358	<0.1				SEEP ONLY
C3363	2.3				
C3365					
C3366					
C3371	1.3				
G3377	3.2				
C3397	1.5	1.5	108.00	>7.50	
C3417	1.3				
C3418	1.6				
C3422	1.2				
C3431	1.2	0.3	134.10	0.02	
C3436	2.0	2.0	73.20	0.07	
C3451	0.9				
C3467	0.0	0.0		0.0	DRY
C3490	3.8	2.1	107.00	10.50	
C3523	0.6				
C3524	0.7				
C3525	2.0	2.0	86.98	25.00	
C3551	4.6	4.6	5.20	7.70	
C3562	0.0	0.0		0.00	DRY
C3576	0.1				
C3615	1.1	1.2	80.80	0.14	
C3616					
C3627	2.5	2.5	118.00	0.13	
C3650	1.8	1.9	28.70	0.09	
C3674	6.3				
C3675	2.1				
C3677	2.1				
C3678					
C3693	1.1				
C3694	2.2	2.1	115.00	0.03	
C3710	3.8	4.5	58.00	22.50	
C3713	0.0	0.0		0.0	WATER LOST AT 72M
C3721	1.0	1.0	115.00	0.01	
C3739	0.8				
C3740	1.4				
C3763	0.7	0.7	73.00	0.01	
C3764	1.3	1.3	67.10	0.04	
C3765	0.9	0.9	54.90	0.05	
C3767	3.0				
C3771	1.9	1.9	82.30	0.04	
C3779	3.8	3.8	36.00	0.15	
C3784	3.8	3.6	63.00	0.06	
C3799	1.5				
C3870	0.0	0.0		0.00	DRY
C3874	1.3				

BOREHOLE NUMBER	YIELD (l/s)	---- PRODUCTION TEST ---- PUMP RATE (l/s)	PUMPED WATER LEVEL (m)	SPECIFIC CAPACITY (l/s/m)	NOTES
C3875	1.3				
C3897	3.5	2.3	65.50	0.08	
C3910	0.2	0.2	105.00	<0.01	
C3919	1.6				
C3924	22.2	22.2	9.65	10.14	
C3925	1.4	0.8	110.00	0.05	
C3929	8.8	8.8	19.00	2.84	
C3932	2.5	2.3	131.80	0.25	
C3937	0.8				
C3939	0.2	0.2	135.00	<0.01	
C3942	1.8	1.8	114.60	0.12	
C3951	0.5	0.5	41.00	0.04	
C3955	4.6	4.6	18.00	0.30	
C3965	2.8	2.8	82.00	0.14	
C3970	0.6	0.6	124.00	<0.01	
C3976	1.9	1.9	61.10	0.40	
C3995	0.8	0.8	91.00	0.01	
C3999	3.7	2.5	99.00	0.05	
C4003	3.7	3.7	53.60	0.07	
C4037	1.3	1.3	122.00	0.02	
C4057	4.7	4.7	30.00	0.17	
C4061					
C4062					
C4077					
C4092	1.3	1.3	14.80	0.18	
C4116	2.2	2.2	178.00	0.07	
C4121	23.6	23.6	168.00	0.32	
C4131	0.0	0.0		0.00	DRY
C4143					
C4152	0.5	0.5	84.00	<0.01	
C4155	9.1	9.1	36.00	1.01	WATER 36C AT 174M
C4157	3.1				
C4161	10.0	10.0	20.00	2.50	
C4168	10.0	10.0	19.00	4.76	
C4174	1.9	1.9	58.50	1.27	
C4177	15.6	15.6	35.00	0.83	
C4178	10.0	10.0	36.88	0.49	
C4179	1.0	1.0	108.00	0.17	
C4185	0.0	0.0		0.00	DRY
C4186					
C4200	7.0	7.0	106.00	0.22	
C4201	9.9	9.1	18.80	3.25	
C4206	5.7	5.7	131.10	0.25	
C4208	10.8	10.8	5.90	36.00	
C4209	10.8	10.8	4.60	36.00	
C4214	0.6	2.5	154.00	0.05	
C4252	1.8	1.8	150.00	0.06	
C4279	4.7	4.7	81.70	1.00	
C4292	0.2				
C4301	8.7	8.7	33.60	9.67	
C4302	50.0	10.3	11.00	10.30	
C4306	1.8	1.8	88.60	0.05	
C4331	0.0	0.0		0.00	DRY
C4332	0.7	0.2	91.30	<0.01	

BOREHOLE NUMBER	YIELD (l/s)	---- PRODUCTION TEST ---- PUMP RATE (l/s)	PUMPED WATER LEVEL (m)	SPECIFIC CAPACITY (l/s/m)	NOTES
C4350	0.7	0.8	148.00	<0.01	
C4360	1.4	1.0	43.00	0.05	
C4369	8.9	8.9	32.00	8.90	
C4370	3.5	3.5	76.20	0.08	
C4397	31.6				
C4403	0.6	1.5	90.00	0.03	
C4413	1.1	1.9	115.00	0.04	
C4416	0.0	0.0		0.00	DRY
C4420					
C4431	3.6				
C4461	1.9				
C4484	2.1				
C4491	4.9	4.9	52.00	0.11	
C4492	1.3				
C4493	3.8				
C4498	1.2	1.3	55.70	0.04	
C4499	0.0	0.0		0.00	DRY
C4500	5.4	5.4	15.80	9.00	
C4501	5.4	5.4	22.00	7.71	
C4502	0.7	0.7	131.00	0.01	
C4504	22.8	22.8	11.90	>114.00	
C4510	32.6	32.6	31.70	8.15	
C4511	3.3	3.3	27.30	11.00	
C4512	3.5				
C4517	3.8	3.8	108.60	0.33	
C4531	1.2	1.2	72.00	0.60	
C4554	1.5				
C4555	4.5	4.5	32.00	1.25	
C4564	3.8	3.8	76.00	0.17	
C4565	0.0	0.0		0.00	DRY
C4575	0.1	0.1	122.70	0.14	
C4591	37.9	37.9	21.50	379.00	
C4594					
C4597	1.6	1.6	187.30	0.02	
C4610	32.6	32.6	33.50	1.86	
C4615	6.3	6.3	62.40	31.50	
C4624	0.9	1.3	73.20	0.03	
C4634	1.7				
C4665	6.8	6.8	55.30	0.37	
C4669	3.2	4.4	33.70	0.34	
C4685	3.6	3.6	85.10	0.88	
C4687	1.8	3.0	40.00	0.12	
C4713	3.8	3.8	60.00	0.22	
C4743	1.6	1.6	19.20	0.12	
C4792	0.7	0.6	121.30	0.02	
C4804	3.3	3.3	120.10	0.06	
C4807	5.0				
C4812	1.3	1.4	97.10	0.08	
C4829	0.0	0.0		0.00	DRY
C4850	6.3	6.3	40.10	0.18	
C4855	1.5				
C4863	1.3	1.1	24.00	0.12	
C4881	2.1	2.1	103.00	0.04	
C4893	0.0	0.0		0.00	DRY

BOREHOLE NUMBER	YIELD (l/s)	PUMP RATE (l/s)	PUMPED WATER LEVEL (m)	SPECIFIC CAPACITY (l/s/m)	NOTES
		---- PRODUCTION TEST ----			
C4897	0.6	0.6	252.00	0.02	
C4907	1.8				
C4909					
C4924	2.0	2.0	150.50	0.44	HOT WATER
C4927	2.0	3.1	148.90	0.10	
C4966	6.1	6.1	93.00	0.31	
C4968	6.1	6.1	75.00	0.38	
C4971	0.0	0.0		0.00	DRY
C4974					
C4981	1.9	1.9	45.00	0.19	
C4986	11.3	11.3	5.53	141.25	
C4989	11.3	11.3	1.75	29.74	
C4997	4.1	2.1	89.40	0.11	
C5002	3.9	2.5	114.00	0.31	
C5029	0.8	0.8	140.00	0.02	
C5111	6.8	2.7	101.50	2.25	
C5117	2.8	2.8	40.00	0.09	
C5143	5.0	5.0	38.00	1.67	
C5161	2.5	2.5	71.80	0.05	
C5175	3.3	3.3	74.80	0.09	
C5206	2.8	1.3	36.70	0.65	
C5257	1.4	2.4	130.10	0.13	
C5343	1.7	1.7	100.10	0.63	
C5348	1.1	1.1	126.30	0.48	
C5375	1.2	1.9	85.70	0.20	
C5411	1.1	1.8	110.00	0.07	
C5520	1.3	2.1	81.50	0.12	
C5564	1.3	1.3	73.00	0.02	
C5754					
C5798	2.1	2.1	47.00	0.23	
C6056	2.1	2.1	49.00	0.06	
C6095					
C6186					
C6211	0.8	0.8	46.00	0.20	
C6213	1.7	1.7	145.00	0.11	
C6271					
C6290					
C6300	1.3	1.3	174.40	0.03	
C630D	1.5				
C6377	0.8	0.8	74.00	0.03	
C6378	1.7	1.7	103.80	0.49	
C6494	5.6	7.3	10.10	1.78	
C6495	0.0	0.0		0.00	DRY
C6524	3.7	3.7	64.30	2.31	
C6613	1.3	1.1	113.00	0.05	
KJ1	0.0	0.0		0.00	DRY
M0001					
P0002	0.3				
P0012	0.4				
P0016	0.5				
P0023	0.4				
P0027					STEAM STRUCK 13M
P0036	0.0	0.0		0.00	ABANDONED. DRY
P0037	0.0	0.0		0.00	ABANDONED. DRY

---- PRODUCTION TEST ----

BOREHOLE NUMBER	YIELD (l/s)	PUMP RATE (l/s)	PUMPED WATER LEVEL (m)	SPECIFIC CAPACITY (l/s/m)	NOTES
P0053	0.4				
P0065	0.6				
P0071	0.0	0.0		0.00	DRY
P0089	0.0	0.0		0.00	DRY
SA58	2.3				

APPENDIX 5

BOREHOLE LOCATION LIST

EASTING	NORTHING	BOREHOLE NUMBER
1391	99697	C0131
1392	99694	C0108
1394	99693	C0132
1397	99705	C2680
1404	99714	C1504
1434	99696	C3925
1440	99684	C0288
1443	99714	C0379
1444	99668	C1033
1446	99605	C3005
1446	99686	C1625
1447	99722	C1641
1453	99658	C3955
1453	99663	C1021
1456	99673	C0376
1456	99704	C0665
1464	99557	C0463
1472	99687	C0423
1478	99696	C0984
1481	99691	C1325
1483	99723	C2564
1508	99595	C0921
1516	99674	C0655
1536	99662	C0258
1538	99654	C0624
1548	99236	C5257
1548	99651	C0208
1549	99671	C0648
1553	99284	C2497
1555	99598	C0164
1560	99705	C1089
1563	99607	C0107
1567	99567	C0227
1567	99595	C0202
1571	99558	C4413
1571	99589	C6271
1572	99602	C4517
1573	99264	C4350
1574	99554	C0223
1574	99606	C0745
1575	99606	C2745
1577	99587	C1749
1578	99593	C3243
1580	98674	C4143
1581	99582	C1585
1582	99625	C0205
1586	99592	C4669
1587	98675	C4131
1587	99615	C0211
1589	99563	C0220
1594	99631	C4206
1595	99596	C5029
1596	99556	C2276

EASTING	NORTHING	BOREHOLE NUMBER
1596	99588	C5206
1596	99627	C1935
1598	99595	C0916
1600	99288	C3351
1605	99629	C4214
1606	99252	C6056
1606	99576	C2894
1608	99627	C3490
1621	99270	C2496
1621	99411	C1545
1624	99627	C3627
1625	99425	C1148
1625	99622	C3467
1626	99634	C1491
1626	99636	C1125
1629	99518	C0953
1634	99586	C3371
1636	99646	C0485
1643	99470	C0741
1644	99565	C4077
1644	99666	C1362
1646	99283	C3650
1649	99273	C3353
1649	99608	C2432
1652	99510	C2448
1656	99280	C1914
1656	99668	C2670
1657	99674	C0214
1663	99292	C1913
1665	99291	C3352
1665	99310	C2482
1665	99339	C3327
1665	99703	C0855
1667	99295	C1911
1668	99293	C1912
1669	99515	C4502
1671	99315	C3397
1680	99619	C0419
1691	99612	C3324
1692	99141	C6495
1696	99702	C0882
1698	99688	C0805
1701	99708	C1535
1704	99468	C4116
1705	99589	C1001
1709	98781	C4332
1721	99406	C0783
1723	99637	C0307
1724	99625	C0306
1754	99468	C1027
1759	99415	C0845
1762	98973	C3562
1764	99350	C2289
1765	99448	C4564
1767	99337	C0261
1783	99301	C3431
1789	99694	C5143
1790	99685	C0408

EASTING	NORTHING	BOREHOLE NUMBER
1791	99687	SA58
1793	99348	C2851
1793	99685	C0152
1795	99661	C3874
1795	99684	C0204
1796	99664	C3047
1797	99416	C1394
1797	99666	C3875
1798	99413	C0079
1798	99444	C2704
1799	99411	C0059
1799	99447	C2059
1801	99248	C3032
1801	99513	C1584
1802	99402	C1941
1802	99678	C0321
1802	99680	C1558
1803	99676	C0719
1803	99676	C0670
1804	99690	C4370
1805	99238	C3024
1805	99657	C1080
1805	99675	C2402
1807	99345	C2288
1808	99479	C2480
1810	99690	C316D
1811	98475	C3525
1812	99405	C1798
1812	99667	C1082
1813	99668	C2269
1814	99667	C1374
1815	99665	C4924
1815	99716	C4512
1816	99668	C0732
1816	99713	C4510
1816	99714	C4369
1816	99715	C4511
1818	98719	C0165
1819	99215	C3932
1820	99664	C1666
1823	99650	C0836
1825	99248	C3164
1828	99389	C0431
1828	99489	C1383
1830	99680	C2128
1831	99598	C0858
1832	99680	C2970
1835	98845	C4331
1836	99418	C0266
1841	99615	C0869
1844	99621	C0822
1844	99677	C2129
1846	99364	C0533
1847	98732	C0511
1847	98788	C0510
1851	99516	C2007
1851	99621	C0813
1853	99629	C1250

EASTING	NORTHING	BOREHOLE NUMBER
1855	99704	C1434
1860	99713	C1436
1861	99682	C2504
1863	99123	C4897
1869	98992	C1970
1869	99371	C1877
1872	99083	C2709
1875	99686	C4493
1877	98998	C2664
1878	99092	C2042
1879	99658	C2493
1881	99706	C3965
1883	99488	C1287
1883	99650	C5111
1886	99689	C4492
1888	99685	C4491
1889	99428	C1990
1889	99431	C0429
1901	99099	C2300
1901	99199	C2241
1902	99153	C1404
1911	99165	C0466
1912	99363	C2541
1915	99325	C2543
1915	99338	C2542
1915	99355	C2600
1918	99193	C4594
1918	99213	C2521
1919	99673	C5754
1920	99003	C2170
1922	99682	C6095
1929	99589	C2499
1934	99305	C2871
1940	99198	C2522
1943	99552	C2234
1944	99552	C0456
1945	99643	C3136
1946	99093	C3767
1947	99295	C2887
1948	99125	C2657
1949	99158	C4499
1949	99595	C2118
1950	99293	C2870
1957	99152	C4591
1959	99106	C0563
1959	99314	C2901
1960	99316	C2900
1961	99138	C4501
1964	99144	C4500
1964	99285	C0704
1965	99296	C0705
1966	99290	C0707
1966	99294	C0706
1966	99335	C2899
1967	99089	C2701
1968	99043	C2885
1969	99120	C2660
1971	99679	C0417

EASTING	NORTHING	BOREHOLE NUMBER
1972	99180	C1464
1973	99176	C2304
1974	99121	C2659
1974	99204	C2813
1975	99194	C1062
1975	99208	C0631
1976	98991	C4061
1978	99678	C2332
1978	99705	C2322
1983	99067	C630D
1984	99203	C1063
1985	99053	C2886
1985	99707	C4252
1986	99386	C0965
1987	99208	C2705
1989	99087	C2069
1990	99012	C4062
1992	99680	C4121
1996	99631	C1358
1998	99203	C3064
2000	98903	C1525
2002	99098	C0581
2002	99206	C2523
2006	99222	C2706
2008	99213	C2538
2008	99403	C6290
2009	98951	C1524
2013	99103	C0579
2014	99720	C0870
2015	99630	C1019
2017	99627	C1082
2019	99405	C0733
2022	99091	C3616
2022	99207	C2539
2022	99552	C0570
2024	99462	C2388
2024	99717	C2109
2025	99216	C2536
2025	99706	C2033
2028	99092	C2071
2030	99467	C2076
2034	99252	C3674
2035	99229	C2535
2035	99720	C2039
2036	99258	C4504
2036	99394	M0001
2038	98844	C0115
2039	99086	C4420
2041	99665	C2097
2043	98563	P0027
2044	99461	C2077
2045	99085	C4397
2046	99208	C2537
2050	99215	C2703
2051	99081	C3924
2059	99553	C1361
2059	99557	C1043
2061	99721	C3066

EASTING	NORTHING	BOREHOLE NUMBER
2062	99313	C3929
2064	99646	C1379
2068	99082	C2863
2069	99078	C1927
2071	99490	C2773
2072	98910	C1402
2074	99497	C2753
2076	99718	C0872
2078	99705	C2292
2079	99702	C0804
2080	98112	C4531
2081	98118	C1662
2084	99724	C0325
2085	99092	C4986
2086	99093	C4989
2087	99374	C0465
2087	99706	C3784
2087	99710	C3779
2090	99257	C0468
2091	99261	C3417
2092	99094	C0210
2094	99054	C1926
2094	99104	C1281
2094	99264	C0054
2095	99577	C1924
2096	99100	C2534
2097	99081	C0910
2098	99631	C3067
2099	98999	C2997
2101	99109	C2636
2101	99606	C2966
2102	99317	C4555
2103	99230	C3299
2104	99114	C4057
2104	99244	C3298
2105	98983	C1843
2107	99148	C0628
2107	99246	C2246
2109	99116	C0562
2110	99263	C4301
2110	99354	C0457
2111	99145	C0667
2112	99121	C1356
2112	99228	C3551
2114	99204	C3217
2114	99235	C3365
2114	99249	C3678
2115	99210	C3216
2119	99125	C0582
2119	99184	C2430
2120	99233	C3366
2120	99237	C4168
2120	99244	C3677
2122	99223	C3675
2123	99566	C1951
2124	99121	C0947
2124	99331	C0458
2125	99039	C0729

EASTING	NORTHING	BOREHOLE NUMBER
2126	99572	C1952
2130	99202	C4209
2130	99294	C2883
2131	99142	C3740
2131	99234	C4178
2132	99233	C4610
2133	99236	C4161
2134	99154	C1652
2134	99215	C3292
2135	99205	C4208
2135	99216	C4157
2136	99215	C4302
2139	99098	C0567
2139	99161	C2117
2139	99166	C1482
2140	99235	C4177
2141	99157	C2058
2141	99649	C2296
2142	99072	C1279
2142	99146	C0580
2143	99198	C0231
2145	99266	C4155
2146	99194	C1947
2146	99196	C0531
2156	99126	C1487
2156	99142	C0467
2157	99257	C1483
2157	99260	C0295
2159	99129	C1486
2163	99658	C2061
2164	99252	C1898
2164	99646	C2697
2180	99223	C1488
2181	98278	C1559
2183	99186	C2347
2185	98051	C4565
2187	99111	C0057
2189	98562	P0037
2189	98565	P0036
2191	99108	C0092
2197	99293	C5002
2199	99025	C2823
2200	99243	C0814
2204	99171	C0939
2210	99559	C2110
2214	99107	C1892
2215	99567	C2160
2225	99293	C1614
2226	99108	C1265
2228	99138	C0572
2234	99004	C1726
2235	99019	C1425
2236	99216	C0946
2237	99119	C1851
2239	99019	C1503
2242	99024	C1161
2246	98723	C4971
2253	97658	C1523

EASTING	NORTHING	BOREHOLE NUMBER
2258	98512	P0023
2258	99201	C1013
2258	99201	C1013
2260	99081	KJ1
2262	99153	C2667
2263	99149	0001C
2264	98939	P0053
2264	99149	C6300
2268	98487	P0016
2268	99185	C0780
2268	99193	C0691
2269	99189	C0692
2271	98458	C2866
2272	98596	C3003
2272	99034	C0264
2273	99406	C5520
2277	97682	C4829
2277	99166	C1997
2278	99078	C1475
2278	99263	C1029
2280	99070	C2662
2281	99212	C2108
2282	99262	C1830
2283	99185	C2062
2288	99102	C2720
2290	99050	C2263
2293	99143	C2005
2294	99072	C1794
2294	99190	C1051
2296	99254	C1795
2296	99254	C1795
2297	99058	C2264
2297	99181	P0089
2299	97899	C4484
2302	99053	C1602
2304	98709	C4174
2306	98606	P0071
2306	98710	C4974
2306	99099	C2063
2309	99094	C2663
2311	98609	C2717
2315	98675	C2758
2315	98764	C4893
2315	98979	C2172
2316	99244	C2149
2317	99074	C0633
2318	98981	C2138
2322	98778	C2910
2324	98668	C2358
2325	98961	C4634
2326	98956	C4152
2327	98695	C0407
2328	99092	C0703
2329	97909	C1390
2329	98636	C4909
2329	99226	C1850
2331	99147	C1000
2337	99139	C1929

EASTING	NORTHING	BOREHOLE NUMBER
2339	99090	C2420
2342	99122	P0065
2345	99316	C0651
2346	98803	C3713
2346	99191	C2197
2347	98678	C2447
2347	99084	C2421
2349	97803	C1499
2349	99126	C0634
2353	98613	C0440
2355	98723	C0416
2355	98775	C3266
2355	99136	C0994
2356	98524	C4575
2361	99247	C2170
2362	98647	C4812
2363	98624	C3087
2363	98645	C4807
2363	98812	C3377
2364	98641	C2902
2364	99139	C1007
2365	98545	C1126
2365	98585	C3280
2365	98653	C3418
2365	98865	C2466
2365	99283	C1112
2366	98644	C4792
2367	98882	C3422
2368	97628	C3939
2369	97893	C1391
2369	98606	C6378
2371	97801	C2468
2371	97908	C3942
2371	98554	C4416
2371	98643	C4431
2371	99150	C2176
2371	99198	C0699
2374	98720	C4597
2375	99219	C0553
2376	98684	C6613
2377	98687	C5343
2380	99130	C4403
2381	97822	C3358
2381	97887	C0605
2382	98697	C6213
2383	98626	C3799
2384	98672	C5348
2385	98514	P0002
2385	98663	C4615
2387	97632	C2647
2387	98503	P0012
2388	99188	C1277
2389	99233	C0677
2390	97883	C0451
2390	97889	C3363
2390	99228	C0678
2391	98478	C6494
2394	98521	C2294

EASTING	NORTHING	BOREHOLE NUMBER
2395	98651	C3710
2395	98666	C4685
2395	98703	C4855
2396	98657	C3615
2397	98483	C6377
2397	98502	C5117
2397	98509	C3937
2397	98606	C3999
2397	98630	C5375
2398	98678	C4461
2399	98442	C5798
2400	98645	C5411
2400	98710	C4037
2402	98715	C3976
2403	98471	C6211
2404	98462	C4743
2405	98675	C4850
2407	98418	C5564
2408	97759	C0875
2408	98377	C3576
2408	98752	C5175
2409	98525	C6524
2410	97886	C3970
2410	98670	C3694
2412	98562	C4804
2413	98410	C1294
2413	98467	C4092
2414	98648	C3764
2414	98802	C4554
2416	97788	C0824
2416	98626	C3765
2420	98413	C1259
2422	98416	C4186
2422	98484	C4907
2422	98486	C4201
2425	98428	C4179
2426	98425	C4863
2427	98466	C4200
2427	98626	C3523
2427	98630	C3524
2428	98502	C4968
2429	98465	C4966
2430	98438	C4997
2430	98440	C4981
2430	98588	C2338
2431	98831	C4279
2432	98255	C1713
2433	98635	C3721
2434	97868	C0381
2435	98563	C0839
2441	98601	C6186
2441	98638	C3763
2442	98536	C4927
2443	98743	C4360
2445	97865	C3436
2448	98498	C4881
2449	98617	C3739
2450	98633	C3693

EASTING	NORTHING	BOREHOLE NUMBER
2451	98436	C5161
2452	98428	C4687
2454	98490	C4624
2458	97868	C3870
2458	98822	C3897
2459	97876	C3951
2459	98696	C4292
2460	98738	C4665
2465	98553	C2620
2466	98633	C3910
2468	97862	C2646
2470	98733	C3995
2471	98013	C4498
2474	98029	C0811
2475	98596	C4306
2480	97692	C3451
2488	97659	C4185
2492	98693	C3771
2493	98457	C4713
2494	98724	C4003
2495	98814	C3919

APPENDIX 6

ESTIMATED HYDRAULIC PROPERTIES OF BOREHOLES

(From Thiem and Logan approximations - Section 3.4.1)

BOREHOLE NUMBER	GRID REFERENCE	TRANSMISSIVITY (m^2/d)	PERMEABILITY (m/d)
C0407	232798695	1139	21.21
C0692	226999189	1139	46.68
C0870	201499720	2	0.19
C1361	205999553	2	0.07
C1404	190299153	10	0.19
C1486	215999129	1	0.02
C1794	229499072	1	0.02
C1795	229699254	17	0.63
C1795	229699254	17	0.63
C1798	181299405	40	3.14
C1830	228299262	22	0.80
C1850	232999226	5	3.04
C1877	186999371	>1015	
C1892	221499107	26	1.30
C1913	166399292	<1	<0.01
C1924	209599577	3	0.21
C1926	209499054	8	0.36
C1929	233799139	4	0.39
C1935	159699627	17	8.54
C1941	180299402	7	3.51
C1947	214699194	185	11.56
C1951	212399566	2	0.07
C1952	212699572	11	37.97
C1970	186998992	1	0.01
C1997	227799166	6	0.37
C2005	229399143	2	0.38
C2033	202599706	31	0.72
C2058	214199157	11	4.58
C2061	216399658	41	5.06
C2062	228399185	3	2.28
C2063	230699099	3	0.21
C2069	198999087	2	0.81
C2071	202899092	>605	>287.98
C2076	203099467	7	0.03
C2097	204199665	2	0.33
C2108	228199212	14	0.72
C2109	202499717	188	31.32
C2118	194999595	3	0.54
C2138	231898981	<1	<0.01
C2160	221599567	9	0.25
C2170	236199247	5	0.21
C2172	231598979	51	0.90
C2176	237199150	8	2.66
C2197	234699191	2	0.05
C2234	194399552	7	0.52
C2246	210799246	11	0.52

BOREHOLE NUMBER	GRID REFERENCE	TRANSMISSIVITY (m^2/d)	PERMEABILITY (m/d)
C2264	229799058	5	0.09
C2269	181399668	7	0.39
C2276	159699556	6	1.06
C2289	176499350	18	0.42
C2294	239498521	6	0.90
C2296	214199649	6	0.38
C2304	197399176	2480	68.88
C2332	197899678	7	1.90
C2338	243098588	35	3.76
C2347	218399186	12	
C2388	202499462	124	5.81
C2402	180599675	>2089	>271.32
C2430	211999184	>3367	
C2448	165299510	8	0.96
C2466	236598865	38	4.81
C2493	187999658	45	5.50
C2496	162199270	19	1.54
C2497	155399284	1082	23.68
C2504	186199682	2	0.24
C2522	194099198	>1814	>3023.77
C2534	209699100	>2107	>296.80
C2536	202599216	>1759	>390.95
C2537	204699208	>2089	>264.45
C2538	200899213	>1975	
C2539	202299207	95	7.00
C2564	148399723	8	0.29
C2600	191599355	>990	>32.99
C2620	246598553	5	0.05
C2636	210199109	538	22.03
C2646	246897862	1	0.11
C2657	194899125	239	
C2659	197499121	269	17.49
C2660	196999120	4453	523.90
C2662	228099070	5	0.12
C2663	230999094	17	
C2701	196799089	204	408.32
C2703	205099215	>4123	>150.49
C2705	198799208	>1539	>127.22
C2706	200699222	2782	118.38
C2709	187299083	22	1.83
C2717	231198609	2	2.14
C2745	157599606	10	1.30
C2813	197499204	>1936	
C2851	179399348	8	0.36
C2866	227198458	7	
C2883	213099294	4	0.29
C2902	236498641	4	0.36
C2910	232298778	3	0.04
C2970	183299680	5	0.51
C2997	209998999	100	3.10
C3005	144699605	57	0.45
C3024	180599238	13	1.04

BOREHOLE NUMBER	GRID REFERENCE	TRANSMISSIVITY (m^2/d)	PERMEABILITY (m/d)
C2264	229799058	5	0.09
C2269	181399668	7	0.39
C2276	159699556	6	1.06
C2289	176499350	18	0.42
C2294	239498521	6	0.90
C2296	214199649	6	0.38
C2304	197399176	2480	68.88
C2332	197899678	7	1.90
C2338	243098588	35	3.76
C2347	218399186	12	
C2388	202499462	124	5.81
C2402	180599675	>2089	>271.32
C2430	211999184	>3367	
C2448	165299510	8	0.96
C2466	236598865	38	4.81
C2493	187999658	45	5.50
C2496	162199270	19	1.54
C2497	155399284	1082	23.68
C2504	186199682	2	0.24
C2522	194099198	>1814	>3023.77
C2534	209699100	>2107	>296.80
C2536	202599216	>1759	>390.95
C2537	204699208	>2089	>264.45
C2538	200899213	>1975	
C2539	202299207	95	7.00
C2564	148399723	8	0.29
C2600	191599355	>990	>32.99
C2620	246598553	5	0.05
C2636	210199109	538	22.03
C2646	246897862	1	0.11
C2657	194899125	239	
C2659	197499121	269	17.49
C2660	196999120	4453	523.90
C2662	228099070	5	0.12
C2663	230999094	17	
C2701	196799089	204	408.32
C2703	205099215	>4123	>150.49
C2705	198799208	>1539	>127.22
C2706	200699222	2782	118.38
C2709	187299083	22	1.83
C2717	231198609	2	2.14
C2745	157599606	10	1.30
C2813	197499204	>1936	
C2851	179399348	8	0.36
C2866	227198458	7	
C2883	213099294	4	0.29
C2902	236498641	4	0.36
C2910	232298778	3	0.04
C2970	183299680	5	0.51
C2997	209998999	100	3.10
C3005	144699605	57	0.45
C3024	180599238	13	1.04

BOREHOLE NUMBER	GRID REFERENCE	TRANSMISSIVITY (m^2/d)	PERMEABILITY (m/d)
C3047	179699664	>9917	>1599.47
C3136	194599643	2	0.15
C3164	182599248	62	2.00
C3280	236598585	1	0.03
C3292	213499215	1613	35.45
C3298	210499244	4802	137.98
C3299	210399230	355	9.75
C3324	169199612	>440	>47.81
C3327	166599339	110	1.83
C3353	164999273	150	16.34
C3397	167199315	>825	>88.67
C3431	178399301	2	0.55
C3436	244597865	8	0.24
C3490	160899627	1196	244.08
C3525	181198475	2848	51.59
C3551	211299228	847	11.96
C3615	239698657	16	2.66
C3627	162499627	15	0.18
C3650	164699283	10	3.42
C3694	241098670	3	0.57
C3710	239598651	2474	651.05
C3721	243398635	1	0.02
C3763	244198638	1	0.05
C3764	241498648	4	0.19
C3765	241698626	6	0.27
C3771	249298693	4	0.21
C3779	208799710	17	0.76
C3784	208799706	6	0.29
C3874	179599661	104	23.20
C3875	179799666	104	6.96
C3897	245898822	9	0.57
C3924	205199081	1058	39.06
C3925	143499696	5	2.64
C3929	206299313	299	6.77
C3932	181999215	27	2.11
C3939	236897628	<1	<0.02
C3942	237197908	14	0.30
C3951	245997876	5	0.05
C3955	145399658	34	1.37
C3965	188199706	15	0.16
C3970	241097886	<1	<0.01
C3976	240298715	46	5.36
C3995	247098733	1	0.09
C3999	239798606	6	0.23
C4003	249498724	7	0.08
C4037	240098710	2	0.13
C4057	210499114	19	0.35
C4092	241398467	19	0.13
C4116	170499468	8	0.47
C4121	199299680	36	4.56
C4152	232698956	<1	<0.08
C4155	214599266	115	

BOREHOLE NUMBER	GRID REFERENCE	TRANSMISSIVITY (m^2/d)	PERMEABILITY (m/d)
C4161	213399236	264	37.65
C4168	212099237	523	130.85
C4174	230498709	145	
C4177	214099235	91	9.13
C4178	213199234	52	1.64
C4179	242598428	19	1.56
C4200	242798466	24	12.10
C4201	242298486	357	7.01
C4206	159499631	28	2.85
C4208	213599205	3848	69.96
C4209	213099202	3848	67.51
C4214	160599629	6	0.06
C4252	198599707	7	0.24
C4279	243198831	114	113.91
C4301	211099263	1009	18.39
C4302	213699215	1086	18.59
C4306	247598596	5	0.16
C4332	170998781	<1	<0.21
C4350	157399264	<1	<0.03
C4360	244398743	6	0.16
C4369	181699714	979	13.41
C4370	180499690	9	0.11
C4403	238099130	3	0.00
C4413	157199558	5	0.76
C4491	188899685	12	0.78
C4498	247198013	5	0.08
C4500	196499144	939	49.45
C4501	196199138	805	89.42
C4502	166999515	1	0.04
C4504	203699258	>11900	>639.79
C4510	181699713	871	18.15
C4511	181699715	1176	21.77
C4517	157299602	38	4.70
C4531	208098112	68	1.42
C4555	210299317	142	2.97
C4564	176599448	18	
C4575	235698524	15	0.08
C4591	195799152	36600	3553.43
C4597	237498720	2	0.07
C4610	213299233	199	7.36
C4615	238598663	3464	65.35
C4624	245498490	3	0.16
C4665	246098738	41	0.77
C4669	158699592	37	0.39
C4685	239598666	94	3.48
C4687	245298428	13	0.51
C4713	249398457	24	2.02
C4743	240498462	13	0.17
C4792	236698644	2	0.02
C4804	241298562	7	0.37
C4812	236298647	9	0.09
C4850	240598675	20	0.66

BOREHOLE NUMBER	GRID REFERENCE	TRANSMISSIVITY (m^2/d)	PERMEABILITY (m/d)
C4863	242698425	13	0.45
C4881	244898498	4	0.08
C4897	186399123	2	0.07
C4924	181599665	48	1.94
C4927	244298536	11	0.61
C4966	242998465	33	2.37
C4968	242898502	40	0.73
C4981	243098440	20	0.46
C4986	208599092	14745	304.01
C4989	208699093	3104	134.98
C4997	243098438	11	1.04
C5002	219799293	34	0.45
C5029	159599596	2	0.03
C5111	188399650	256	1.51
C5117	239798502	10	0.10
C5143	178999694	184	1.75
C5161	245198436	6	0.05
C5175	240898752	10	
C5206	159699588	74	1.19
C5257	154899236	15	0.25
C5343	237798687	69	2.66
C5348	238498672	53	8.51
C5375	239798630	22	2.75
C5411	240098645	8	1.28
C5520	227399406	14	0.49
C5564	240798418	2	0.18
C5798	239998442	25	0.37
C6056	160699252	7	0.05
C6211	240398471	23	0.42
C6213	238298697	13	0.31
C6300	226499149	3	0.10
C6377	239798483	3	0.02
C6378	236998606	54	4.14
C6494	239198478	196	2.36
C6524	240998525	247	5.37
C6613	237698684	6	0.11

Appendix 7 - List of Geochemical Sampling Sites (BGS and UNDP) including Grid Reference and Sample Source

SITE NO.	BGS HYDROCHEM REF	SITE NAME	GRID REF	SAMPLE SOURCE
1	85/967	Little Magadi 1	AJ973092	Spring, 85°
2	85/968	Little Magadi 2	AJ970094	Spring, 81°
3	85/973	Little Magadi 3	AJ967092	Spring, 85°
4	85/974	Little Magadi 4	AJ968090	Spring, 81°
5	85/975	Little Magadi 5	AJ965099	Spring, 79°
6	85/976	Little Magadi 6	AJ962098	Stream, 83°
7	85/977	Little Magadi 7	AJ961101	Spring, 82°
8	85/978	Little Magadi 8	AJ962105	Spring, 83°
9	85/971	NW Lagoon 1, L. Magadi	AH903954	Spring, 45°
10	85/972	NW Lagoon 2, L. Magadi	AH904933	Spring, 44°
11	85/982	NE Lagoon 1, L. Magadi	BJ001059	Spring, 67°
12	85/983	NE Lagoon 2, L. Magadi	AJ999054	Spring, 60°
13	85/980	Magadi E2	AH963834	Spring, 40°
14	85/981	Magadi E2	AH964835	Spring, 39°
15	85/984	Magadi E3	AH999888	Spring, 34°
16	85/965	Bird Rock 1, L. Magadi	AH948794	Spring, 41°
17	85/966	Bird Rock 2, L. Magadi	AH948794	Spring, 41°
18	85/979	Magadi S1	AH919783	Spring, 45°
19	85/986	Magadi Causeway	AH970921	Lake, surface brine
20	85/969	Ewasongiro	AG714957	River, ambient
21	85/970	Oloibortot	AJ712001	River, ambient
22	85/985	Oltepesi	BJ181278	Borehole, ambient
23	85/987	Olorgesailie	BJ156256	Rain
24	85/998	Naivasha	BK109150	Lake
25	85/993	C4635, Kijabe RVA	BJ32 95	Borehole, 35°
26	85/991	Kijabe, Spring	BJ318980	Spring, 43°
27	85/992	Kijabe, Stream	BJ318980	Stream, ambient
28	85/995	Mayer's Farm	BJ31 82	Spring, 28°
29	85/994	Mount Margaret	BJ273887	Fumarole
30	85/997	Suswa, S. Slope	BJ022693	Shallow well
31	85/996	Akira Ranch	BJ082903	Fumarole
32	85/990	Ewasongiro	AJ077730	River, ambient
33	85/988	Majiyamoto 1	ZP013521	Spring, 51°
34	85/989	Majiyamoto 2	ZP013522	Spring, 52°
35	86/596	Kariandusi	AK988527	Spring, 40°
36	86/597	Kariandusi	AK977530	Spring, 23°
37	86/598	Meroronyi	AK894699	Spring, 30°
38	86/599	Meroronyi	AK893699	Spring, 24°
39	86/600	Chamuka	AK93 69	Spring, 29°
40	86/601	Ngosorr	AK778660	River
41	86/602	Elmenteita	AK938485	Spring, 45°
42	86/603	Elmenteita	AK938485	Spring, 38°
43	86/604	Eburru	AK966335	Fumarole
44	86/605	Lorusio S1	AM788387	Spring, 77°
45	86/606	Lorusio S2	AM788387	Spring, 81°
46	86/607	Lorusio N1	AM788388	Spring, 76°
47	86/608	Lorusio N2	AM788388	Spring, 75°

SITE NO.	BGS HYDROCHEM REF	SITE NAME	GRID REF	SAMPLE SOURCE
48	86/609	Kapedo S1	AM776298	Spring, 50°
49	86/610	Kapedo S2	AM776298	Spring, 50°
50	86/611	Kapedo S3	AM778293	Spring, 27°
51	86/612	Kapedo N	AM780306	Spring, 50°
52	86/613	Kapedo	AM767293	River
53	86/614	Bala S2	XQ696515	Spring, 72°
54	86/615	Bala S2	XQ696515	Spring, 35°
55	86/616	Bala S3	XQ697514	Spring, 58°
56	86/617	Bala S3	XQ697514	Spring, 75°
57	86/618	Bala S4	XQ686513	Spring, 36°
58	86/619	Homa Limeworks	XQ62 43	Lake Victoria
59	86/620	Simbi, Kisumu	XQ82 59	Lake Simbi
60	86/621	Homa Bay	XQ62 43	Lake Victoria
61	86/622	Bogoria SE	AL79 23	Spring, 97°
62	86/623	Bogoria SE	AL79 21	Stream
63	86/624	Bogoria S	AL78 20	Stream
64	86/625	Bogoria SW	AL77 23	Spring, 45°
65	86/626	Bogoria 1	AL77 25	Lake
66	86/627	Bogoria 2	AL76 27	Lake
67	86/628	Bogoria 3	AL75 37	Lake
68	86/629	Bogoria W1	AL75 27	Spring, 96°
69	86/630	Bogoria W2	AL75 29	Spring, 96°
70	86/631	Baringo	AL72 68	Lake
71	86/632	Olkokwe Island	AL76 69	Spring, 94°
72	86/633	Emerit	BJ19 41	Borehole, 37°
73	86/634	Magadi N	AJ98 05	Spring, 63°
74	86/635	Magadi NW	AH90 95	Spring
75	86/636	Oltepesi	BJ181278	Borehole
76	86/637	Naivasha	BK12 15	Lake
77	86/638	Nasagum	ZR31 52	River
78	86/639	Tigeri	ZR31 52	River
79	86/640	Malewa	BK090264	River
80	86/661	C4989	BK086094	Borehole, 21°
81	86/663	C567	BK139096	Borehole, 22°
82	86/664	C4178	BK131233	Borehole, 20°
83	86/665	C563	AK959105	Borehole, 26°
84	86/666	C1487	BK156126	Borehole, 21°
85	86/667	C5002	BK198293	Borehole, 20°
86	86/668	C1063	AK983202	Borehole, 26°
87	86/669	C1488	BK180223	Borehole, 26°
88	86/670	C467	BK156142	Borehole, 24°
89	86/671	C580	BK144146	Borehole, 25°
90	86/672	C814	BK200243	Borehole, 18°
91	86/673	Kanyamwi Farm	BK021552	Spring, 24°
92	86/674	C570	BK022552	Borehole, 22°
93	86/675	C3784	BK087706	Borehole, 23°
94	86/676	C307	AK723638	Borehole, 19°
95	86/677	C1190	AK704612	Borehole, 24°
96	86/678	P65	BK342121	Borehole, 23°
97	86/679	C3955	ZQ132657	Borehole, 23°
98	86/680	C2063	BK306099	Borehole

SITE NO.	BGS HYDROCHEM REF	SITE NAME	GRID REF	SAMPLE SOURCE
99	86/681	C4179	BJ425425	Borehole, 26°
100	87/218	C1404, Ndabibi	AK902155	Borehole, 26°
101	87/219	Kokot, Maiella	AJ878992	Gallery, ambient
102	87/220	Nakuru	AK787629	Lakewater
103	87/221	Hell's Gate (Ol Njorowa)	BJ012954	Seepage
104	87/222	Hell's Gate (Ol Njorowa)	BJ017965	Seepage, 20°
105	87/223	Hell's Gate (Ol Njorowa)	BJ016973	Seepage
106	87/224	Hell's Gate (Ol Njorowa)	BJ015977	Seepage, 52°
107	87/225	Hell's Gate (Ol Njorowa)	BJ011992	Seepage, 32°
108	87/226	Hell's Gate (Ol Njorowa)	BK015010	Seepage, 23°
109	87/227	Hell's Gate (Ol Njorowa)	BK014007	Seepage, 72°
110	87/368	Well 2, Olkaria	BK00070015	Geothermal well
111	87/369	Well 26, Olkaria	BK01110244	Geothermal well
112	87/370	Well 22, Olkaria	BK01100114	Geothermal well
113	87/371	Well 16, Olkaria	BK00620107	Geothermal well
114	87/372	Well 23, Olkaria	BK01300167	Geothermal well
115	87/373	Well 21, Olkaria	BK00840086	Geothermal well
116	87/374	Well 5, Olkaria	BK00260120	Geothermal well
117	87/375	Well 10, Olkaria	BK00260161	Geothermal well
118	87/382	Lanet, Nakuru No. 7 W.S.	AK797664	Borehole, 28°
119	87/376	EF-2, Eburru	AK946297	Fumarole
120	87/377	EF-13, Eburru	AK947315	Fumarole
121	87/378	C431, ADC Farm	AK826389	Borehole, 37°
122	87/379	C1798, ADC Farm	AK811405	Borehole, 35°
123	87/383	West Olkaria Fumarole	AK968993	Fumarole
124	87/380	DEL, Soysambu	AK857430	Borehole, 32°
125	87/381	C1990, Soysambu	AK889428	Borehole, 28°
126	87/384	F-3, Suswa	BJ056776	Fumarole
127	87/385	F-15, Domes	BJ063983	Fumarole
128	87/386	F-23, Longonot	BJ164998	Fumarole
129	87/387	C3525, Mosiro	AJ811475	Borehole, ambient
F-1		Suswa, caldera floor	BJ063760	Fumarole
F-2		Suswa, caldera rim	BJ072778	Fumarole
F-3		Suswa, caldera rim	BJ056776	Fumarole
F-4		Suswa, caldera rim	BJ026764	Fumarole
F-5		Suswa, caldera floor	BJ046759	Fumarole
F-6		Suswa, caldera floor	BJ073751	Fumarole
F-7		Suswa, caldera rim	BJ062780	Fumarole
F-8		Suswa, ring graben	BJ027732	Fumarole
F-9		Suswa, caldera rim	BJ003751	Fumarole
F-10		Suswa, caldera rim	BJ042775	Fumarole
F-11		Suswa, caldera rim	BJ053775	Fumarole
F-12		Suswa, ring graben	BJ041744	Fumarole
F-13		Suswa, ring graben	BJ045708	Fumarole
F-14		Suswa, ring graben	BJ042713	Fumarole
F-15		Domes	BJ063983	Fumarole
F-16		Domes	BJ061982	Fumarole
F-17		Domes	BJ051972	Fumarole
F-18		Hell's Gate (Ol Njorowa)	BJ010959	Fumarole
F-19		Hell's Gate (Ol Njorowa)	BJ008953	Fumarole
F-20		Domes	BJ041989	Fumarole

SITE NO.	BGS HYDROCHEM REF	SITE NAME	GRID REF	SAMPLE SOURCE
F-21		Domes	BJ045971	Fumarole
F-22		Domes	BJ016974	Fumarole
F-23		Longonot, crater	BJ164998	Fumarole
F-24		Longonot, crater	BJ173986	Fumarole
F-25		Longonot, crater	BJ171999	Fumarole
F-26		Longonot, S.E. slopes	BJ187944	Fumarole
F-27		Mount Margaret	BJ272884	Fumarole
F-28		Suswa, central island	BJ072740	Fumarole
F-29		Suswa, S. slopes	BJ056635	Fumarole
F-30		Suswa, central island	BJ076736	Fumarole
H-1		Akira Ranch	BJ082904	Borehole, steam
H-2		Hell's Gate (Ol Njorowa)	BJ010948	Borehole, steam
K-1		Meru, Kingua 1	E. side Mt. Kenya	Spring, 21^{o}
K-2		Meru, Kingua 2	E. side Mt. Kenya	Spring, 19^{o}

F, H and K prefixes - samples collected by Dr H Armannsson of the UNDP

ISBN 0 85272 175 7

£15 net

Natural
Environment
Research
Council